SYMMETRICAL AND ASYMMETRICAL SALEN-TYPE SCHIFF BASE LIGANDS AND THEIR TRANSITION METAL COMPLEXES

A thesis presented to the University of London in partial fulfilment of the requirements for the degree of PhD

By

MIHAELA DIANA POP

University College London Chemistry Department

Christopher Ingold Laboratories

20 Gordon Street

London WC1H 0AJ

2003

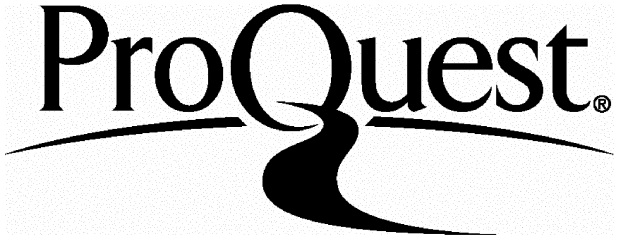

Motto: 'Be like the circle, the end is the beginning'

Japanese saying

This thesis is dedicated to my family

Acknowledgements

Firstly I would like to thank my supervisor Dr Graeme Hogarth for giving me the opportunity to work on this project, for his enthusiasm and support he gave me during these years.

I would like to thank my family for the love, help and patience they had while waiting the news from me or to go home, for the things they sacrificed for me and their daily thoughts toward me. I want to thank T. for making my life so enjoyable, for the friendship and support he gave me, encouragement throughout of it. For being next to me during hard periods.

I am grateful to Dr Graeme Hogarth and Dr John Steed for solving the crystal structures of the compounds that I made. I want also to thank Dr Graeme Hogarth for reading this thesis and for the suggestions he made. I want to thank Professors Robin Clark and David Williams for the strong support they gave to me in obtaining the grants, which allowed me to do this PhD. Without their help this thesis would not be now.

I want to thank Dr Alan Spivey (Sheffield University) for the advice, the encouragement and support he gave me while I was writing this thesis. I was deeply moved by his generosity and the help he gave me in this final year. I want to thank Professors Henning Lund and Steen U. Pedersen (Aarhus University, Denmark) for showing me what research means, how to plan and make it. For opening my eyes to the beauty of it and important contributions to the way I am thinking now.

My thanks go to Dr Andrea Sella for the help he gave me, for the things that I learned from him. I am grateful to Professor Tony Deeming and Dr Derek Tocker for the general advice they gave me which proved very useful over time, also for their interesting courses they taught to me. I want to thank Professor Sally Price and Mrs Anne McDonald from Graduate School for their kindness, support and dedication they had in helping me and other PhD students.

I want to thank D. for healing my hands and the advice I received from him which helped me stay healthy and cope with the hard work and stressful periods that I had. Thank you for your poems. I am very grateful to Jorge Outeirino for the advice he gave me in making my latest grant application that helped me in completing this research. I want to thank Maria Christofi and Denise Marinou for their friendship and for sharing with me so many happy and not so happy moments during these years. Thank you, Dave for being such a nice mate, for understanding me and the help you gave, for encouraging me to finish writing. To all those friends who were not next to

me, but they lit a candle for me, prayed and sent their loving thoughts toward me I want to thank.

My thanks go to my mates: Shahbanu, Venus, Idris, MRR and Sarah, Anthony and Romano for putting up with me in the lab, for the nice time we shared on tea breaks and lunches we had together.

Thank you all !

Abstract

This thesis describes synthetic studies towards symmetrical and asymmetrical double Schiff bases with N_4, N_3O and N_2O_2 donor atoms and their metal complexes.

The thesis begins with an introduction to salen complexes describing possible types of co-ordination to the metal ions and ways in which chirality is introduced in these complexes. A review on applications of salen complexes in asymmetric synthesis is then presented which aims to illustrate how careful catalytic system design led to significant discoveries in asymmetric synthesis.

Preparation of 2-amino-R-benzaldehydes, unstable intermediates, using multistep organic synthesis is presented and the stability of these compounds generated by three different routes is assessed. Further on, synthesis of ambch ligands, which combine the donor atom environment of porphyrins with ready incorporation of chirality and arene functionalisation familiar to salen ligands, was achieved. It is followed by synthesis and characterisation of their nickel, copper, manganese, cobalt, and vanadium complexes. The structures of these complexes are discussed based on NMR, IR and X-ray crystallography data.

The strategies proposed in the literature for preparation of asymmetrical ligands were tested in synthesis of ligands **178, 180** and **183**. Original strategies were developed in the search for better synthetic procedures to compounds **178-183**. The results demonstrated that the route to asymmetrical ligands is not general and has to take into account the difference in reactivity of the two aldehydes and the nature of the diamine involved in the condensation reaction. Synthesis of asymmetrical nickel salchsal and ambchsal complexes were achieved under mild conditions in high yields. The influence of changing the co-ordination sphere from N_2O_2 to N_3O and N_4 in the ligands and nickel complexes on the structure of these compounds is discussed based on NMR and X-ray crystallography data. The asymmetrical complexes allow a better tuning of the electronic and structural properties than symmetrical ones. The study demonstrates for the first time that the difference between the two aromatic moieties of the asymmetrical complexes can be tuned by appropriate substitution of the aromatic rings.

Abbreviations

Ac	acetyl
acac	acetylacetonate
BINOL	1, 1'-bis-2-naphthol
br	broad
Bn	benzyl
Bu	butyl
Bz	benzoyl
Ch	1,2-diaminocyclohexane
d	doublet
DCC	Dynamic Combinatorial Chemistry
DCM	dichloromethane
DMF	*N*,*N*-dimethylformamide
DMSO	dimethylsulfoxide
Et	ethyl
HKR	Hydrolytic Kinetic Resolution
HMT	hexamethylenetetramine
m-CPBA	*m*-chloroperbenzoic acid
Me	methyl
MOM	methoxymethyl
Ms or mesyl	methanesulfonyl
NBS	*N*-bromosuccinimide
NMI	*N*-methyl-imidazole
NMR	nuclear magnetic resonance
Ph	phenyl
PPNO	phenyl-pyridine-*N*-oxide
py	pyridine
q	quartet
SES	2-(trimethylsilyl)ethanesulfonyl
s	singlet
t	triplet
TBDMS	*tert*-butyldimethylsilyl
TBME	*tert*-butyl-methyl-ether
TFA	trifluoroacetic acid
Tf	trifluoromethanesulfonyl
THF	tetrahydrofuran
TMEDA	*N*, *N*, *N'*, *N'*-tetramethylethylenediamine
TMS	trimethylsilyl
Ts	*para*-toluenesulfonyl

Contents

Chapter 1. Introduction **14**

1.1 Salen ligands 14

1.2 Conformational aspects 14

1.3 Chirality of salen complexes 16

1.3.1 Chiral salen ligands 16

1.3.2 Induced chirality 17

1.4 Applications of salen complexes in asymmetric synthesis 20

1.4.1 Epoxidation 20

1.4.2 Aziridination 29

1.4.2.1 Aziridination with epoxidation type catalysts 29

1.4.2.2 Aziridination with cyclopropanation-type catalysts 35

1.4.3 Cyclopropanation 37

1.4.4 Kinetic resolution by ring opening of epoxides 42

1.4.4.1 Kinetic resolution with $TMSN_3$ 43

1.4.4.2 Ring opening of epoxides with acids 47

1.4.4.3 Hydrolytic kinetic resolution 48

1.4.4.4 Kinetic resolution with phenols 50

1.5 References 52

1.6 Nomenclature of symmetrical salen and amben type ligands 55

1.7 Aims of the project 56

Chapter 2. Synthesis of ambch ligands **58**

2.1 Introduction 58

2.1.1 Synthesis of substituted nitrobenzaldehydes 58

2.1.2 Reduction of nitrobenzaldehydes 61

2.1.3 Synthesis of amino-benzyl-alcohols 63

2.1.4 Oxidation of amino-benzyl-alcohols 64

2.1.5 Other methods 64

2.2 Results and discussions 65

2.2.1 Synthesis of substituted nitrobenzaldehydes 65

2.2.2 Reduction of 2-nitro-benzaldehydes 68

2.2.3 Duff reaction 70

2.2.4 Synthesis of amino-benzaldehydes from amino-benzyl-alcohols 76

2.2.5 Bromination of 5-methoxy-2-nitro-toluene 77
2.2.6 Methylation of 5-hydroxy-2-nitro-benzaldehyde 78
2.2.7 Synthesis of ambch ligands 80
2.3 Conclusions 81
2.4 References 83

Chapter 3. Synthesis of symmetrical ambch complexes 84

3.1 Nickel double Schiff base complexes 84
3.1.1 Nickel amben type complexes 84
3.1.2 Synthesis of Ni(R-ambch) complexes 85
3.1.3 IR spectra of Ni(R-ambch) complexes 85
3.1.4 NMR spectra of Ni(R-ambch) complexes 87
3.1.5 Crystal structure of Ni(ambch) 87
3.2 Copper double Schiff base complexes 91
3.2.1 Copper amben and salen type complexes 91
3.2.2 Synthesis of Cu(R-ambch) complexes 95
3.2.3 IR spectra of Cu(R-ambch) complexes 96
3.2.4 Crystal structure of Cu(ambch) 97
3.3 Manganese double Schiff base complexes 100
3.3.1 Manganese salen type complexes 100
3.3.2 Synthesis of Mn(R-ambch) complexes 103
3.4 Cobalt double Schiff base complexes 106
3.4.1 Cobalt amben and salen type complexes 106
3.4.2 Synthesis of Co(R-ambch) complexes 111
3.4.3 Reactivity of Co(ambch) towards O_2 112
3.5 Vanadyl double Schiff base complexes 119
3.5.1 Vanadyl salen type complexes 119
3.5.2 Synthesis of vanadyl ambch complexes 122
3.6 Conclusions 127
3.7 References 128

Chapter 4. Asymmetrical Schiff base ligands and their nickel complexes 131

4.1 Introduction 131
4.2 Nomenclature of asymmetrical salch and amch ligands 133
4.3 Strategies applied for synthesis of asymmetrical salchsal

	and ambchsal ligands	133
4.3.1	Stepwise procedure	134
4.3.1.1	Study of the reactivity of different aromatic aldehydes toward 1,2-diaminocyclohexane	134
4.3.1.2	Procedure 1	137
4.3.1.3	Procedure 2	139
4.3.1.4	Procedure 3	140
4.3.1.5	Characterisation of symmetrical and asymmetrical salen ligands by ^{1}H-NMR	141
4.3.1.6	Attempt to synthesize N-(2-hydroxy-benzylidene)-1,2-diamino cyclohexane	143
4.3.2	Synthesis involving blocking of one of the active sites in the diamine	144
4.3.3	Attempted synthesis of Ni complex of the mono Schiff base	147
4.4	Synthesis of asymmetrical Ni (salchsal) and Ni (R-ambchsal)	152
4.4.1	Synthesis from the free ligand	152
4.4.2	Synthesis of Ni (R-ambchsal)	153
4.4.3	NMR spectra of asymmetrical Ni complexes	156
4.4.4	Crystal structures of Ni(salchsal) and Ni(ambchsal)	159
4.5	Conclusions	164
4.6	References	165
Chapter 5. Experimental		**166**
5.1	Preparation and instrumentation	166
5.2	Preparation of 2-nitro-benzaldehydes	167
5.3	Reduction of R-nitro-benzaldehydes (R = H, 5-Cl, 3-MeO, Mixture of MeO)	169
5.4	Duff reaction	171
5.4.1	Attempt to synthesize 2-amino-3,5-dimethyl-benzaldehyde	171
5.4.2	Attempt to synthesise 2-amino-5-methyl-benzaldehyde	173
5.5	Oxidation of amino-R-benzyl alcohols (R = H, 3-Me, 5-Me)	174
5.6	Bromination of 5-methoxy-2-nitro-toluene	176
5.7	Methylation of 5-hydroxy-2-nitro-benzaldehyde	177
5.8	Synthesis of symmetrical R-ambch ligands (R = H, 5-Cl, 3-MeO, 3-Me, 5-Me)	178
5.9	Synthesis of symmetrical ambch complexes	182
5.9.1	Synthesis of Ni (R-ambch) complexes (R = H, 5-Cl, 3-MeO, 3-Me, 5-Me)	182
5.9.2	Synthesis of Cu (R-ambch) complexes (R = H, 5-Cl, 3-MeO, 3-Me, 5-Me)	187

5.9.3	Synthesis of Mn (R-ambch) complexes (R = H, 3-Me)	190
5.9.4	Synthesis of Co (R-ambch) complexes (R = H, 3-Me, 5-Me)	194
5.9.5	Oxidation of Co (II) ambch	195
5.10	Synthesis of VO(ambch) complexes	201
5.10.1	Complexation of ambch with $VO(acac)_2$	201
5.10.2	Complexation of ambch with $VO(acac)_2$ in presence of a base	202
5.10.3	Complexation of ambch with $VOSO_4$	204
5.11	Synthesis of asymmetrical Schiff base ligands	205
5.11.1	Reactivity of different benzaldehydes toward 1,2-diaminocyclohexane	205
5.11.2	Stepwise syntheses of asymmetrical ligands	206
5.11.2.1	Procedure 1	206
5.11.2.2	Procedure 2	208
5.11.2.3	Procedure 3	209
5.11.2	Attempt to synthesize of N-(2-hydroxy-benzylidene)-1,2-diamino cyclohexane	210
5.11.4	Synthesis involving blocking of one of the active sites of the diamine	211
5.11.5	Synthesis from nickel complexes of the mono Schiff bases	212
5.12	Synthesis of asymmetrical nickel complexes salchsal and ambchsal	215
5.12.1	Synthesis of Ni (salchsal)	215
5.12.2	Study of the equilibrium between symmetrical and asymmetrical double Schiff base ligands	216
5.12.3	Synthesis of Ni(ambchsal)	216
5.12.4	Synthesis of Ni(3-Me-ambchsal)	217
5.12.5	Synthesis of Ni(5-Me-ambchsal)	218
5.13	References	219
Appendix		220

List of Figures

Figure 1.1 – Salen ligand
Figure 1.2 – Co-ordination modes of salen ligands
Figure 1.3 – Non-planar co-ordination modes
Figure 1.4 – Chiral Mn(salen) complexes
Figure 1.5 – Equilibrium of enantiomers in non-chiral salen complexes
Figure 1.6 – Chiral salen complexes with induced (**19**) or axial chirality (**6a**)
Figure 1.7 – Jacobsen's and Katsuki's (first generation) epoxidation catalysts
Figure 1.8 – Olefin approach to the reaction centre in epoxidation using **21** and **22**
Figure 1.9 – Axial donor ligands
Figure 1.10 – Katsuki's Mn(salen) catalyst from the second generation
Figure 1.11 – Diastereomeric Mn(salen) complexes **6c** and **6d**
Figure 1.12 – *Trans*-Olefin approaching planar and folded salen complexes
Figure 1.13 – Mn(salen) catalysts possessing axial chirality
Figure 1.14 – CoN_4 catalyst used in epoxidation with molecular oxygen
Figure 1.15 – Olefin approach to the reaction centre in epoxidation vs aziridination
Figure 1.16 – Possible orientations of N-sulfonyl group and the olefin approach
Figure 1.17 – Epoxidation – Mn(salen) catalysts of different reactivity
Figure 1.18 – Active species involved in synthesis of oxazolines
Figure 1.19 – Chiral ligands used in aziridination of olefins
Figure 1.20 – Olefin approach in cyclopropanation
Figure 1.21 – Ru(salen) catalyst with high *cis*-selectivity
Figure 1.22 – Tunning the catalysts for *cis*-selective cyclopropanation
Figure 1.23 – Ring opening of *meso*-epoxides
Figure 1.24 – Compounds obtained by ring opening of terminal epoxides
Figure 1.25 – Active species in asymmetric ring opening; mechanism of action
Figure1.26 – Dimers tested in reactions with $TMSN_3$ and catalysts used for ARO of epoxides with acids
Figure1.27 – Intermediate in KR reaction with phenols
Figure 2.1 – Products from nitration of 3-hydroxy-benzaldehyde
Figure 2.2 – Products from nitration of 3-methoxy-benzaldehyde
Figure 2.3 – Products from reduction of chloro-aminobenzaldehydes
Figure 2.4 – Amino-3-methoxy-benzaldehydes synthesized
Figure 2.5 – Substrates used in Duff reaction and position of substitution
Figure 2.6 – Aniline derivatives employed in Duff reaction
Figure 2.7 – Structure of the intermediate Schiff bases
Figure 2.8 – Electrophilic attack in the free and protonated aniline **95 a,b**
Figure 2.9 – Structures of the intermediate Schiff bases **104-105**
Figure 2.10 – Products from bromination of 5-methoxy-2-nitro-toluene
Figure 2.11 – Product from methylation of 5-hydroxy-2-nitro-benzaldehyde
Figure 2.12 – Symmetrical ambch ligands
Figure 3.1 – Green and Tasker's Ni(amben) type complexes
Figure 3.2 – Related Ni(salen) complexes
Figure 3.3 – Ni(R-ambch) complexes synthesized
Figure 3.4 – Crystal structure
Figure 3.5 – Ni(ambch) and related nickel complexes
Figure 3.6 – Cu(amben) and other R-substituted copper complexes
Figure 3.7 – Crystal structures

Figure 3.8 – Macrocyclic N_4 double Schiff bases
Figure 3.9 – Copper N_4 complexes derived from 2-pyridyl-carboxaldehyde
Figure 3.10 – Copper ambch complexes synthesized
Figure 3.11 – Crystal structure
Figure 3.12 – Cu(ambch) complex and related CuN_4 and Cu(salch) complexes
Figure 3.13 – Jacobsen's manganese complexes
Figure 3.14 – Katsuki's manganese salch complexes
Figure 3.15 – Mn salen type complexes prepared by ligand substitution or complexation with $MnCl_2$
Figure 3.16 – Cobalt amben type complexes previously reported
Figure 3.17 – Co(ambch) complexes prepared (**154-156**) cf. related Cobalt complexes
Figure 3.18 – Equilibrium mixture of two enantiomers in non-chiral salen complexes
Figure 3.19 – Co(ambch)(O-C_6H_4-Bu^t)
Figure 3.20 – Possible by-product from oxidation of Co(ambch)
Figure 3.21 – Co(salch)(OR) complex
Figure 3.22 – Asymmetrical vanadyl complexes
Figure 3.23 – VO(salstien)
Figure 3.24 – Polymeric structure of VO(salstien) in orange form
Figure 3.25 – Asymmetrical ligand ambchac **171** vs related ligand **172**
Figure 3.26 – Asymmetrical VO(ambchac) complex **173** and related VO complexes
Figure 4.1 – Jacobsen's monomer and dimer – catalysts in ring opening of epoxides
Figure 4.2 – Gilheany's asymmetrical chromium salen epoxidation catalysts
Figure 4.3 – Planar cf. bent conformation in Cr(salch) complexes
Figure 4.4 – Asymmetrical salchsal and ambchsal ligands synthesized
Figure 4.5 – Structure of the mono Schiff base when R is an electron-withdrawing substituent
Figure 4.6 – Symmetrical salch and asymmetrical salchsal ligands
Figure 4.7 – Nguyen's and Gilheany's asymmetrical salchsal ligands
Figure 4.8 – Asymmetrical ligands generated by Elder's strategy
Figure 4.9 – Nickel asymmetrical salprt-sal prepared by Elder's strategy
Figure 4.10 – Compound with biological activity dicovered by DCC
Figure 4.11 – Asymmetrical Ni(R-ambchsal) complexes synthesized
Figure 4.12 – Symmetrical and asymmetrical ligands synthesized
Figure 4.13 – Crystal structure
Figure 4.14 – Symmetrical and asymmetrical N_2O_2 and N_3O complexes
Figure 4.15 – Crystal structure

List of Tables

Table 3.1 Stretching frequencies of imine group in Ni(R-ambch) complexes
Table 3.2 Selected bond lengths (Å) in Ni(ambch) and related complexes
Table 3.3 Selected bond angles (°) for Ni(ambch)and related complexes
Table 3.4 Stretching frequencies of imine group in Cu(R-ambch) complexes
Table 3.5 Selected bond lengths (Å) in Cu(ambch) and related complexes
Table 3.6 Selected bond angles (°) in Cu(ambch) and related complexes
Table 3.7 Selected IR frequencies (cm^{-1}) of starting materials and **158a**

Table 3.8 Selected IR frequencies (cm^{-1}) of Co(ambch)(OAc) and related Co(salen) complexes
Table 3.9 Selected IR frequencies (cm^{-1}) in $VO(acac)_2$ and VO(ambch) complexes
Table 4.1 Reactivity of X-C_6H_4-CHO **184a-d** toward 1,2-diaminocyclohexane
Table 4.2 Reactivity of benzaldehydes **187a-d** toward 1,2-diaminocyclohexane
Table 4.3 Variation of imine protons chemical shift (δ, ppm) in symmetrical and asymmetrical complexes
Table 4.4 Variation of imine protons chemical shift (δ, ppm) in N_3O complexes **198-200**
Table 4.5 Selected bond lengths (Å) in Ni(ambchsal) **198**, Ni(salchsal) **197** and related complexes
Table 4.6 Selected bond angles (°) for Ni(ambchsal)**198**, Ni(salchsal) **197** and related complexes
Table 5.1 Composition of the bromination mixture in time
Table 5.2 Reactivity of benzaldehydes toward 1,2-diaminocyclohexane
Table 5.3 Results obtained using Procedure 1
Table 5.4 Results obtained using Procedure 2
Table 5.5 Results obtained using Procedure 3
Table 5.6 Optimization of the work-up procedure for the first step condensation

Chapter 1. Introduction

1.1 Salen ligands

Salen ligands (**1**) are products of the condensation reaction between a diamine and two moles of salicylaldehyde or its derivatives. Since their metal complexes are readily available and have structural and chemical properties similar to porphyrins, the chemistry of metal-salen complexes has attracted attention of chemists for a long time. However, it was only in mid-80s that metal-salen complexes were tested for their catalytic activity and since then they have been successfully applied in various enantioselective reactions such as epoxidation [**1**], aziridination [**2**], cyclopropanation [**3**], the Diels-Alder [**4**], and Strecker reactions [**5**] and in kinetic resolution of racemic epoxides [**6**].

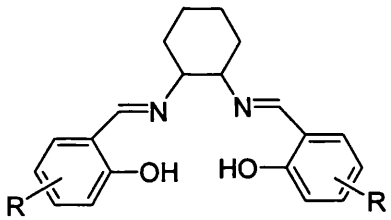

1

Figure 1.1. Salen ligand

1.2 Conformational aspects

Salen ligands are tetradentate double Schiff bases with an N_2O_2 donor atom set. In most complexes salen has a planar co-ordination around the metal (**2a**), with the four donor atoms nearly coplanar. Variations of this type of co-ordination are displayed in structures **2b** and **2c**.

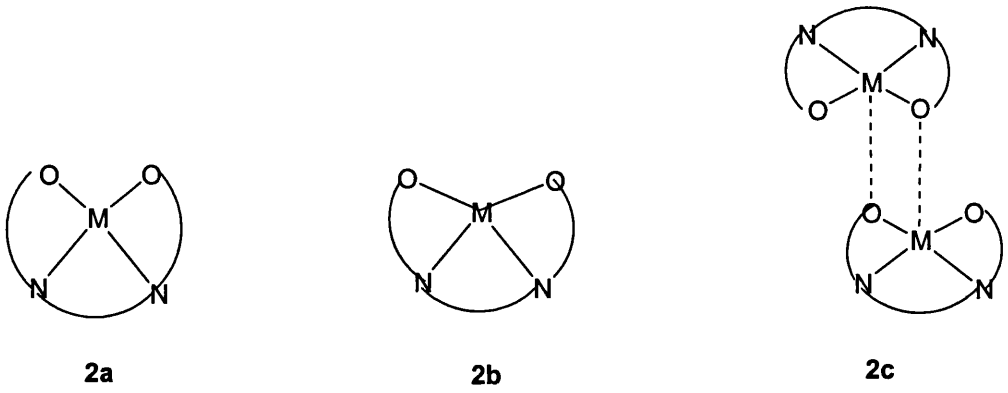

Figure 1.2. Co-ordination modes of salen ligands

In complex **2b** the metal atom is located above the N_2O_2 plane, while in **2c** two molecules of metal salen complex are arranged such that the oxygen atom from one ligand co-ordinates also to the metal atom from a neighbouring molecule generating a dimeric structure. The relative flexibility of these ligands allows distortions of the Schiff base, depending on the metal and/or volume of apical or axial ligands, leading to umbrella or stepped geometries [7].

Salen can also adopt a non-planar co-ordination in which one of its oxygen donors occupies an axial position as in [Co(acac)(salen)] **3** and in $[Co_2(3\text{-MeO-salen})_3]$ **4** [**8, 9**]. In the latter, each cobalt atom has an octahedral geometry in which two salen ligands present a non-planar arrangement and act as tetradentate ligands, while the third salen molecule acts as a bidentate ligand bridging the two cobalt atoms.

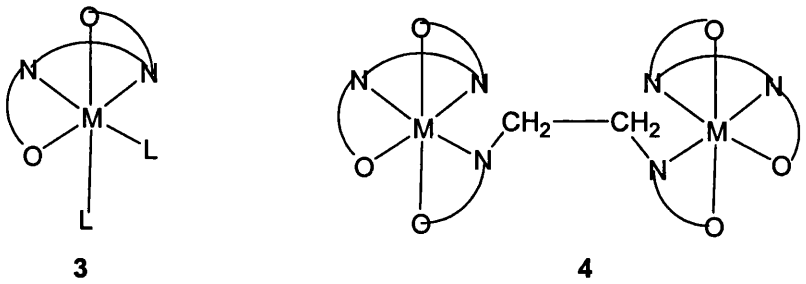

Figure 1.3. Non-planar co-ordination modes

1.3 Chirality of salen complexes

1.3.1 Chiral salen ligands

The chirality of salen ligands is determined by the presence of stereogenic centres either at the diimine bridge as in **5a** or, together with these, of chiral axes at the 3,3'-positions in the aromatic rings as in **6a, 7**.

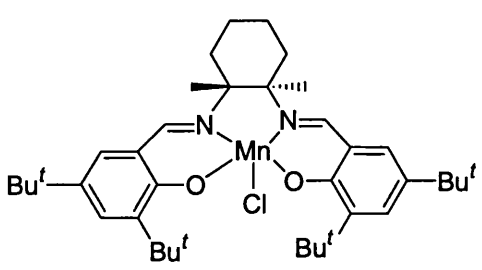

5a

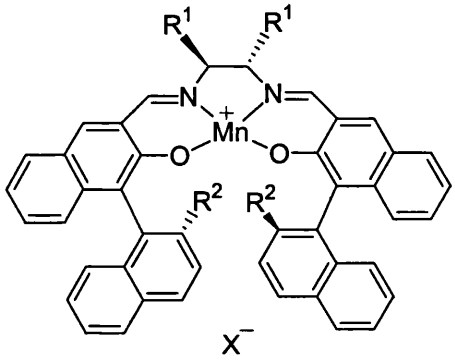

6a : R^1 = 3, 5-$(CH_3)_2$-C_6H_3; or R^1, R^1 = -$(CH_2)_4$-;
R^2 = Ar, X = PF_6 ;
7: R^2 = OCOBu^t, X = Cl

Figure 1.4. Chiral Mn salen complexes

Ligands such as that in **5a** can be easily obtained using chiral diamines in the condensation reaction with salicylaldehyde derivatives [**10**]. Racemic diamines were resolved by treating the mixture of enantiomers with tartaric acid, mandelic acid, camphorsulfonic acid, each of them being commercially available at low cost in optically pure form.

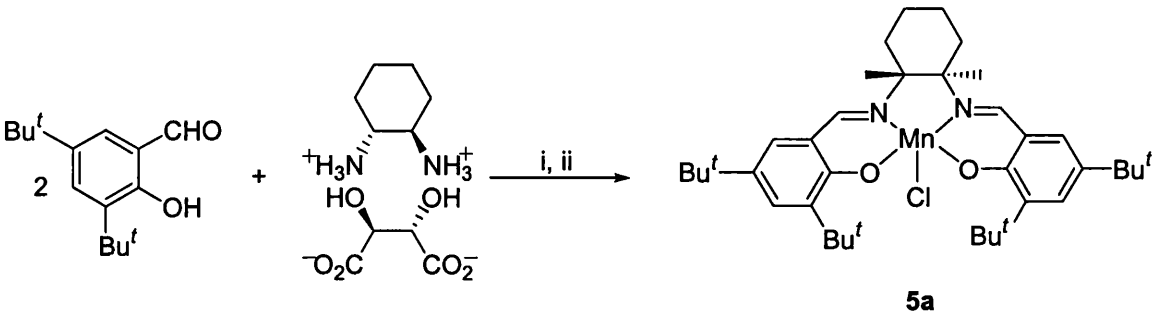

5a

i: K_2CO_3, H_2O-EtOH, 80 °C
ii: $Mn(OAc)_2 \cdot 4\ H_2O$, toluene-ethanol, 80-85 °C, air, NaCl

Scheme 1.1. Synthesis of chiral salen ligands

The synthesis of complex **6a** [**11**] starts with the coupling of Grignard reagent **8** and triflate **9**, followed by protection as a MOM ether. The resulting ether **10** was converted into the aldehyde **11** by the sequence: *ortho*-lithiation, formylation and subsequent deprotection with trimethylsilyl bromide to give **11**. Aldehyde **11** was then converted into manganese complex **6a** by template synthesis.

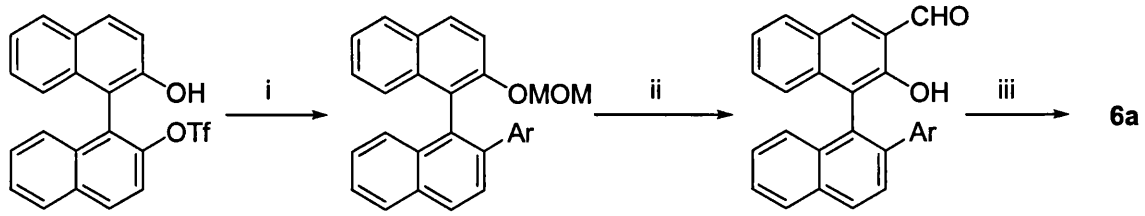

9 **10** **11**

i: 1. ArMgBr **8**, $NiCl_2$(dppe), THF, reflux, 90 % yield; 2. MOMCl, NaH, THF, DMF, 83 % yield
ii: 1. ^{t}BuLi, TMEDA, THF, -78 °C; 2. DMF, -78 °C to rt, 91 % yield; 3. TMSBr, DCM, 0 °C, 95 % yield
iii: 1. $Mn(OAc)_2$, diamine, EtOH, 50 °C, air; 2. $NaPF_6$

Scheme 1.2. Synthesis of a chiral salen complexes **6a** possessing axial chirality

The synthetic route to another chiral aldehyde **14** from bis-MOM-protected BINOL **12**, used in preparation of sterically hindered chiral manganese salen complexes **7**, is summarised in Scheme 1.3 [**12**].

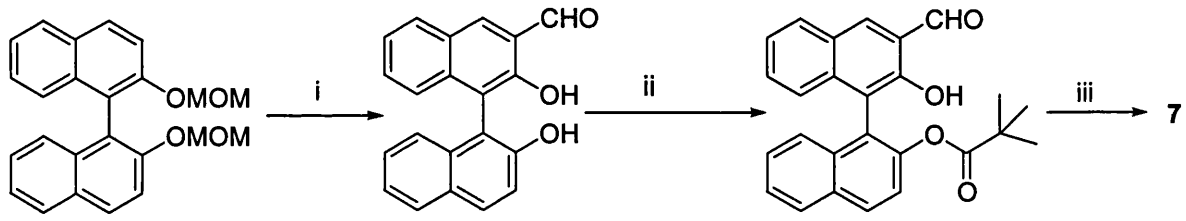

12 **13** **14**

i: 1. t-BuLi, DMF, THF, -78 °C; 2. HCl, EtOH, 65 % yield
ii: NaH, pivaloyl chloride, THF, 89 % yield
iii: 1. diamine, EtOH, reflux; 2. $Mn(OAc)_2$, EtOH, reflux, O_2; 3. LiCl, EtOH

Scheme 1.3. Synthesis of chiral salen complexes **7** possessing axial chirality

1.3.2 Induced Chirality

While chiral manganese salen complexes exist as one conformer due to the regulation of the diamine as described before, the corresponding achiral oxo complex exists as a mixture of two enantiomeric conformers in equilibrium (**15a**, **15b**). Conformer **15a** in

which the R groups take a sterically favourable pseudo-equatorial orientation is more stable, the diaxial conformer (**15b**) being destabilised by steric repulsion between R groups and the axial ligands (oxo and the donor ligand).

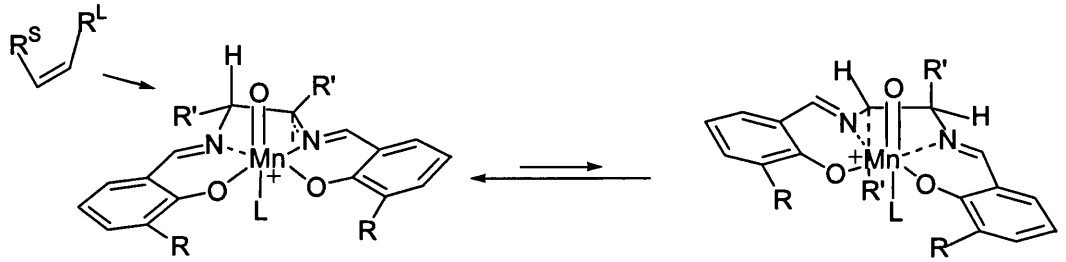

15a **15b**

Figure 1.5. Equilibrium of enantiomers in non-chiral salen complexes

Katsuki observed that by shifting this equilibrium, an achiral catalyst (**16a**) could act as a chiral one. He showed that this equilibrium changed when an apical chiral ligand was co-ordinated to an achiral salen complex. Asymmetric epoxidation of 6-acetamido-2,2-dimethyl-7-nitro-2H-chromene [**13a**] in the presence of (–)-sparteine (**17a**) as a chiral ligand gave the corresponding epoxide with 73 % enantioselectivity. Even better results (82 % ee) were obtained [**13b**] on this substrate with (+)-bipyridine *N,N'*-dioxide **17b**.

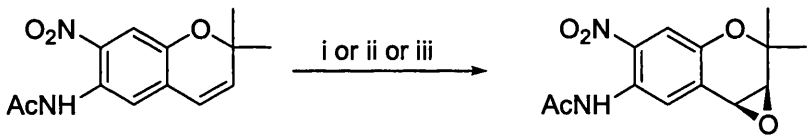

i: PhIO, -20 °C, DCM, (+)-ligand — 73 % ee with **16a** and **17a**; 82 % ee with **16a** and **17b**

ii: PhIO, — 99 % ee with **19**

iii: NaOCl — 99 % ee with **6a**

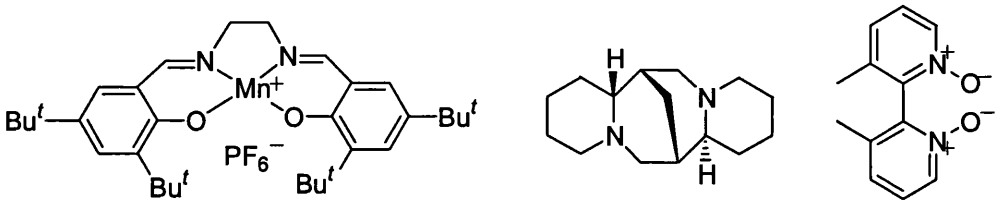

16a **17a** **17b**

Scheme 1.4. Epoxidation of substituted chromenes catalysed by non-chiral Mn(salen) complex **16a** or chiral complexes **19** and **6a** as catalysts

Another way of regulating the conformation of the achiral ligand involves the use of an ethylenediamine backbone that contains co-ordinating groups R (*e.g.* carboxylate in **19**)

[14]. The axially oriented group coordinates to the metal and will determine an inversion in ligand conformation to the axial, axial conformer. Due to this, olefins approach the M=O bond in complex **18** from the opposite side compared with that in **6a**.

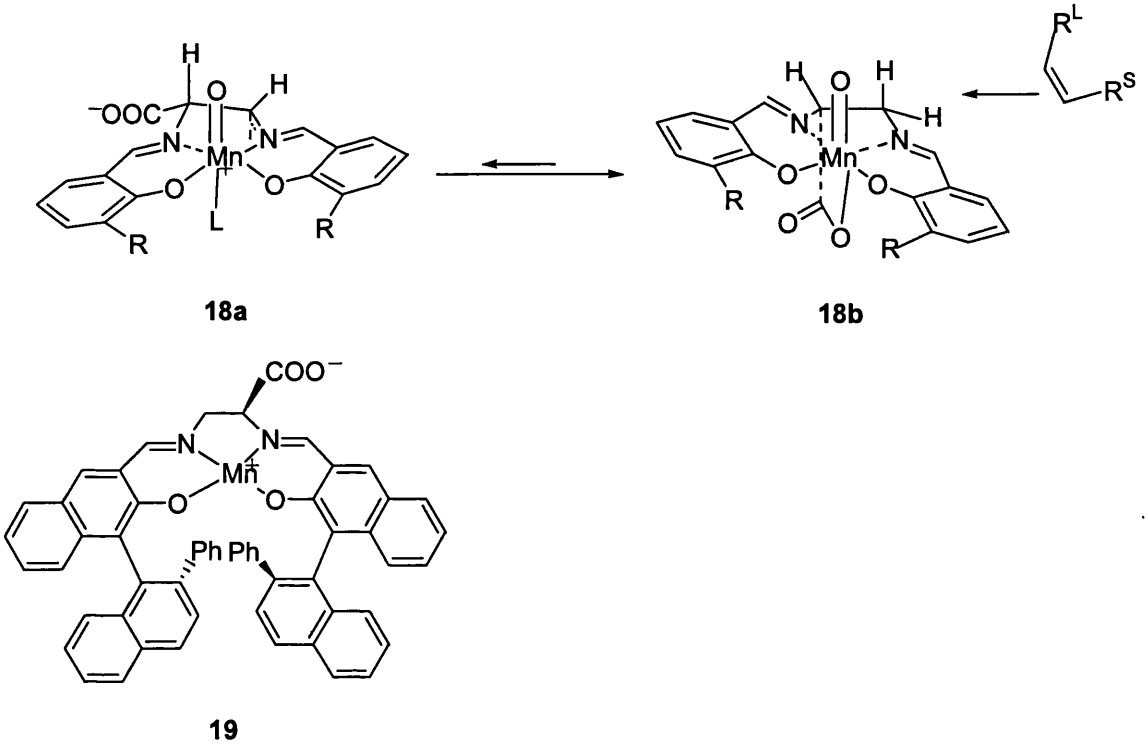

Figure 1.6. Chiral salen complexes with induced **19** or axial chirality **6a**

Ligands with the C_2-symmetry were not employed in this case as the second R group would intercept the approaching olefin. Accordingly, an unsymmetrical monosubstituted diamine was chosen. Asymmetric epoxidation of 2,2-dimethyl-chromenes with the catalyst **19** having a monocarboxylate group on the ethylenediamine moiety and 2'-phenylnaphthyl groups as bulky C-3, C-3' substituents provided the corresponding epoxides in high yield and with high enantioselectivity (Scheme 1.4). The reaction occurred in the absence of a donor ligand and required only a small amount of catalyst (2 mol % or less). Another synthetic advantage was the high turn-over number (9200) achieved.

1.4 Applications of salen complexes in asymmetric synthesis

In the following, several processes which employ salen complexes are presented, the selection of these examples aims to emphasize how careful catalytic system design led to significant discoveries in the asymmetric synthesis. The examples were chosen among those using metal salen complexes related to the amben complexes synthesized in Chapter 3 of this thesis and are organised by the catalytic process developed.

1.4.1 Epoxidation

Epoxides are versatile intermediates for organic synthesis. Nucleophilic ring-opening of epoxides is a regio and stereospecific reaction that allows the control of one or two stereogenic centres in a synthetic scheme. As a result, a lot of work has been concentrated on developing catalysts able to provide routes toward such compounds. In 1986 Kochi et al. reported [**15**] that the cationic [Mn(III)(salen)] complexes **16** were catalysts for epoxidation of simple olefins and proposed that the epoxidation proceeds through an oxo(salen)manganese (V) complex (Scheme 1.5).

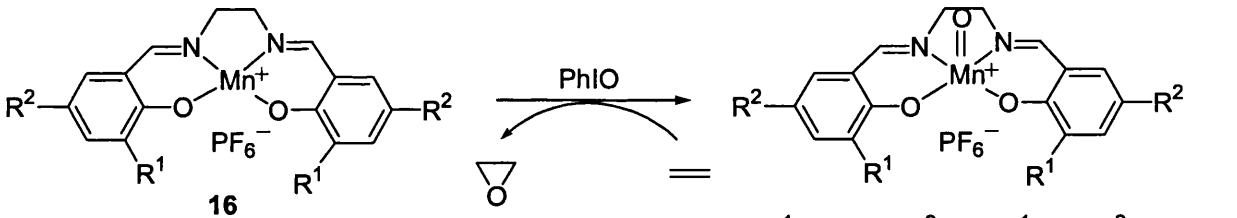

Scheme 1.5. Kochi's epoxidation of olefins

Following this work, Jacobsen and Katsuki independently reported manganese salen catalysed asymmetric epoxidation of unfunctionalized olefins using complexes **5** and **20** as catalysts.[**16, 17**]

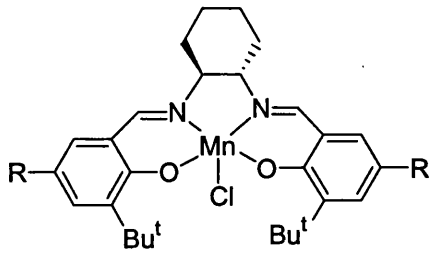

5 a-d

R = ^{t}Bu, H, (^{i}Pr)$_3$SiO, MeO

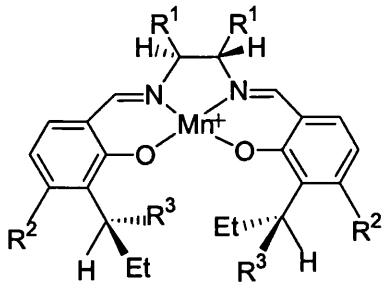

20

a. R^1 = Ph, R^2 = H, R^3= Ph

b. R^1, R^1= -$(CH_2)_4$-, R^2 = CH_3, R^3 = ^{t}Bu-C_6H_4-

Figure 1.7. Jacobsen's and Katsuki's (first generation) epoxidation catalysts

While in complex **5** the chiral co-ordination sphere around the metal is determined by the asymmetric carbons at the ethylene diamine bridge, complex **20** has asymmetric centres both here and in the aromatic rings. These complexes show a good level of enantiomeric excess in epoxidation of conjugated *cis*-di- and trisubstituted olefins using iodosylbenzene [**15**] and sodium hypochlorite [**18, 19**] as a stoichiometric oxidant.

Two structural properties of the ligand are important in order to attain good enantioselectivities in epoxidation of alkenes by manganese salen complexes, namely: a non-symmetric diimine bridge obtained from a C_2-symmetric diamine and bulky substituents in 3,3' positions of the salicylidene site. Similar enantioselectivities were found for catalysts derived from 1,2-diphenylethane and 1,2-cyclohexane diamine. The substituents in the 5,5'-positions influence the selectivity, but they are less important compared with the elements presented above. In general, electron-donating and sterically demanding groups increase the enantioselectivity, while electron-withdrawing groups have the opposite effect.

The increase of enantioselectivity in the mentioned complexes has been explained by alkene approach to the reaction centre *via* pathway **a** or **b**, with the bulky olefinic substituent away from the groups in 3, 3', while the other competing ways are blocked. In this way the stereochemical communication between the catalyst and the substrate is maximised [**20**].

Although they have not been isolated, high valent [Mn(O)(salen)] complexes **21-22** are considered to be the active species involved in Jacobsen-Katsuki epoxidation of olefins.

Jacobsen's opinion [**16a**] is that complex **21** is planar, similar with Mn(III)salen complexes which are planar as found from X-ray studies. This implies that alkenes are approaching complex **21** from upside (path **a**) to avoid steric repulsion with the 5'-*tert*-butyl group.

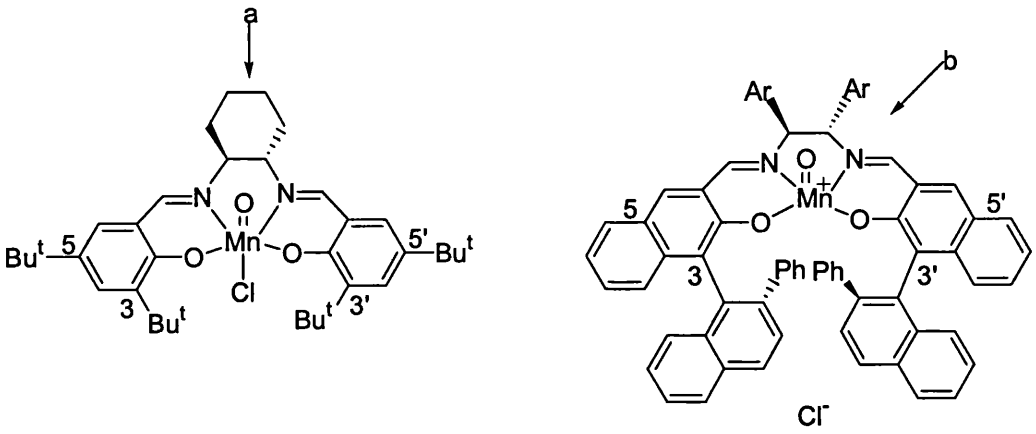

21 **22**: Ar = 3,5-$Me_2C_6H_3$

Figure 1.8. Olefin approach to the reaction centre in epoxidation using **21** and **22**

Katsuki considers [**21**] that [Mn(O)(salen)(Cl)] complexes like **22** have a non-planar conformation of the ligand in analogy with oxo(salen)chromium(V) complexes[**22**]. In addition to this, the bond Mn–O_{equat} becomes shorter with the increase of manganese oxidation state and amplifies the non-planarity of the ligand. He suggested that salen ligands of oxo(salen)-Mn(V) complexes take a non-planar stepped conformation, olefins approaching complex **22** over its downward benzene ring (path **b**). Due to the ligand conformation the 5'-substituent will not disturb this approach, while that in position 5 effectively blocks the undesired path.

Electronic effects of the substituents from the 5,5'- positions on the enantioselectivity are subtle, but have a direct influence on the reactivity of the metal oxo intermediates [**23**]. Electron-withdrawing groups destabilise the oxo manganese intermediate, making it a more reactive oxidant compared to intermediates substituted with electron-donating groups. According to Hammond postulate, the more reactive oxidants effect epoxidation *via* a more reactant-like transition state, with greater separation between substrate and catalyst and therefore poorer steric differentiation of diastereomeric intermediate

structures. A milder oxidant will effect epoxidation *via* a more product-like transition state.

For substrates that undergo the reaction sluggishly it was found that addition of pyridine N-oxide derivatives **23** improves the catalyst turnovers and enantioselectivities. Although the mechanism of the axial donor ligand action is not clear, its role is considered to be multifold. It causes not only conformational change of 3,3'-substituents of salen ligand and change in the geometry of oxo-Mn(salen), but also reduces the reactivity of metal-oxo species and destabilises the undesired diaxial conformation.

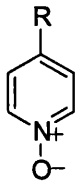

23: R=Ph, NMe_2, ^tBu

Figure 1.9. Axial donor ligands

Enantioselectivities were further improved during the second generation of catalysts designed by Katsuki [**24**], for example in complexes **6b**, in which the bulky substituents from the 3,3' positions having a $C(sp^3)$ were replaced with $C(sp^2)$ substituents (*e.g.* binaphthyl subunit substituted with phenyl groups).

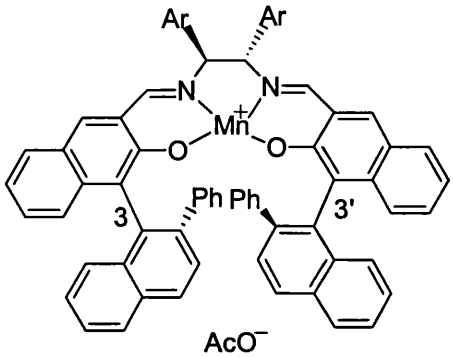

6b: Ar = 3,5-$Me_2C_6H_3$

Figure 1.10. Katsuki's Mn (salen) catalyst from the second generation

This is the result of protrusion of the phenyl groups in complexes **6b** towards the reaction centre, thus increasing the steric and Coulombic repulsions between the ligand and the olefin.

X-ray analyses of diastereomeric manganese complexes **6c** and **6d** revealed that they have considerably different ligand conformations [**25**]. The conformation of the basal salen ligand is determined by several factors, not only by the conformation of the five membered chelate ring formed by manganese ion, two nitrogen and two carbon atoms from the diimine bridge. An important role is played by the interaction between the 2"-phenyl naphthyl group and the apical ligand at the manganese ion that could be a molecule of water or alcohol. This is an attractive OH-π interaction and manifests itself in the same way in both diastereomers. However, the effect of the mentioned interaction can reinforce the effect caused by the chelate ring formation (as in complex **6d**) or the two effects tend to cancel each other (as in complex **6c**) leading to different ligand conformations. Thus, complex **6d** adopts a deeply folded stepped conformation, while complex **6c** takes a slightly folded one.

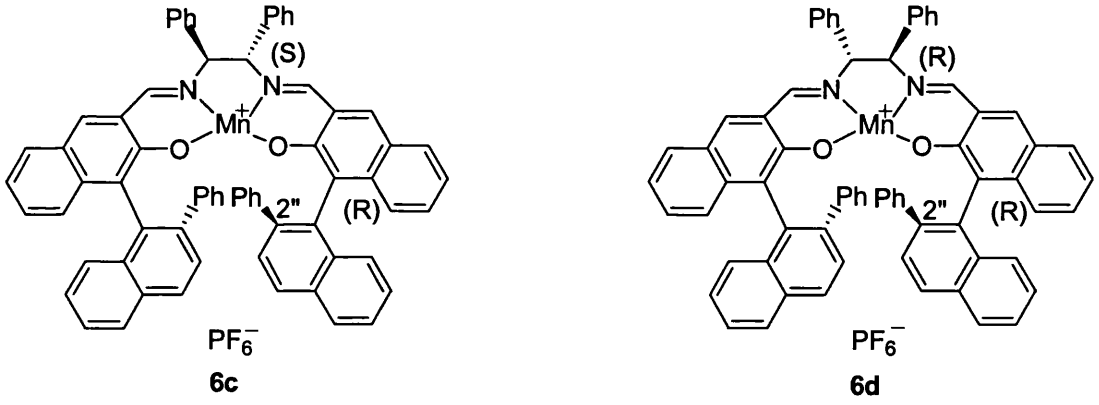

Figure 1.11. Diastereomeric Mn(salen) complexes **6c** and **6d**

These data imply that introduction of an apical ligand which cannot interact attractively with the 2"-phenyl ring reduces the folding in **6d** and increases it in **6c**. Therefore, the ligand conformation in manganese salen complexes can be modulated by the choice of the apical ligand and together with it the catalyst performance.

Manganese salen complexes like **5** did not show high enough enantioselectivity in epoxidation of *trans*-olefins, probably due to the interaction between one olefinic substituent and the salen ligand which destabilise the desired orientation of the substrate (Figure 1.12).

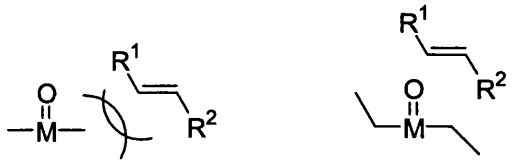

Figure 1.12. *trans*-Olefin approaching planar and folded salen complexes

Using catalyst **24** possessing stereogenic centres only at 3,3'- positions, *trans*-stilbene was epoxidized with 61% ee. This result demonstrates that stereochemical elements at the 3,3'- positions have little influence in the case of *cis*-olefins, but they are the dominant factors in the epoxidation of *trans*-olefins [**26**]. Later, Katsuki revealed [**27**] that manganese salen complexes such as **25a** are efficient catalysts for epoxidation of *trans*-olefins due to the deeply folded conformation of the ligand in the corresponding oxo-Mn(salen) (Scheme 1.6).

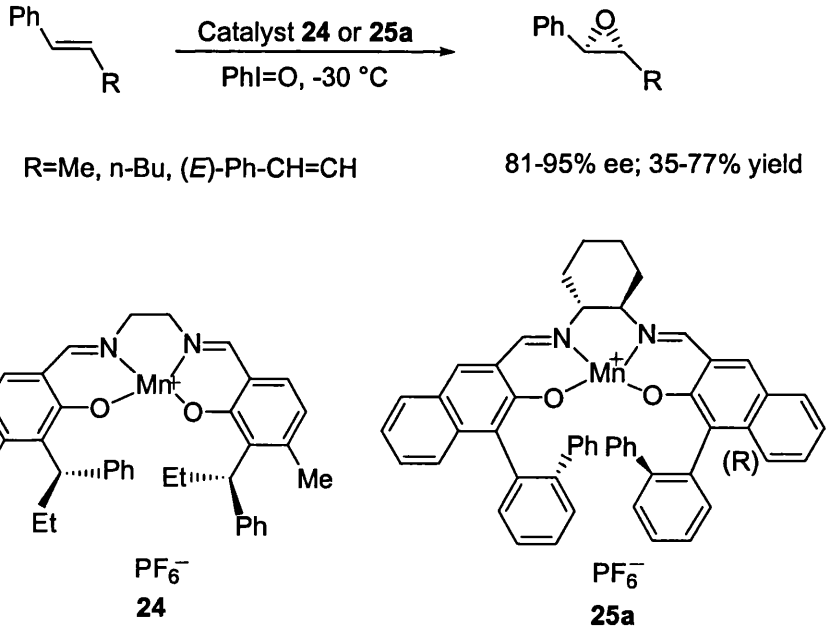

Scheme 1.6. Epoxidation of *trans*-olefins

It was also shown that manganese complex **26** bearing electron-withdrawing groups is a good catalyst for epoxidation of *trans*-β-methyl-styrene [**28**]. The ligand of this complex lacks the bulky groups in 3, 3'-positions, but the binaphthyl diamine unit induces the non-planar conformation of the ligand.

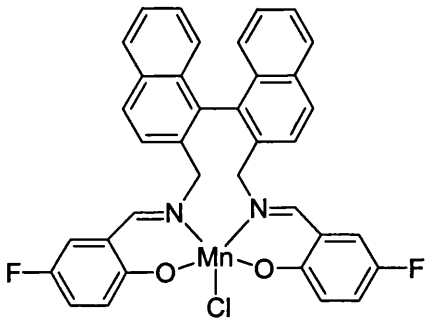

26

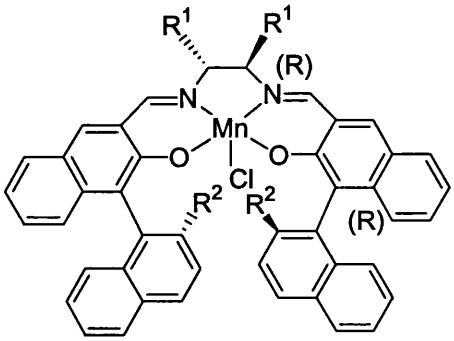

7: R^1 = Ph, -$(CH_2)_4$-; R^2 = -$COOBu^t$

Figure 1.13. Mn(salen) catalysts possessing axial chirality

Recently, syntheses of complexes **7** has been reported [**12**] which were found to be efficient catalysts (ee up to 99 %) for the epoxidation of *cis*-disubstituted alkenes in the presence of NaOCl. These complexes are more easily prepared than **6**, and the presence of polar ester groups in the catalyst facilitates the transfer of the oxidant between the phases in the biphasic reaction system leading to higher turnovers of the catalyst.

Epoxidation of unfunctionalized alkenes with NaOCl and *m*-CPBA[**29**] using Mn(III)(salen)complexes **27** obtained from the (*S,S*) diamines and di-*tert*-butyl-salicylaldehyde proceeded with moderate enantioselectivity (up to 69 %). The reversed asymmetric induction found with **27** was attributed to the participation of diaxial conformer of the catalyst. Due to the presence of the second axial ligand, enantioselectivities were not good. The yield and enantioselectivity of the reaction depend on the R group in the diamine, with higher levels being obtained for benzyl group.

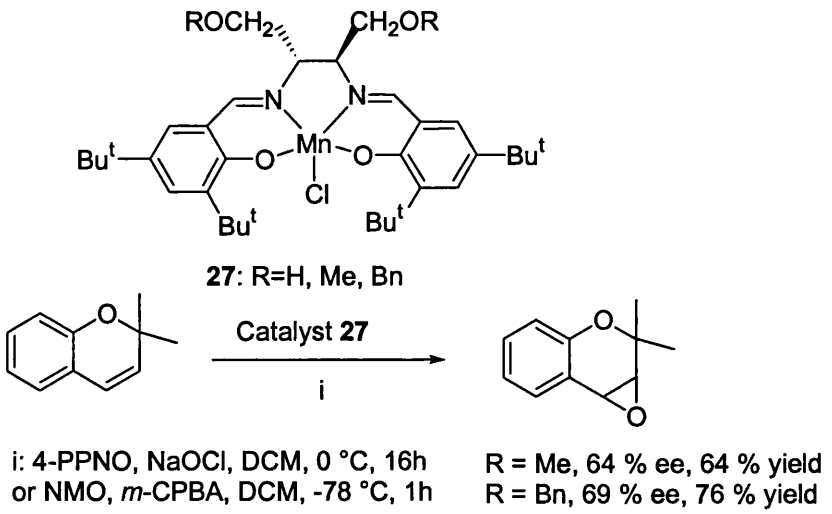

Scheme 1.7. Mosset's epoxidation procedure

Higher asymmetric induction was obtained in epoxidation of *trans*-β-methylstyrene than for the *cis*- isomer with Cr(III)(salen) complex **28** in the presence of triphenylphosphine oxide as an axial ligand [**30**]. These different results compared to those obtained with Mn(III)(salen) and Mn(III)(porphyrin) complexes were explained by the twisting of the salen complex (Scheme 1.8) which allows for a better interaction with the *trans*-olefin.

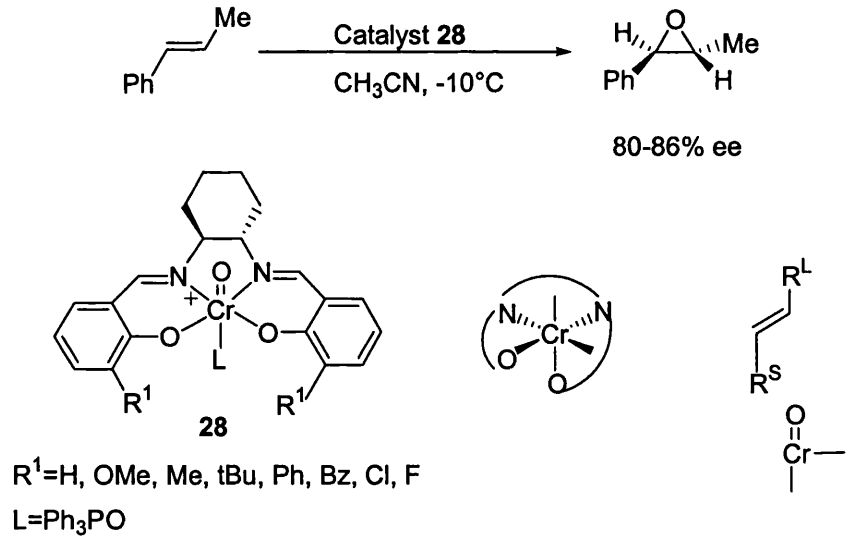

Scheme 1.8. Gilheany's epoxidation of *trans*-olefins

It was also observed that Cr(salen) catalysts do not require bulky groups in 3,3'-positions as Mn(salen) complexes. All the former complexes substituted with different R^1 groups (R^1 = H, Me, ^{t}Bu, Ph, Bz, Cl, F) except methoxy derivatives, in the presence of the suitable axial donor ligand gave enantiomeric excess higher than 80 %.

Apart from terminal oxidants previously mentioned (iodosylbenzene, sodium hypochlorite and *m*-CPBA), epoxidation of olefins was also performed with molecular oxygen in the presence of pivalaldehyde and salen complex **5e** [31], however, the results obtained poorer than those obtained with NaOCl.

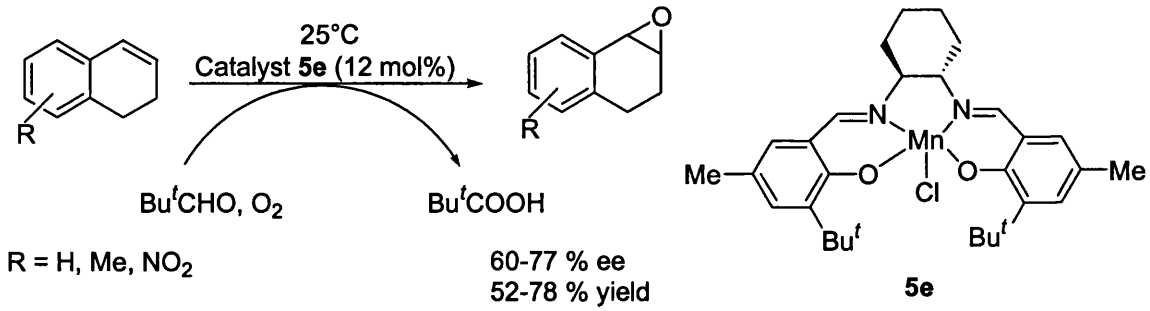

Scheme 1.9. Epoxidation of olefins with molecular oxygen

Highly regioselective alkene epoxidation with molecular oxygen was achieved [32] using Co(II) Schiff base complexes **29** and a range of neutral axial donor ligands (*e.g.* pyridine, DMF, aliphatic aldehydes and ketoesters). The reaction occurred without affecting other groups (carbonyl, ester, hydroxy) in the substrate and when more double bonds were present, the ring double bond was epoxidized exclusively. The product distribution depended on the employed carbonyl compound.

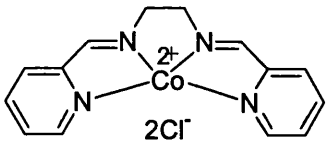

29

Figure 1.14. CoN_4 catalyst used in epoxidation with molecular oxygen

The latter helps in the formation of the cobalt(III)-dioxygen complex and subsequently acts as a reducing agent during oxygen atom transfer to the organic substrate.

1.4.2 Aziridination

Aziridines are nitrogen equivalents of epoxides and are useful building blocks in synthesis of compounds containing nitrogen functionalities. Enantioselective

aziridination can be achieved either by transfer of a nitrene group to an olefin or by reaction between diazoesters and imines. In this section only aziridination *via* imido transfer to alkenes in the presence of metal salen complexes is presented. The analogy of aziridination with the epoxidation and cyclopropanation reactions determined the research in the area to evolve from the catalysts previously designed for these two asymmetric processes.

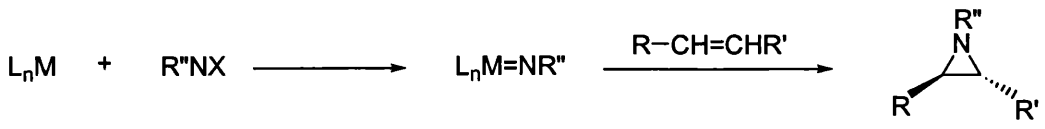

Scheme 1.10. Metal-catalysed aziridination of olefins

1.4.2.1 Aziridination with epoxidation type catalysts

Early reports on aziridination of olefins using PhI=NTs and complexes **30, 20a, 20c [33, 34]** provided aziridines only in low yields and with poor enantioselectivities.

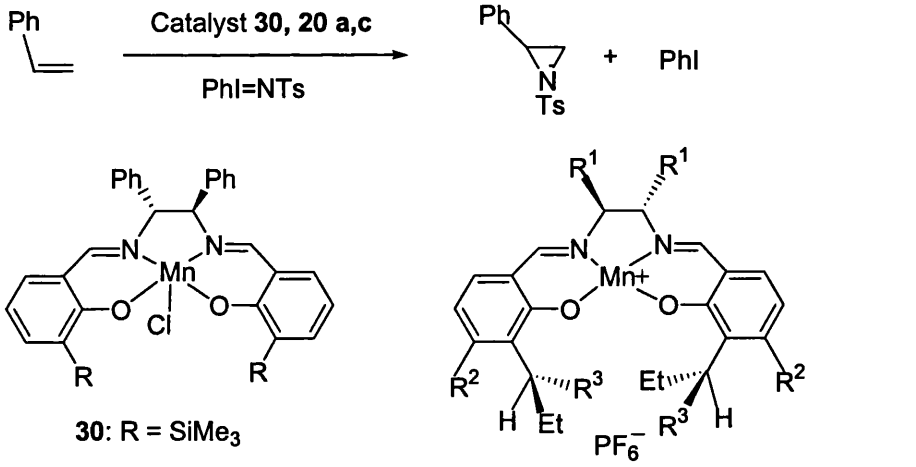

Scheme 1.11. First reports of the aziridination of olefins using salen complexes

These results compared with those reported for epoxidation were ascribed to the difference between the structure of the intermediates, namely the presence of a *p*-toluenesulfonyl group at the metal nitrenoid, while the metal oxenoid has no substituent at the oxygen atom. Katsuki suggested that in catalyst **31** the *p*-toluenesulfonyl group is

likely to occupy the open space between the substituent at C8' of the diimine bridge and the aromatic ring (Figure 1.15) thus blocking olefin approach from that direction and at the same time reducing the yield of the reaction.

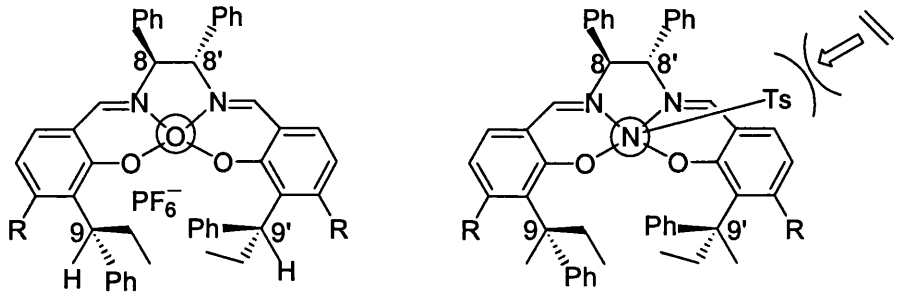

Figure 1.15. Olefin approach to the reaction centre in epoxidation *cf.* aziridination

If the *N*-tolylsulfonyl group leans toward C8 or C9' substituents (Figure 1.16), the olefin can approach the metal-nitrene bond following path a or path b. This implies that the enantioselectivity of the reaction will depend on the steric repulsion between the two respective groups of C8 (or C9') substituent, *N*-tolylsulfonyl group and the olefinic substituents. Based on this model it was predicted that asymmetric induction would be improved by tuning the C8 and C9' substituents.

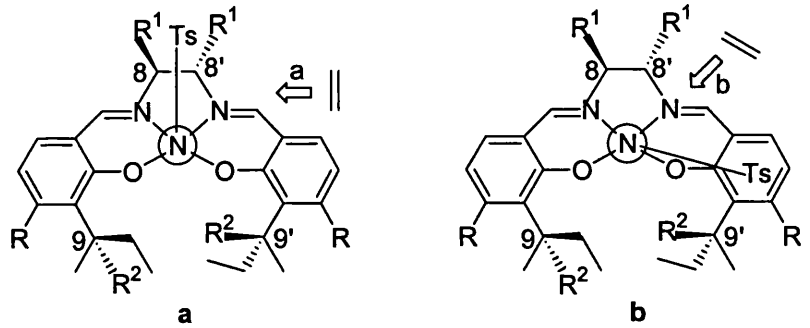

Figure 1.16. Possible orientations of *N*-tolylsulfonyl group and the olefin approach

Reducing the bulkiness of the substituents (R^1) from the diamine bridge (*i.e.* phenyl was replaced by CH_3 or H) led to the discovery of catalyst **20c** [**34**] which showed moderate enantioselectivity (61 %), but again low chemical yield (9 %).

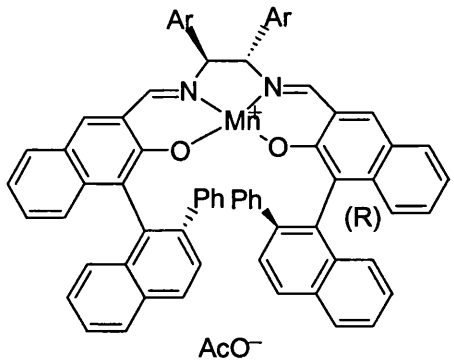

Ar = 3, 5-$(CH_3)_2$-C_6H_3

6b

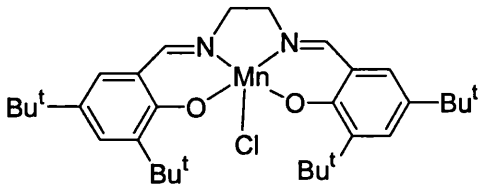

16a

Figure 1.17. Epoxidation Mn(salen) catalysts of different reactivity

Epoxidation studies using complex **6b** have shown that the reaction is two or three times faster than the one employing complex **16a** and prompted the authors to examine aziridination of styrene with catalyst **6b**. This led to a significant improvement in the yield (60 %), but the enantioselectivity was diminished (8 % ee). Later the R^1 substituents at the bridge were replaced by methyl groups and the R^2 substituents were tuned to find the optimum bulkiness for this side of the catalyst. Among the complexes tested, catalyst **25b** gave the best results (70-75 % yields, 80-94 % ee) for the aziridination of styrene and its derivatives, however, the reaction did not give good results for other substrates [35].

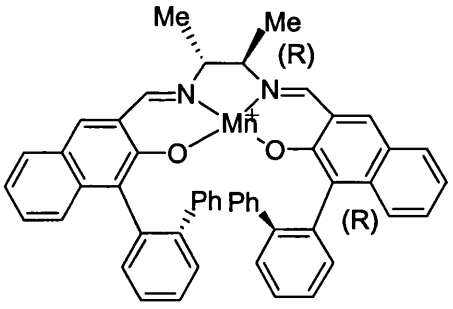

25b

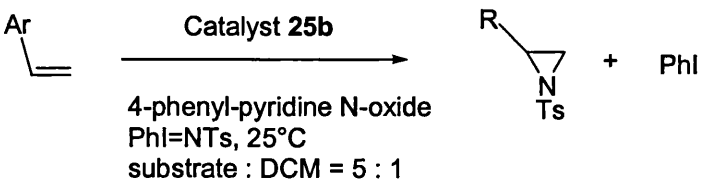

Substrate	Yield (%)	ee (%)
styrene	76	94
4-chloro-styrene	70	86
4-methyl-styrene	75	81

Scheme 1.12. Katsuki's aziridination protocol

For stoichiometric imido transfer reactions to alkenes the manganese nitrido complex **32**, was employed by Carreira and co-workers [**36**] in amination of silyl enol ethers and glycals (Scheme 1.13), reaction proceeding in good yield of racemic synthetically useful products. Although not isolated, it is believed that aziridine intermediates are involved in these reactions.

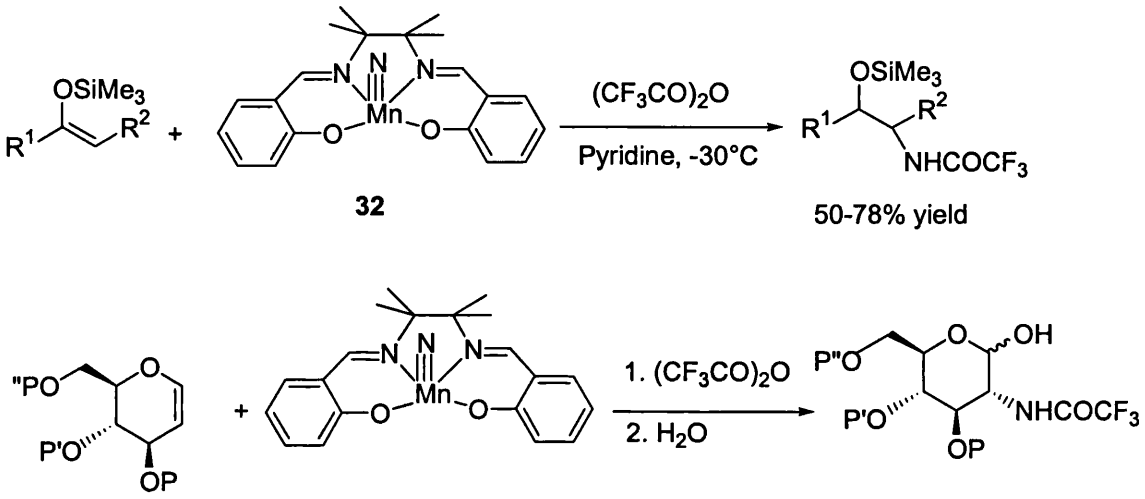

Scheme 1.13. Carreira's amination reactions using complex **32**

Chiral analogues were studied by Komatsu [**37**] who reported the asymmetric aziridination of certain *trans*-styrene derivatives with complex **33** to give aziridines in good yields (53-78 %) and with excellent enantioselectivity. Additives play an important role in this reaction, *p*-toluenesulfonic anhydride (Ts_2O) was the most effective reagent in the activation of the catalyst and the use of pyridine N-oxide was necessary to obtain high enantioselectivities (85-94 % ee for *trans*-styrenes). An alternative procedure for this reaction, involving cheaper alkyl sulfonyl chlorides and $AgClO_4$ as additives, was later developed [**38**]. It gave promising results (50-70 % yields, 83-93 % ee) for *trans*-substituted styrenes, while lower enantioselectivity was obtained for styrene.

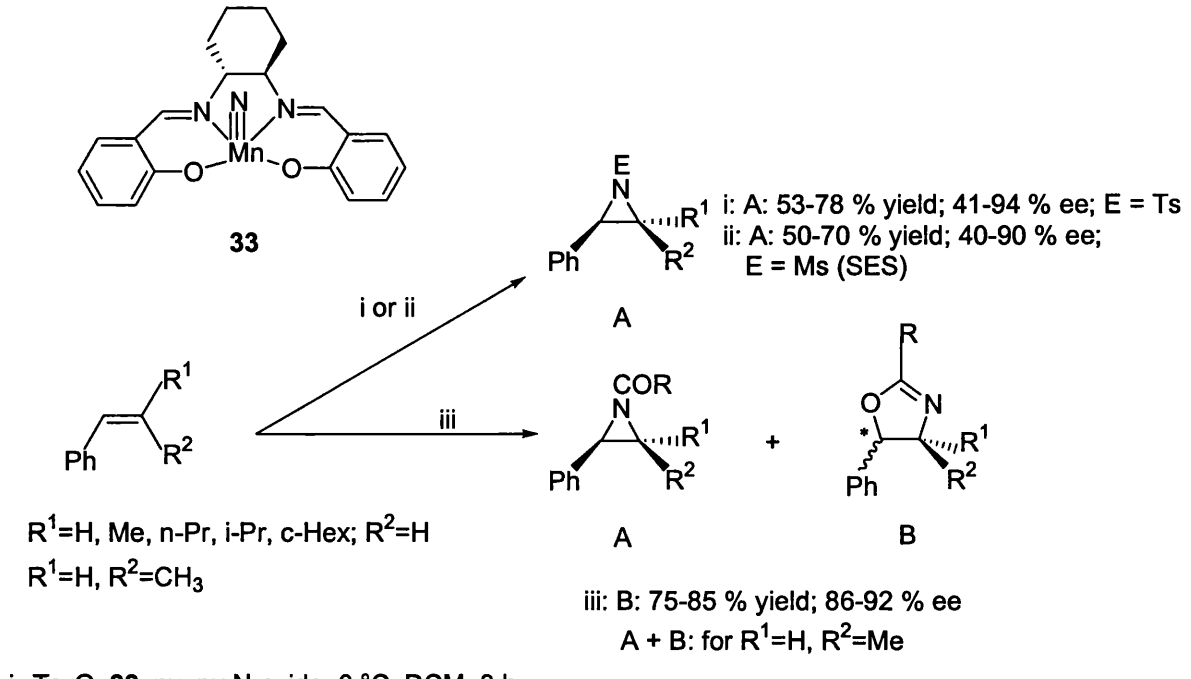

i: Ts_2O, **33**, py, py N-oxide, 0 °C, DCM, 3 h
ii: MsCl (SESCl), **33**, py, py N-oxide, $AgClO_4$, 0 °C, DCM, 18 h (9 h)
iii: RCOCl, **33**, py N-oxide, $AgBF_4$, DCM, 0 °C, 24-48 h

Scheme 1.14. Formation of aziridines and oxazolines catalysed by complex **33**

Performing the reaction in the presence of an acyl chloride as activator, alkenes could be converted into 2-oxazolines and/or *N*-acylaziridines [**38, 39**]. The former are highly versatile heterocycles which are present in a variety of biologically active compounds and also find applications as chiral ligands for asymmetric synthesis.

The reaction of *trans*-substituted styrene derivatives led to *trans*-2-oxazolines stereoselectively in good yields (75-85 %) with high enantioselectivity (86 %). c*is*-β-Methyl styrene treated under the same conditions gave a mixture of *cis*- and *trans*-oxazolines together with important amounts of *cis*-aziridines. The mechanism proposed for this transformation involves formation of imido complex **34** upon reaction of acyl chlorides with **33** in the presence of $AgBF_4$, followed by nitrene transfer to the alkene giving the aziridine products which isomerize to oxazoline in the presence of a Lewis acid (Mn(III)salen complex or $AgBF_4$).

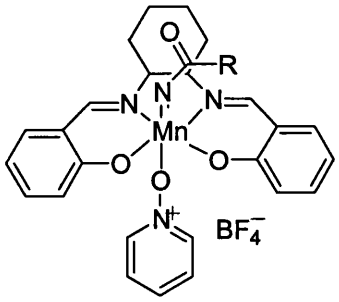

34

Figure 1.18. Active species involved in synthesis of oxazolines

Complex **1.47** was further employed for aziridination of a range of unfunctionalized 1,3-dienes [**40**]. Aziridination procedeed selectively *via* a [2+1] type addition, with no detectable formation of the [4+1] addition product or of the bis-aziridinated product.

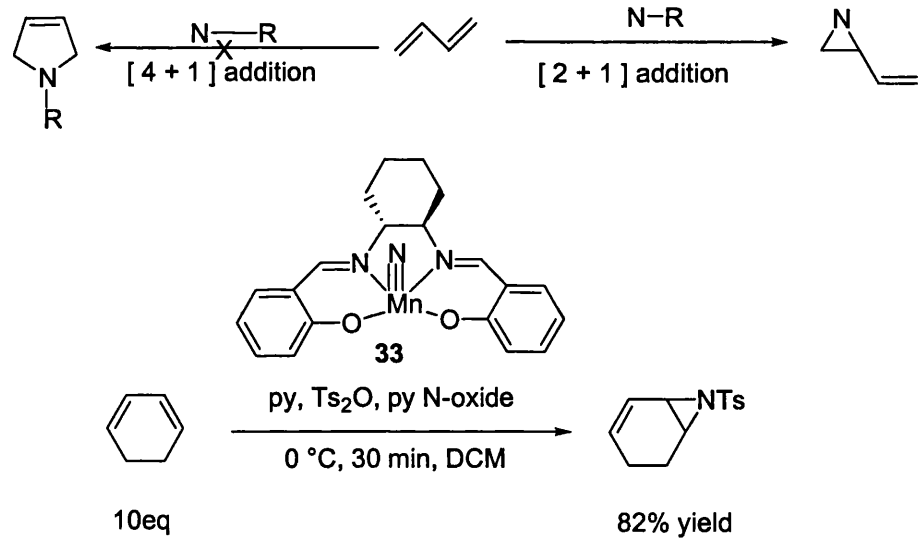

Scheme 1.15. Aziridination of dienes catalysed by **33**

Recently Ho and co-workers have investigated the activation of manganese nitrido complexes by Brønsted and Lewis acids towards the aziridination of styrene, α and β-methyl-styrene[**41**] and reported good to high yields (72-92 %) using achiral catalyst **35a** and trifluoroacetic acid. Chiral catalysts **35b** and **35c** gave similar yields in aziridination of styrene (35 %), but a high enantioselectivity (81 % ee) was obtained only with **35c**, while the use of catalyst **35d** resulted in very low yields (7 %). Good asymmetric induction (91 % ee) was also obtained with **35c** for *trans*-β-methyl-styrene with low yields. The high enantioselectivity obtained with complex **35c** compared to

that obtained with **35b** suggested the formation in this transformation of a less bulky (salen)Mn=NH reactive intermediate.

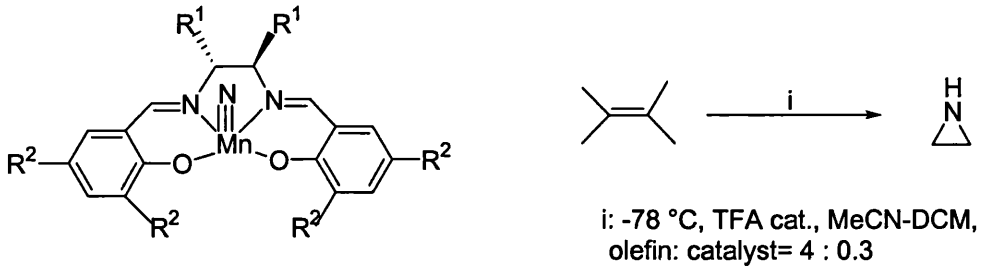

35a: $R^1 = R^2 = H$; **35b**: $R^1 = -(CH_2)_4-$; $R^2 = H$;
35c: $R^1 = -(CH_2)_4-$, $R^2 = {}^tBu$; **35d**: $R^1 = Ph$, $R^2 = {}^tBu$

Scheme 1.16. Aziridination of olefins with nitrido complexes **35a-d**

1.4.2.2 Aziridination with cyclopropanation type catalysts

In early 1990's Evans discovered that low valent metal ions used for cyclopropanation, were also good catalysts for aziridination of olefins with PhI=NTs [**42**]. Copper (I) and copper(II) salts proved to be effective catalysts for the preparation of a wide range of racemic aziridines.

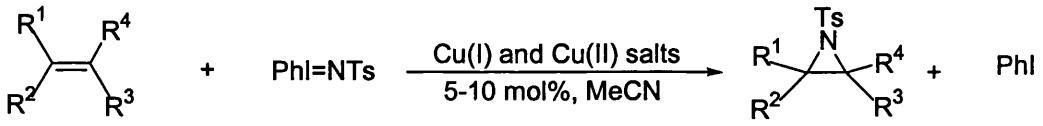

a. $R^1 = R^3 = R^4 = H$, $R^2 = Ar$; 78 - 90 % yield
b. $R^1 = Me$, $R^2 = Ar$, $R^3 = R^4 = H$; 78 % yield
c. $R^1 = R^3 = H$, $R^2 = Ph$, $R^4 = CO_2Me$; 75 % yield
d. $R^1 = R^4 = H$, R^2, $R^3 = -(CH_2)_4-$; 77 % yield

Scheme 1.17. Evan's aziridination of olefins with Cu salts

Inspired by this report, Jacobsen designed his own catalytic system involving CuOTf or $CuPF_6$ and ligand **36** [**43**]. Although high levels of enantioselectivity were observed for alkenes with a variety of substitution patterns (Scheme 1.18), the reaction required the presence in the substrate of at least one aromatic group conjugated to the alkene [**44**].

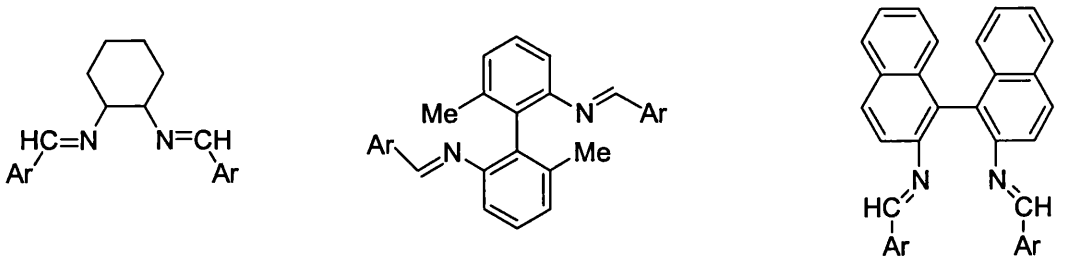

36 **37** **38**

Ar = 2,6-dichloro-benzene

Figure 1.19. Chiral ligands used in aziridination of olefins

Later Scott[**45**] and Shi[**46**] independently investigated aziridination of cinnamate esters with different copper (I) salts and similar diimine ligands **37-38.**

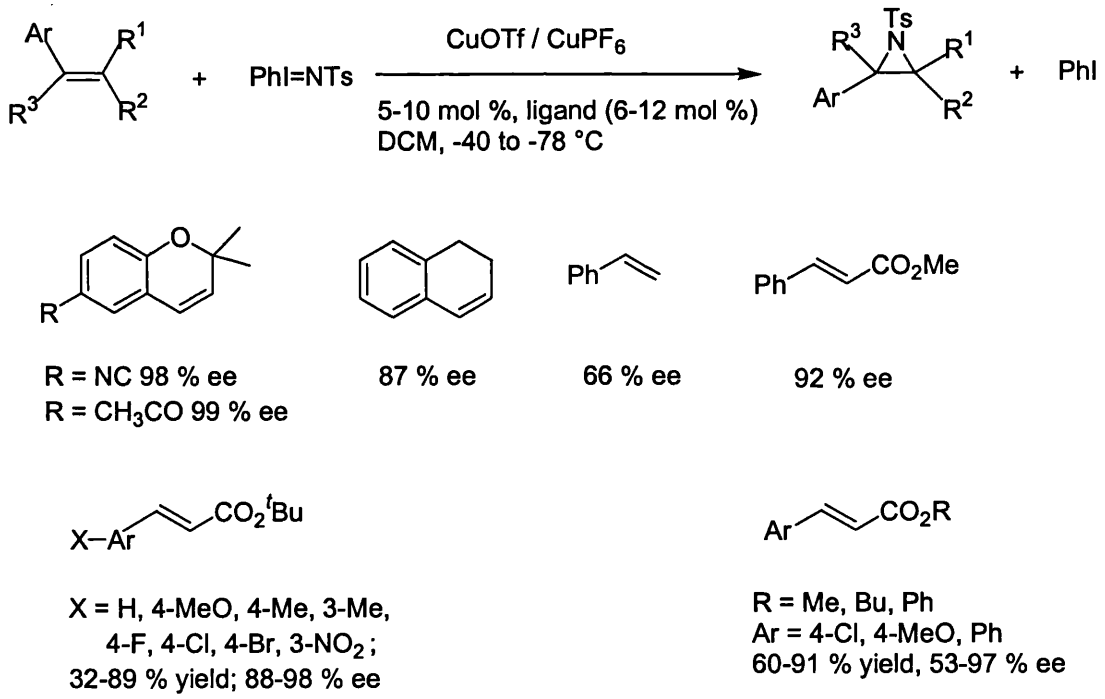

Scheme 1.18. Aziridination of olefins using chiral Cu(I)salen complexes

1.4.3 Cyclopropanation

Metal-salen complexes are useful catalysts not only for oxo and nitrene transfer, but also for carbene transfer. While in asymmetric epoxidation and aziridination the main stereochemical issue is the differentiation of the enantiotopic faces of double bonds, in

cyclopropanation together with this is another stereochemical issue, *cis-trans* selectivity, imposed by the presence of a substituent at the carbenoid carbon. Accordingly, simultaneous control of these two stereochemical problems is necessary for achieving highly efficient cyclopropanation.

In 1978 Nakamura reported cyclopropanation using a chiral Co(II) salen complex as catalyst, although with low enatioselectivities [**47**]. While studying different salen catalysts in the epoxidation of olefins, Katsuki found that the results of the reaction were affected to a large extent by the nature of the axial ligand. This prompted him to examine cyclopropanation of styrene with *t*-butyl 2-diazoacetate in the presence of iodo(salen)Co(III) complexes and found that complexes **39** and **40** bearing substituents at C3 and C3' had no or very poor catalytic activity, while the unsubstituted complex **41** gave preferentially the *trans*-isomer with moderate enantioselectivity (64%) [**48a,b**].

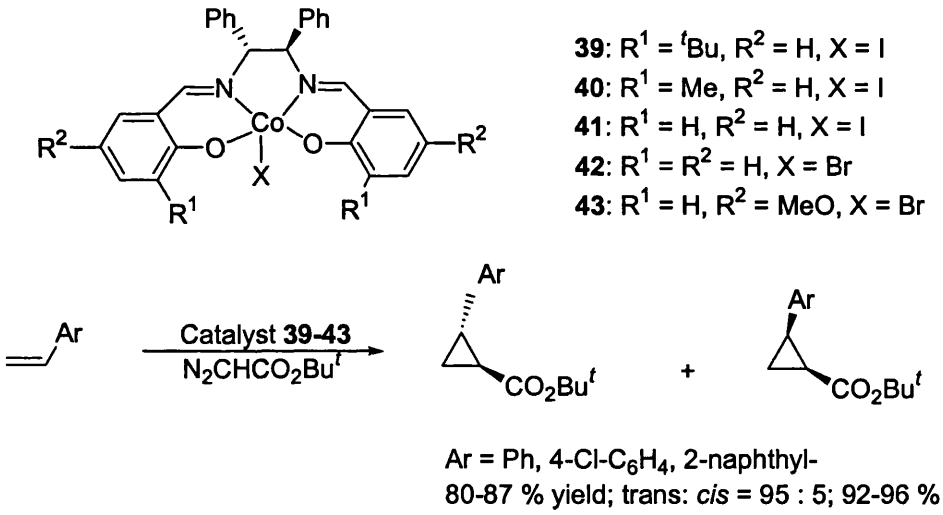

Scheme 1.19. Katsuki's catalyst with high *trans* selectivity

Furthermore, he tried to improve the asymmetric induction by changing the electronic properties of the complex. The iodide ligand was replaced with bromide, the obtained complex **42** showed better enantioselectivity due to a weaker *trans*-effect of the latter ligand which reduces the reactivity of the metal carbene. He also tuned the substituents of the salen ligand and found for the complex **43**, having electron-donating methoxy groups at C5 and C5', a high enatioselectivity (93 % ee), while preserving the high *trans*-selectivity (*trans* : *cis* = 96 : 4) in the cyclopropanation of styrene and its derivatives.

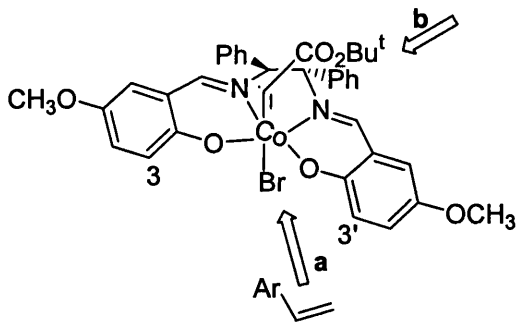

44

Figure 1.20. Olefin approach in cyclopropanation

In analogy with oxo Mn(V) salen complexes where the non-planarity of the salen ligand determined the asymmetric induction in epoxidation of alkenes, Katsuki assumed a non-planar structure for the ligand in metal carbene **44**. He suggested that the alkene could approach the carbenoid carbon from the front side (Figure 1.20), along the O-Co bond, which is in agreement with the stereochemistry of the products obtained with catalyst **43** and explains the lack or poor activity of catalysts **39** and **40** bearing substituents at $C_3/C_{3'}$ which interfere with the incoming olefin [**49**].

Based on this model he predicted that chiral Ru(salen) complex **45a** having longer Ru-O_{equat} bonds and a larger distance between $C_3/C_{3'}$ substituents would allow the approach of the alkene to the reactive centre from the C3 and C3' side even in presence of substituents at the mentioned positions. It was also expected that salen ligands like that in **45a** would impose a non-planar conformation of the catalyst with one 3 or 3' substituents inclined outward, leaving an open space above C3 or C3', while the second substituent from the mentioned positions would prevent counter clockwise rotation of the olefin favouring selective formation of the *cis*-product. Indeed, complex **45a** showed high *cis*-selectivity (*cis* : *trans* = 93 : 7) and enantioselectivity (98 % ee), but low chemical yield (36 %) due to an undesired reaction leading to fumaric and maleic acid esters [**50a, b**].

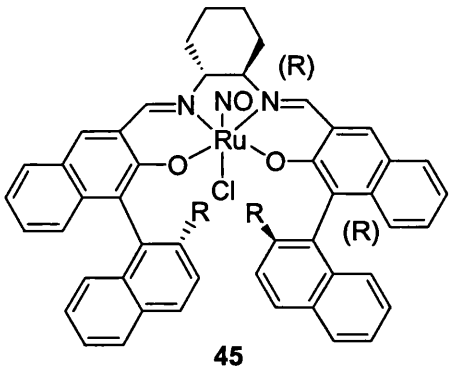

45

a: R = Ph, **b**: R = Me, **c**: R = H

Figure 1.21. Ru(salen) catalyst with high *cis* selectivity

Studies continued in this area using cobalt(II)salen complexes that have Co-O_{equat} bonds roughly equal to those in Co(III)salen complexes and are able to adopt various ligand conformations depending on the substituents in the aromatic ring and the apical ligand. Katsuki gradually modified the structure of cobalt(III)salen complexes in order to favour alkene approach of the metal carbene along Co-N bond (Figure 1.20). Complex **46** showed moderate *trans*- and enantioselectivity, while the sense of *ee* was opposite to that induced by **43**, suggesting that the ligand conformation in the two complexes was different.

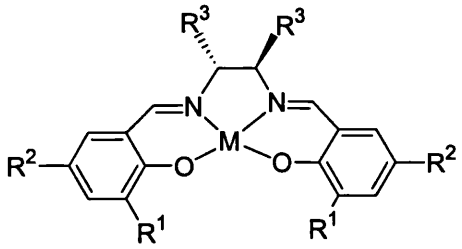

43: M = Co-Br; R^1 = H, R^2 = OMe, R^3 = Ph
46: M = Co, R^1 = H, R^2 = OMe, R^3 = Ph
47: M = Co, R^1 = Cl, R^2 = Cl, R^3 = Ph
48: M = Co, R^1 = R^2 = *t*-Bu, R^3,R^3 = -$(CH_2)_4$-

Figure 1.22. Tuning the catalysts for *cis*-selective cyclopropanation

It was found that complexes **47** and **48** bearing substituents at $C_3/C_{3'}$ catalyse the reaction with moderate *trans* selectivity and in low yield. However, the enantioselectivities of the minor *cis*-isomer were good to high and prompted them to test complex **49a** which exhibited high *cis*- and enantioselectivity in good yield. This

complex was further used under the optimised conditions in cyclopropanation of other substrates and showed good to excellent *cis*-regioselectivity and high enantioselectivity [**51**].

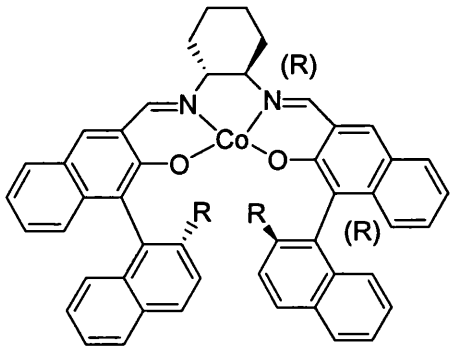

49

a: R = Ph, **b:** R = Me, **c:** R = H

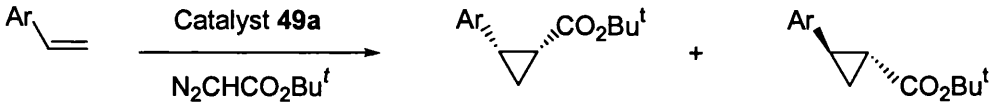

Ar = Ph, 4-Cl-C_6H_4, 4-MeO-C_6H_4

84-89 % yield,
cis: 95-98 % ee, *cis* : *trans* >97: 3

Scheme 1.20. Katsuki's procedure for *cis*-cyclopopanation

Recently Nguyen [**52**] revealed that Ru(II) salen complexes **50** were efficient catalysts (90-96 % yield) for asymmetric cyclopropanation of different electron-rich, electron poor and aliphatic olefins with ethyl-diazoacetate, leading predominantly to *trans*-products with high enantioselectivity. Apart from the good results obtained, the procedure has the advantage of employing ethyldiazoacetate which is the most readily available diazoester, while previous studies used bulky *t*-butyldiazoacetate in order to attain high levels of asymmetric induction.

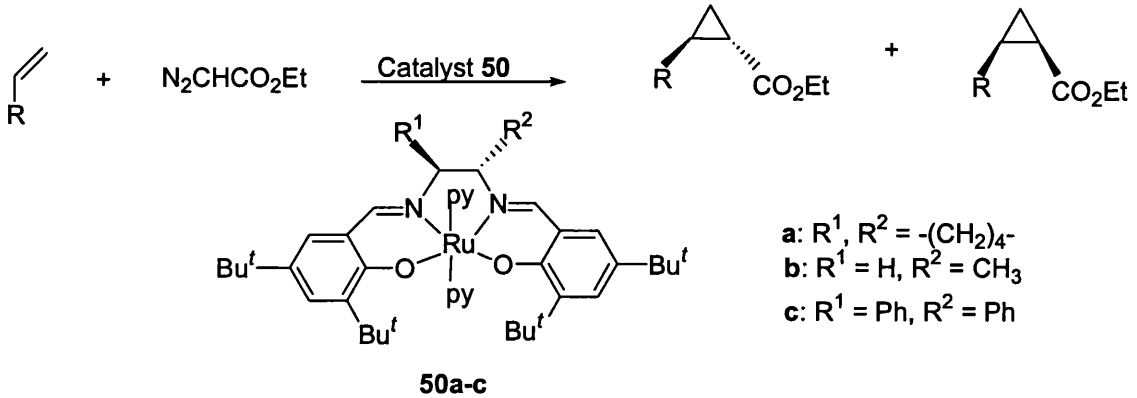

50a-c

a: R^1, R^2 = -$(CH_2)_4$-
b: R^1 = H, R^2 = CH_3
c: R^1 = Ph, R^2 = Ph

Scheme 1.21. Nguyen's *trans*-cyclopropanation using ethyl-diazoacetate

Following these results for intermolecular cyclopropanation reactions, Katsuki investigated different complexes for their catalytic activity in intramolecular cyclopropanation and achieved this transformation for several *trans*-cinnamyl-α-diazoacetates under photo-irradiated conditions with good enantioselectivity using ruthenium complexes **45a-c** as catalysts [**53**].

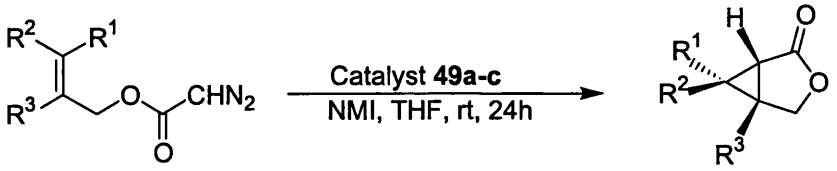

R^1 = H, Me, Ph

R^2 = Ph, 4-Cl-C_6H_4, 4-MeO-C_6H_4, 4-Br-C_6H_4

R^3 = H

65-93 % yield, 74-98 % ee

Scheme 1.22. Katsuki's intramolecular cyclopropanation

However, the dimerization of the substrate in the presence of ruthenium complexes accompanied by the decrease in chemical yield led to testing of the cobalt (II) complexes **49a-c** of the same ligands in absence of light [**54**]. Among these, **49b** and **49c** proved to be good catalysts (70-93 % yield and 96-98 % ee) for asymmetric intramolecular cyclopropanation of E-allyl-α-diazoacetates (R^1=R^3=H; $R^2 \neq$H) under high substrate concentration. The results obtained for other substrates in which the diazoacetate contains R^1 or $R^3 \neq$ H were not so good due to steric interactions, which appeared between the substrate and the catalyst in the transition state.

1.4.4 Kinetic resolution by ring opening of epoxides

Kinetic resolution is a process in which enantiomers of a racemic substrate (S) react at different rates to form a product (P) that may or may not be chiral. In catalytic kinetic resolution the relative rates of reaction for the substrate enantiomers, expressed as k_{rel}, depends on the difference in energies $\Delta G^{\neq}$ between the transition states of each enantiomer.

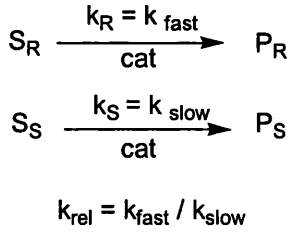

Scheme 1.23. Kinetic resolution

The attractive aspect of this methodology is that unreacted substrate can be recovered in high ee (>99 %) even if k_{rel} is not very high, simply by carrying the reaction to high enough conversion. Calculations showed that a selectivity factor of 10 allows the isolation of unreacted substrate in 98 % ee with a 30 % recovery. In contrast, high enantioselectivity factors are necessary in order to obtain high product enantioselectivities by kinetic resolution. The enantiomeric ratios in the first cycles of the reaction correspond to k_{rel} ($k_{rel} = 10$, er ≈ 10), but as the reaction proceeds, the ee of the product decreases. Therefore a k_{rel} of ≥ 50 is generally required if a product of high enantiomeric purity is to be obtained in useful yield.

As detailed in section **1.4.1**, epoxides are very useful chiral building blocks in organic synthesis and for this reason a substantial effort was directed toward development of practical routes to these compounds by asymmetric catalysis. In spite of the progress made in the area, there are still some important classes of epoxides (*e.g.* terminal epoxides) which are not accessible in this way. Kinetic resolution is an appealing strategy for accessing chiral terminal epoxides because racemic substrates from this class are inexpensive or are readily available by epoxidation of terminal alkenes. Classical resolution cannot be applied as they do not form stable salts or complexes with usual resolving agents. Terminal epoxides are liquids at room temperature, making enantioenrichment of non-racemic mixtures by recrystallization impossible. In contrast, kinetic resolution can provide access to material that is highly enantiopure.

1.4.4.1 Kinetic resolution with $TMSN_3$

Jacobsen investigated the possibility of achieving the asymmetric ring opening of epoxides by a mechanism involving substrate activation by a chiral Lewis acid metal salen complex. A preliminary screen of metal salen complexes indicated that

Cr(salen)(Cl) **51** was an effective catalyst for nucleophilic ring-opening of *meso*-epoxides with $TMSN_3$, with regard to both the reactivity and enantioselectivity [**55**]. The fact that the other tested metal salen complexes showed lower reactivity and asymmetric induction as compared to complex **51** suggested that the reaction with this catalyst did not proceed by a simple Lewis acid mechanism. Co(salen) complex **52a** gave promising results in terms of enantioselectivity, although was less reactive in the reaction with the nucleophile.

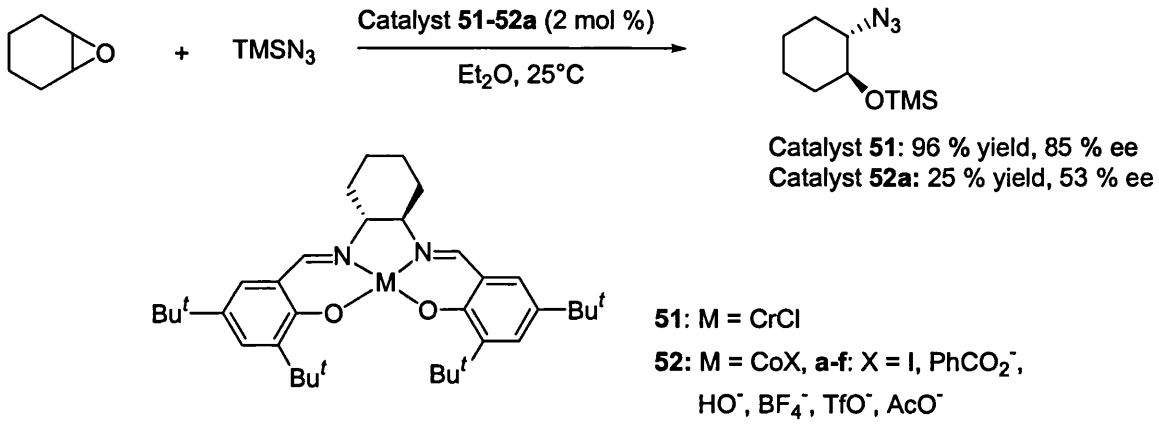

Scheme 1.24. Asymmetric ring opening of epoxides with $TMSN_3$

Complex **51** was employed for enantioselective ring opening of a variety of *meso* epoxides (Figure 1.23) [**55, 56**]. The reaction was quite sensitive to the environment surrounding the epoxide. Thus, five-membered-ring-fused epoxides afforded higher enantioselectivity (93 % ee) than six-membered-ring analogues (85 % ee), the asymmetric induction decreased even more for cycloheptene oxide (42 % ee) while cyclooctene was unreactive. This effect was illustrated also in asymmetric ring opening of epoxide **53a-b** for which the results showed a strong dependence on the protective groups present in the substrate [**57**].

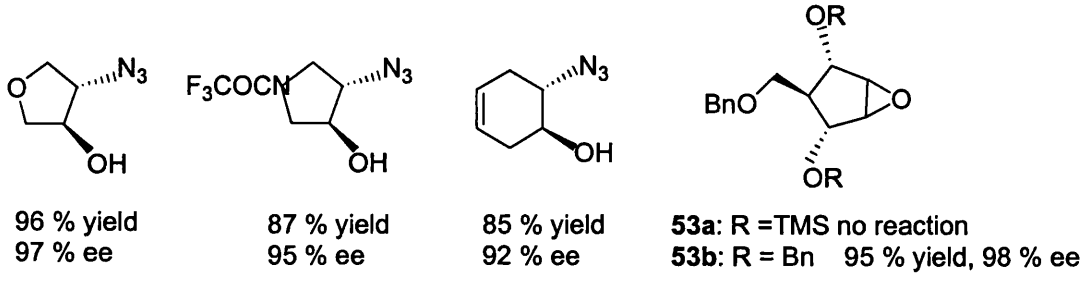

Figure 1.23. Ring opening of *meso*-epoxides

Later, asymmetric ring opening with $TMSN_3$ was extended to terminal epoxides (Figure 1.24). While styrene oxide and epichlorohydrin proved to be difficult substrates due to competing side reactions [**55, 58**], good to excellent results were obtained for other terminal epoxides [**59**].

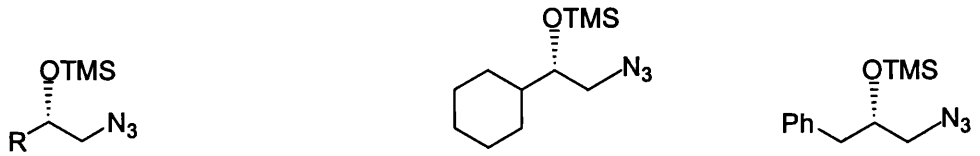

R = Me, Et, *n*-Bu, CH_2-OTBS, CH_2-CN
82-98 % yield
97 % ee

84 % yield
97 % ee

94 % yield
93 % ee

Figure 1.24. Compounds obtained by ring opening of terminal epoxides

The method also has other positive features that make it attractive for synthesis of 1, 2-amino alcohol derivatives. These are the high stability of the catalyst in the system, the easy separation of the product from the unreacted epoxide and the ability to carry out the reaction under solvent free conditions.

Jacobsen isolated and characterized the active species in the process, $Cr(salen)N_3$ **54** [**60**]. He has shown that the catalyst is able to activate both the nucleophilic and electrophilic reacting partners by acting as a Lewis acid for the epoxide and as azide delivery agent through the complex **54**. The presence of a donor ligand in the system, able to co-ordinate to the metal (*e.g.* THF), severely inhibited the reaction, while catalytic amounts of water were found to be essential for the reaction to take place.

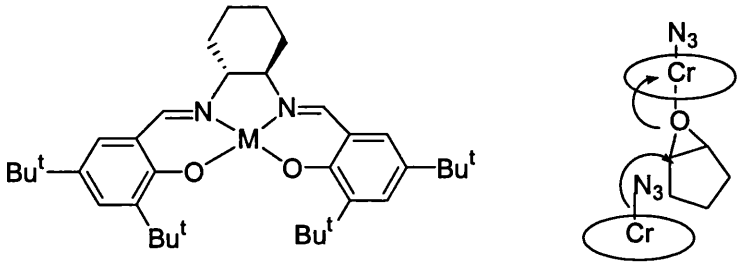

54: $M=CrN_3$

Figure 1.25. Active species in asymmetric ring opening; mechanism of action

The kinetic study carried out on cyclopentene oxide showed that the rate of the reaction obeyed the law:

$$\text{Rate} = k \cdot [\text{catalyst}]^2 \cdot [\text{epoxide}]^{-1} \cdot [HN_3]^0 \qquad (1.1)$$

Thus, the reaction between the epoxide and azide was inhibited by one and independent of the other. The second order dependence on the concentration of the catalyst provided key evidence that the reaction requires two molecules of catalyst in the rate determining step.

In order to demonstrate the cooperative catalysis between two chromium centres, Jacobsen synthesized several dimeric Cr(salen)(Cl) complexes and tested their catalytic activity. He envisaged two limiting geometries possible in these complexes, a head-to-head alignment in which the diamine backbones were in an eclipsed orientation (**55a**), or a head-to-tail arrangement in which one salen unit is rotated with 180 ° relative to the other one (**55b**).

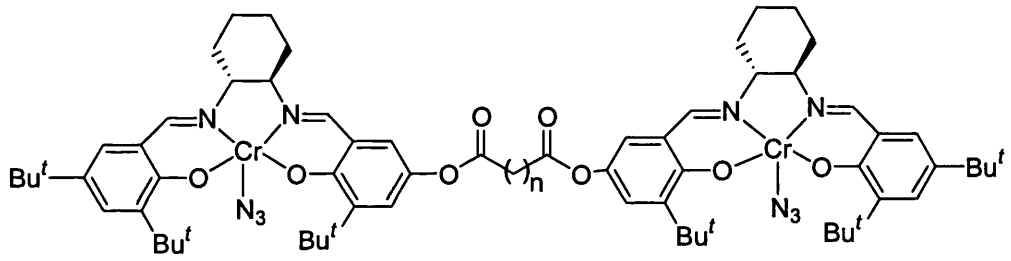

55b: n = 2-10; 90-94 % ee

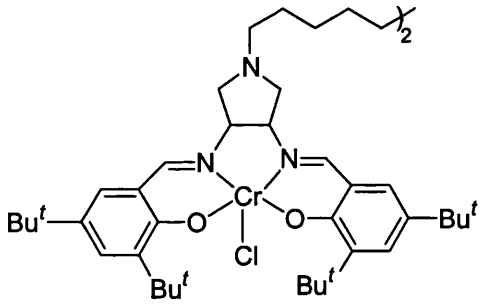

55a: 8 % ee

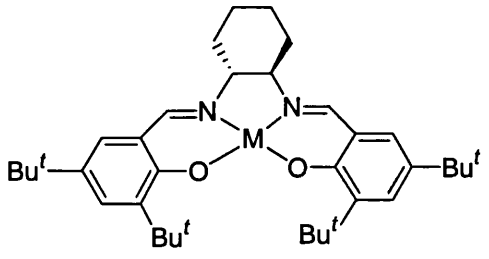

48: M = Co
56: M = $Co(O_2CR)$

Figure 1.26. Dimers tested in reactions with $TMSN_3$ and catalysts **48-56** used for asymmetric ring opening of epoxides with acids

When tested in asymmetric ring opening of cyclopentene oxide, only **55b,** consisting of two chromium salen units connected by a diester linkage, gave enantioselectivities (90-94% ee) comparable with monomeric compounds **51** [**61**]. While monomeric complexes displayed second order dependence on the catalyst concentration, reaction with dimers had a more complicated rate expression (Eq 1.2).

$$\text{Rate} = k_{intra} \cdot [\text{Catalyst}] + k_{inter}\,[\text{Catalyst}]^2 \qquad (1.2)$$

k_{intra}, k_{inter} = rate constants for intra and intermolecular paths

Dimeric catalysts display reactivity 1-2 orders of magnitude greater than that of the monomeric catalyst **51**, which is due to the presence of intramolecular path and also enhancement of intermolecular path in Eq 1.2, implying the participation of highly reactive multimetallic assemblies in the asymmetric ring opening of the epoxides.

1.4.4.2 Ring opening of epoxides with acids

In spite of the good results obtained with $TMSN_3$, this method involved the use of a valuable nucleophile that was not recovered at the end of the reaction and it also generates azides which can cause problems in manipulation on a large scale due to their heat sensitivity. In searching for other nucleophiles, which would be cheaper and easier to handle, Jacobsen discovered that the Co(II) catalyst **48** mediated clean transformation of *meso*-epoxides to the ring opened product with benzoic acid [**62**]. Experimentally it was found that the rate, enantiomeric excess and the yield of the process improved in the presence of $^{i}Pr_2NEt$. Other organic and inorganic bases showed a smaller effect, while those able to coordinate to the metal center inhibited the reaction.

The enantioselectivity of the transformation depended on the nature of the acid, the most useful nucleophiles were benzoic acid and its derivatives (ee $\approx$ 77 %). Acetic acid showed 40 % ee, while the more hindered pivalic acid gave 73 % ee, although the reaction was slow. Stronger acids (TFA, TsOH and trichlorobenzoic acid) gave several side reactions and generated racemic products. The active species in the reaction was Co(III)(salen)(O_2CR) **56** formed by aerobic oxidation of the catalyst in the presence of carboxylic acid. The reactivity of several Co(salen)(X) (X= $PhCO_2$-, HO-, I-, BF_4-, TfO-) complexes **52** was similar, however, for practical reasons [Co(III)(salen)(O_2CR)] was generated *in situ* from Co(II)(salen) and the carboxylic acid prior to the epoxide addition.

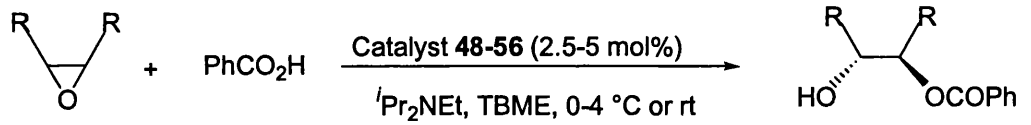

R= -$(CH_2)_n$-, n=3-5, Me, Ph

52-97 % yield, 55-92 % ee

n=4: 98 % yield, 77 % ee;
after recrystallization: 75 % yield, 98 % ee

Scheme 1.25. Ring opening of epoxides with acids

The optimised procedure was applied on several *meso*-epoxides and led to the corresponding 1,2-diol mono-esters in 52-98 % yield and 55-93 % ee. The crystallinity of the product allowed improvement of enantioselectivity by recrystallization (Scheme 1.25).

1.4.4.3 Hydrolytic kinetic resolution (HKR)

While trying to extend this procedure involving Co(salen) **48** as a catalyst to terminal epoxides, it was found that a significant amount of 1, 2-diol product was generated in this reaction with high enantioselectivity.

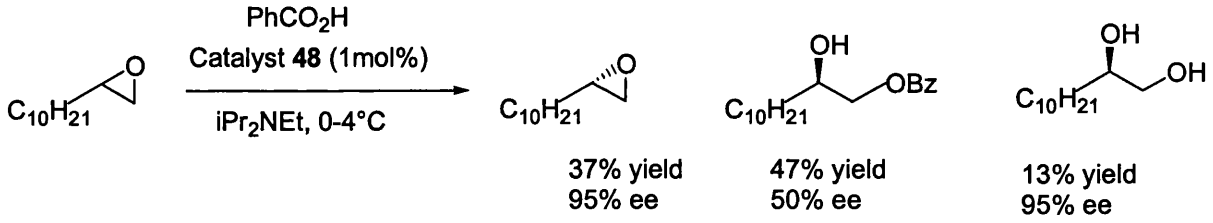

Scheme 1.26. Asymmetric ring opening with acids

Later it was shown that the nucleophilic ring-opening of epoxide occurred due to water contamination and was promoted by acetic acid present in small amounts in the system leading to the discovery of HKR of terminal epoxides with the Co(III) catalyst **52f** [**63**]. The process is very efficient and gives high selectivities with low catalyst loadings for a wide range of substrates [**64**]. In all cases the epoxide was recovered in high ee and good to excellent yield, while diols were also isolated in high ee.

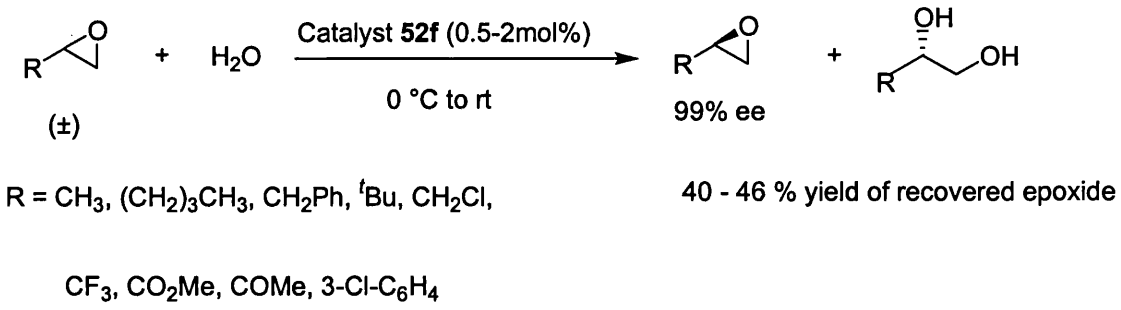

Scheme 1.27. Jacobsen's hydrolytic kinetic resolution of terminal epoxides

These were easily separated one from another by distillation or extraction. This is especially useful as there was no other general and practical method for generation of enantiomerically pure terminal epoxides. The HKR was carried out under solvent-free conditions in most cases, except for the very hydrophobic epoxides that had low solubility in water and required small amounts of polar co-solvents (*e.g.* THF). The reaction was run effectively on milligram to multiton scale.

HKR of terminal epoxides was also achieved efficiently using polymer supported chiral cobalt (salen) complexes **57-58** [**65**]. The procedures developed solved several technological problems associated with the isolation of the reaction products generated from specific substrates (Scheme 1.28). Other advantages of heterogeneous catalysts over their homogeneous counterparts included the simplification of the procedure employed for catalyst recycling and the possibility of using the catalyst in continuous-flow processes.

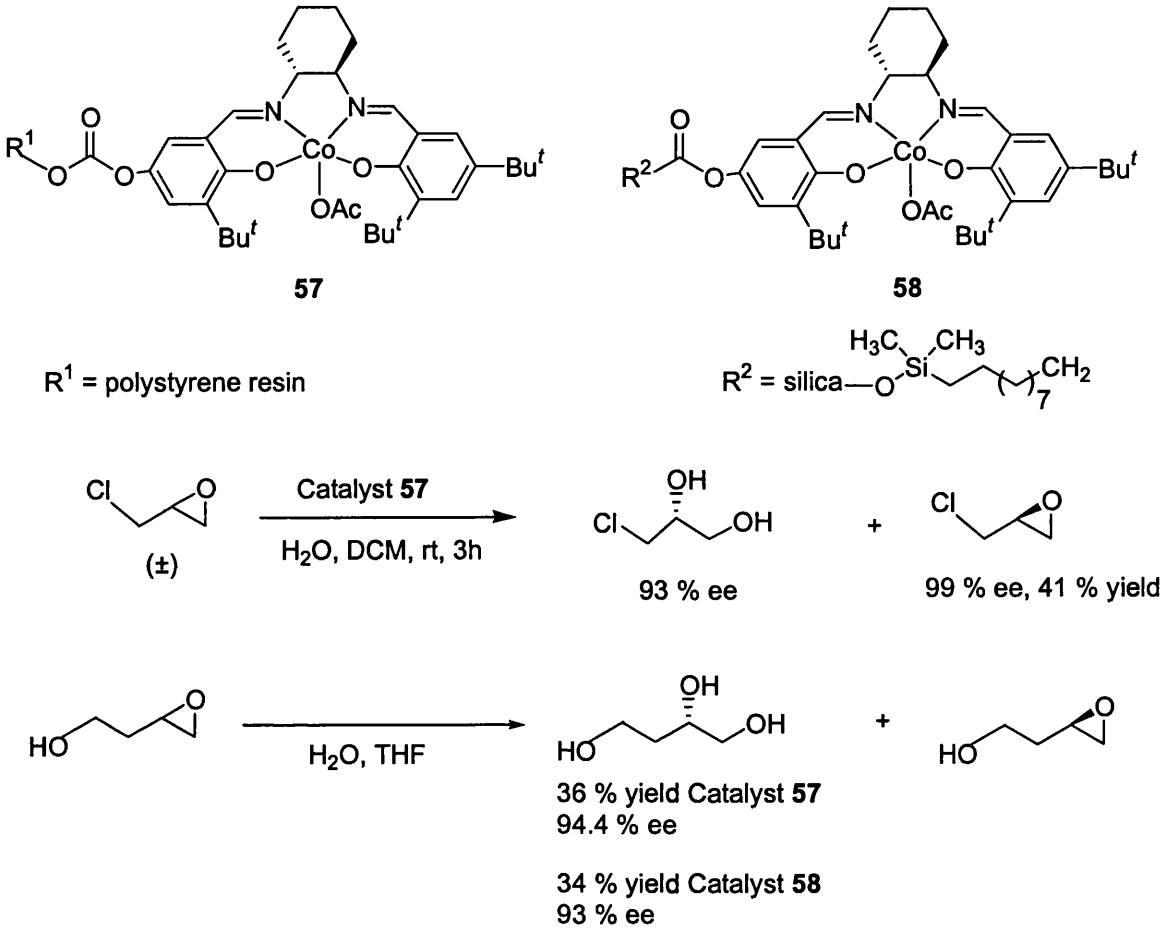

Scheme 1.28. Polymer supported Co(III) salen catalysts used in HKR

1.4.4.4 Kinetic resolution with phenols (KR)

Jacobsen has revealed that phenols are also effective nucleophiles for Co(salen) catalized KR of terminal epoxides providing direct access to α-aryloxy alcohols, which are valuable synthetic intermediates [**66**].

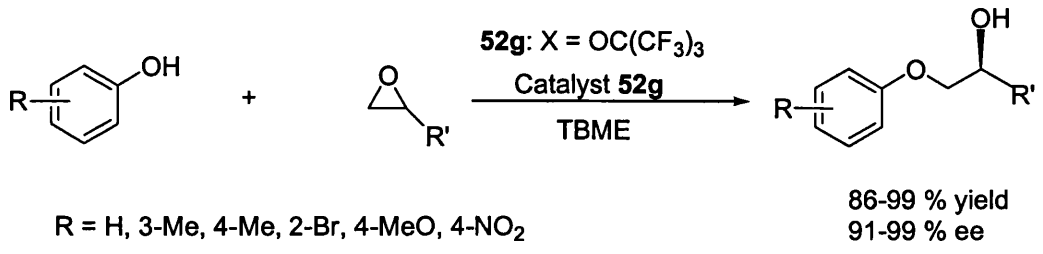

Scheme 1.29. KR of terminal epoxides with phenols

The counterion X of the Co(salen)(X) complex influences the obtained results, among the screened axial ligands complex **52g** exhibited the best catalytic activity. The optimised procedure was applied to both electron-rich and electron-poor epoxides giving the corresponding α-aryloxy alcohols in excellent yields and enantioselectivities. The reaction had complete regioselectivity for all substrates except for styrene oxide when a mixture of regioisomers was obtained. The stereoselectivity of the process displayed strong temperature dependence, enantioselectivity being significantly improved by lowering the temperature to around –20 °C.

The scope of the reaction was also broad with respect to the phenol. Phenols with a wide range of electronic properties (Scheme 1.29) participated in the process with high yields and enantioselectivities apart from, *o*-methyl-phenol which presented poor reactivity (yield below 5 %). Although the mechanism of the reaction is not completely elucidated, Jacobsen prepared the Co(salen)(phenoxide) complex **59** from 3,5-difluoro phenol and proved that it was an intermediate in the ring-opening reaction.

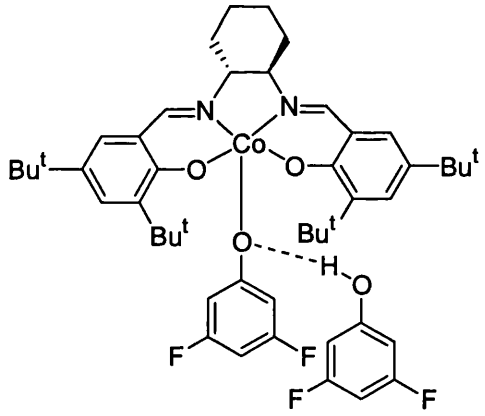

59

Figure 1.27. Intermediate in KR reaction with phenols

The extraordinary generality of this reaction with respect to the nature of terminal epoxide and phenol prompted him to apply this methodology in synthesis of parallel libraries of ring-opened products [**67**] using a polymer-supported Co(salen) complex **57**.

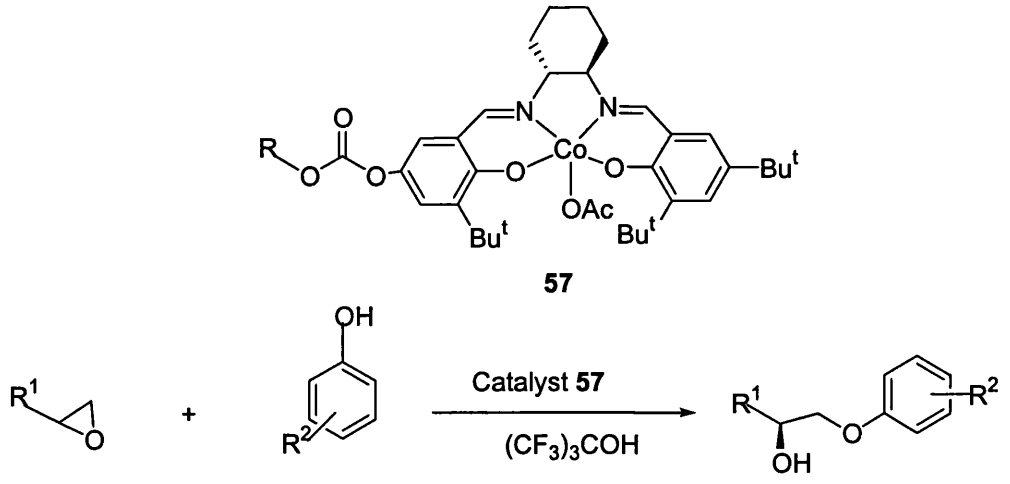

Scheme 1.30. Polymer-supported Co(salen) – catalysts in KR of terminal epoxides

Racemic epoxides were used as reaction medium in the catalytic process which was carried out until completion of phenols. Filtration of the catalyst followed by evaporation of the excess of epoxides afforded the 1-aryloxy-2-alcohols in high yield, purity and enantiomeric excess. Separation of the product from unreacted epoxide relied on the high difference in volatility (more than a hundred degrees) between the two compounds.

Phenols bearing electron-withdrawing substituents in the *para*-position afforded slightly lower results, with product enantioselectivities between 81 and 93.5 %, whereas all the others gave products in 93 to 99 % ee. Using *ortho*-halophenols, the products were obtained with ee higher than 90 %, while *ortho*-alkyl-phenols proved unreactive in the same reaction conditions.

1.5 References

1. E. N. Jacobsen, *Catalytic Asymmetric Synthesis*, Ed. I. Ojima, VCH publishers, Inc., New York, **1993**, 159.
2. K. Noda, N. Hosoya, R. Irie, Y. Ito, T. Katsuki, *Synlett*, **1993**, 469; H. Nishikori, T. Katsuki, *Tetrahedron Lett.*, **1996**, *37*, 9245.
3. T. Fukuda, T. Katsuki, *Synlett*, **1995**, 825; T. Fukuda, T. Katsuki, *Tetrahedron*, **1997**, *53*, 7201.
4. Y. Yamashita, T. Katsuki, *Synlett*, **1995**, 829; S. E. Schaus, J. Branalt, E. N. Jacobsen, *J. Org. Chem.*, **1998**, *63*, 403.
5. M.S. Sigman, E.N. Jacobsen, *J. Am. Chem. Soc.*, **1998**, *120*, 5315.
6. J. F. Larrow, S.E. Schaus, E.N. Jacobsen, *J. Am. Chem. Soc.*, **1996**, *118*, 7420.
7. M. Calligaris, G. Nardin, L. Randaccio, *Coord. Chem. Rev.*, **1972**, *7*, 385.
8. M. Calligaris, G. Manzini, G. Nardin, L. Randaccio, *J. Chem. Soc., Dalton Trans.*, **1972**, 543.
9. M. Calligaris, G. Nardin, L. Randaccio, *Chem. Comm.*, **1970**, 1079.
10. J.F. Larrow, E.N. Jacobsen, *J. Org. Chem.*, **1994**, *59*, 1939.
11. T. Hamada, R. Irie, J. Mihara, K. Hamachi, T. Katsuki, *Tetrahedron*, **1998**, *54* , 10017.
12. K.H. Ahn, S.W. Park, S. Choi, H-J. Kim, C.J. Moon, *Tetrahedron Lett.*, **2001**, *42*, 2485.
13. a) T. Hashihayata, Y. Ito, T. Katsuki, *Tetrahedron*, **1997**, *53*, 9541; b) K. Miura, T. Katsuki, *Synlett*, **1999**, 783.
14. Y. Ito, T. Katsuki, *Tetrahedron Lett.*, **1998**, *39*, 4325.
15. K. Srinivasan, P. Michaud, J.K. Kochi, *J. Am. Chem. Soc.*, **1986**, *108*, 2309.
16. a) W. Zhang, J. L. Loeback, S.R. Wilson, E.N. Jacobsen, *J. Am. Chem. Soc.*, **1990**, *112*, 2801; b) E.N. Jacobsen, W. Zhang , L.C. Muci, J.R. Ecker, L. Deng, *J. Am. Chem. Soc.* **1991**, *113*, 7063.
17. a) R. Irie, K. Noda, Y. Ito, N. Matsumoto, T. Katsuki, *Tetrahedron Lett.* **1990**, *31*, 7345; b) R. Irie, K. Noda, Y. Ito, T. Katsuki *Tetrahedron Lett.* **1991**, *32*, 1055; c) N. Hosoya, R. Irie, T. Katsuki, *Synlett*, **1993**, 261.
18. B. Meunier, E. Guilmet, M. –E. De Carvalho, R. Poilblanc, *J. Am. Chem. Soc.*, **1984**, *106*, 6668.
19. W. Zhang, E.N. Jacobsen, *J. Org. Chem.*, **1991**, *56*, 2296.

20. E.N. Jacobsen in *Comprehensive Organometallic Chemistry*, 2nd ed., (Eds. E.W. Abel, F.G.A. Stone, G. Wilkinson), Pergamon, New York, **1995**, vol. 12, 1097.
21. T. Katsuki, *J. Mol. Catal. A.*, **1996**, *113*, 87.
22. K. Srinivasan, J.K. Kochi, *Inorg. Chem.*, **1985**, *24*, 4671.
23. E.N. Jacobsen, W. Zhang, M.L. Guller, *J. Am. Chem. Soc.*, **1991**, *113*, 6703.
24. a) N. Hosoya, A. Hatayama, R. Irie, H. Sasaki, T. Katsuki *Tetrahedron*, **1994**, *50*, 4311; b) H. Sasaki, R. Irie, T. Katsuki, *Synlett*, **1994**, 356; c) H. Sasaki, R. Irie, T. Hamada, K. Suzuki, T. Katsuki, *Tetrahedron*, **1994**, *50*, 11827; d) D. Mikame, T. Hamada, R. Irie, T. Katsuki, *Synlett*, **1995**, 827.
25. a) T. Punniyamurthy, R. Irie, T. Katsuki, M. Akita, Y. Moro-oka, *Synlett*, **1999**, 1049; b) T. Hashihayata, T. Punniyamurthy, R. Irie, T. Katsuki, M. Akita, Y. Moro-oka, *Tetrahedron* **1999**, *55*, 14599.
26. N. Hosoya, R. Irie, Y. Ito, T. Katsuki, *Synlett*, **1991**, 691.
27. H. Nishikori, C. Ohta, T. Katsuki, *Synlett*, **2000**, 1557.
28. E.N. Jacobsen, M.H. Wu, in *Comprehensive Asymmetric Catalysis*, (Eds. E.N. Jacobsen, A. Pfaltz, H. Yamamoto), Springer, Berlin, **1999**, Vol. 2, 649.
29. A. Scheurer, P. Mosset, M. Spiegel, R.W. Saalfrank, *Tetrahedron*, **1999**, *55*, 1063.
30. K. M. Ryan, C. Bousquet, D.G. Gilheany, *Tetrahedron Lett.*, **1999**, *40*, 3613.
31. T. Yamada, K. Imagawa, T. Nagata, T. Mukaiyama, *Chem. Lett.*, **1992**, 2231.
32. T. Punniyamurthy, B. Bhatia, M.M. Reddy, G.C. Maikap, J. Iqbal, *Tetrahedron*, **1997**, *53*, 7649.
33. K.J. O' Connor, S.-J. Wey, C. Burrows, *Tetrahedron Lett.*, **1992**, *33*, 1001.
34. K. Noda, N. Hosoya, R. Irie, Y. Ito, T. Katsuki, *Synlett*, **1993**, 469.
35. H. Nishikori, T. Katsuki, *Tetrahedron Lett.*, **1996**, *37*, 9245.
36. a) J. Du Bois, J. Hong, E.M. Carreira, M.W. Day, *J. Am. Chem. Soc.*, **1996**, *118*, 915; b) J. Du Bois, C.S. Tomooka,, J. Hong, E.M. Carreira, M.W. Day, *Angew. Chem., Int. Ed.* , **1997**, *36*, 1645; c) J. Du Bois, C.S. Tomooka,, J. Hong, E.M. Carreira, *Acc. Chem. Res.*, **1997**, *30*, 364.
37. S. Minakata, T. Ando, N. Nishimura, I. Ryu, M. Komatsu, *Angew. Chem., Int. Ed. Engl.*, **1998**, *37*, 3392.
38. M. Nishimura, S. Minakata, T. Takahashi, Y. Oderaotoshi, M. Komatsu, *J. Org. Chem.*, **2002**, *67*, 2101.
39. S. Minakata, M. Nishimura, T. Takahashi, Y. Oderaotoshi, M. Komatsu, *Tetrahedron Lett.*, **2001**, *42*, 9019.

40. M. Nishimura, S. Minakata, S. Thongchant, I. Ryu, M. Komatsu, *Tetrahedron Lett.*, **2000**, *41*, 7089.

41. C-M. Ho, T-C. Lau, H-L. Kwong, W-T. Wong, *J. Chem. Soc., Dalton Trans.*, **1999**, 2411.

42. a) D.A. Evans, M.M. Faul, M.T. Bilodeau, *J. Org. Chem.*, **1991**, *56*, 6744; b) D.A. Evans, M.M. Faul, M.T. Bilodeau, *J. Am. Chem. Soc.*, **1994**, *116*, 2742.

43. Z. Li, R.W. Quan, E.N. Jacobsen, *J. Am. Chem. Soc.*, **1995**, *117*, 5889.

44. Z. Li, K.R. Conser, E.N. Jacobsen, *J. Am. Chem. Soc.*, **1993**, *115*, 5326.

45. K.M. Gillespie, E.J. Crust, R. J. Deeth, P. Scott, *Chem. Commun.*, **2001**, 785.

46. M. Shi, C-J. Wang, A.S.C. Chan, *Tetrahedron Asymm.*, **2001**, *12*, 3105.

47. A. Nakamura, A. Konishi, Y. Tatsuno, S. Otsuka, *J.Am.Chem.Soc.*, **1978**, *100*, 3443.

48. a) T. Fukuda, T. Katsuki, *Synlett*, **1995**, 825; b) T. Fukuda, T. Katsuki, *Tetrahedron*, **1997**, *53*, 7201.

49. T. Fukuda, T. Katsuki, *Tetrahedron Lett.*, **1997**, *38*, 3443.

50. a) T. Uchida, R. Irie, T. Katsuki, *Synlett*, **1999**, 1163; b) T. Uchida, R. Irie, T. Katsuki, *Synlett*, **1999**, 1793.

51. T. Niimi, T. Uchida, R. Irie, T. Katsuki, *Tetrahedron Lett.*, **2000**, *41*, 3647.

52. J.A. Miller, W. Jin, S.T. Nguyen, *Angew. Chem., Int. Ed.*, **2002**, *41*, 2953.

53. B. Saha, T. Uchida, T. Katsuki, *Synlett*, **2001**, 114.

54. T. Uchida, B. Saha, T. Katsuki, *Tetrahedron Lett.*, **2001**, *42*, 2521.

55. L.E. Martinez, J.L. Leighton, D.H. Carsten, E.N. Jacobsen, *J. Am. Chem. Soc.*, **1995**, *117*, 5897.

56. a) J.L. Leighton, E.N. Jacobsen, *J. Org. Chem.*, **1996**, 61, 389; b) L.E. Martinez, W.A. Nugent, E.N. Jacobsen, *J. Org. Chem.*, **1996**, 61, 7963; c) M.H. Wu, E.N. Jacobsen, *Tetrahedron Lett.*, **1997**, 38, 1693; d) S.E. Schaus, J.F. Larrow, E.N. Jacobsen, *J. Org. Chem.*, **1997**, 62, 4197.

57. D. J. Kassab, B. Ganem, *J. Org. Chem.*, **1999**, 64, 1782.

58. S.E. Schaus, E.N. Jacobsen, *Tetrahedron Lett.*, **1996**, 37, 7939.

59. a. J.F. Larrow, S.E. Schaus, E.N. Jacobsen, *J. Am. Chem. Soc.*, **1996**, *118*, 7420; b. H. Lebel, E.N. Jacobsen, *Tetrahedron Lett.*, **1999**, 40, 7303.

60. K.B. Hansen, J.L. Leighton, E.N. Jacobsen, *J. Am. Chem. Soc.*, **1996**, *118*, 10924.

61. R.G. Konsler, J. Karl, E.N. Jacobsen, *J. Am. Chem. Soc.*, **1998**, *120*, 10780.

62. E.N. Jacobsen, F. Kakiuchi, R.G. Konsler, J.F. Larrow, M. Tokunaga, *Tetrahedron Lett.*, **1997**, *38* , 773.

63. M. Tokunaga, J.F. Larrow, F. Kakiuchi, E.N. Jacobsen, *Science*, **1997**, *277*, 936.

64. M.E. Furrow, S.E. Schaus, E.N. Jacobsen, *J. Org. Chem.*, **1998**, *63*, 6776.

65. D.A. Annis, E.N. Jacobsen, *J.Am.Chem.Soc.*, **1999**, *121*, 4147.

66. J.M. Ready, E.N. Jacobsen, *J.Am.Chem.Soc.*, **1999**, *121*, 6086.

67. S. Peukert, E.N. Jacobsen, *Org. Lett.*, **1999**, *1*, 1245.

1.6 Nomenclature of symmetrical salen and amben type ligands

Abbreviated names for symmetrical salen and amben ligands are obtained by joining together the abbreviated names of the aldehyde and diamine, the two components involved in the condensation reaction by which these compounds are generated. Abbreviations for the aromatic aldehydes salicylaldehyde, 3,5-di-*tert*-butyl-salicylaldehyde, 2-amino-benzaldehyde, *n*-R-2-amino-benzaldehyde are as follows sal, 3,5-di-*t*-Bu-sal, amb and *n*-R-amb (where n indicates the position of R in the aromatic ring). Abbreviations for diamines 1,2-diaminoethane, 1,3-diaminopropane, 1,2-diaminocyclohexane are en, pr, ch. For example, salen is the double Schiff base derived from salicylaldehyde and 1,2-diaminoethane.

Salen ligands are also N_2O_2 ligands, this name associated to the family of double Schiff bases derived from salicylaldehyde is used to indicate the donor atoms involved in the co-ordination sphere. On the other hand amben type ligands, porphyrins and corrins are considered N_4 ligands for similar reasons.

1.7 Aims of the project

Catalytic asymmetric oxidation of various organic compounds has attracted the attention of synthetic chemists in the last decade. Research studies involving metal porphyrins and metal salen complexes were carried out in order to understand various oxidation reactions which are involved in many fundamental biological processes and in an attempt to mimic the activity of different enzymes. These results led to the development of effective chiral catalysts which achieve various asymmetric transformations; among them salen complexes proving to be very versatile.

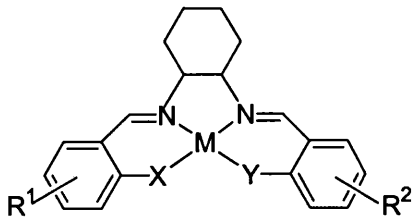

X=Y=O or N; $R^1=R^2$ or $R^1 \neq R^2$
X=O; Y=N; R^1, R^2 variable, $R^1 \neq R^2$
60

The studies so far employed various metal salen complexes possessing an N_2O_2 donor atom set around the metal, which were synthesized from different diamines and salicylaldehyde derivatives. We were interested in obtaining new symmetrical ligands in which the oxygen donor atoms are replaced with other donors such as nitrogen. The amben (N_4) ligands have received much less attention due to the problems associated with synthesis and manipulation of aminobenzaldehyde derivatives. This type of ligand combines the donor atom environment of porphyrins with ready incorporation of chirality and arene functionalization familiar to salen ligands. It will be therefore interesting to obtain symmetrical N_4 double Schiff base ligands derived from different 2-amino-benzaldehydes. We also considered using 1,2-diaminocyclohexane in the condensation reaction as this diamine can be easily resolved leading to chiral ambch complexes.

It was also of interest to develop routes toward synthesis of asymmetrical ligands (**60**) in which the outer donors would be either the same (X=Y) and the two aromatic rings will be differently substituted, or the donor atoms would be different (X≠Y) and study the changes in electronic and structural properties determined by variation of direct co-ordination sphere around the metal ion in these complexes.

Chapter 2 Synthesis of symmetrical ambch ligands

2.1 Introduction

A retrosynthetic analysis of aminobenzaldehydes **61** indicates that there are three possible routes to these compounds: by reduction of the corresponding nitro-benzaldehydes **62**, by formylation of substituted anilines **63** and by oxidation of amino-benzyl alcohols **64**.

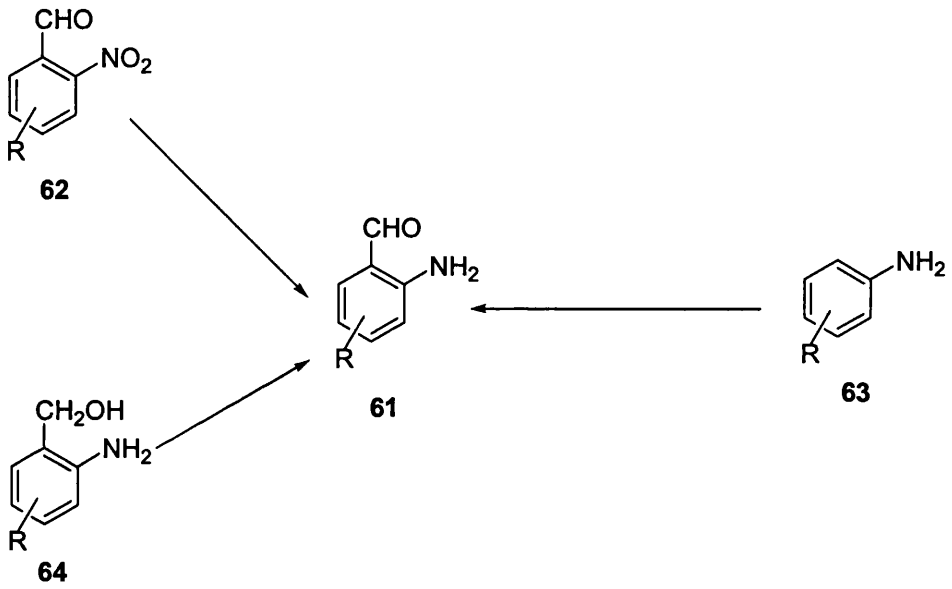

Scheme 2.1. Possible routes toward amino-benzaldehydes **61**

All these routes were investigated in a search for an optimum synthetic procedure towards the target 2-amino-R-benzaldehydes which would involve cheap starting materials and could be applied to various R groups. The following sections describe the challenges encountered in the synthesis of these compounds and the solutions that we proposed to overcome them. The chapter closes with synthesis of C_2-symmetric ambch ligands.

2.1.1 Synthesis of substituted nitrobenzaldehydes

Previous work in the area has shown that nitrobenzaldehydes can be prepared either by conversion of the methyl group of substituted nitrotoluenes into a carbonyl group, by nitration of benzaldehyde derivatives or *via* nucleophilic substitution of nitro-

derivatives. For example, synthesis of 2-nitro-4-methoxy-benzaldehyde by oxidation of nitrotoluene **65** was achieved in moderate yields with chromyl chloride in CS_2[1].

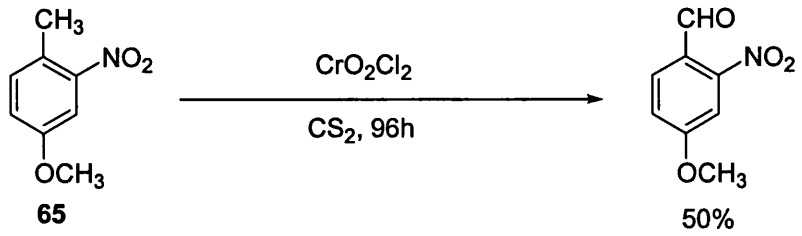

Scheme 2.2. Synthesis of nitro-benzaldehyde **65** by oxidation

In a different approach 2,4-dinitro-benzaldehyde **62** was obtained by acidic hydrolysis of dinitro-benzylidene-*p*-amino-dimethylaniline **66**, previously prepared by the condensation of *p*-nitroso-dimethylaniline with 2,4-dinitrotoluene[2].

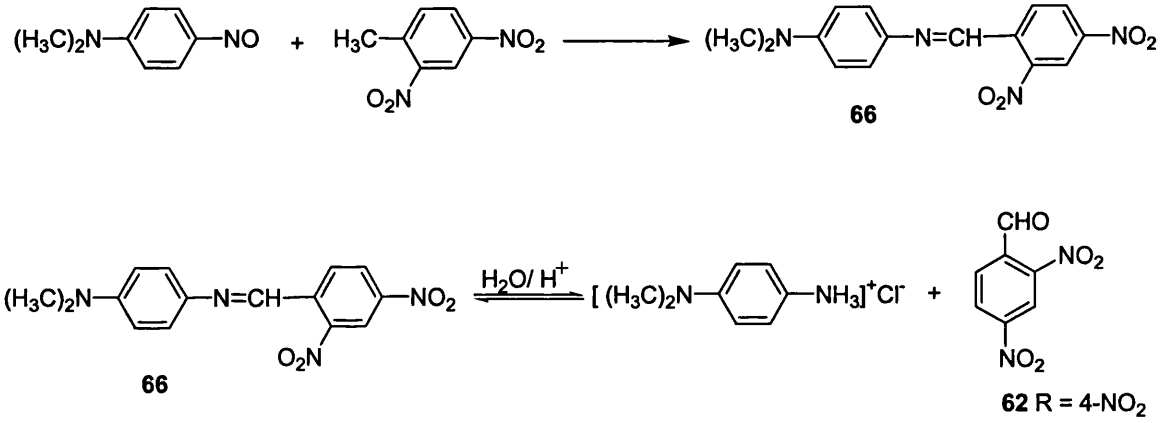

Scheme 2.3. Synthesis of nitro-benzaldehyde **62** by hydrolysis

Electrophilic substitution of 3-hydroxy-benzaldehyde with nitric acid at 50-55 °C has been reported [3] to give a mixture of 2-nitro, 4-nitro and 6-nitro-3-hydroxy-benzaldehyde. From it the pure regioisomers were isolated by recrystallisation from hot benzene followed by steam distillation.

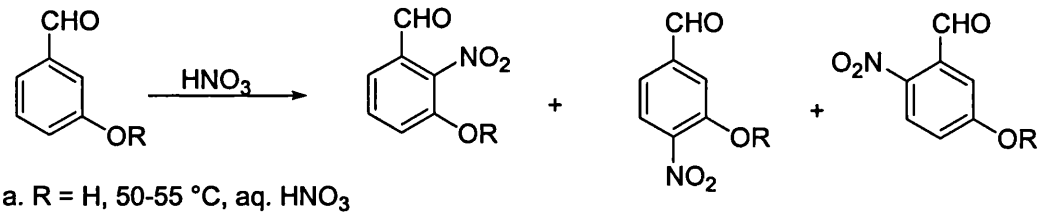

a. R = H, 50-55 °C, aq. HNO_3
b. R = CH_3, 20 °C, conc. HNO_3

Scheme 2.4. Nitration of 3-hydroxy and 3-methoxy-benzaldehydes

Nitration of the 3-methoxy-benzaldehyde was accomplished with concentrated nitric acid at room temperature[4]. The products, 2-nitro and 6-nitro-3-methoxy-benzaldehyde, were separated by recrystallisation from benzene.

In both procedures the presence of hydroxy and methoxy groups in the substrates activates the aromatic ring towards electrophilic substitution, therefore nitration can be carried out in the absence of sulfuric acid. Milder reaction conditions are required in the presence of carbonyl group which is prone to oxidation under harsher conditions.

Direct formylation of the nitro-derivatives by electrophilic substitution is not possible due to the presence of the nitro group which deactivates the aromatic ring toward such reactions. However, Makosza and co-workers were successful in formylation of such substrates by nucleophilic substitution. They reported [5] that reaction of nitro-arenes **67** with chloroform in the presence of ^{t}BuOK in THF/DMF at -70°C followed by acidic quenching afforded the dihalide **68** in high yields. This was further hydrolyzed in refluxing formic acid under nitrogen to give compound **62** in moderate yields.

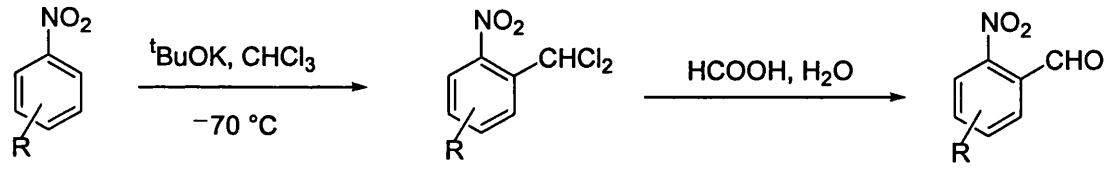

67 **68** **62**

Scheme 2.5. Synthesis of nitrobenzaldehyde **62** by nucleophilic substitution

Another approach [6] to substituted nitrobenzaldehydes (Scheme 2.6) uses nitrobenzyl aryl sulfones **70** which are accesible from nitroarenes **67** and chloromethyl aryl sulfones **69** by nucleophilic substitution[7]. Electrophilic amination of the anions of the sulfones **70**, generated by the treatment of **70** with sodium hydride in DMF, led to aminosulfones **72** which can be cleaved in acidic medium to give aldehydes or ketones **62**, aryl sulfinates and ammonia.

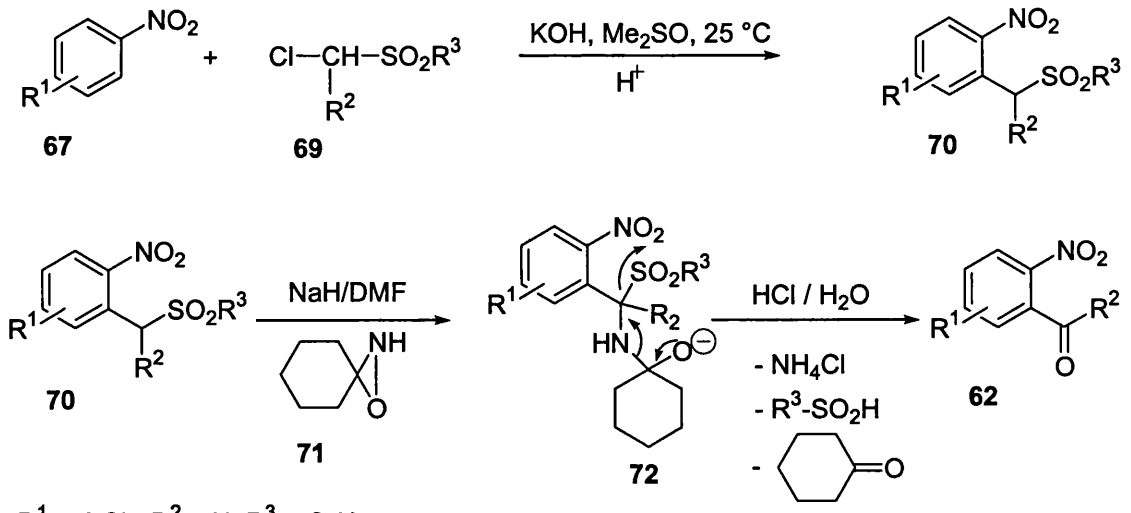

R^1 = 5-Cl-, R^2 = H, R^3 = C_6H_5-;
R^1 = 5-F-, R^2 = H, R^3 = 4-CH_3-C_6H_4-;
R^1 = 5-CH_3O-, R^2 = H, R^3 = 4-CH_3-C_6H_4-.

Scheme 2.6. Synthesis of nitro-benzaldehyde **62** by nucleophilic substitution

The 2-nitro-5-R-benzaldehydes **62** (R = 5-Cl, 5-F, 5-OCH_3) were obtained in moderate yields due to the base-catalyzed decomposition of oxaziridine **71,** which competes with the main reaction.

2.1.2 Reduction of nitrobenzaldehydes

Selective reduction of the nitro group in substituted nitrobenzaldehydes is a challenging process that requires the use of special reducing agents which do not affect the aldehyde and the other groups present in the substrate. The products also have a limited stability under the reaction conditions in which they are generated due to their propensity to undergo self-condensation reactions. Iron sulfate and ammonia were originally used for the reduction of 2-nitro-benzaldehyde[8] and later this procedure was applied to the reduction of a variety of nitro-benzaldehydes in aqueous solution or a mixture of water and ethanol.

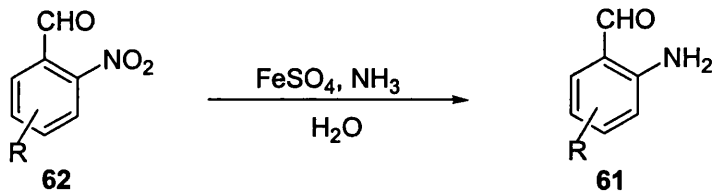

R = H, Cl, CF_3, CH_3, CH_3O

Scheme 2.7. Reduction of nitrobenzaldehydes by Opie's procedure

After reduction, the product was isolated from the complex reaction mixture either by fast steam distillation, followed by induced precipitation, or by filtration and extraction of the filtrate with chloroform[**9**]. In general, good to high yields were obtained for amino benzaldehydes substituted with electron-withdrawing groups (Cl, CF_3), while lower yields were obtained in the case of electron-donating groups (CH_3, CH_3O) [**9, 10, 11**].

Reduction of 4-methoxy-2-nitro-benzaldoxime with H_2S/ NH_4OH in an ethanol-water mixture was reported [**1**] to give the corresponding protected amino-benzaldehyde in high yield (80% yield), but the product was contaminated with sulfur.

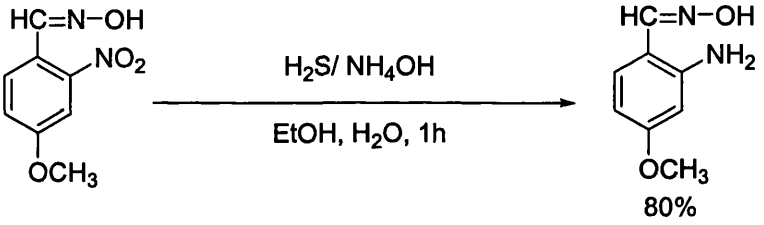

Scheme 2.8. Reduction of nitrobenzaldehydes with H_2S/ NH_4OH

Moderate yields of aminobenzaldehyde were obtained upon reduction of 4-nitro-3-methoxy-benzaldehyde **73** and 5-chloro-2-nitro-benzaldehyde **74** with Na_2S_2 and $Na_2S_2O_4/Na_2CO_3$
[**12, 13**].

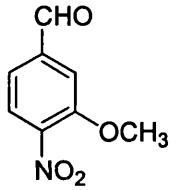

73

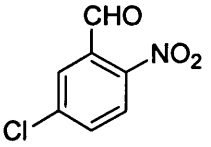

74

Scheme 2.9. Reduction of nitrobenzaldehydes **73, 74** with Na_2S_2 and $Na_2S_2O_4$

Reduction of 3-nitro-benzaldehyde with $SnCl_2$ in acidic medium [**14**] afforded the 3-amino-benzaldehyde hydrochloride salt as red-orange crystals which was further used in synthesis without isolation of the free 3-aminobenzaldehyde. The reaction was strongly

exothermic and required careful control of the temperature and manipulation of the reagents to avoid explosions.

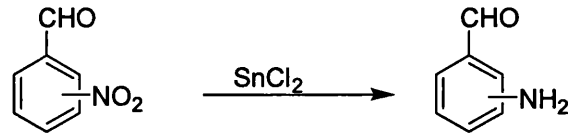

a: 3-NO_2, **b**: 4-NO_2

Scheme 2.10. Reduction of 3- and 4-nitrobenzaldehydes with $SnCl_2$

A milder procedure was reported for reduction of 4-nitrobenzaldehyde with $SnCl_2$ in non-acidic conditions[**15**]. The reaction proceeded in hot ethanol or ethyl acetate under nitrogen in 96 % yield. Many authors mentioned that they encountered difficulties during synthesis and the generated aminobenzaldehydes were used immediately after preparation.

2.1.3. Synthesis of amino-benzyl-alcohols

Another route to obtain substituted aminobenzaldehydes is *via* oxidation of the corresponding amino benzyl alcohols **64** with MnO_2. These can be prepared in high yields either by reduction of substituted amino-benzoic acids **75** with $LiAlH_4$ [**16, 17**] or *via* reduction of nitro-benzyl-alcohols **76** with $NaBH_4$ and $NiCl_2$[**18**] (Scheme 2.11).

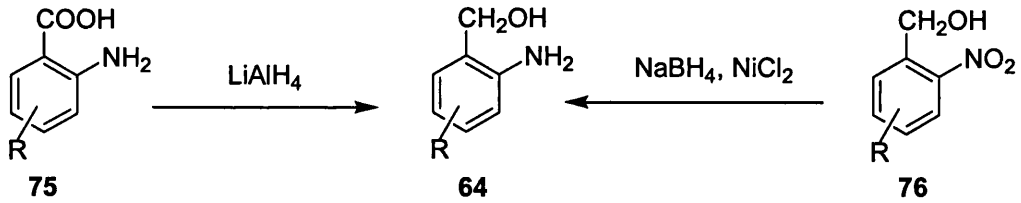

75 **64** **76**

Scheme 2.11. Synthesis of amino-benzyl-alcohols

A previous report in the literature showed that nitro-benzyl alcohol **79a** was accesible *via* bromination of nitrotoluene **77a** with NBS, followed by the hydrolysis of the intermediate benzyl bromide **78a** with sodium carbonate in boiling water[**11**].

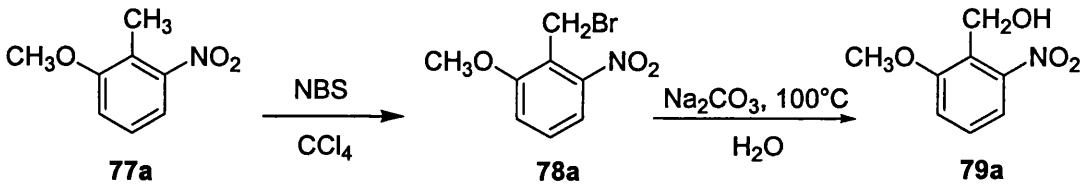

77a **78a** **79a**

Scheme 2.12. Synthesis of nitrobenzyl alcohol **79a** by the hydrolysis of **78a**

2.1.4 Oxidation of amino-benzyl-alcohols

Oxidation of substituted amino-benzyl-alcohols to the corresponding benzaldehyde derivatives by MnO_2 is a free radical process [**17**] (Scheme 2.13).

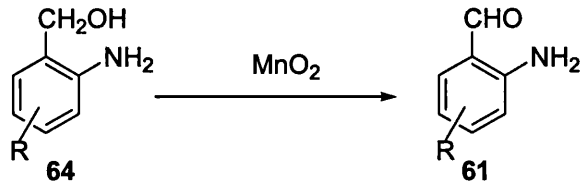

Scheme 2.13. Oxidation of amino-benzyl-alcohols to corresponding benzaldehydes

The process depends on the nature of substituents in the aromatic ring; a change in electron-attracting ability of the substituents gradually increased the rate of the reaction. Methoxy compounds, however, exhibited a different behaviour which was explained in terms of their different adsorption on solid MnO_2.

2.1.5 Other methods

An alternative way of synthesis of aminobenzaldehydes is summarised in the scheme below:

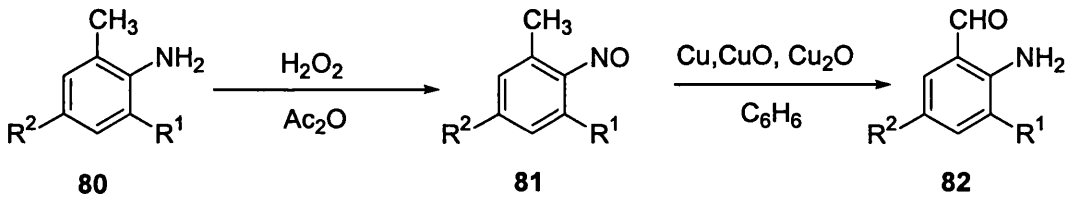

a: $R^1=CH_3$, $R^2=Br$; **b**: $R^1=Br$, $R^2=CH_3$;
c: $R^1=CH_3$, $R^2=Cl$; **d**: $R^1=CH_3$, $R^2=H$.

Scheme 2.14. Synthesis of aminobenzaldehydes **82** from aniline derivatives **80**

The aniline derivative **80** was oxidized with H_2O_2 at room temperature to give the nitrosotoluene **81**. This, in the presence of Cu, CuO or Cu_2O in refluxing benzene rearranged to the aminobenzaldehyde **82**[**19**].

2.2 Results and discussion

2.2.1 Synthesis of nitrobenzaldehydes

There is not a general procedure for preparation of aminobenzaldehyde derivatives **61** However, synthesis by reduction of R-nitrobenzaldehydes **62** with iron(II) sulfate and ammonia uses cheap starting materials and the fact that most of the literature reports in the area utilise this route[**8**], suggesting that the methodology could be applied to different R groups, prompted us to start our investigation with this approach.

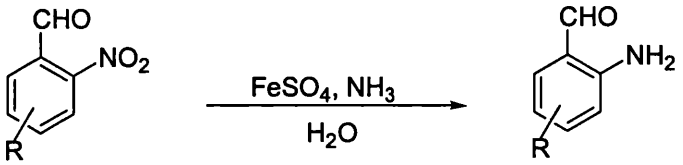

62 **61**

Scheme 2.15. Synthesis of aminobenzaldehydes **61** by reduction of corresponding nitrobenzaldehydes

While 2-nitro-benzaldehyde and 5-chloro-2-nitro-benzaldehyde are commercially available, the other R-nitro-benzaldehydes such as 3- and 5-hydroxy, 3- and 5-methoxy-nitrobenzaldehydes could be obtained by nitration of the 3-hydroxy, respectively 3-methoxy benzaldehyde and separation of the desired isomers. For certain R groups where reduction with with iron sulfate and ammonia would not be efficient, it was hoped that using other reducing agents and different reaction conditions an improved method could be obtained.

Nitration of 3-hydroxy and 3-methoxy benzaldehyde with nitric acid resulted in substitution of *ortho-* and *para-* positions relative to hydroxy, respectively methoxy group with formation of a mixture of three regio-isomers (Scheme 2.16).

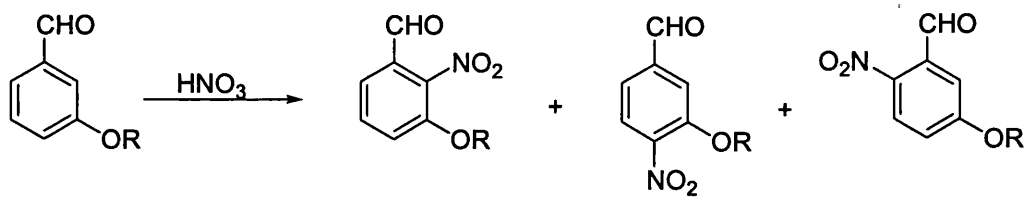

a: R = H	Molar ratio:	1.2	1.4	1.0
b: R = CH_3	Molar ratio:	4.8	1.0	2.1

Scheme 2.16. Nitration of 3-hydroxy and 3-methoxy benzaldehyde

In the reported procedure for nitration of 3-hydroxy-benzaldehyde[**3**], the heat generated during the reaction was used to maintain the mixture at 50-55 °C, the temperature being controlled by a careful addition of the substrate to the mixture of concentrated nitric acid and water. We carried out the reaction on a much smaller scale on which the heat generated during the reaction was not enough to increase the temperature of the reaction mixture more than 20 °C. Therefore, after addition of all of the aldehyde, the temperature was increased gradually to 50-55 °C and maintained for 4 h. Following the usual work-up procedure for nitration reactions, the crude product was obtained as a yellow precipitate and its ^{1}H-NMR spectrum showed it to be a mixture of three isomers. The elemental analysis of the crude indicated the absence of polynitrated products.

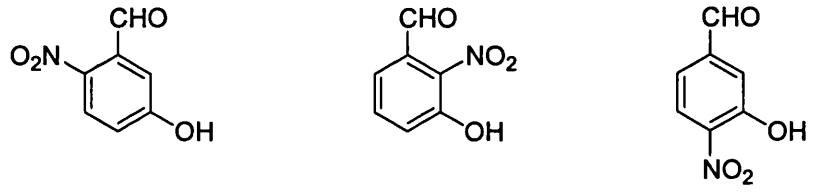

83 **84** **85**

Figure 2.1. Products from nitration of 3-hydroxy-benzaldehyde

We found that a good separation of the three isomers could be achieved by fractional crystallisation from hot benzene. Upon cooling the mixture, brown 2-nitro-5-hydroxy-benzaldehyde (**83**) precipitated from the warm benzene solution and was separated by filtration. Cooling the mixture to room temperature led to precipitation of orange 2-nitro-3-hydroxy-benzaldehyde (**84**), while evaporation of the solvent from the obtained filtrate gave the yellow 4-nitro-3-hydroxy-benzaldehyde (**85**). The identity of all three isomers was established by ^{1}H-NMR. Further purification by steam distillation as previously described [**3**] was not necessary.

Following the procedure reported for nitration of 3-methoxy-benzaldehyde [**4**] no precipitate was formed after the usual work-up procedure. The two liquid layers were separated and the ^{1}H-NMR of the organic layer showed that it contained unreacted starting material with traces of product. Unreacted substrate was also recovered when the nitration was performed using the conditions employed in the case of 3-hydroxy-benzaldehyde.

The reaction took place only when concentrated nitric acid was used in excess (aldehyde : nitric acid = 1 : 5) and the mixture was heated gradually to 50 °C. A 50 % conversion of 3-methoxy-benzaldehyde was obtained after 4 h and even after longer reaction periods the conversion was still not complete. After 3-4 h the concentration of the nitric acid in the mixture decreases considerably and the water generated during the process transforms the initial homogeneous system into a heterogeneous one, moving the reaction from the bulk of the liquid phase to the interface between the two liquid phases. Both these factors decrease the rate of the nitration to such an extent that the reaction almost stops.

In order to achieve complete conversion of the aldehyde, the aqueous layer was separated from the organic phase, fresh nitric acid was added to it and the temperature was gradually increased to 50 °C. This procedure was repeated until all of the 3-methoxy-benzaldehyde reacted. At the end of the reaction the crude product was subjected to the usual work-up procedure to give a yellow precipitate (65 % yield).

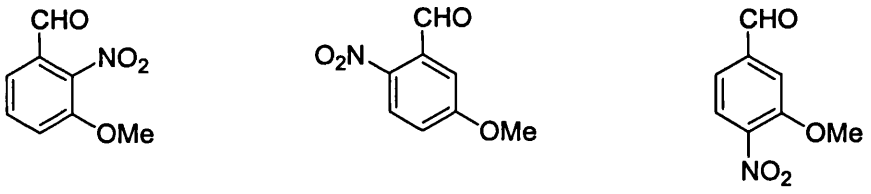

86 **87** **88**

Figure 2.2. Products from nitration of 3-methoxy-benzaldehyde

The ^{1}H-NMR showed it was a mixture of the expected three isomers: 2-nitro-3-methoxy (**86**), 2-nitro-5-methoxy (**87**) and 4-nitro-3-methoxy-benzaldehydes (**88**) (Figure 2.2) which were separated by fractional crystallisation from benzene, the most insoluble being 3-methoxy-2-nitro-benzaldehyde. Separation was more difficult than in the case of the crude mixture obtained from nitration of 3-hydroxy-benzaldehyde.

2.2.2 Reduction of 2-nitro-benzaldehydes

Reduction of nitrobenzaldehyde to 2-amino-benzaldehyde **61a** with iron sulfate and ammonia was performed according to Opie's procedure [**8**]. To avoid degradation of the product *via* self-condensation reaction, this was separated from the reaction mixture by

fast steam distillation. Saturation of the aqueous distillate with sodium chloride led to precipitation of **61a** as a light yellow solid (70 % yield).

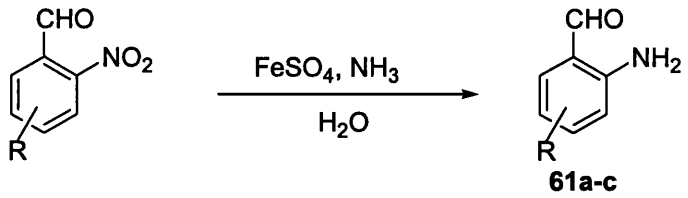

61a-c

a: R=H, **b**: R=5-Cl, **c**: R=3-CH_3O

Scheme 2.17. Synthesis of amino-benzaldehydes **61 a-c**

5-Chloro- and 3-methoxy-2-amino-benzaldehydes (**61b, 61c**) were prepared in a similar way from the appropriate nitro-benzaldehydes in 55 and 50 % yield respectively. 5-Chloro-2-nitrobenzaldehyde is commercially available as a technical mixture containing small amounts of 3-chloro-4-nitro-benzaldehyde, 5-chloro-2-nitro-benzoic acid and sulfuric acid. In this case the reducing agent was added in excess so that all the nitro-derivatives present in the technical 5-chloro-2-nitro-benzaldehyde were reduced to the corresponding aromatic amines. Separation of the product **61b** from the reaction mixture was possible due to the difference in volatility between 5-chloro-2-amino-benzaldehyde (**61b**) and 3-chloro-4-amino- benzaldehyde (**89**).

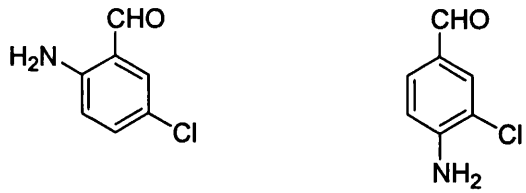

61b **89**

Figure 2.3. Products from reduction of chloro-aminobenzaldehydes

An experiment was set up to compare the difference in reactivity and stability of the three methoxy-nitro-benzaldehydes in the reduction with iron(II) sulfate and ammonia in aqueous solution. After the reduction of a nitro-benzaldehydes mixture was performed, the reaction mixture was either steam distilled or the products were extracted in dichloromethane and the composition of these mixtures was determined by ^{1}H-NMR.

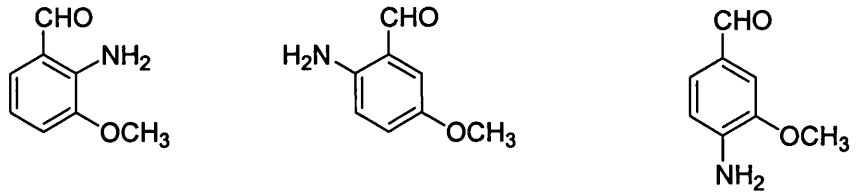

61c **61d** **61g**

Figure 2.4. Amino-3-methoxy-benzaldehydes synthesized

From the experiment involving steam distillation we found that 2-amino-3-methoxy-benzaldehyde **61c** was the most volatile product, 4-amino-3-methoxy **61g** showed low volatility (ratio **61c** : **61g** was 9 : 1), while 2-amino-5-methoxybenzaldehyde (**61d**) was not volatile. Using a work-up procedure involving extraction in dichloromethane it was found that the yield of 2-amino-5-methoxy-benzaldehyde (**61d**) was approximately half of that for 2-amino-3-methoxy isomer (**61c**), while 4-amino-3-methoxy-benzaldehyde (**61g**) was obtained in high yield from the corresponding nitro-benzaldehyde. As there was no unreacted 3-methoxy-nitro-benzaldehyde in the dichloromethane extract (by ^{1}H-NMR), these results imply that the stability of the mentioned amino-3-methoxy-benzaldehydes decreases in the order **61g** > **61c** > **61d**. This is in agreement with the work published by Wall [**11**], who reported that the yield of methoxy aminobenzaldehydes resulted by reduction of nitrobenzaldehydes with iron sulfate and ammonia depends on the position of the methoxy group relative to the carbonyl group in the aromatic ring. Thus, 3-methoxy-nitrobenzaldehyde **61c** was prepared in moderate yield (67%), while a low yield (29 %) was obtained in synthesis of 5-methoxy-2-aminobenzaldehyde **61d**.

Based on these results it was concluded that reduction of 2-nitro-3-methoxy-benzaldehyde (**61c**) following the mentioned procedure does not require a high purity starting material, the difference in volatility between the 2-amino-3-methoxy-benzaldehyde and the other regio isomers being high enough for separation of the former as a pure product. The reducing system iron sulfate and ammonia cannot be applied for reduction of 2-nitro-5-methoxy-benzaldehyde as the generated aldehyde (**61d**) gives rapid degradation due to side reactions.

2-Amino-benzaldehydes have been reported to be unstable at room temperature due to a self-condensation reaction. They cannot be dried completely as removal of water

favours this process and it was recommended to be used immediately after synthesis. However, we found that it is possible to preserve the 2-amino-benzaldehydes **61a** and **61b** for two weeks without degradation in a small amount of mother solution. Other amino-benzaldehydes having electron-donating substituents (*e.g.* OCH_3, CH_3) in the ring are more prone to self-condensation which is even faster in presence of metal ions (Fe^{2+} and Fe^{3+}) as in Opie's procedure. These results determined us to investigate a different synthetic route toward them using the Duff reaction.

2.2.3 Duff reaction

The Duff reaction involves the transformation of aniline **63** into Schiff base(s) **90**, followed by acidic hydrolysis to the desired aldehyde.

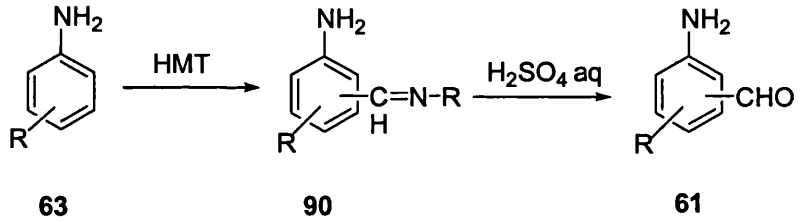

63 **90** **61**

Scheme 2.18. Duff reaction on anilines

The method was previously applied on *N,N'*-substituted anilines and *ortho-*, *para-*, *meta-* toluidines giving 4-formyl-anilines **91** in 35-45 % yield [**20**]. Duff reported that *o* and *p*-toluidines did not react in the same way, but did not give further details of these results. Better yields (55-95 %) were obtained in formylation of alkylbenzenes such as **92** (Figure 2.5) with hexamethylenetetramine and CF_3COOH. For 2,6-dimethyl-phenol and 2,6-dimethylanisole **93 a-b**, substitution was directed by the hydroxy/methoxy groups and not by the methyl groups [**21**].

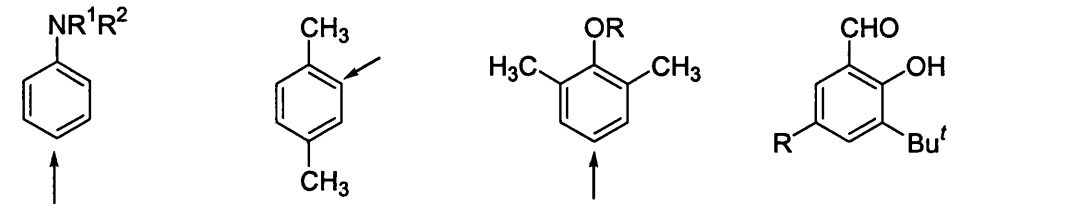

91 **92** **93** **94**

Figure 2.5. Substrates used in Duff reaction and position of substitution

More recently, the Duff reaction was employed by Jacobsen [22] towards the synthesis of a series of 3-*t*-butyl-5-substituted salicylaldehydes **94** from the corresponding phenol derivatives. In this case formylation occurs in the *ortho-* and *para-* position relative to the hydroxy group. We attempted to adapt this procedure for formylation of 2,4-dimethyl-aniline **95** and 4-methyl-aniline **96**.

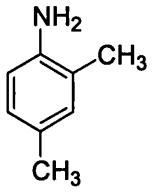

95

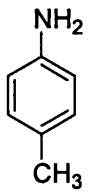

96

Figure 2.6. Aniline derivatives employed in Duff reaction

For these methyl anilines, which have already a substituent in the *para* position, formylation is expected to take place only in *ortho-* relative to the amino group. The Duff reactions on both substrates **95** and **96** were performed using the conditions described by Jacobsen [22]. Reaction of hexamethylenetetramine with 2,4-dimethyl-aniline **95** in hot acetic acid (100 °C) led to a mixture of aldehydes and Schiff bases (Scheme 2.19).

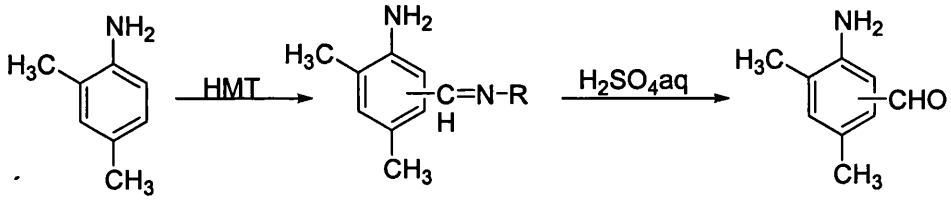

95 **97-98** **61h**

Scheme 2.19. Duff reaction on 2, 4-dimethyl-aniline

Hydrolysis with sulfuric acid followed by addition of diethyl ether to the cold mixture led to formation of a red-orange precipitate which was separated by filtration. The ^{1}H-NMR spectrum of the precipitate revealed a mixture of three Schiff bases in the ratio 1 : 17 : 3, having the imine protons at δ 8.57, 8.36 and 8.21. The major compound in the mixture exhibits a singlet at δ 8.36 corresponding to the imine group proton, two doublets at δ 7.35 and 7.13 due to H^{5*} and H^{6*}, together with three singlets at δ 7.14, 6.94 and 6.64, which correspond to H^6, H^{3*} and H^4. The spectrum has also a singlet at δ

4.91 which was assigned to the protons from the NH_2 group and four singlets at δ 2.41, 2.35, 2.33, 2.28 corresponding to the four different methyl groups.

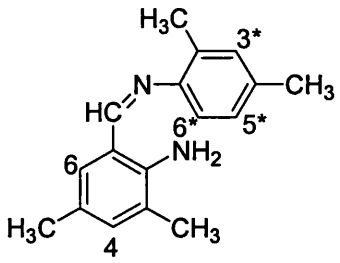

97

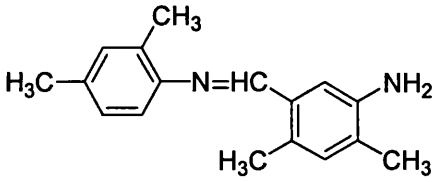

98

Figure 2.7. Structures of the intermediate Schiff bases

It could then be concluded that formylation had occured mainly in one position of the aromatic ring, however it was not possible to distinguish between the two possible structures **97** and **98** (Figure 2.7) of the product. In analogy with the mechanism proposed for formylation of alkyl phenols, the compounds **97-98** are obtained by a sequence of steps summarised in Scheme 2.20.

Aniline **95** reacts with hexamethylenetetramine to give benzylamine **100** by electrophilic substitution. Previous reports proposed the electrophile **99** based on 0.4 - 0.5 rate order in concentration of HMT for this step. The amine **100** is dehydrogenated in the system to the imine **101** which hydrolyses leading to the aminobenzaldehyde **61**. The dehydrogenating agent changes from compound **102** which acts in early stages of the process, to compound **103** formed later on in the system. The aminobenzaldehyde **61** undergoes condensation with different amines present in the system and this explains the large number of imine protons which appear in the ^{1}H-NMR spectrum of the reaction mixture before and after hydrolysis. It is expected that Schiff base **97-98** is one of the major compounds in the mixture as 2,4-dimethylaniline **95** is present in larger amount than the other amines.

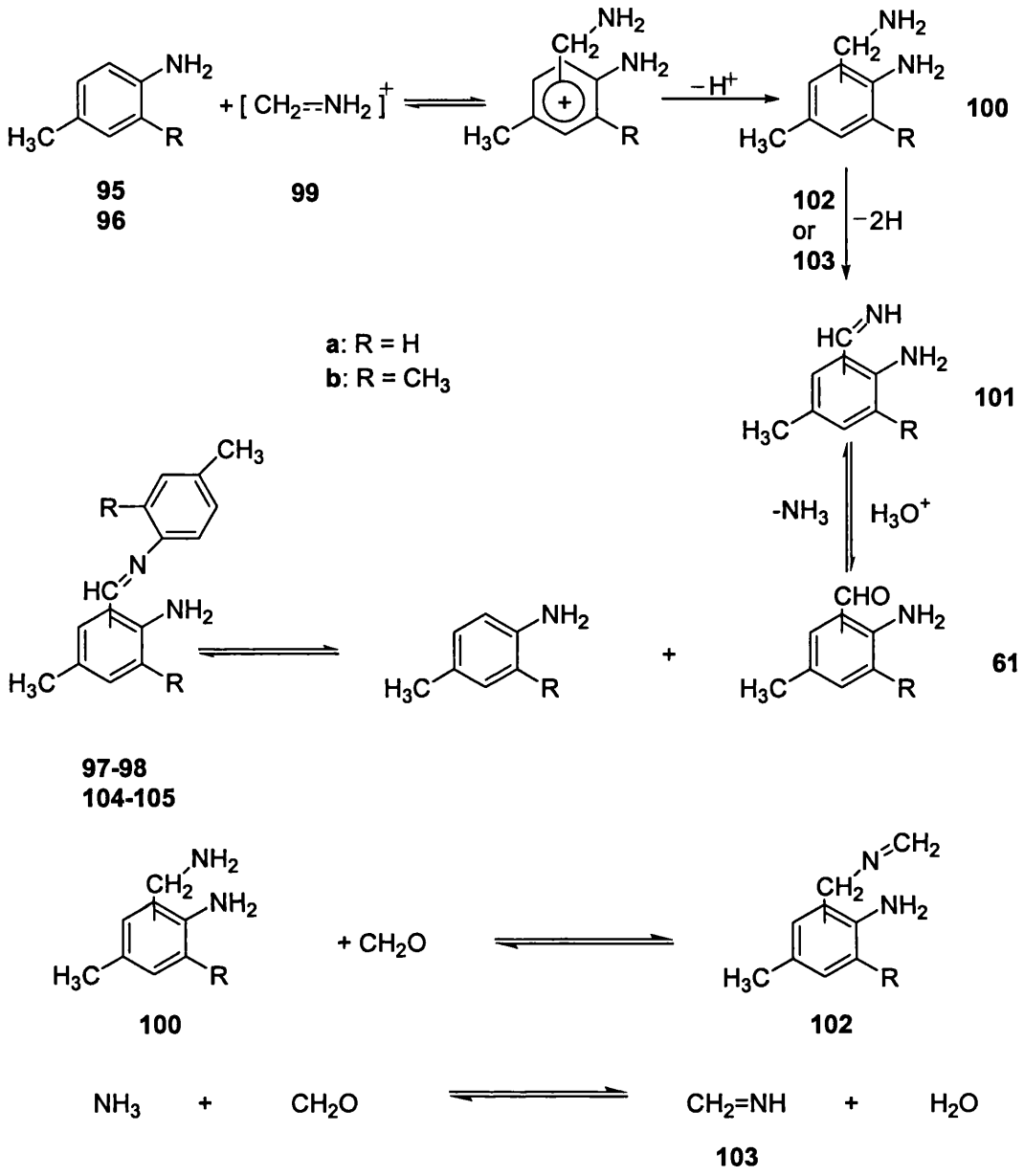

Scheme 2.20. Mechanism of Duff reaction

Acetic acid is present in excess which implies that at least part of the aromatic amine is protonated (Figure 2.8). While for 2,4-dimethyl-aniline (**95a**) one would expect electrophilic attack to take place mainly in the sixth position of the aromatic ring, in the protonated aniline **95b,** the attack will occur in the fifth position. Thus, the composition of the reaction mixture depends on the amount of free aniline in the system and also on the difference in reactivity of the two positions (5^{th} and 6^{th}) in the free and protonated substrate.

95a R = H, CH_3 **95b**

Figure 2.8. Electrophilic attack in the free and protonated aniline **95 a, b**

The presence of aromatic amine groups in these Schiff bases (Figure 2.7) hampers the hydrolysis by preventing the protonation of the imine nitrogen. Using more acid and longer periods for hydrolysis of the orange-red precipitate did not help in completion of the reaction and it is also likely that the amino-benzaldehyde generated in strong acidic conditions did not survive. Steam distillation of the reaction mixture followed by extraction of the distillate with dichloromethane indicated the presence of small amounts of 3,5-dimethyl-2-amino-benzaldehyde by ^{1}H-NMR.

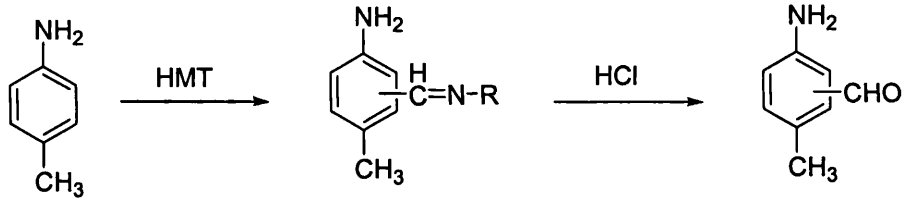

Scheme 2.21. Duff reaction on 4-methyl-aniline **96**

Formylation of 4-methyl-aniline **96** with hexamethylenetetramine in acetic acid was performed under similar conditions to those employed for 2,4-dimethyl-aniline **95**, but in the hydrolysis of the Schiff bases hydrochloric acid was used since it generates salts which are more unstable toward hydrolysis than those obtained from sulfuric acid [**20**].

Upon addition of ether, an orange precipitate was formed which was separated by filtration. The ^{1}H-NMR spectrum of the precipitate indicated a major Schiff base that presents a singlet at δ 8.27 which was assigned to the imine group. Two doublets at δ 7.49 and 7.15 were assigned to H^4 and H^3, while those from δ 7.34 and 7.26 to H^{2*} and H^{3*} based on their integrals. The H^6 proton resonates at δ 6.89. The spectrum also contains a singlet at δ 5.15 corresponding to the protons from the NH_2 group and two other singlets at δ 2.42 and 2.35, corresponding to the two methyl groups. These data suggest the structure **104-105** for the intermediate Schiff base.

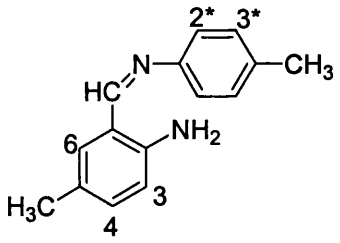

104

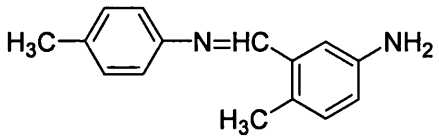

105

Figure 2.9. Structures of the intermediate Schiff bases **104-105**

Different attempts were carried out to hydrolyse the mixture of Schiff bases. Adjusting the pH of an ethanolic solution of the orange precipitate, to 8-9 with saturated aqueous sodium carbonate, followed by heating led to disappearance of the peak corresponding to the Schiff base **104-105** by ^{1}H-NMR (δ 8.27). However, the same spectrum gave no indication that the sample contained free amino-benzaldehyde, implying that it had probably decomposed under these conditions.When the ether layer was washed with base (Na_2CO_3) and water until neutral pH, then dried and separated on an alumina column, all the fractions collected were mixtures of aldehydes and Schiff bases by ^{1}H-NMR, the major compound showing a singlet at δ 8.77, however the complexity of the spectra prevented further interpretation.

As this route did not seem viable, we considered achieving the synthesis of methyl-amino-benzaldehydes by oxidation of the corresponding amino benzyl alcohols **64** with MnO_2, although this involved more expensive starting materials.

2.2.4 Synthesis of aldehydes from amino-benzyl-alcohols

The general procedure for oxidation of benzyl alcohols by manganese dioxide[**17**] was adapted for synthesis of 2-amino-R-benzaldehydes (R = H, 3-CH_3, 5-CH_3) (**61a, 61e, 61f**) from the corresponding 2-amino-benzyl alcohols.

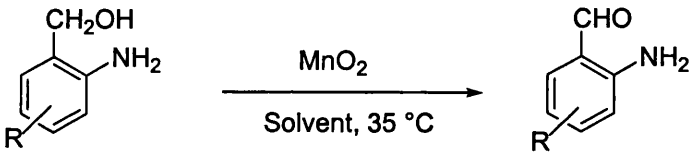

64 a, e, f **61a, e, f**

a: R = H, **e**: R = 3-CH_3, **f**: R = 5-CH_3

Scheme 2.22. Synthesis of amino-benzaldehydes **61a, 61e, 61f** by oxidation of corresponding amino-benzyl-alcohols

Activation of manganese dioxide was achieved according to Goldman's procedure[**23**], the wet catalyst being heated in refluxing benzene and water gradually being removed as an azeotrope from the system in a Dean-Stark trap. Addition of 2-amino-3-methyl-benzyl alcohol (**64e**) as a benzene solution to the activated manganese dioxide in dry degassed benzene was performed under nitrogen, then the system was heated gently (35 °C) with stirring overnight. The product 2-amino-3-methyl benzaldehyde (**61e**) was separated next day by filtration as a yellow solution. The solubility of the product in benzene is not high, therefore after filtration, the black solid residue was extracted a few times with dry degassed dichloromethane and filtered under nitrogen in order to obtain a good yield.

Syntheses of 2-amino-5-methyl-benzaldehyde and 2-amino-benzaldehyde (**61f, 61a**) were achieved using similar procedures. Other solvents (ether, dichloromethane) were employed to avoid some practical problems related with the low solubility of 2-amino-R-benzyl-alcohols **64** in benzene at room temperature. The oxidation is a selective process, 2-amino-R-benzaldehyde (R = H, 3-CH_3, 5-CH_3) being the only isolated product as confirmed by ^{1}H-NMR. The 2-amino-benzaldehydes **61a, 61e, 61f** were preserved at room temperature under nitrogen as dichloromethane solutions. They proved to be stable under these conditions for few weeks without degradation (by ^{1}H-NMR).

2.2.5 Bromination of 5-methoxy-2-nitro-toluene

A previous report in the literature showed that nitrobenzyl alcohol **79a** was accesible *via* bromination of nitrotoluene **77a** with *N*-bromosuccinimide (NBS), followed by the hydrolysis of the intermediate benzyl bromide **78a** with sodium carbonate in boiling water[**11**].

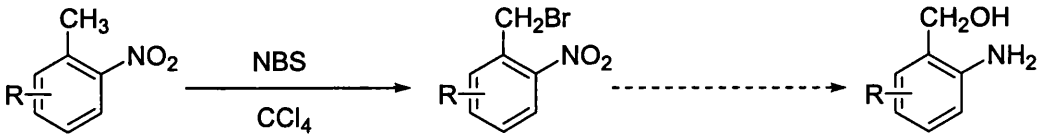

77 **78** **79**

a: R = 6-CH_3O **a**: R = 6-CH_3O
b: R = 5-CH_3O **b**: R = 5-CH_3O

Scheme 2.23. Synthetic route toward 5-methoxy-amino-benzyl-alcohol

We adapted this procedure for bromination of 5-methoxy-2-nitro-toluene (**77b**). Thus, the reaction took place upon stirring **77b** with *N*-bromosuccinimide and benzoyl peroxide in tetrachloromethane for 5-6 days at reflux. During this time, samples were taken from the reaction mixture and analysed by ^{1}H-NMR. In spite of addition of more benzoyl peroxide and upon employing a longer reaction time than that reported for its regioisomer **77a**, the conversion of the starting material was not complete (67 %). After the above mentioned period, the mixture was cooled and filtered. Attempts to induce crystallisation of the product **78b** by addition of ether-hexane to the tetrachloromethane solution were not successful.

The ^{1}H-NMR spectrum of the crude mixture showed together with the signals associated to the starting materials, the formation of two different compounds in the ratio 2.8 : 1. The major compound presented in the aromatic region a doublet at δ 8.15 (J = 9.1 Hz), a doublet of doublets at δ 6.92 (J = 9.1 and 2.8 Hz) and another doublet at δ 7.02 (J = 2.8 Hz). This suggested that the first two protons (H^3 and H^4) were attached to adjacent carbon atoms in the aromatic ring, while the last two were in *meta-* to one another (H^4 and H^6). The compound presented two singlets at δ 4.86 and 3.91, corresponding to the protons from methylene and methoxy groups. Based on this data it was concluded that this compound was 2-nitro-5-methoxy-benzyl bromide (**78b**).

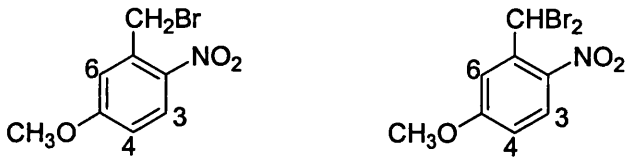

78b **106**

Figure 2.10. Products from bromination of 5-methoxy-2-nitro-toluene

The ^{1}H-NMR signals for the minor product indicated that this was 5-methoxy-2-nitro-benzylidene dibromide (**106**). Due to the long reaction time and the problems related with separation of the product it was decided to use a different synthetic route to 5-methoxy-2-nitro-benzaldehyde.

2.2.6 Methylation of 5-hydroxy-2-nitro-benzaldehyde

We have seen in section **2.2.1** that nitration of 3-methoxy-benzaldehyde is a slower process than nitration of related 3-hydroxy-benzaldehyde and for this reason it required a longer reaction time and harsher reaction conditions (*i.e.* concentrated nitric acid in excess). At the same time, separation of 5-methoxy-2-nitro-benzaldehyde from 3-methoxy-4-nitro-benzaldehyde proved more difficult than the isolation of the 5-hydroxy-2-nitro-benzaldehyde from the corresponding nitration mixture. These results prompted us to investigate an alternative route to 5-methoxy-2-nitrobenzaldehyde (**62d**) and the corresponding amino-benzyl-alcohol, as summarised in Scheme 2.24.

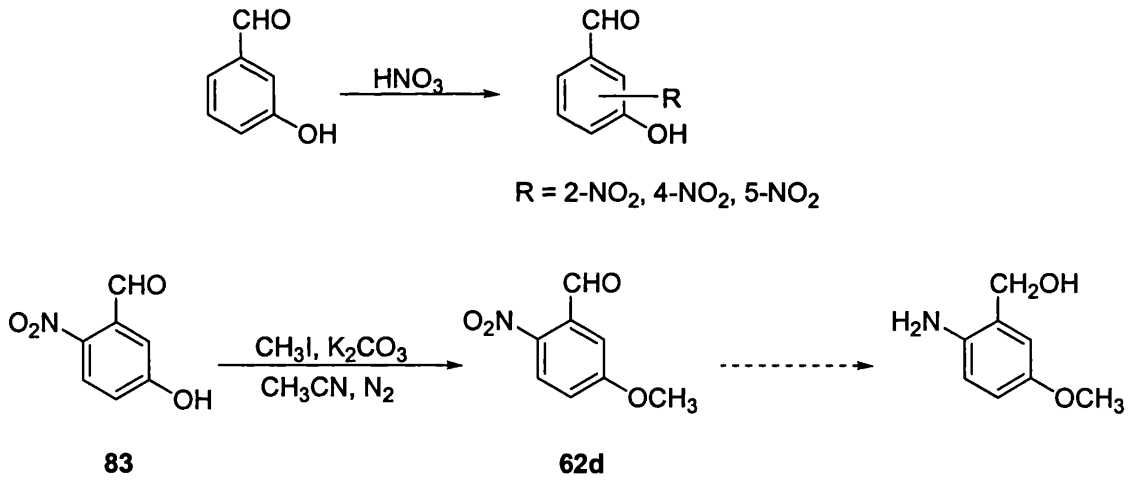

Scheme 2.24. Synthetic route to 5-methoxy-amino-benzyl alcohol

The general procedure for protection of phenols[**24**] as their methyl ethers was adapted for methylation of 5-hydroxy-2-nitro-benzaldehyde (**83**). 5-Hydroxy-2-nitro-benzaldehyde reacted quantitatively with methyl iodide under basic conditions (K_2CO_3), in dry acetonitrile at 55 °C, to give the corresponding 5-methoxy-2-nitro-benzaldehyde (**62d**). A gentle nitrogen flow ensured protection of the reaction mixture against moisture, this preventing the hydrolysis of methyl iodide. After cooling to room temperature the product, which is soluble in acetonitrile, was separated from small

amounts of brown precipitate (unreacted substrate) by filtration. Removal of the solvent under vacuum gave an orange powder of 5-methoxy-2-nitro-benzaldehyde (**62d**).

The ^{1}H-NMR spectrum of this compound displayed a singlet at δ 10.5 assigned to the carbonyl group proton, two doublets at δ 8.17 and 7.34 corresponding to H^3 and H^6 and a doublet of doublets at δ 7.16 assigned to H^4 by its couplings with the adjacent H^3 and the *meta*- H^6. The protons corresponding to the methoxy group appear at δ 3.97. These data are consistent with the proposed structure **62d**.

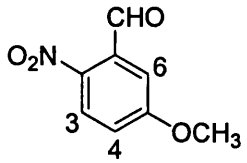

62d

Figure 2.11. Product from methylation of 5-hydroxy-2-nitro-benzaldehyde

2.2.7 Synthesis of ambch ligands

Synthesis of *N,N'*-bis-(2,2'-iminobenzylideneimino)-cyclohexane (**107**) was achieved upon condensation of 2-amino-benzaldehyde (**61a**) with 1,2-diaminocyclohexane in refluxing ethanol. At the end of the reaction the solvent was removed and the product was obtained as a light yellow powder on recrystallization from ethanol or by precipitation from CH_2Cl_2 with petroleum spirit.

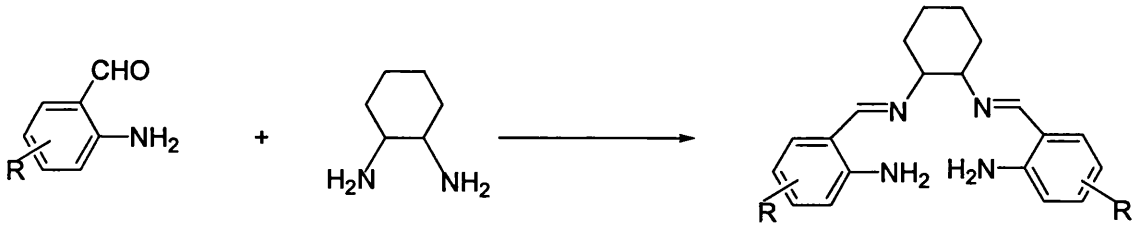

61a-c, e, f

Compound (yield)
107: R = H (81 %)
108: R = Cl (76 %)
109: R = 3-CH_3O (82 %)
110: R = 3-CH_3 (85 %)
111: R = 5-CH_3 (78 %)

Scheme 2.25. Preparation of ambch ligands

The formation of side products from self-condensation reaction of 2-amino-benzaldehyde **61a** is kinetically unfavourable. This is because the aromatic amino group is less reactive than the aliphatic diamine in the nucleophilic attack toward the carbonyl compound. One way of approximating the electron density around the nitrogen atom and therefore the nucleophilicity of the two amines present in the system is by comparing the basicity of the two types of amines. While the basicity constant for aliphatic amines is $\approx 10^{-4}$, that for aromatic amines is $\approx 10^{-10}$, which makes the latter less reactive in the condensation reactions with carbonyl compounds.

The ^{1}H-NMR spectrum of this ligand (**107**) shows a singlet at δ 8.25 corresponding to the proton from the imino group. It also exhibits an asymmetric quintet at δ 7.08 which results from the overlap of a doublet and triplet for H^6 and H^4 respectively. The other two protons H^3, H^5 also overlap and give an asymmetric triplet at δ 6.60. The protons from the amino group appear at δ 6.29 and those from cyclohexylidene moiety give multiplets at δ 3.24 and between δ 1.46 - 1.92.

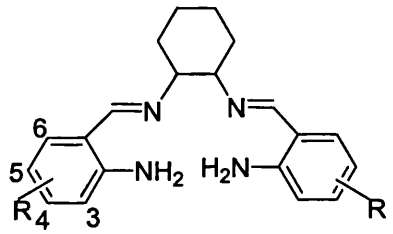

107-111

Figure 2.12. Symmetrical ambch ligands

Other double Schiff bases **108-111** derived from substituted amino-benzaldehydes were prepared in a similar way and their structure was confirmed by ^{1}H-NMR, IR and mass spectroscopy. Introducing a substituent R in the aromatic ring in the third (CH_3, CH_3O) or the fifth position (CH_3, Cl) determined a shift in the position corresponding to the imine proton toward lower field and respectively higher field. The effect of the substituent in the fifth position (0.06-0.11 ppm) was bigger than the one induced by the substituent in the third position. The signal assigned to the amino group protons showed a bigger shift downfield (0.11-0.21 ppm) in the 3-substituted igands, while only small variations in the chemical shifts of 5-substituted ligands were found. The IR spectra of these ligands present very strong absorptions between 1627 and 1630 cm^{-1} corresponding to the imine group.

2.3 Conclusions

Three different synthetic routes toward synthesis of 2-amino-R-benzaldehydes (**61**) were investigated, namely: reduction of 2-nitro-R-benzaldehydes by Opie's procedure, Duff reaction and oxidation of 2-amino-benzyl alcohols with manganese dioxide.

Applying the first route 2-amino-benzaldehyde and 2-amino-5-chloro-benzaldehyde (**61 a, b**) were obtained in good to moderate yield. A comparative study performed for reduction of an equimolecular mixture of 2-nitro, 4-nitro and 6-nitro-3-methoxy-benzaldehydes has shown that these substrates were reduced to the corresponding amino-benzaldehydes in a yield which depended on the relative position between the nitro- and the methoxy- groups in the aromatic ring. The yield for reduction of 2-nitro-3-methoxy-benzaldehyde was moderate, while that for 6-nitro-3-methoxy-benzaldehyde was low. Among the products resulted from reduction of the mentioned nitro-benzaldehydes, only 3-methoxy-2-amino-benzaldehyde (**61c**) was volatile enough to allow separation from the reaction mixture by steam distillation. Using a different work-up procedure for reduction of 3-methoxy-6-nitro-benzaldehyde, small amounts of corresponding amino-benzaldehyde were isolated, although in low yield and it was decided to test other routes towards synthesis of this amino-benzaldehyde.

Syntheses of 2-amino-3,5-dimethyl-benzaldehyde and 2-amino-5-methyl-benzaldehyde were attempted by Duff reaction. A Schiff base was isolated from the mixture in each reaction and the NMR analysis indicated that formylation did occur, however it was not clear if it took place in the *ortho-* position relative to amino or to the methyl group. This possible change in expected regioselectivity could be determined by the acidic conditions employed. Different hydrolysis conditions were tested, however either the Schiff base was too stable to hydrolysis (acidic conditions) or the amino-benzaldehydes were not stable (the others). The higher stability of these amino-Schiff bases toward hydrolysis than usual Schiff bases was determined by the presence of amino-groups in the aromatic ring.

Oxidation of 2-amino-R-benzyl-alcohols (R = H, 3-Me, 5-Me) with manganese dioxide led to the corresponding amino-benzaldehydes (**61 a, e, f**) in 81-85 % yield. These results prompted us to apply this route to synthesis of 2-amino-5-methoxy-benzaldehyde

(**61d**). The first steps towards synthesis of 5-methoxy-2-amino-benzylalcohol from 5-methoxy-2-nitro-toluene and from 5-hydroxy-2-nitro-benzaldehydes were also performed. Bromination of the former led to a mixture of mono and dibromo-products, while methylation gave the desired 5-methoxy-2-nitro-benzaldehyde in high yield. The results obtained from the synthetic routes investigated have indicated that the stability of 2-amino-benzaldehydes varies with the nature of R group, its position in the aromatic ring and also with the reaction conditions in which the amino-benzaldehydes are generated. Careful manipulation allows storage and use of these intermediates for few weeks without degradation.

The chapter concludes with the synthesis of R-ambch ligands **107-111** (R = H, 5-Cl, 3-MeO, 3-Me and 5-Me) by condensation of 1,2-diaminocyclohexane with the R-substituted-2-amino-benzaldehydes in good yield.

2.4 References

1. W. R. Boon, *J.Chem. Soc.*, **1949**, S 230.
2. G.M. Bennett, E.V. Bell, *Org. Syn. Coll., II*, **1947**, 223.
3. W.S. Saari, S.W. King, V.J. Lotti, A. Scriabine, *J. Med. Chem.*, **1974**, *17*,1086.
4. H.H. Hodgson, H.G. Beard, *J. Chem. Soc.*, **1927**, 2375.
5. M. Makosza, Z. Owczarczyk, *Tetrahedron Lett.*, **1987**, *28*, 3021.
6. J. P. Wulf, K. Sienkiewicz, M. Makosza, E. Schmitz, *Liebigs Ann.Chem.*, **1991**, 537.
7. M. Makosza, J. Golinski, J. Baran, *J.Org.Chem.*, **1984**, *49*, 1488.
7. L.I. Smith, J.W. Opie, *Org. Syn.*, **1948**, *28*, 11.
8. M.C. Wani, A.W. Nicholas, G. Manikumar, M.E. Wall, *J. Med. Chem.*, **1987**, *30*, 1774.
9. P. Shanmugam, R. Palaniappan, N. Soundararajan, T.K. Thiruvengadam, K. Kanakarajan, *Monatsh. Chem.*, **1976**, *107*, 259.
10. M.C. Wani, M.E. Wall, *J. Org. Chem.*, **1969**, *34*, 1364.
11. H.H. Hodgson, H.G. Beard, *J. Chem. Soc.*, **1925**, *127*, 875.
12. J.K. Horner, D.W. Henry, *J. Med. Chem.* **1968**, *11*, 946.
13. J.S. Buck, W.S. Ide, *Org. Syn.Coll., II*, **1947**, 130.
14. F.D. Bellamy, K. Ou, *Tetrahedron Lett.*, **1984**, *25*, 839.

15. D.S.C. Black, C.H.B. Vanderzalm, L.C.H. Wong, *Aust. J. Chem*, **1982**, 2435.

16. R.F. Nystrom, W.G. Brown, *J. Am. Chem. Soc.*, **1947**, *69*, 2548.

17. G.H. Jones, M.C. Venuti, R. Alvarez, J.J. Bruno, A.H. Berks, A. Prince, *J. Med. Chem.*, **1987**, *30*, 295.

18. V.I. Rybinov, M.Ya. Mustafina, M.V. Gorelik, *J. Org. Chem. USSR*, **1992**, 1786.

19. J. Duff, *J. Chem. Soc.*, **1945**, 276.

20. W.E. Smith, *J. Org. Chem.*,**1972**, *37*, 3972.

21. J.F. Larrow, E.N. Jacobsen, *J. Org. Chem.*, **1994**, *59*, 1939.

22. I. M. Goldman, *J. Org. Chem.*, **1969**, *34*, 1979.

23. T. W. Green, P.G.M. Wuts, *Protective Groups in Organic Synthesis*, 3rd ed., Wiley, New York, **1999**, p 23.

Chapter 3 Synthesis of symmetrical ambch complexes

3.1 Nickel double Schiff base complexes

3.1.1 Nickel amben type complexes

Green and Tasker [1] have reported the preparation of several nickel amben type complexes **112a-h** possessing different diimine bridges (Figure 3.1) in which the ligands were derived from 2-aminobenzaldehyde, *N*-methyl-2-aminobenzaldehyde or 2-aminobenzophenone. Synthesis was easily achieved for complexes with the strongest ligand fields and the least strained arrangement of the nitrogen donor atoms. The methods employed were: (i) addition of a methanolic solution of a nickel salt to the free ligand in refluxing methanol in the presence or absence of sodium methoxide; (ii) addition of an aqueous solution of nickel(II) sulfate and ammonia to the ligand in refluxing methanol; (iii) reduction of the aromatic nitro double Schiff base with hydrogen in methanolic solution of nickel(II) acetate containing a palladium-charcoal catalyst; (iv) the reaction of nickel(II) acetate with the ligand formed *in situ* by condensation of the appropriate aldehyde and diamine.

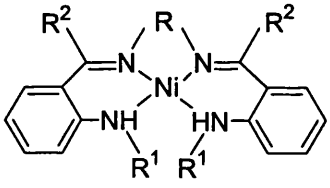

112 a-h

R: $-(CH_2)_n-$; n = 2, 3, 4, 10
$-CH(CH_3)-CH_2-$, *o*-C_6H_4, $R^1 = R^2 = H$;
R: $-(CH_2)_2-$; $R^1 = CH_3$, $R^2 = H$
R: $-(CH_2)_2-$; $R^1 = H$, $R^2 = Ph$

Figure 3.1. Green and Tasker's Ni(amben) type complexes

It was found that using the first procedure, the yield of the complexation varied with the anion in the nickel salt. For example with amben, the highest complexation yield was obtained from nickel(II) acetate (81 %), while nickel(II) sulfate and nickel(II) nitrate gave lower yields (72 % and 68 % respectively). Method (iii) was developed in order to avoid some difficulties encountered during the synthesis of the amben type ligands.

Addition of the nickel(II) acetate to the reaction mixture from the beginning of reduction is necessary because it prevents, by complexation of the ligand generated *in situ*, further reduction of the imine group. At the end of the reaction (24 h) the nickel complex was separated from the catalyst (Pd-C) by extraction into DMF and was then precipitated with methanol.

3.1.2 Synthesis of Nickel (R-ambch) complexes

The nickel ambch complex **113** was synthesised by reaction of nickel(II) acetate, added in stoichiometric amount as a powder, with the free ligand in ethanol at room temperature. After 3 h, filtration of the reaction mixture afforded a red precipitate of **113** in 60% yield. A similar procedure was used for preparation of complex **114** in 91 % yield.

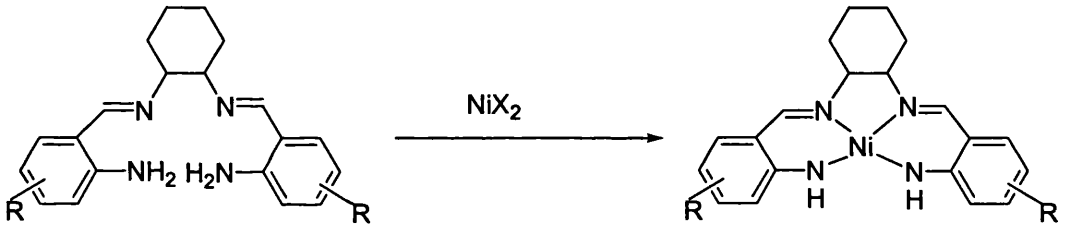

113: R = H
114: R = Cl
115: R = 3-CH_3O
116: R = 3-CH_3
117: R = 5-CH_3

Scheme 3.1. Complexation of R-ambch ligands with nickel

Due to a higher basicity of amine groups in ambch ligands containing electron-donating substituents (R = 3-MeO-, 3-CH_3-, 5-CH_3-) in the aromatic rings, complexation of these ligands leading to **115-117** took place only at 60-65°C in the presence of a base, the products again precipitating from solution (in 62 %, 85 % and 32 % yield).

3.1.3 IR spectra of nickel ambch complexes

The IR spectra of nickel ambch complexes (**113-117**) exhibit very strong bands between 1609-1624 cm^{-1} which correspond to the stretching frequency of C=N double bond. These bands are shifted to a lower frequency than those in the free ligands, indicating

the involvement of the nitrogen atom in donation from the ligand to the metal. As one could see from Table 3.1, introduction of a substituent (R) in the aromatic ring does not produce significant changes in the $\bar{\upsilon}_{C=N}$ frequencies, except for the case in which R is 5-methyl.

Table 3.1. Stretching frequencies of imine group in Ni(R-ambch) complexes

Complex No	R	$\bar{\upsilon}_{CN}$ (cm^{-1})
113	H	1609
114	5-Cl	1610
115	3-MeO	1610
116	3-Me	1609
117	5-Me	1622, 1601

The spectrum of complex **117** presents two bands at 1622 and 1601 cm^{-1}, while all the other complexes have only one band in this region. This is similar with what was found for nickel salen complex **118** for which the strong resonances at 1621 cm^{-1} and 1600 cm^{-1} were assigned to the C=N stretch and to a vibration determined by a conjugated ring interaction, respectively[2].

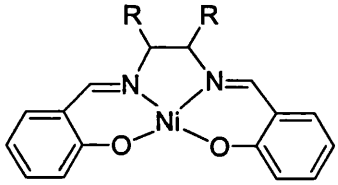

118: R=H
119: R, R= -$(CH_2)_4$-

Figure 3.2. Related Ni(salen) complexes

Nickel salch **119** also shows two resonances in this region, at 1619(vs) and 1600 cm^{-1}(s). The crystal structure reported for this complex showed that it had a slightly distorted geometry in which the two oxygen atoms were situated above and below the plane determined by the nickel and the two imine nitrogen atoms [3]. This distorsion could make the two imine groups in **119** non-equivalent leading to different IR resonances.

3.1.4 ^{1}H-NMR spectra of nickel ambch complexes

The singlet corresponding to the imine group of the nickel ambch complexes **113-117** appears between δ 7.59 (R = 5-Cl) and 7.70 (R = 3-CH_3) compared with δ 7.36 which was reported for nickel salch (**119**) [**3**]. Complexation with nickel results in a shift of 0.59 - 0.6 ppm to higher field relative to the position of this proton in the free ligands, which is less than the shift found in related nickel salch complexes (*e.g.* in **119** is 0.9 ppm). The data also shows that introduction of a CH_3 substituent in the 3rd-position has a slightly larger influence on imine proton chemical shift than when it is introduced in the 5th-position.

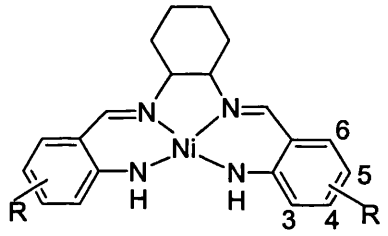

113-117

113: R = H, **114:** Cl, **115:** 3-CH_3O, **116:** 3-CH_3, **117:** 5-CH_3

Figure 3.3 Ni(R-ambch) complexes synthesized

The signals assigned to the aromatic protons in these complexes are also shifted to higher field. Greater variations in chemical shift due to complexation were found as expected for H^5 and H^4 in complexes **113, 115** and **116** ($\Delta\delta$ = 0.14 - 0.38 ppm) which are in *para-* positions relative to the amino and imine groups. In **117** variations of 0.1 ppm were noticed only for H^4 and H^6. The shifts exhibited by the rest of aromatic protons are below this value.

3.1.5 Crystal structure of nickel (II) ambch

The molecular geometry of complex **113** is shown in Fig. 3.4 together with the atom labelling scheme. The asymmetric unit cell contains two molecules which are nearly identical. The small differences between them are considered to arise from the crystal

packing effects. Each nickel centre has a square planar environment provided by the N_4 donor ligand set.

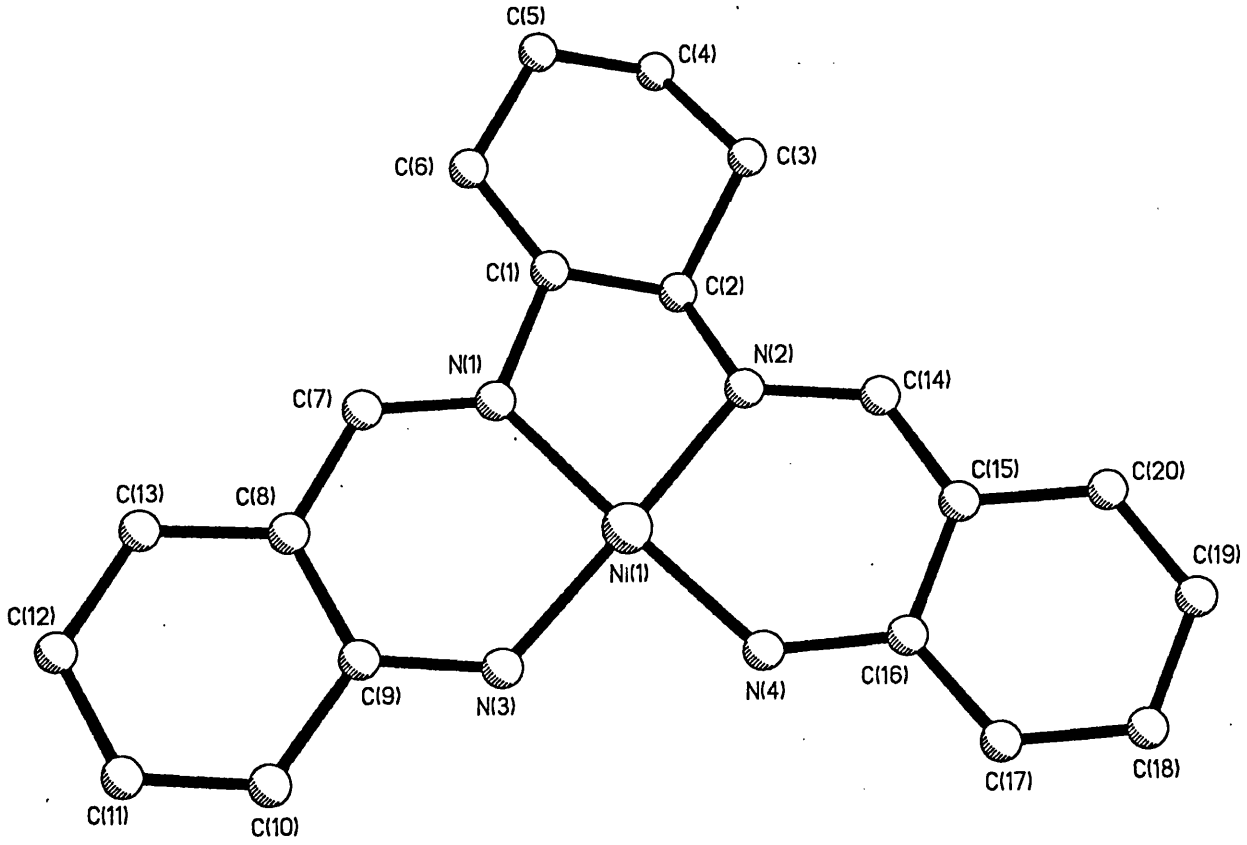

Ni(1)–N(1)	1.874(15)
Ni(1)–N(2)	1.910(10)
Ni(1)–N(3)	1.888(10)
Ni(1)–N(4)	1.833(15)
N(1)–Ni(1)–N(2)	85.03(55)
N(3)–Ni(1)–N(4)	88.27(57)
N(1)–Ni(1)–N(4)	178.15(38)

Figure 3.4 Crystal structure of Ni(ambch) **113** with selected bond lengths (Å) and angles (°)

The bond lengths between nickel and the deprotonated nitrogen donors are shorter than those between nickel and the neutral imine donors. This is similar with the situation found in complex **112b** , but opposite to that corresponding to complex **112a** (Figure 3.5, Table 3.2).

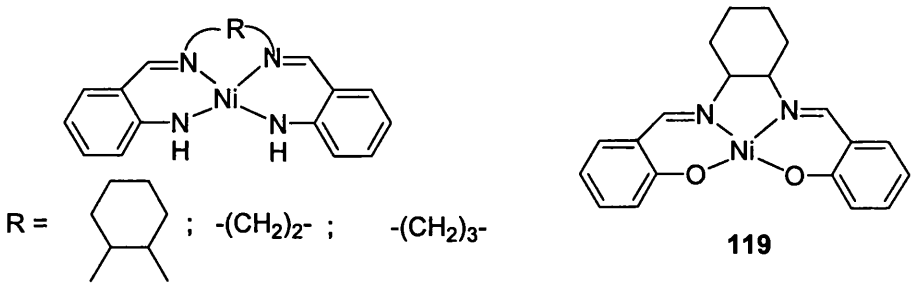

Figure 3.5. Ni(ambch) and related nickel complexes

Table 3.2. Selected bond lengths (Å) in nickel ambch(**113**) and related complexes

Complex	Imine bridge	Ni-X*	Ni-N	Ref.
113	C_6	1.833(15) 1.888(10)	1.874(15) 1.910(10)	-
112a	C_2	1.87(1) 1.86(1)	1.88(1) 1.83(1)	**4**
112b	C_3	1.860(7)	1.923(7)	**5**
119	C_6	1.835(3) 1.852(3)	1.861(4) 1.852(4)	**3**

*X = N for all, but salch where X = O.

The data presented in Table 3.2 show that in nickel complexes **113** and **112a** three Ni-N bonds are statistically equal, the fourth bond being different; while in **112b,** the nickel-outer donor bonds are equal and different from those between nickel and the inner nitrogen donors. A similar situation with that in the first two complexes was found for complex **119** in which one oxygen atom is at closer distance from the nickel, while the other three donor atoms are placed at almost the same distance from the metal ion.

In **113** the angle between the outer nitrogen atoms and nickel is only few degrees (3°) bigger than the one between nickel and the imine nitrogen. In **112a** this difference is

almost double (6.8°) and in **112b** it is even larger (-10°). Furthermore, the angle with the neutral nitrogen atoms becomes bigger than the angle with anionic nitrogen atoms. This was also found in **119** where the difference between the angles is -1.2° (Table 3.3).

Table 3.3. Selected bond angles (°) for Ni ambch(**113**) and related complexes

Complex	Imine bridge	X-Ni-X α	N-Ni-N β	Difference α-β	Ref
113	C_6	88.27(57)	85.03(55)	3.24	-
112a	C_2	92.7(5)	85.9(6)	6.8	**4**
112b	C_3	84.9(3)	94.9(3)	-10	**5**
119	C_6	84.5(1)	85.7(2)	-1.2	**3**

The values of (α-β) reflect a higher flexibility of the ligands in **112a** and **112b** introduced by the diimine bridge compared with that found in **113**.

As mentioned earlier, **113** has a square-planar geometry in which the nickel atom lies only 0.002 (molecule A) and 0.01 Å (molecule B) out of the plane defined by the four nitrogen donors. This is less than the deviation of nickel in **112b** which is 0.04 Å out of the donor atom plane. At the same time, **119** was described as having a slightly tetrahedrally distorted square-planar environment which was explained by intermolecular steric effects on the ligand atoms in the co-ordination plane. The same conclusion results from comparison of the angles between *trans*- donor nitrogen atoms and nickel in these complexes. In **113** these angles are 178.4 ° compared with 175.6(6) ° in **112a**, 175.0(3) ° in **112b** and 176.6(2) ° in **119**.

The dihedral angles between the phenyl rings are 9.6 ° and 12.6 ° in complex **113** which show that the molecule has an umbrella shape. The conformation of the 5-membered ring containing the nickel, azomethine nitrogen and the two carbon atoms of the bridge is a half-chair. Complex **113** is a monomer with no intermolecular interactions between the two molecules in the unit cell. This is similar to what was found for **112a** and **112b** complexes.

3.2 Copper double Schiff base complexes

3.2.1 Copper amben and salen type complexes

Copper salen complexes were obtained by treating the free ligand with copper(II) acetate or copper(II) nitrate in the presence or absence of a base[**6**]. They were also prepared by reaction of substituted salicylaldehyde copper complex with a diamine in ethanol[**7**]. Later it was reported the synthesis of copper amben by reaction of copper(II) methoxide with the free ligand in refluxing methanol [**8**]. Filtration of the reaction mixture lead to the desired products and crystals suitable for X-ray studies were obtained from acetone.

Conformational flexibility of the salen ligand together with electronic properties determined by the substituents (R) in the aromatic rings of this ligand and the axial ligand have a major influence on the reactivity at the metal centre. Bhadbhade and Srinivas showed the effect of substitution of copper salen complex (**120**) with either a methoxy- or a chloro- group at the C-5 position in the aromatic ring on the geometry and electronic structure of complexes **121** and **122** [**9**].

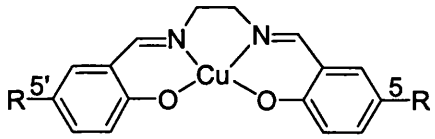

120 - 127

120: R=H, **121**: MeO, **122**: Cl, **123**: Me
124: I, **125**: HO, **126**: Br, **127**: NO_2

Figure 3.6. Cu(amben) and other R-substituted copper complexes

They found that complex **120** consists of strong dimers (Figure 3.7) in which copper has a tetragonally elongated square-pyramidal configuration with the donor atoms N_2O_2 forming a perfect basal plane and the apical bond (Cu...O_1') with the oxygen atom from the second molecule almost perpendicular to this plane. The complex has a stepped conformation in which the two benzene rings of the salen ligand bend asymmetrically with respect to the N_2O_2 plane. This change in the conformation of the ligand provides a closer approach for the fifth donor atom (O_1) and reduces the steric interaction between

Figure 3.7. Effect of aromatic ring on crystal structure of Copper complexes **120 - 122**

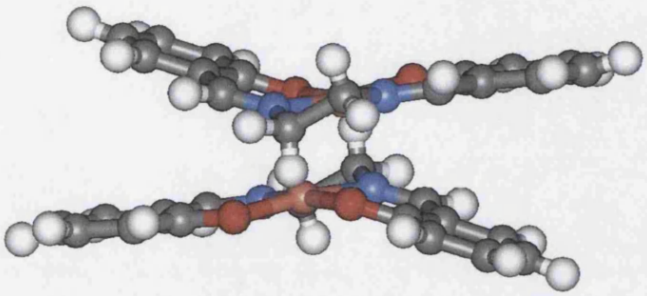

a. R=H: Dimers in stepped conformation

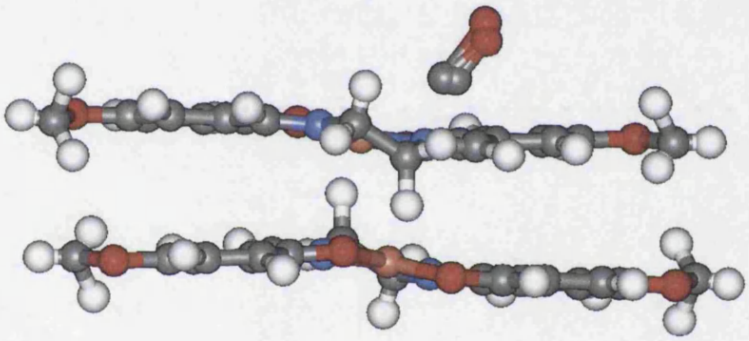

b. R=5-MeO: Weak dimers with planar geometry

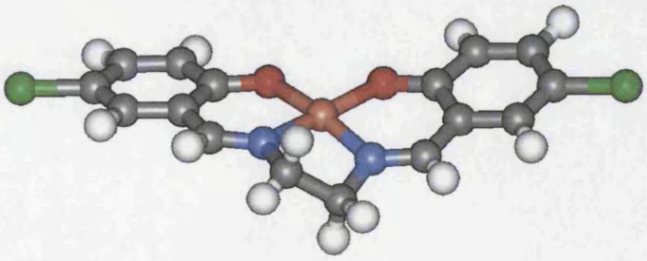

c. R=Cl: Monomer

the benzene rings. Also as an effect of the involvement of one oxygen atom (O_1) in the dimer bridge, the C-N bonds are equal, while the C-O bonds show significant differences, the C-O_1 bond being longer.

Complex **121** (R = MeO) forms weak dimers with a solvent molecule (MeOH) in the lattice. The N_2O_2 atoms are almost in a plane and the displacement of the copper atoms from this plane is small (0.06 Å). Although the ethylenediamine conformation is identical to that in complex **120**, the molecule is now planar and the arene rings are bent symmetrically with the N_2O_2 plane. A weaker (Cu...O_1') apical bond may determine a planar conformation and reduces the steric interactions between the benzene rings. Methanol is included in the crystal lattice in some channels generated upon packing of the molecules and forms hydrogen bonds with O_2 of the ligand which is not involved in the dimer formation.

Complex **122** (R = Cl) is a monomer with a tetrahedrally distorted square-planar geometry around copper. The Cu-O bonds are similar, while the Cu-N distances are shorter than in complex **120**, determined by a decrease in co-ordination number from 5 to 4. The absence of dimeric interactions in this complex was attributed to the chlorine substitution.

Complexes **120 - 122** show colour isomerism in solid-state and solvatochromism. The change in colour which goes in parallel with the changes in the ligand field strength is determined not only by the change in the co-ordination number of the copper and the conformational flexibility of the ligand, but also by more subtle factors such as weak interactions of the ligand with the solvent molecules or changes in the ethylenediamine conformation.

The formation of addition compounds of 5,5'-disubstituted salen copper (II) complexes **120 -127** (R = CH_3, OCH_3, I, H, HO, Br, NO_2 , Cl) (Figure 3.6) with propionic acid, phenol, chloroform and ethanol was examined [**7, 10**] and the authors suggested that the rapid change in colour of complexes from green to purple (in less than 10 min) was the result of the conversion from a tetra-coordinate planar structure to a pyramidal structure. They also reported that the tendency to form five co-ordinate complexes decreased in the order: 5-CH_3 > 5-OCH_3 > 5-I > 5-H > 5-HO > 5-Br > 5-NO_2 > 5-Cl.

Related to amben complexes are the macrocyclic N_4 ligands with the general structure **128 a, b** in which an ethylene or propylene unit connects the two aromatic amine groups.

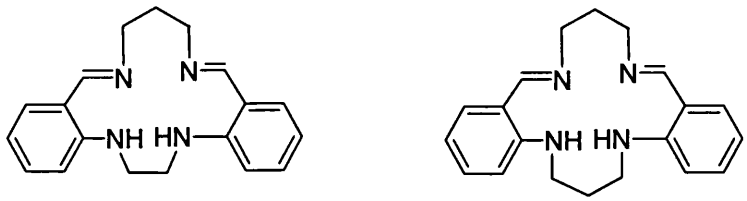

128 a **128 b**

Figure 3.8. Macrocyclic N_4 double Schiff bases

Studies concerning the reactivity of copper, nickel and cobalt complexes of these ligands towards oxygen revealed that oxidation of the metal centre could lead to subsequent ligand to metal electron-transfer, ultimately resulting in oxidative degradation of the ligand. Examples of ligand oxidation processes which were found are presented in the following scheme [**11**].

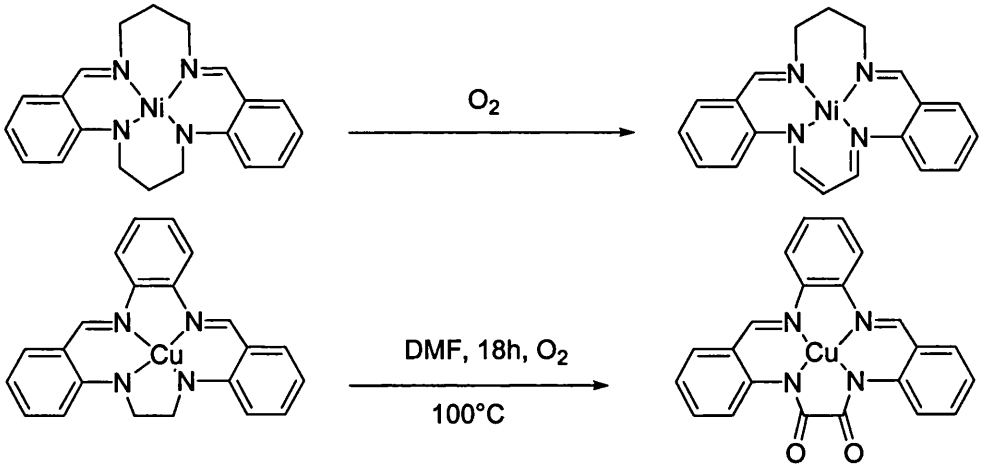

Scheme 3.2. Ligand oxidation in nickel and copper N_4 complexes

The interest in this area arises from the fact that ligand oxidation is an important step involved in oxidation of substrates by metal complexes and is also one of the factors responsible for autoxidation of transition metal dioxygen carriers.

In searching for model complexes which can mimic the redox function of copper site in copper-zinc superoxide dismutase (CuZnSOD), an enzyme that catalyses the dismutation of superoxide radical anions to molecular oxygen and hydrogen peroxide, the N_4 double Schiff base copper complex **129** was prepared [**12, 13**]. CuZnSOD is a dimeric molecule in which the two subunits are bonded non-covalently; copper(II) ion, which is N_4 co-ordinated in square-planar geometry with tetrahedral distortion, is the redox partner of the superoxide radical anion in the catalytic process.

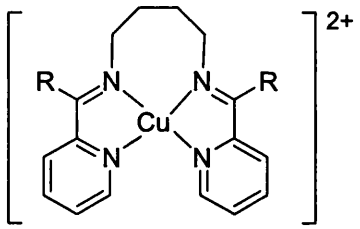

129: R = H; **130**: R = Me; **131**: R = Ph

Figure 3.9. Copper N_4 complexes derived from 2-pyridinecarboxaldehyde

Complex **129** proved to have SOD, anti-carcinogenic and anti-rheumatic activity [**14a, b**]. Introduction of substituents R = Me and R = phenyl at the imine carbon atoms of the ligand increased the stability of the corresponding copper complexes, **130** and **131**, and the SOD activity.

3.2.2 Synthesis of Cu(R-ambch) complexes

Copper ambch complexes **132, 133** were prepared by addition of copper(II) acetate to a solution of ligand and triethylamine in ethanol at room temperature. The product precipitated from the reaction mixture and was separated by filtration in 59 and 80 % yield. In the case of ligands substituted with electron-donating groups (3-MeO; 3-Me) complexation was performed in a similar way, but at a higher temperature (55-60 °C), the products (**134, 135**) being isolated in 49 % and 80 % yield.

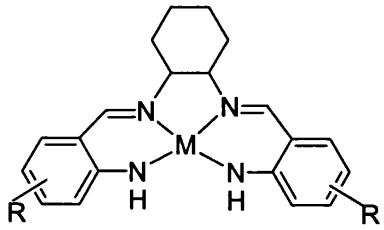

132-135: M = Cu, R = H, Cl, 3-MeO, 3-Me
136a: M = CuOAc; R = 5-Me
136b: M = CuCl; R = 5-Me

Figure 3.10. Copper ambch complexes synthesized

3.2.3 IR spectra of Cu(R-ambch) complexes

The Cu(R-ambch) complexes (**132 - 136**) have very strong absorption bands for the imine group between 1609-1629 cm^{-1}. While in Ni(R-ambch) complexes introduction of the R- group in the ligand does not have a significant effect on the C=N stretching frequencies, the analogous copper complexes present more important variations of $\bar{\upsilon}_{CN}$ with the nature of the R- group (Table 3.4).

Table 3.4. Stretching frequencies of imine group in Cu (R-ambch) complexes

Complex No	R	$\bar{\upsilon}_{CN}$ (cm^{-1})
132	H	1616
133	5-Cl	1609
134	3-MeO	1608
135	3-Me	1612
136a	5-Me	1628, 1616
136b	5-Me	1629, 1612

Complexation of 5-Me-ambch **111** with copper(II) acetate was achieved using reaction conditions similar to those employed for the other ambch ligands possessing electron-donating groups. At the end of the reaction, the solvent was removed under low pressure to give a brown-black residue. This was washed with petroleum spirit and after decanting the liquid phase, the solid was dried under vacuum and analysed. The mass spectrum of this compound had peaks at *m/z* = 469 which was assigned to the $[\mathbf{136a}]^+$ fragment and at *m/z* = 410 corresponding to [**136a**-CH_3COO] ion. The spectrum also

contained fragmentation peaks up to *m/z* = 838, however we could not exclude the fact that such peaks could have resulted due to the experimental conditions in which the the mass spectrum was run. Analytical data suggested that the molecular formula of this complex was Cu(5-Me-ambch)(OAc) · $3H_2O$ (**136a**). The compound exhibited two bands (1628, 1616 cm^{-1}) in the region corresponding to $\bar{\upsilon}_{CN}$, while absorption due to carbonyl group in the co-ordinated carboxylate appeared at 1581 cm^{-1} and the one at 1419 cm^{-1} was assigned to δ_{CH3}.

When copper(II) chloride was used instead of copper acetate, a black precipitate was formed during the reaction which was separated by filtration. Complete evaporation of the solvent from the filtrate led to a black residue. The elemental analysis of the latter sample suggested that the product (**136b**) was Cu(5-Me-ambch)(Cl) · $3H_2O$. Similar to the data obtained for compound **136a**, the IR spectrum of compound **136b** presents two stretching frequencies for the C=N bond (1629 and 1612 cm^{-1}).

The results obtained for complexation of 5-Me-ambch with copper are in agreement with the data reported [**7, 10**] for analogous salen complexes, Cu(5-Me-salen), which had the highest tendency to form 5-coordinate complexes among a series of 5, 5'-substituted salen complexes.

3.2.4 Crystal Structure of Cu(ambch) complex 132

The crystal structure of copper ambch (**132**) shows that it is a tetrahedrally distorted square-planar complex (Figure 3.11) in which copper is coordinated by four nitrogen atoms. In this complex the outer nitrogen donors are placed in closer proximity to the copper ion than the inner nitrogen donors, similar to the situation reported for complexes **137** and **138**.

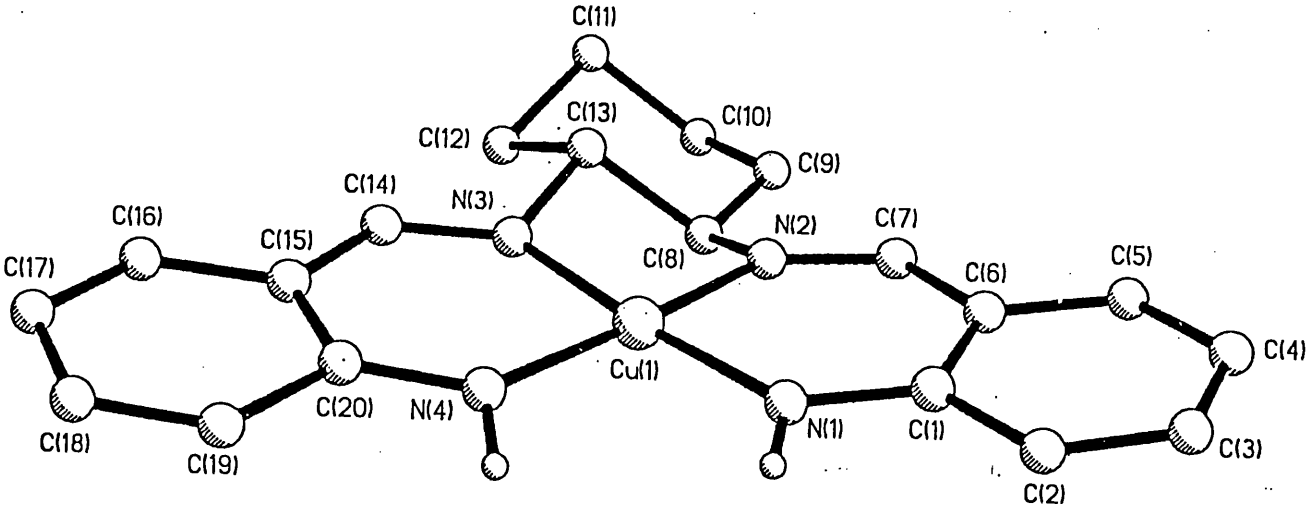

Cu(1)–N(3)	1.946(6)
Cu(1)–N(2)	1.956(6)
Cu(1)–N(4)	1.923(6)
Cu(1)–N(1)	1.907(6)
N(3)–Cu(1)–N(2)	83.2(2)
N(1)–Cu(1)–N(4)	94.8(3)
N(1)–Cu(1)–N(3)	173.6(3)

Figure 3.11. Crystal structure of Cu(ambch) **132** with selected bond lengths (Å) and angles (°)

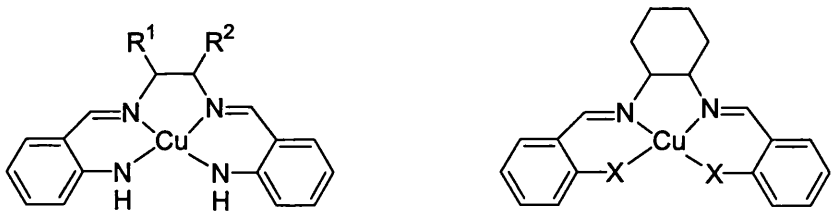

137: $R^1=R^2=H$
138: $R^1=Me$; $R^2=H$

132: X=NH
139: X=O

Figure 3.12. Cu(ambch) complex and related CuN_4 and Cu(salch) complexes

Table 3.5 shows the gradual modifications in the values of Cu-N bonds determined by the change in the diimine bridge from C_6 to C_3 and C_2 [**8, 15, 16**].

Table 3.5. Selected bond lengths (Å) in Cu(ambch) **132** and related complexes

Complex	Diimine bridge	Cu-X	Cu-N	Ref
132	C_6	1.907(6) 1.923(6)	1.946(6) 1.956(6)	-
137	C_2	1.97(1) 1.88(1)	1.96(1) 1.95(1)	**8**
138	C_3	1.899(11) 1.930(11)	1.880(13) 1.945(12)	**15**
139	C_6	1.896(3) 1.901(2)	1.927(3) 1.935(3)	**16**

A closer look to the structure of these molecules reveals that while in **132** the bonds between copper and the deprotonated nitrogen donors are statistically different from those with the neutral imine donors, in complexes **137** and **138**, three Cu-N bonds have similar values and only the fourth is statistically different.

The angle between the anionic NH donors and Cu (94.8 °) is bigger than the angle between neutral nitrogen donors and Cu (83.2 °)(Table 3.6), the difference between them being 11.6 ° as compared with 15.5 ° in **137** and 12.4 ° in **138**. The angle N(1)-Cu(1)-N(3) (Fig. 3.11), where N(1), N(3) are in *trans* position one relative to the other, is 173.9(3) °, while this angle in **137** is 171.9(5) ° and in **138** is 171.8(5) °. These values

show that in **132** the tetrahedral distorsion is not as large as in the other two copper N_4 complexes mentioned. A similar trend was observed for nickel N_4 complexes **113** and **112 a, b**. However, all the data (bond lengths and angles) suggest that the influence of the diimine bridge on the geometry of the complex is less important in copper complexes than in the analogous nickel complexes.

Table 3.6. Selected bond angles (°) in Cu(ambch) and related complexes

Complex No	Diimine bridge	X-Cu-X α	N-Cu-N β	Difference α-β	Ref
132	C_6	94.8(3)	83.2(2)	11.6	-
137	C_2	97.4(4)	81.9(5)	15.5	8
138	C_3	95.0(5)	82.6(5)	12.4	15
139	C_6	89.1(1)	84.6(1)	4.5	16

In comparison with nickel ambch complex **113**, the copper complex **132** of the same ligand shows metal-nitrogen bonds longer with both types of nitrogen donors. In the same time, the angle between the metal and the inner nitrogen donors decreases slightly on changing the metal ion from nickel to copper, while the outer nitrogen donors are placed farther one from another.

The influence of the change in co-ordination sphere around copper may be seen in the comparison between the structure of the present complex and that of **139** (Tables 3.5 and 3.6) [**16**]. Complex **132** has longer bond lengths with all the donor atoms, a structure less tetrahedrally distorted with bigger difference between the α and β angles than **139**. Both complexes have the Cu-outer donor bonds equal and statistically different than those with inner N donors.

3.3 Manganese double Schiff base complexes

3.3.1 Manganese salen complexes

Jacobsen synthesized several manganese salen complexes (**5**) by reaction of the free ligand with an excess of manganese(II) acetate in refluxing ethanol or a mixture of ethanol-water. The reaction was carried out in aerobic conditions which transformed the

intermediate Mn(II) salch complex into Mn(III) species [**17, 18**]. The conditions employed varied depending on the structure of the ligand. In some cases such as for R^1 = Cl, MeO and O-Si(O^iPr)$_3$ oxidation of Mn(II) to Mn(III) was completed by bubbling air through the solution. The [Mn(salen)(OAc)] formed in this way, reacted further with an excess of NaCl or LiCl at room temperature or reflux to give the desired product. This was extracted in toluene or dichloromethane, washed and separated by filtration.

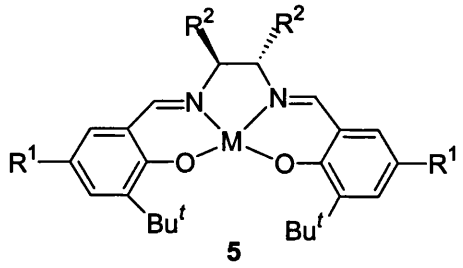

5

M = MnCl; R^1 = MeO, Bu^t, Me, H, Cl, NO_2, -OSi(O^iPr)$_3$
R^2 = Ph or R^2, R^2 = -$(CH_2)_4$-

Figure 3.13. Jacobsen's manganese complexes

For ligands containing electron-withdrawing groups (*e.g.* 3-Br, 5-NO_2) it was reported that reaction of manganese acetate with the free ligand in air led to the corresponding Mn(II)(salen) complex which was transformed into the Mn(III) species by chemical oxidation with ferricinium tetrachloroferrate or hexafluorophosphate [**19, 20**]. Katsuki's catalysts (*e.g.* **6a**) were obtained by a template synthesis in the presence of manganese(II) acetate[**21**]. The reagents, added in stoichiometric amounts, reacted in ethanol at room temperature under aerobic conditions. The [Mn(salen)(OAc)] precipitated from the solution and was separated by filtration. From it, upon treatment with $NaPF_6$ in excess, the [Mn(salen)PF_6] was obtained which was purified by column chromatography.

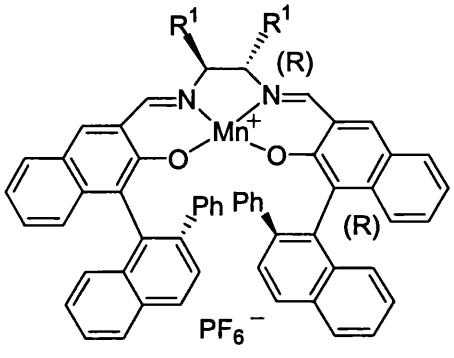

6a

Figure 3.14. Katsuki's manganese salch complexes

Syntheses of $[Mn(III)(salpn)]^+$ complexes **140** and **141** were accomplished by ligand exchange from [Mn(salpn)(acac)] [**22**]. This latter complex results from reaction of $[Mn(acac)_3]$ with the free ligand. [**23**]

$$Mn(acac)_3 + salpn \rightarrow Mn(acac)(salpn) + 2\ acac$$

$$Mn(acac)(salpn) + Me_3SiCl \rightarrow Mn(salpn)(Cl)\ \textbf{(140)}$$

$$Mn(acac)(salpn) + RCOOH \rightarrow Mn(salpn)(OCOR)\ \textbf{(141)}$$

The reaction with Me_3SiCl took place in anhydrous acetonitrile under nitrogen from which the product **140** precipitated upon cooling. The replacement of acac ligand by a carboxylate group occurred upon heating the reagents in ethanol at reflux. At the end of the reaction the mixture was concentrated and the [Mn(salpn)(OCOR)] complex (**141,** R = Me, Et, Pr^n, Bu^n, Pr^i, Bu^t) precipitated in diethyl ether from this solution.

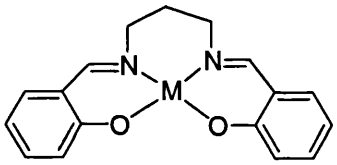

140-141

M = MnCl, or $Mn(O_2CR)$

R = Me, Et, Pr^n, Bu^n, Pr^i, Bu^t

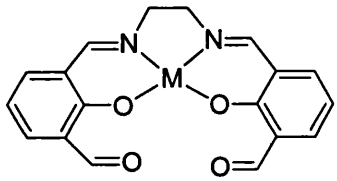

142

M = MnCl

Figure 3.15. Mn salen type complexes prepared by ligand substitution or complexation with $MnCl_2$

Mn(III)salen type complexes with auxiliary carboxylate ligands (**141**) were also isolated from reaction of the free ligand with a stoichiometric quantity of the appropriate Mn(II) carboxylate salt in ethanol under aerobic conditions [**24**].

A direct synthetic route to manganese complex **142,** from the free ligand and $MnCl_2$ in hot ethanol was reported[**25**]. The reaction took place in presence of air, the product precipitated from the reaction mixture and was separated by filtration.

3.3.2 Synthesis of Mn(R-ambch) complexes

Synthesis of Mn(III)(ambch) complex **143** was attempted following a procedure similar to the one utilised by Jacobsen [**17**] for the related manganese salch complex (**5**). A solution of ambch in toluene was added slowly to an ethanolic solution containing excess of manganese acetate (ratio 1 : 3) heated at reflux. After 3 h, air was bubbled gently through the solution and heating continued for other 6 h to oxidise the Mn(II) ambch to Mn(III) ambch complex.

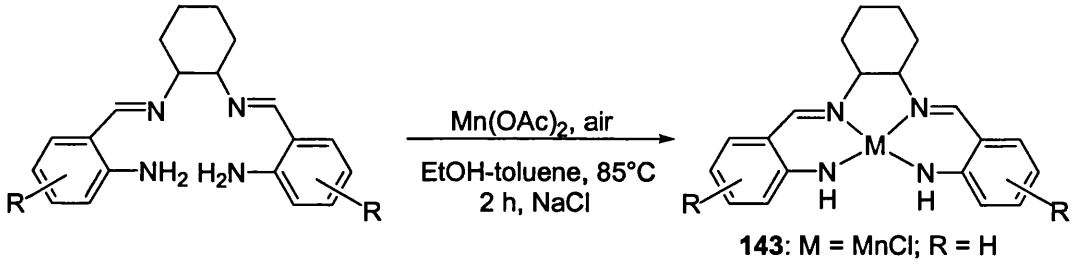

Scheme 3.3. Complexation of ambch with $Mn(OAc)_2$

The reaction mixture was then treated with NaCl in order to exchange the acetyl group with chloride and then it was extracted in toluene. After the solvent was removed, the residue obtained was redissolved in dichloromethane and addition of hexane led to separation of a brown precipitate containing the impure product **143** as resulted from its analytical data. During extraction the product seemed to have a low solubility in toluene, while the obtained organic layer was brown-orange indicating that oxidation of Mn(II) to Mn(III) ambch complex **143** was probably not complete.

Following these observations it was decided to perform the synthesis in a one phase system (ethanol) which should increase the rate of the reaction and allow solvent removal at a lower temperature. Triethylamine was added to the suspension of ligand and manganese acetate in ethanol and the reaction was monitored by IR. The mixture was stirred for 2.5 h at 90 °C and then air was bubbled gently through it for another 3.5 h. The reaction mixture changed its colour from yellow to brown during reflux and became black within 5-10 min after bubbling air. After this time, aqueous NaCl was added and the reflux continued for other 30 min.

After cooling, the reaction mixture was filtered and the black filtrate was evaporated to dryness to give a black residue which was extracted in dichloromethane. The obtained solution was concentrated and upon addition of petroleum spirit, a brown precipitate separated overnight which was analysed by MS, IR and elemental analysis.

The mass spectrum of this compound showed a peak at *m/z* = 372 which was assigned to the species formed by loss of Cl from the molecular ion. This is similar with the data reported for related Mn(salch)(Cl) complexes [**17**]. The compound presents two bands (at 1627 and 1609 cm^{-1}) in the region corresponding to the (C=N) stretching bond. It also exhibits absorptions at 1564 and 1538 cm^{-1} which is an indication of an impurity having an acetate group [either manganese acetate or Mn(ambch)(OAc)]. The elemental analysis also showed that the product was contaminated with an impurity which could be $Mn(OAc)_2$. The ether solution turned from orange to brown on standing in air indicating the possible incomplete conversion of Mn(II) ambch to $[Mn(III)\ ambch]^+$.

Due to the problems encountered with synthesis and purification of the manganese ambch complex **143,** it was decided to use $MnCl_2$ as the manganese salt in the complexation reaction in analogy with complexation of **142** [**25**]. This approach has the advantage of reducing the number of parameters which influence the complexation reaction.

Mn(ambch)(Cl) complex (**143**) is insoluble in $CDCl_3$ and this prompted us to use it as a solvent in NMR samples which were taken during the reaction, to monitor the consumption of the free ligand in time. The advantage of using $CDCl_3$ is twofold, the low solubility of the product in it prevents practical problems in running the NMR experiments determined by the paramagnetism of the complex and then, the signals due to the ligand do not overlap with those of the product making the interpretation of the spectra easier.

Addition of $MnCl_2$ to a solution of ambch ligand and triethylamine in ethanol determined a change in the colour of the solution from yellow to orange and then brown indicating formation of Mn(II)(ambch) complex, which was oxidized in air to give **143**. Complexation took place at 55-60 °C and it was monitored by ^{1}H-NMR. At the end of

the reaction the product, a brown powder, precipitated and it was isolated by filtration in 53.4 % yield.

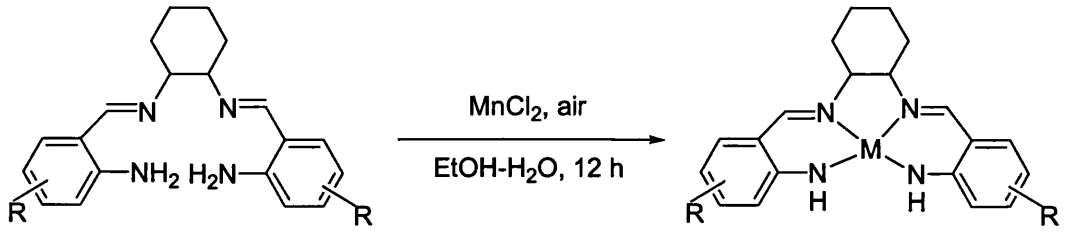

143: M = MnCl; R = H
144: M = MnCl; R = 3-Me

Scheme 3.4. Synthesis of manganese salch complexes

Synthesis of 3-methyl substituted analogue **144** was performed using a similar procedure as the one described above (47 % yield). After removal of the brown precipitate, the filtrate was concentrated and layered with diethyl ether, resulting in precipitation of more product. Both manganese ambch complexes (**143**, **144**) were analysed by IR, MS and elemental analysis. Their IR spectra resemble with those of other metal ambch complexes. The stretching frequency for the C=N bond appears at 1606 cm^{-1} (in both complexes), whereas that for C=C bond is present at 1537 cm^{-1} (in **143**) and 1546 cm^{-1} (in **144**). The bands corresponding to deformation of CH_2 groups from the bridge are between 1450 and 1350 cm^{-1}, with additional absorptions (1429, 1327, 1221 cm^{-1}) due to the CH_3 substituent in the complex **144**. Also characteristic for these compounds are the bands at 758 cm^{-1} (**143**) and 795, 748 cm^{-1} (**144**) determined by deformations of C-H aromatic bonds.

3.4 Cobalt double Schiff base complexes

3.4.1 Cobalt amben and salen type complexes

In a search for analogues of vitamin B_{12}, the CoN_4 complexes **145 a-g** (Figure 3.16) were prepared using methods similar to those employed for preparation of Ni(amben) and Co(salen) derivatives [**26a,b**].

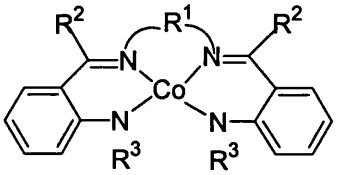

145a: R^1 = -$(CH_2)_2$-, **b**: -$CH(CH_3)$-CH_2-,
c: *o*-C_6H_4-, **d**: -$(CH_2)_3$-; $R^2 = R^3 = H$
145e-f: R^1 = -$(CH_2)_2$-, R^2 = Ph or CH_3, R^3 = H
145g: R^1 = -$(CH_2)_2$-, R^2 = H, $R^3 = CH_3$

Figure 3.16. Cobalt amben type complexes previously reported

The synthesis was carried out under nitrogen to prevent oxidation to Co(III) and formation of peroxycobalt (II) species. The methods used were: i) addition of cobalt(II) acetate in methanol to a solution of ligand in methanol at reflux in the presence or absence of sodium methoxide; ii) template synthesis from *o*-amino-arylcarbonyl compound, the appropriate diamine and cobalt(II) acetate in methanol; iii) reduction of the nitro- double Schiff base in the presence of cobalt(II) acetate with a palladium-charcoal catalyst and hydrogen. The authors mentioned that they encountered some difficulties during the synthesis and purification of these complexes. Based on the similarity of the IR and electronic spectra of nickel and cobalt amben complexes it was concluded that they had similar geometries.

This was confirmed by Higson and McKenzie [**27**] who reported that complexes **145a-d** separated out from the reaction mixture upon addition of a hot aqueous solution of cobalt (II) acetate to a boiling ethanol solution of ligand. The products were filtered from the hot mixture, washed with ethanol and dried in air. From the similarity of the electronic spectra of complexes **145a-d** in different solvents and in solid phase it was deduced that the complexes preserve the planar structure in solution even in donor solvents such as pyridine. This is different from what was found in the case of related salen type complexes which tend to increase their co-ordination number, either by dimerisation or polymerisation (more likely for Co(II) and Cu(II) complexes) [**28**] or by addition of donor molecules[**29**].

The electrochemical data recorded in DCM [**27**] showed that the oxidation potential for the redox couple Co(II)/ Co(III) varies with the nature of the bridge in the N_4 ligands in

the order: **145d** > **145c** > **145a**, which implies that the last complex is the easiest oxidised in the series. In CV experiments, **145d** gave a reversible wave, while the other two complexes had a quasireversible and an irreversible behaviour which suggest the instability of the Co(III) species in solution for these complexes.

The reactivity of complex **145c** toward oxygen was studied and showed that it was air stable in dry pyridine or DMF solutions saturated with oxygen. This contrasts with the reactivity of N_2O_2 salen type complexes and the N_4 complexes derived from porphyrin and corrin [**30 a,b**]. Oxidation of **145c** took place in hydroxylic solvents (*e.g.* ethanol) or in wet DMF solutions which changed colour from red to brown leading to amorphous products. In the same time, salen complexes **146a-e** gave irreversible oxidation in presence of different alcohols with formation of Co(salen)(OR) species. Kinetic studies on this reaction revealed that the mechanism of the reaction depends on steric and electronic nature of the salen ligand and also on the nature of alcohol [**31a**].

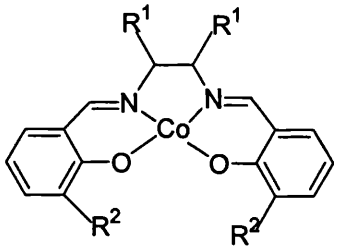

146a-d: R^1 = H, R^2 = H, MeO, Bu^t, Cl
146e: R^1, R^1 = -$(CH_2)_4$-, R^2 = H

$$\text{Co(salen)} + \frac{1}{4}\,O_2 + \text{ROH} \longrightarrow [\,\text{Co(salen)(OR)}\,] + \frac{1}{2}\,H_2O$$

Scheme 3.5. Oxidation of Co(salen) complexes **146a-e** in alcohol

Crystalline products were obtained from reaction with oxygen of both salen and amben type complexes in the presence of β-diketone and malononitrile [**31 c, d**].
Cobalt salen type complexes such as **146a** display homogeneous catalysis for oxidation of phenols with molecular oxygen in organic media [**32**]. These complexes react reversibly with oxygen giving an equilibrium mixture of cobalt superoxo complex **147** and the dimeric peroxo-complex **148** in a ratio which depends on the nature of the cobalt complex and the reaction conditions employed. The presence of electron-

releasing groups in the ligand increases the oxygen affinity and the concentration of **147**, while electron-withdrawing or bulky substituents have the opposite effect.

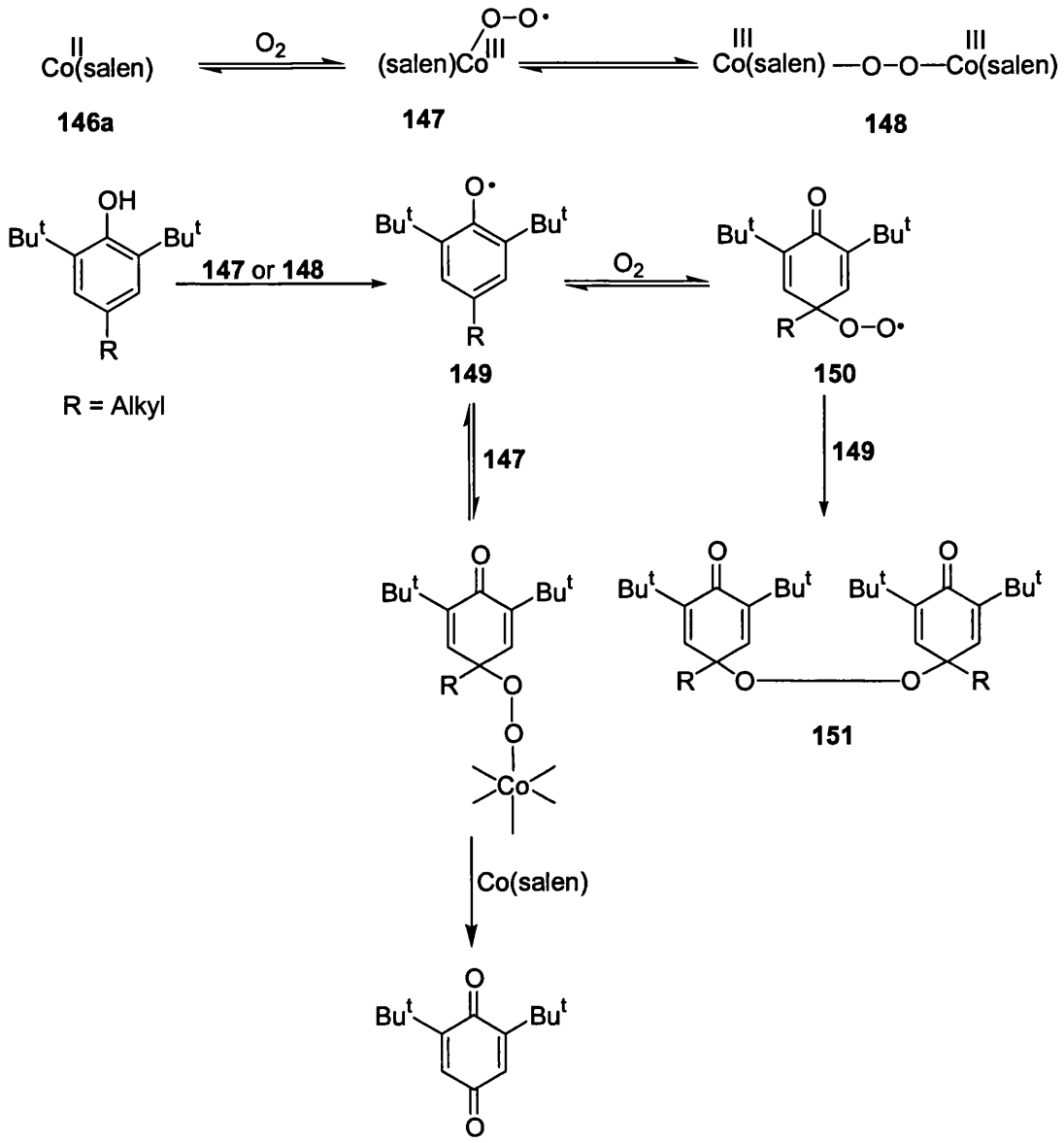

Scheme 3.6. Oxidation of *para*- substituted phenols catalysed by **146a**

The ratio **147** : **148** influences the composition of the final reaction mixture, [Co(salen)] **146a** leading to formation of peroxide **151** by the mechanism summarised in Scheme **3.6** [**33**]. Examining the influence of different substituents in the phenol ring it was concluded that electron donating substituents promote the oxidation. On the other hand, for substrates having lower reactivity competitive deactivation of the catalyst by irreversible oxidation occured.

Cobalt amben type complexes (**145 a, c, d**) reacted quickly with bromine or iodine in DCM giving the corresponding CoN_4X (X = Br, I) complexes which precipitated from the reaction mixture and were separated by filtration [**27**]. The analogous CoN_4Cl were prepared by reaction of the $Co(II)N_4$ complexes with $CHCl_3$ or CCl_4 in air at room temperature. The compounds CoN_4X (X = Cl, Br, I) presented similar X-ray powder diffraction patterns implying that they were isomorphous. They were paramagnetic and had a five-co-ordinate square pyramidal structure.

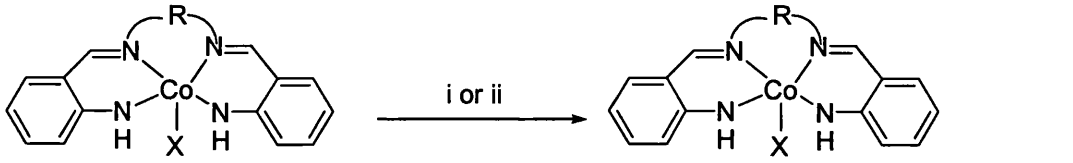

145 a, c, d

R = $-(CH_2)_2-$, $-CH(CH_3)-CH_2-$, $-o-C_6H_4-$
X = Cl, Br, I

i: Br_2 or I_2, DCM, 25 °C, X = Br, I ; ii: $CHCl_3$, CCl_4, 24 h, 25 °C, X = Cl

Scheme 3.7. Halogenation of CoN_4 complexes

The crude Co(amben)Cl samples, especially those obtained from hot $CHCl_3$ solution, gave high chlorine analyses and had poorly defined IR spectra. The reversibility of the reaction between this complex and pyridine (Py), leading to the octahedral [Co(amben)PyCl], was employed to obtain pure [Co(amben)Cl]. In the spectrophotometric titration of **145c** and **145d** with bromine and iodine the changes observed in the UV-VIS spectra beyond the 1 : 1 end-point were considered to be determined by the formation of polyhalogenated compounds.

Other studies on cobalt Schiff base complexes used as vitamin B_{12} models were focused on the reduction to Co(I) and formation of Co-C bonds. The Co(I) species are powerful reducing agents and nucleophiles [**34**]. Due to their facile homolytic cleavage (thermal or photochemical), a range of alkyl and acyl cobalt Schiff base complexes (*e.g.* **152, 153**) were used as precursors to the corresponding carbon centred radicals. The utility of these complexes in organic synthesis was explored by Pattenden and co-workers [**35**].

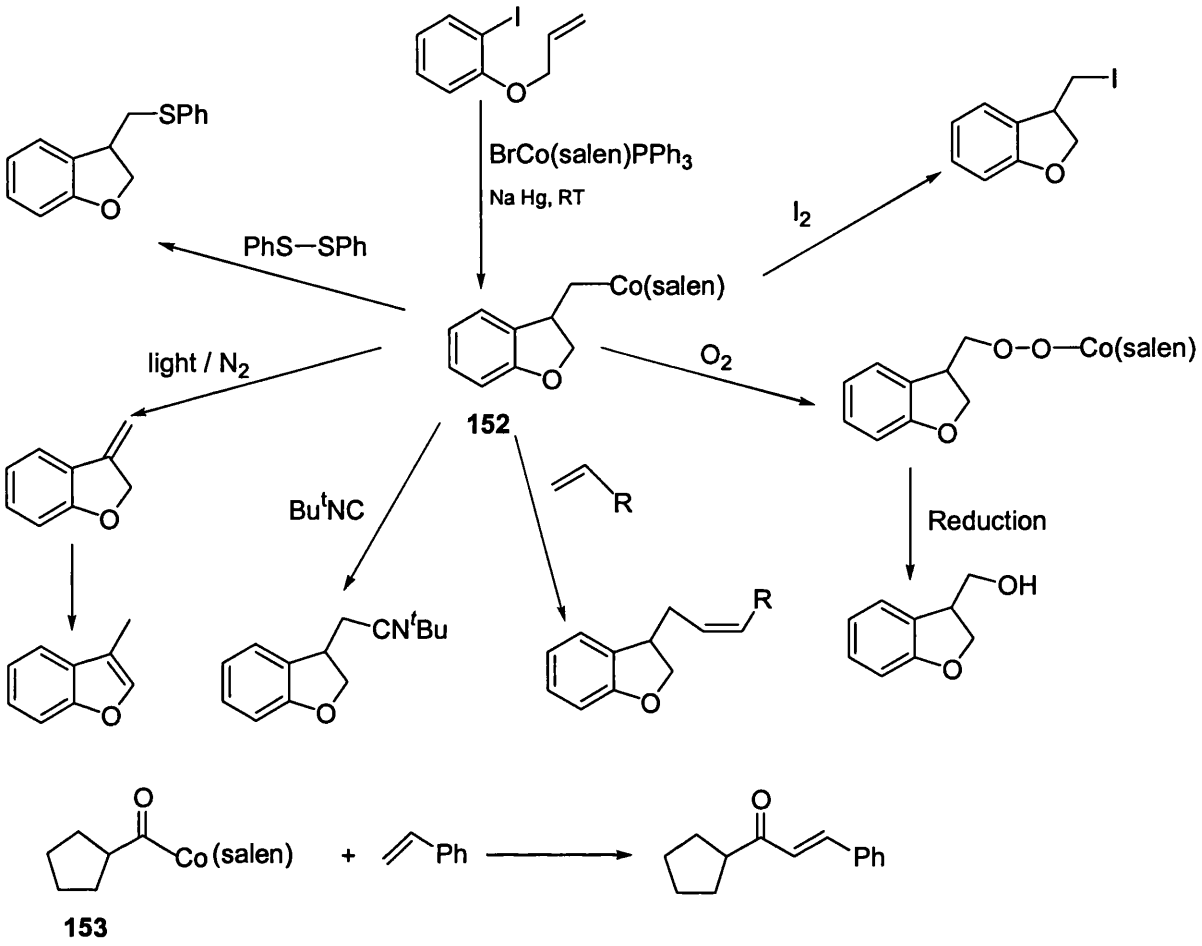

Scheme 3.8. Applications of alkyl and acyl Co salen complexes in organic synthesis

In Scheme 3.8 are presented two examples of how the generated radical can be manipulated to introduce different functionality in the substrate or can give addition to deactivated C=C bond leading to new alkene products.

3.4.2 Synthesis of Co(R-ambch) complexes

Synthesis of cobalt complexes **154 - 156** was performed under an inert atmosphere. Anhydrous conditions were not necessary because water does not co-ordinate to the metal centre[**26**] as in [Co(salen)] complexes. Dropwise addition of an aqueous solution of cobalt(II) acetate to a hot solution of ambch ligand in ethanol led to formation of a bright red precipitate of Co(ambch) (**154**) which was filtered and dried under vacuum (61 % yield). The product was air stable and was characterised by elemental analysis and IR. Preparation of complexes **155** and **156** was achieved in a similar way, except that the ligand was deprotonated with a base to increase the rate of complexation. They were obtained as red powders in 73 % and 80 % yield.

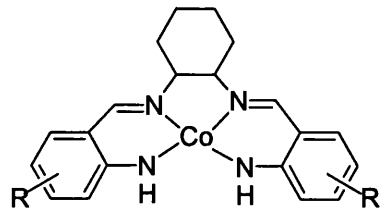

154 - 156: R = H, 3-CH_3, 5-CH_3

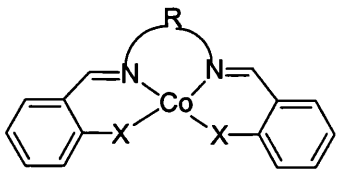

145a-b: R = -$(CH_2)_2$-, -$(CH_2)_3$-; X = NH
146a : R = -$(CH_2)_2$-, X = O

Figure 3.17. Co(ambch) complexes prepared (**154 - 156**) *cf.* related cobalt complexes

In cobalt ambch (**154**) the band for C=N bond vibration appears at lower frequency (1602 cm^{-1}) than in cobalt complexes **145a** and **145b** (1607 $cm^{-1}$and 1613 cm^{-1} in Nujol)[**26b**]. Substitution of the benzene ring with a methyl group determines changes in the IR frequency of this band, namely it decreases slightly for *ortho-* substitution in **155** (1600 cm^{-1}) and increases considerably for *para-* substitution in **156** (1623 cm^{-1}), becoming closer to the value reported for [Co(salen)] complex **146a** (1625 cm^{-1}). This might be explained by a better conjugation between the imine group, benzene ring and methyl group in the 5-Me-ambch complex **156**. The same effect of substitution was also observed in the IR spectra of nickel and copper ambch complexes (sections **3.1.3** and **3.2.3**).

3.4.3 Reactivity of Co(II) ambch complex toward oxygen

We decided to investigate oxidation of Co(II) ambch complexes to Co(III) species in air in the presence of different nucleophiles. Some of the reactions were directed to obtain compounds analogous to cobalt salen complexes which proved to be active in ring-opening of epoxides and cyclopropanation of olefins. Introduction of a ligand X in the axial position of the cobalt complex would provide a new means of tuning the electronic properties and a way of introducing asymmetry/ chirality in the obtained Co(III) complexes.

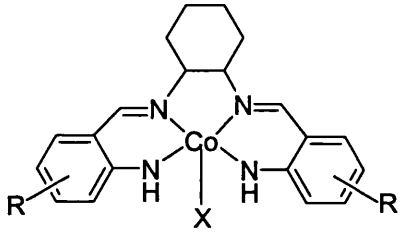

Non-chiral metal salen complexes can exist in solution as an equilibrium mixture of two enantiomeric conformational isomers (**157 a, b**). Katsuki demonstrated that for a non-chiral manganese salen complex this equilibrium could be shifted towards conformer **157a** by using a chiral axial ligand L (*e.g.* sparteine) [**36**], in this way the catalyst could act as a chiral complex.

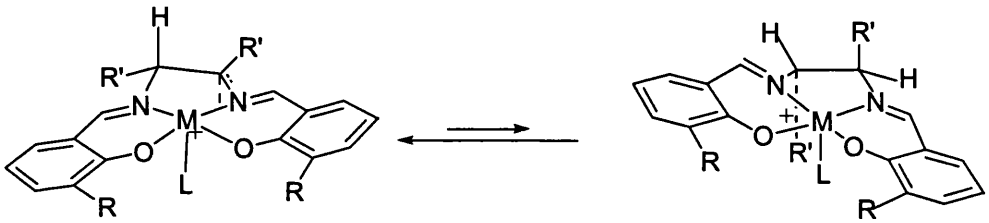

Figure 3.18. Equilibrium mixture of two enantiomers in non-chiral salen complexes

The mechanism involved in controlling the chirality is not well understood and using cobalt instead of manganese complexes in such a study has the advantage that the former complexes are expected, in analogy with [Co(III) salen] complexes, to be diamagnetic; this allowing to gain more information about their structure and the mentioned equilibrium by NMR.

Firstly, oxidation of Co(ambch) complex **154** with air in the presence of *t*-butyl-phenol was studied by ^{1}H-NMR in $CDCl_3$. When the reaction was carried out using an excess of *t*-butyl-phenol, broad signals corresponding to Co(II) complex could be seen in the sample after 30 min. These disappeared after approximately 1 h and the product was diamagnetic. The ^{1}H-NMR spectrum revealed the formation of only one product possessing a *t*-butyl group (δ = 1.1 ppm). The signals of the unreacted *t*-butyl-phenol overlapped in the aromatic region with those from the ambch ligand in the complex and for this reason the latter could not be interpreted.

In order to avoid this, the reaction was performed using stoichiometric amounts of the Co(II) ambch complex and *t*-butyl-phenol. In this case the broad signals determined by Co(II) ambch complex are present even after 1 h and problems with shimming of the sample were encountered. A new peak appeared at δ = 3.54 ppm which could be due to a possible product formed in the reaction of Co(II) amben complex with $CDCl_3$. The

signals in the aromatic region are broad and they overlap preventing further interpretation of the spectrum, while two resonances for *t*-butyl groups were observed, one of them corresponding to the unreacted phenol.

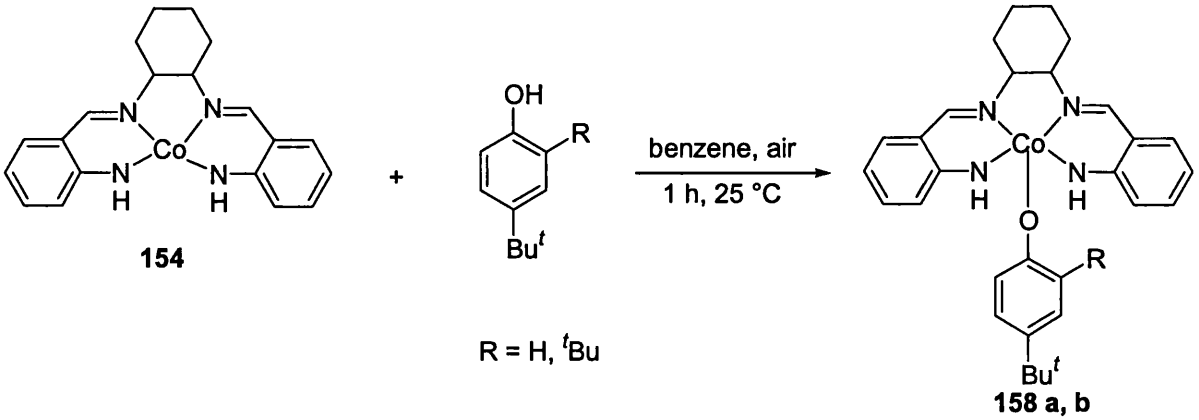

Scheme 3.9. Oxidation of Co(ambch) with O_2 in presence of phenols

Following these preliminary tests, it was decided to use benzene instead of chloroform as a reaction medium to avoid contamination of the product due to possible side reactions.

Addition of Co(ambch) **154** to a solution of *t*-butyl-phenol in benzene led to rapid dissolution of the solid and formation of a red solution. This changed its colour within a few minutes to brown red and later to brown-black indicating the change in oxidation state of the metal ion from Co(II) to Co(III). At the end of the reaction, the mixture was filtered and the product **158 a** precipitated as a black solid on addition of diethyl ether to the concentrated benzene solution.

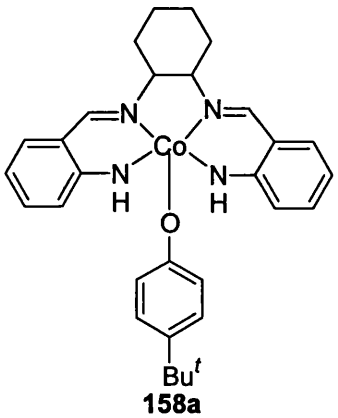

Figure 3.19. Co(ambch)(O-C_6H_4-Bu^t)

The IR spectrum of this precipitate **158a** shows resonances for both ambch ligand and co-ordinated 4-*t*-butyl-phenoxide. These together with selected bands for [Co(II)ambch] and 4-*t*-butyl-phenol are presented in Table 3.7. The co-ordination of the phenoxide to the cobalt centre is confirmed by the absence of $\bar{\upsilon}_{OH}$ at 3248 cm^{-1} and by the shift of the $\bar{\upsilon}_{CN}$ toward a higher frequency than in cobalt N_4 complex.

Table 3.7. Selected IR frequencies (cm^{-1}) of starting materials and **158a**

Characteristic absorptions	4-*t*-butyl-phenol	Co(ambch)(OAr) **158a**	Co(ambch) **154**
$\bar{\upsilon}_{(OH)}$	3247	-	-
$\bar{\upsilon}_{CH(CH_3)}$	2960; 2868	2947	-
$\bar{\upsilon}_{CN}$	-	1608	1602
$\bar{\upsilon}_{C=C}$	1600; 1514	1535; 1514	1581; 1539
$\delta_{CH(CH_3)}$	1363; 1242	1361; 1240	-
δ_{CHarom}	825	833, 746	746

Variations also appear in the bands for $\bar{\upsilon}_{(CH(CH_3))}$ and $\delta_{(CHarom)}$ of the phenoxide ligand. The structure was in agreement with the analytical data. Reaction of 2,4-di-*t*-butyl-phenol with Co(ambch) **154** under similar conditions to those described above for 4-*t*-butyl-phenol, gave a red-brown precipitate containing Co(II)ambch ($\bar{\upsilon}_{(CN)}$ = 1603 cm^{-1}; $\delta_{(CHarom)}$ = 748 cm^{-1}) and 2,4-di-*t*-butyl-phenol ($\bar{\upsilon}_{(OH)}$ = 3246 cm^{-1}; $\delta_{(CHarom)}$ = 825 cm^{-1}) as results from the IR spectrum of this material. In addition a strong band is present at 737 cm^{-1} ($\delta_{(CHarom)}$) together with a small one at around 840 cm^{-1}. The latter could be assigned to the 2,4-di-*t*-butyl-phenol. The bands for the stretching frequencies of *t*-butyl groups and methylene groups from the diimine bridge of ambch ligand overlap preventing further interpretation.

The IR spectrum of the residue obtained after evaporation of the solvent from the filtrate shows several peaks in the region corresponding to $\bar{\upsilon}_{(CO)}$ and $\bar{\upsilon}_{(CN)}$ between 1654 to 1603 cm^{-1}. It also exhibits three bands for the $\delta_{(CHarom)}$ (760 cm^{-1}; 748 cm^{-1}; 737 cm^{-1}). The IR spectra of both precipitate and filtrate presented bands which could indicate the

presence of quinones (*e.g.* in Figure 3.20) in the reaction mixture. These bands at 1654, 1590, 824 cm^{-1} were more intense in the filtrate, while in the precipitate were weak. These results show that oxidation of Co(ambch) in presence of 2,4-di-*t*-butyl-phenol to the Co(III) ambch was not selective and due to time constrains it was decided to stop our investigation here.

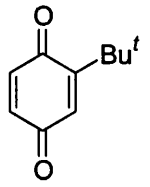

Figure 3.20. Possible by-product from oxidation of Co(ambch) in presence of 2,4-di-tert-butyl-phenol

A further step in this study was the oxidation of Co(ambch) (**154**) in 2-butanol. Oxidation in this solvent was slow, no colour change was observed after stirring this complex in 2-butanol at room temperature for 30 min. Dichloromethane and a small amount of water were added, but the solution preserved its initial colour. In order to increase the reaction rate, the mixture was heated to 50 °C and stirred at this temperature overnight. After filtration to remove the unreacted Co(II) complex, the black solution was concentrated and was layered with petroleum spirit. However, this resulted in more red cobalt(II) complex being deposited overnight. Removal of the solvent from the filtrate gave a brown solid (**159**) which exhibited three signals in the IR spectrum in the region corresponding to C=O and C=N stretchings at 1653, 1632 and 1607 cm^{-1}. These data correlate well with those reported for Co(III) salen complex **160** ($\bar{\upsilon}_{(CN)}$ =1636, 1608 cm^{-1}) [**37**], while the stretching frequencies for the alkyl C-H bonds in the ambch ligand and the product overlap preventing further interpretation. The $\delta_{(CHarom)}$ is present at 763 cm^{-1} as a broad band. Attempts to purify this material were not successful.

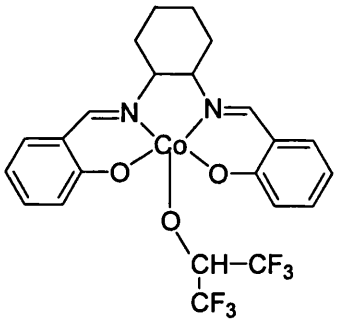

160

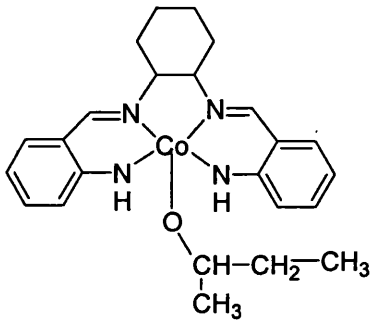

159

Figure 3.21. Co(salch)(OR) complex

A possible reason why the oxidation of Co(II) complex is so slow in this solvent is the low amount of water present in 2-butanol which, according to previous reports, is necessary for promoting the oxidation to Co(III) species [**27**]. Another explanation would be a lower acidity of the 2-butanol compared with the ethanol and perfluoro-*t*-butanol used in synthesis of **160**. Finally, it is likely that Co(ambch)(OBu^i) gives decomposition *via* a mechanism similar to that reported for analogous salen type complexes [**31b**].

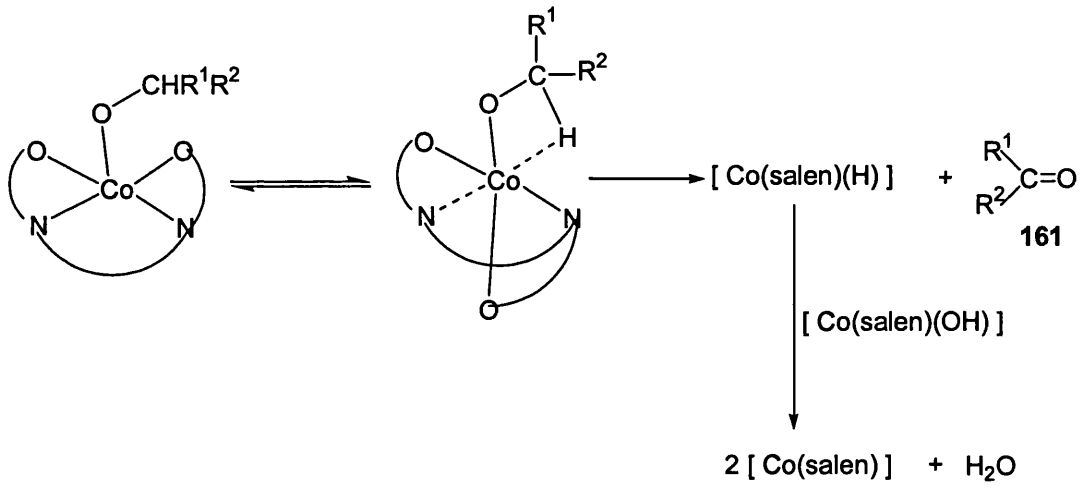

Scheme 3.10. Mechanism of decomposition of Co(salen)(OCHR^{1}R^2) complexes when R^1, R^2 ≠ H

The reaction involves conformational change of the ligand followed by β-elimination with formation of the carbonyl compound **161** and regeneration of Co(II) salen complex. The process is much faster for secondary alcohols (*e.g. i*-propanol) than for primary alcohols (methanol, ethanol) as result of steric interaction between the salen ligand and the R^1, R^2 substituents in the alcohol leading to a favourable non-planar conformation. This also depends on the flexibility of the ligand imposed by the diimine bridge, however, salen and salch cobalt complexes exhibited comparable reactivity in their reactions with *i*-propanol. At the same time oxidation of cobalt amben in the presence of β-diketones proved that these complexes such as Co(amben)(acac) can also adopt a non-planar conformation. All these explain why apparently oxidation of Co(ambch) in 2-butanol is slow and the peak at 1653 cm^{-1} could be assigned to $\bar{\upsilon}_{(CO)}$ from 2-butanone.

Oxidation of Co(ambch) in chlorofom was also studied. A solution of Co(ambch) in this solvent, stirred in air at room temperature, changed its colour over a few minutes from bright red to brown and subsequently the reaction mixture became heterogeneous. When the reaction was carried in an NMR tube both formation of the suspension and the paramagnetism of the product prevented us from obtaining good NMR spectra. The mixture was left under stirring overnight and the product (**162**) was isolated by filtration as a black-grey solid. The IR spectrum of this solid presented a very strong absorption at 1603 cm^{-1} which was assigned to $\bar{\upsilon}_{(CN)}$ and two weak bands for $\bar{\upsilon}_{(C=C)}$ at 1570 and 1553 cm^{-1}. The strong and medium bands corresponding to deformation of CH_2 groups from the bridge appeared between 1441 and 1356 cm^{-1}. It also exhibited a strong absorption at 758 cm^{-1} in the region corresponding to $\delta_{(CHarom)}$. Analytical data suggested that this complex was Co(ambch)(Cl) · CH_2Cl_2. Based on these data and in analogy with similar reactions given by salen and amben type complexes it was concluded that this solid contained Co(ambch)(Cl) **162**.

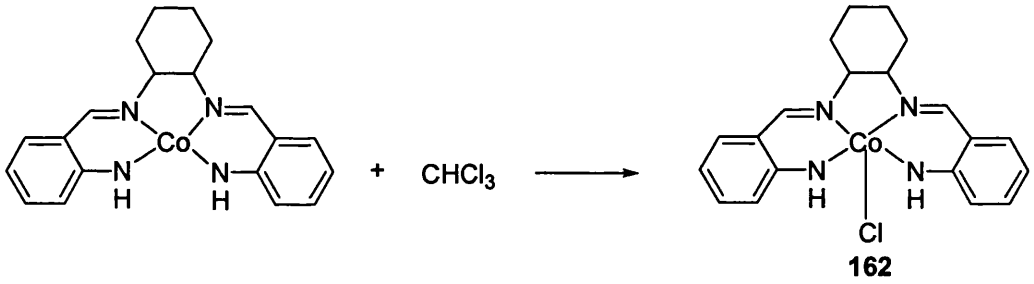

162

Scheme 3.11. Oxidation of Co(ambch) in chloroform

Further on, a reaction mixture containing Co(ambch) (**154**), generated as described in section **3.4.2**, was opened to the air and oxidation proceeded under stirring at room temperature. Formation of [Co(III) ambch] complex was indicated by the change in the colour of this solution within few minutes from red to brown-red and later to black.

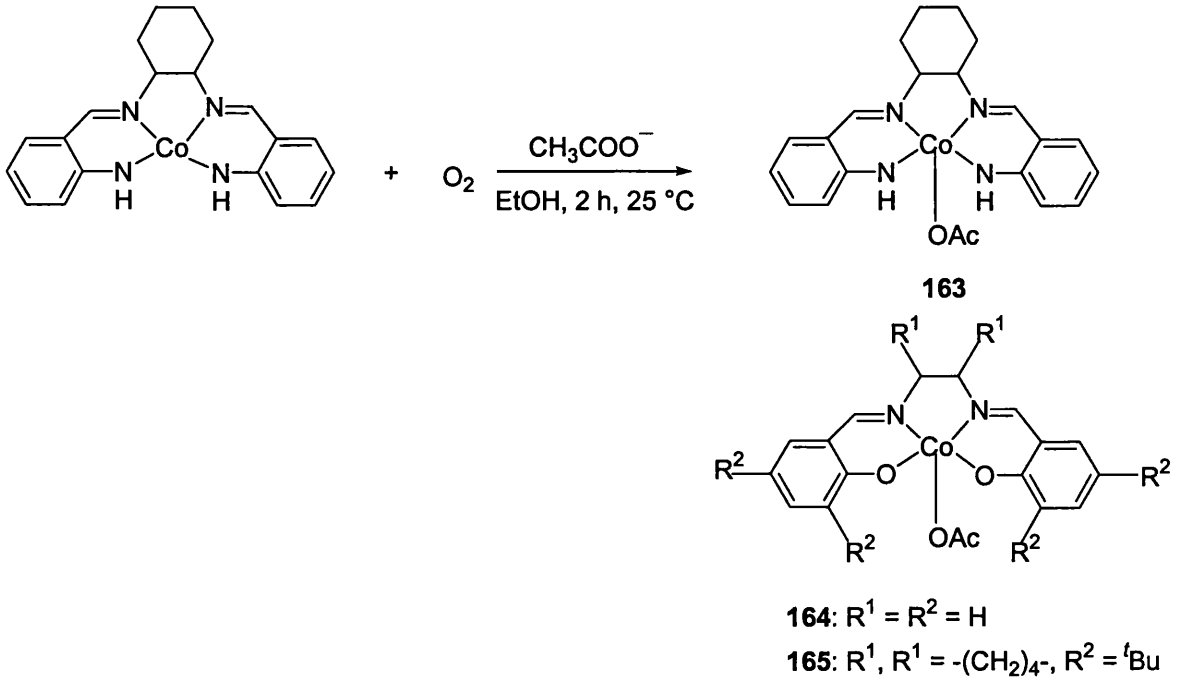

Scheme 3.12. Oxidation of Co(ambch) in presence of CH_3COO^- in EtOH

After 2 h the solvent was removed and the residue obtained was purified by washing with petroleum spirit to give [Co(ambch)(OAc)] (**163**). The structure of this complex was proposed based on the results from the IR and elemental analysis which were compared with data reported for similar compounds (Table 3.8)[**38**].

Table 3.8. Selected IR frequencies in [Co(III)ambch(OAc)](**163**) and related Co(III) salen complexes

Characteristic Absorptions (cm^{-1})	Co(ambch)(OAc) **163**	Co(salch)(OAc) **164**	Co(salen)(OAc) **165**
$\bar{\upsilon}_{(CN)}$	1649	1638	1620
$\bar{\upsilon}_{(CO)}$	1596; 1569	1611; 1545	1610, 1590
$\delta_{(CHarom)}$	764	783	750

3.5 Vanadyl double Schiff base complexes

3.5.1 Vanadyl salen type complexes

Oxovanadium double Schiff base complexes have been extensively studied. They can be obtained either from $VO(acac)_2$ or from $VOSO_4$ and the free ligand in an alcoholic solution. VO(acen) (**166**) was prepared using the former vanadyl source [**39**] in which the equilibrium established was shifted to the right by removing the acetylacetone from the system upon heating at 250 °C.

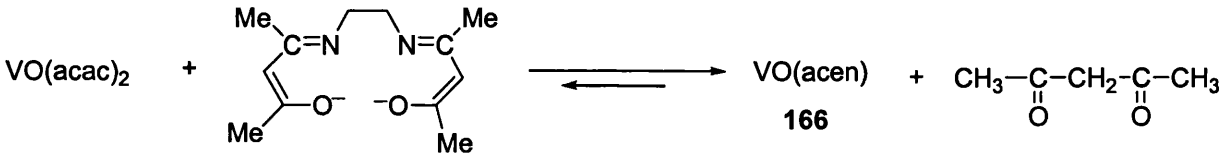

Scheme 3.13. Synthesis of VO(acen)

In the synthesis of asymmetrical VO complexes **167** this was achieved at 25 °C or lower temperature by choosing an appropriate solvent (EtOH) or a mixture of solvents (*e.g.* ethanol-chloroform or DCM-ether) to induce precipitation of the product from the system [**40**].

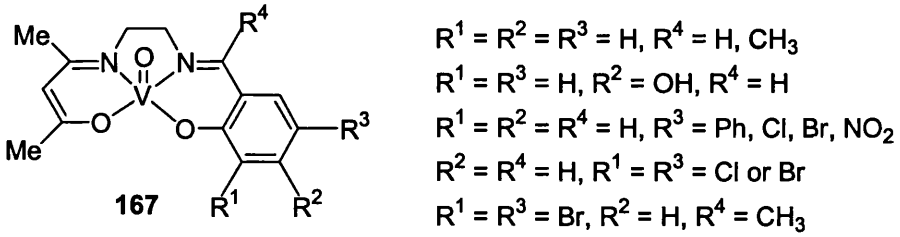

Figure 3.22. Asymmetrical VO complexes

When vanadyl sulfate was used as starting material [**41**], the ligand was deprotonated before complexation with a base and the product was separated in a similar manner as described for the previous procedure.

The colour of the complexes depends on the solvent from which they are isolated, being green or blue powders from methanol or chloroform and orange when isolated from acetonitrile. The green-blue complexes have a monomeric 5-coordinate square-pyramidal structure while the orange or red complexes have a polymeric structure which consists of individual complexes stacked to give an infinite linear chain of VO bonds.

Most oxovanadium (IV) complexes containing tetradentate Schiff base ligands derived from 1,2-diamines take the monomeric green forms; those from 1,3-diamines give orange polymeric VO complexes while green forms have not been obtained. In the case of the complex **168** derived from 1,2-diphenyl-1,2-ethanediamine both orange and green forms were obtained and the crystal structures of VO(salstien) · MeOH (green) **168a**, VO(salstien) · $CHCl_3$ (green) **168b** and VO(salstien) · CH_3CN(orange) **168c** determined by X-ray allowed a direct comparison of their structure [**42**].

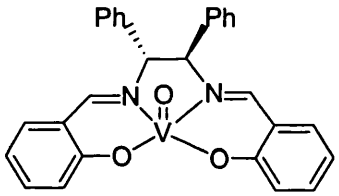

168

Figure 3.23. VO(salstien)

In the first two structures (**168 a, b**), the geometry around the vanadium atom is a distorted square pyramid with the tetradentate Schiff base ligand occupying the basal sites, each complex containing two independent molecules A and B in the unit cell. The 5-membered central chelate ring determined by vanadium, two nitrogens and two carbon atoms from the diimine bridge takes a gauche conformation with the phenyl groups in the equatorial positions. A and B differ from one another with respect to the orientation of the 1, 2-(*R,R*)-stien phenyl groups, the chelate ring of B being more severely distorted than that of A. The two molecules face each other, disposing the VO groups in opposite directions.

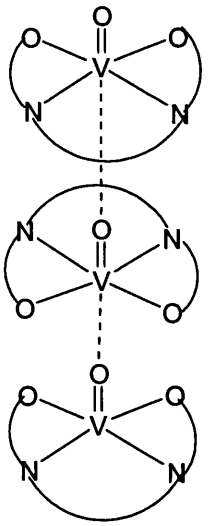

Figure 3.24. Polymeric structure of VO(salstien) in orange form

In the orange crystal form (**168c**) an oxo ligand bridges two vanadium atoms and a linear chain structure with V=O....V=O....bonds is constructed. The geometry around the vanadium atom is a distorted octahedron. The two metal complex subunits in the unit cell have identical structural parameters, but are rotated with 180 ° one relative to the other. The VO bond lengths are larger than in the green forms since the oxo ligand coordinates at the position *trans-* to the oxo ligand of the neighboring complex. The IR spectra of oxovanadium complexes in Nujol mulls showed VO stretching at 990 cm^{-1} for the monomeric form and around 860 cm^{-1} for the polymeric linear chain structure. These values are consistent with longer VO bond lengths and weaker bonds for polymeric forms than for monomers as found from the X-ray studies.

The orange complexes show mechanochromism, their colour changes from orange to green upon grinding. This is believed to be determined by the destruction of the polymer chains and the IR spectrum of such a sample will present VO bands for both the monomer and polymer forms. The ratio between these bands depends on the extent of grinding. It was found that the green complexes turn orange when heated at 120 °C for a few minutes. The orange crystals turn green when exposed to $CHCl_3$ vapor, while the green crystals turn orange upon exposure to CH_3CN vapour.

3.5.2 Vanadyl ambch complexes

VO(salen) complexes are air stable compounds, while an VO(L)(L = **169**) complex which was prepared in air as an orange solid, turned brown in time [**43**]. Following this report it was decided to carry out the synthesis of VO(ambch) complex **170** under a protective nitrogen atmosphere.

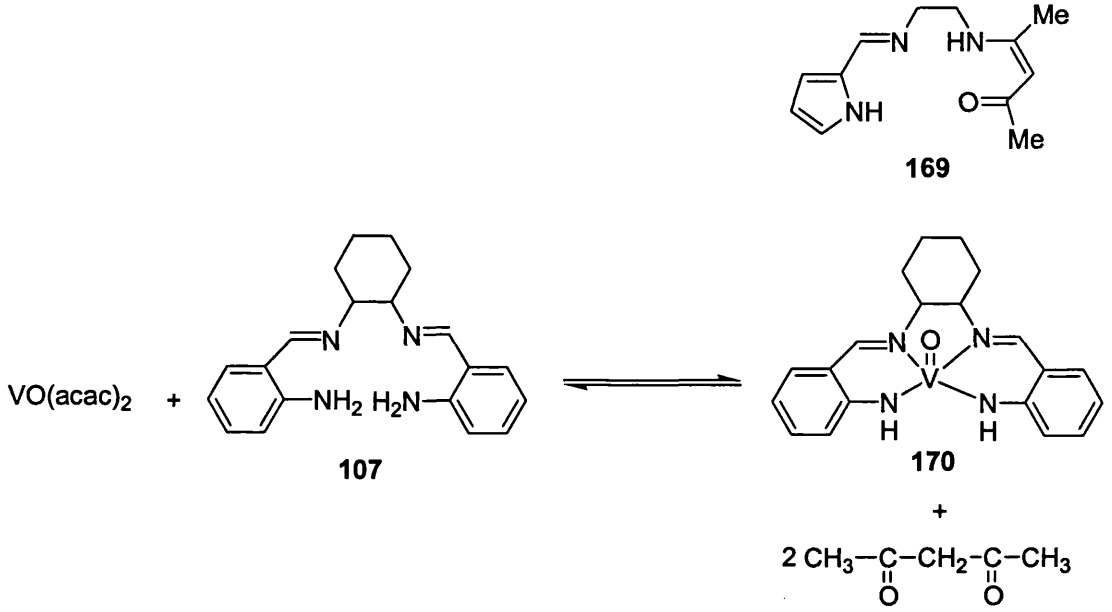

Scheme 3.14. Complexation of ambch **107** with $VO(acac)_2$

Complexation occurred upon dropwise addition of a $VO(acac)_2$ solution in ethanol over a warm ethanolic solution of ligand. At the end of the addition, the temperature was raised to 90 °C, then heating and stirring continued for 3 h. Filtration of the reaction mixture while still hot gave a green-black precipitate and a green-yellow solution. The filtrate was concentrated to half of the initial volume and upon cooling overnight, light-blue crystals were formed.

The liquid phase was decanted from these crystals with a cannula and evaporation of solution gave a brown-orange oil. This was washed with dry petroleum spirit to give a yellow solution and a brown-orange solid. The blue crystals were unreacted $VO(acac)_2$. The yellow solution was evaporated to give a light yellow solid which was analysed by ^{1}H-NMR. The spectrum of this sample showed that it contained the ambch ligand (**107**) ($\delta_{(CH=N)}$ = 8.25 ppm) and another Schiff base (**171**) ($\delta_{(CH=N)}$ = 8.50 ppm, H^7) in the molar ratio 1: 1. The latter compound has a broad peak at δ 10.9 which was assigned to NH

proton (H^{11}), two doublets at δ 8.05 and 7.88 (H^6 and H^3) and two triplets at δ 7.80 and 7.55 (H^4 and H^5) in the aromatic region. It also exhibits three singlets at δ 4.73 due to the olefinic proton H^9 and at δ 2.93 and 2.74, corresponding to the protons from the methyl groups (H^{10} and H^8). Comparing this data with those obtained for symmetrical ambch **107** and related asymmetrical ligand **172** [**44**] the structure **171** for the unknown Schiff base was proposed. The colour of the solid (brown-orange) indicated contamination with oxygen and was not analysed.

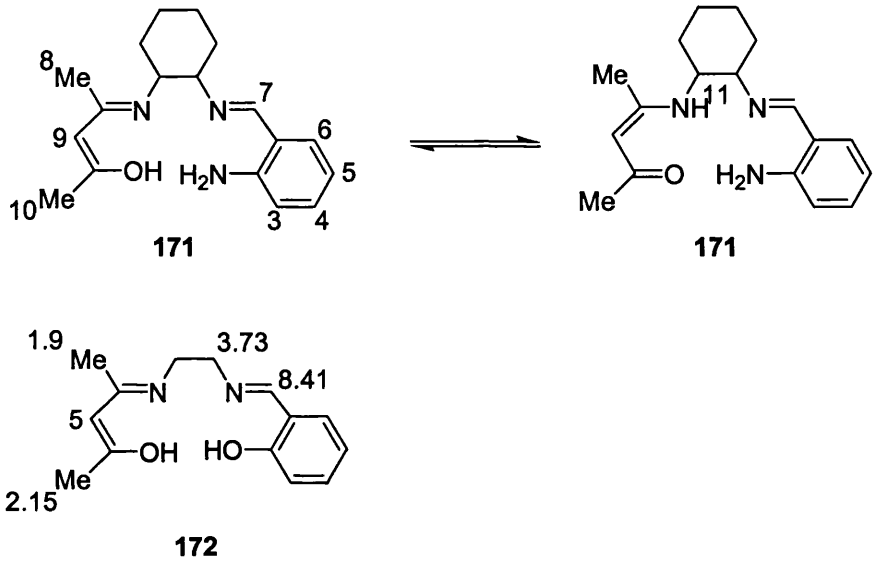

Figure 3.25. Asymmetrical ligand ambchac **171** *cf.* related ligand **172**

These results imply that the desired product **170** is more soluble in ethanol than $VO(acac)_2$ and cooling of the solution at the end of the reaction is not a suitable way to isolate it. The presence of asymmetrical ligand **171** in the yellow fraction together with the free, uncomplexed, ambch ligand (**107**) showed that complexation is not that fast and is a reversible process. This is not surprising as the synthesis of VO(ambch) complex **170** from $VO(acac)_2$ would involve breaking of four V-O bonds and forming four weaker V-N bonds which is enthalpically unfavourable. However the process is accompanied by an increase of the entropy in the system and at a certain temperature it is expected to become thermodynamically possible. Experimentally it was found that acetylacetone generated upon complexation reacts with the mono Schiff base formed by partial hydrolysis of **107** to give the asymmetrical ligand **171**. The latter can also undergo complexation, therefore a mixture of two paramagnetic, air-sensitive compounds **170** and **173** is expected to be obtained at the end of the reaction.

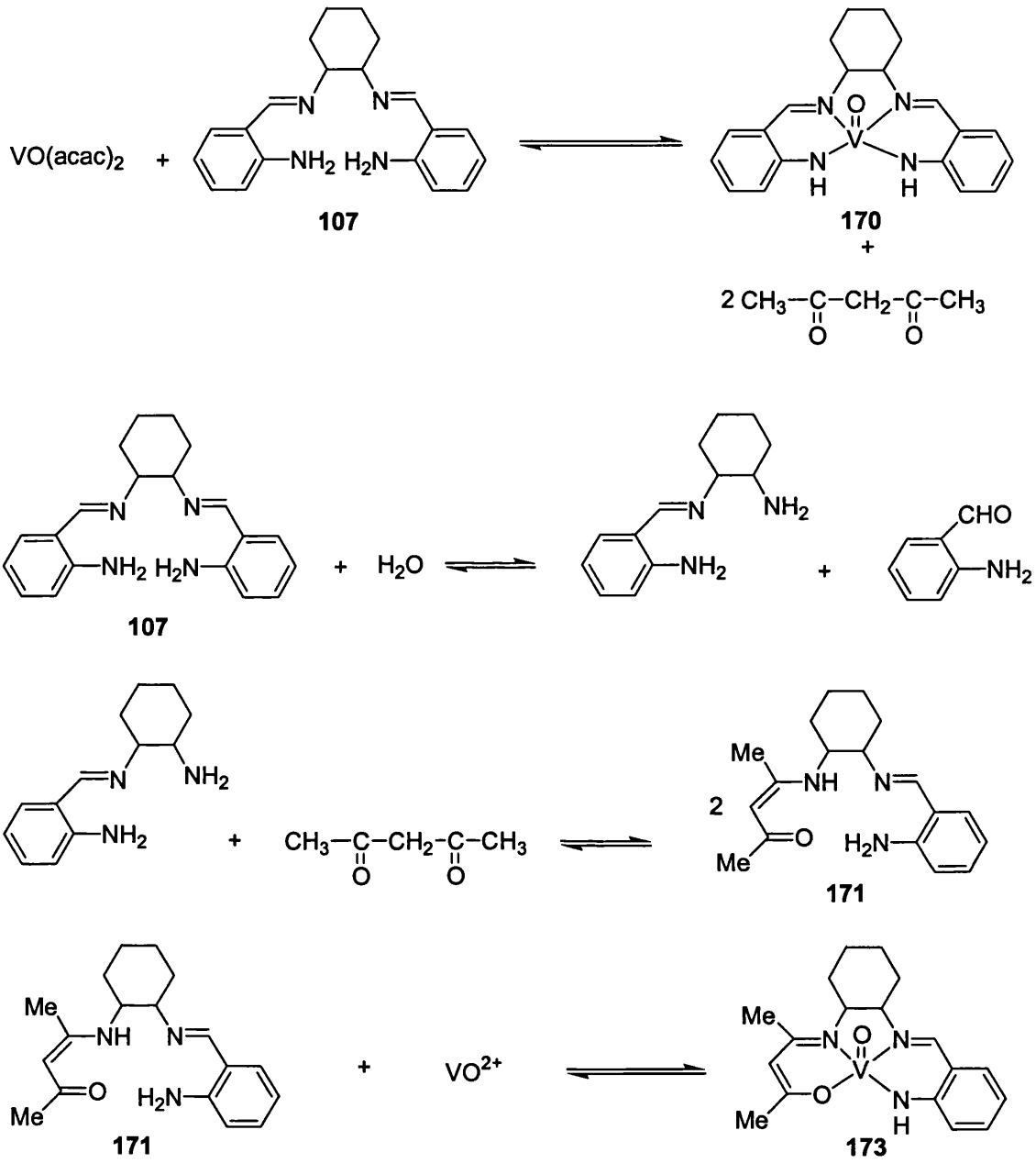

Scheme 3.15. Mechanism of ambch complexation with $VO(acac)_2$

Based on these results it was decided to modify the initial procedure. Addition of $VO(acac)_2$ was done over a hot solution of deprotonated ligand, a higher temperature was expected to increase the rate of the complexation reaction and dropwise addition to keep the concentration of acetyl acetone low at the beginning of the reaction. At the end of the complexation reaction, the salt formed by reaction of $NHEt_3^+$ with acetyl acetone (white precipitate) was separated by filtration from a dark green filtrate. Evaporation of this to dryness under reduced pressure produced an orange-brown oil. This was dissolved in DCM and a green-brown precipitate was formed by addition of diethyl ether to the mentioned solution. Upon addition of more ether and after shaking the

Schlenk tube, the precipitate became yellow-orange and solution turned brown. It is not clear if these changes in colour of both the precipitate and solution were determined by the change from a monomeric (green) to a polymeric structure (orange) of the complex or are two different VO complexes which pass from solution to the precipitate by changing the ratio between the two solvents.

Filtration of the system and evaporation of the filtrate under vacuum led to a brown solid. This was extracted twice with hot toluene to give a green solution and an orange solid, the liquid phase being decanted with the cannula. The product changed its colour, becoming darker orange, upon scratching with a spatula on the walls of the Schlenk tube inside a dry box and while mixing with KBr. The IR spectrum of the orange compound showed a very strong absorption at 1611 cm^{-1} corresponding to the stretching of C=N bond and strong bands at 1594 and 1524 cm^{-1} due to $\bar{\upsilon}_{(CO)}$ and $\bar{\upsilon}_{(C=C\ aliphatic)}$. These are in the same region with the data reported for the analogous VO complex **174** ($\bar{\upsilon}_{(CO)}$, $\bar{\upsilon}_{(C=C\ aliphatic)}$ = 1570-1580 cm^{-1}) [**40**] and $VO(acac)_2$ (Table 3.9).

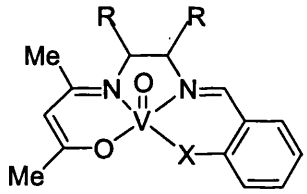

173: R, R = $-(CH_2)_4-$, X = NH
174: R = H, X = O

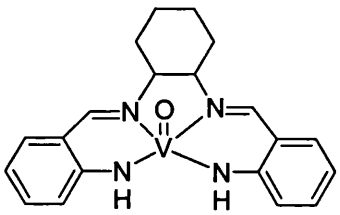

170

Figure 3.26. Asymmetrical VO(ambchac) complex **173** isolated and related VO complexes

The IR spectrum of the product (**173**) resembles with the spectrum of VO(ambch) (**170**) obtained using a different procedure (**5.10.3**), but it is not the same (Table 3.9). The difference in the structure of the symmetrical and asymmetrical complexes (**170** and **173**) is revealed by the presence in the spectrum of the bands for $\bar{\upsilon}_{(CO)}$, $\bar{\upsilon}_{(C=C\ aliphatic)}$, $\bar{\upsilon}_{(VO)}$, $\bar{\upsilon}_{(CH=CR_2)}$ and $\delta_{(CH_3)}$ which appear at different values than the corresponding frequencies in $VO(acac)_2$. The green fraction was a mixture of $VO(acac)_2$ and **173** as revealed by the IR spectrum.

Table 3.9. Selected IR frequencies (cm^{-1}) in $VO(acac)_2$ and VO(ambch) complexes

Characteristic absorptions	$VO(acac)_2$	VO(ambchac) **173**	VO(ambch) **170**
$\bar{\upsilon}(CH_3)$, $\bar{\upsilon}(CH_2)$	Low intensity	2929; 2856	2935; 2858
$\bar{\upsilon}(C=N)$	-	1611	1614
$\bar{\upsilon}(CO)$, $\bar{\upsilon}$(C=C aliphatic)	1558; 1529	1594; 1524	-
$\bar{\upsilon}$(C=C aromatic)	-	1543	1545
$\delta(CH_3)$	1374; 1358	1389; 1356	-
$\bar{\upsilon}(VO)$	997	962	962
$\delta(RCH=CR_2)$	799	806	-
$\delta(CH_3)$	-	750	752

Due to the problems encountered with the isolation of the product (**170**), it was decided to use $VOSO_4$ as source of vanadyl ions. A mixture of ligand and triethylamine in ethanol was heated to obtain a homogeneous system and $VOSO_4$ was added dropwise to it as an aqueous solution. In few minutes the solution changed its colour from yellow to orange and the system became heterogeneous. The product **170** precipitated from the reaction mixture and was separated by filtration as an orange powder (47.3 % yield).

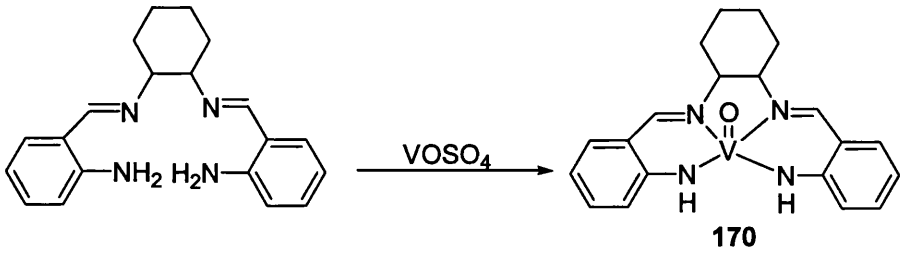

170

Scheme 3.16. Complexation of ambch with $VOSO_4$

The synthesis was also achieved by rapid addition of the deprotonated ligand to solid $VOSO_4$ under stirring at room temperature, then the temperature was increased to 60 °C and preserved until the end of the reaction. This was done to avoid the loss of the product in the aqueous layer in which it is soluble. The product did not change colour upon collection with the spatula from the Schlenk tube in the glove box.

Selected characteristic IR absorptions for compound **170** are given in Table **3.9**. The band for the C=N group appears at 1614 cm^{-1}, displaced to lower frequency than the free ligand indicating a decrease in the C=N bond order due to the involvement of N in the co-ordination of the metal. The stretching frequency from 962 cm^{-1} was assigned to $\bar{\upsilon}_{(VO)}$. The value is intermediate between the values reported for monomeric and polymeric VO salen type complexes, closer to the monomeric form [**42**].

3.6 Conclusions

Syntheses of *N,N'*-bis(2,2'-imino-R-benzylideneimino)-cyclohexane nickel, copper, manganese, cobalt and vanadyl complexes were performed and the products were characterized using different techniques. While complexation with nickel and copper gave the corresponding M(II)(ambch) complexes (M = Ni, Cu) for most ligands used, complexation of 5-Me-ambch with $Cu(OAc)_2$ and $CuCl_2$ in air resulted in formation of Cu(III) species. This is similar to previous studies carried out on 5-R-salen ligands which indicated that the ligand with R=Me has the highest tendency to form 5-coordinated complexes.

Manganese R-ambch complexes (R=H, 3-Me) were obtained via complexation of the ligand with $MnCl_2$, while the product proved hard to isolate pure from the route involving complexation with $Mn(OAc)_2$ followed by ligand exchange. After synthesis of Co(R-ambch)(R=H, 3-Me, 5-Me) complexes, the reactivity of the unsubstituted complex toward oxygen in presence of different nucleophiles was investigated. Co(III)(ambch) complexes were isolated in reaction of Co(ambch) with 4-t-Bu-phenol, $CHCl_3$ and ethanol/ AcO^-. The process depends on the solvent and the nucleophile employed. Further studies are necessary in order to obtain more information regarding oxidation in presence of 2,4-di-*t*-Bu-phenol and 2-butanol.

Complexation with $VO(acac)_2$ resulted in formation of the asymmetrical ligand **171** and of the corresponding vanadyl complex **173**, which is thermodynamically more favourable than formation of VO(ambch). Synthesis of the latter complex was achieved by employing a different vanadyl source, $VOSO_4$.

3.7 References

1. M. Green, P.A. Tasker, *J. Chem. Soc.* (A), **1970**, 2531.
2. E.J. Olszewski, D.F. Martin, *J. Inorg. Nuclear Chem.*, **1964**, *26*, 1577.
3. A. Wojtczak, E. Szlyk, M. Jaskolski, E. Larsen, *Acta Chem. Scand.*, **1997**, *51*, 274.
4. G. Brewer, J. Jasinski, W. Mahany, L. May, S. Prytkov, *Inorg. Chim. Acta,* **1995**, *232*,183.
5. N.A. Bailey, E.D. McKenzie, J.M. Worthington, *J. Chem. Soc., Dalton Trans.*, **1974**, 1363.
6. S. Bunce, R. Cross, L.J. Farrugia, S. Kunchandy, L.L. Meason, K.W. Muir, M. O'Donnell, R.D. Peacock, D. Stirling, S.J. Teat, *Polyhedron*, **1998**, 17, 4179.
7. T. Tanaka, *Bull. Chem. Soc. Jpn.*, **1960**, *33*, 259.
8. T. Tanaka, *J. Am. Chem. Soc.*, **1958**, *80*, 4108.
9. G. Brewer, J. Jasinski, W. Mahany, L. May, S. Prytkov, *Inorg. Chim. Acta,* **1995**, *232*,183.
10. M.M. Bhadbhade, D. Srinivas, *Inorg. Chem.*, **1993**, *32*, 6122.
11. G. Brewer, P. Kamaras, S. Prytkov, M. Shang, W.R. Scheidt, *J. Chem. Soc., Dalton Trans.*, **1999**, 4511.
12. J. Lange, H. Elias, H. Paulus, *Inorg. Chem.*, **2000**, *39*, 3342.
13. R.H. Holm, P. Kennepohl, E.I. Solomon, *Chem. Rev.*, **1996**, *96*, 2239.
14. a. M. Linss, U. Weser, *Inorg. Chim. Acta*, **1986**, *125*, 117, b. M. Linss, U. Weser, *Inorg. Chim. Acta*, **1987**, *138*, 163.
15. D. Hall, T.N. Waters, P.E. Wright, *J. Chem. Soc., Dalton Trans.*, **1973**, 1508.
16. K. Bernardo, S. Leppard, A. Robert, G. Commenges, F. Dahan, B. Meunier, *Inorg. Chem.*, **1996**, *35*, 387.
17. J.F. Larrow, E.N. Jacobsen, *J. Org. Chem.*, **1994**, *59*, 1939.
18. M. Palucki, N.S. Finney, P.J. Pospisil, M.L. Gueler, T. Ishida, E.N. Jacobsen, *J. Am. Chem. Soc.*, **1998**, *120*, 948.
19. M.R. Bermejo, A. Castineiras, J.C. Garcia-Monteagudo, M. Rey, A. Sousa, M. Watkinson, C.A. McAuliffe, R.G. Pritchard, R.L. Beddoes, *J. Chem. Soc, Dalton Trans.*, **1996**, 2935.
20. T. Hamada, R. Irie, J. Mihara, K. Hamachi, T. Katsuki, *Tetrahedron*, **1998**, *54*, 10017.
21. H. Nishikori, C.Ohta, E. Oberlin, R. Irie, T. Katsuki, *Tetrahedron*, **1999**, *55*, 13937.

22. M. Watkinson, M. Fondo, M.R. Bermejo, A. Sousa, C.A. McAuliffe, R.G. Pritchard, N. Jaiboon, N. Aurangzeb, M. Naeem, *J. Chem. Soc., Dalton Trans.*, **1999**, 31.
23. E.J. Larson, V.L. Pecoraro, *J. Am. Chem. Soc.*, **1991**, *113*, 3810.
24. N. Aurangzeb, C.E. Hulme, C.A. McAuliffe, R.G. Pritchard, M. Watkinson, A. Garcia-Deibe, M.R. Bermejo, A. Sousa, *J. Chem. Soc., Chem. Comm.*, **1992**, 1524.
25. D. Das, C.P. Cheng, *J. Chem. Soc., Dalton Trans.*, **2000**, 1081.
26. M. Green, P.A. Tasker, *J. Chem. Soc. (A)*, **1970**, 3105.
27. B.M. Higson, E.D. McKenzie, *J. Chem. Soc., Dalton Trans.*, **1972**, 269.
28. S. Brückner, M.Calligaris, G. Nardin, L. Randaccio, *Acta Cryst.*, **1969**, *B25*, 1671.
29. R.H. Bailes, M. C alvin, *J. Am. Chem. Soc.*, **1947**, *69*, 1886.
30. a) F.A. Walker, *J. Am. Chem. Soc.*, **1970**, *92*, 4235; b) J.H. Bayston, N.K. King, F.D. Looney, M.E. Winfield, *J. Am. Chem. Soc.*, **1969**, *91*, 2775.
31. a) A. Nishinaga, T. Kondo, T. Matsuura, *Chem. Lett.*, **1985**, 905; b) A. Nishinaga, T. Kondo, T. Matsuura, *Chem. Lett.*, **1985**, 1319; c) M. Calligaris, G. Nardin, L. Randaccio, *J. Chem. Soc., Chem. Comm.*, **1969**, 1248; d) N.A. Bailey, B.M. Higson, E.D. McKenzie, *Inorg. Nuclear Chem. Letters,* **1971**, *7*, 591.
32. J.J. Bozell, B.R. Hames, D.R. Dimmel, *J. Org. Chem.*, **1995**, *60*, 2398.
33. A. Nishinaga, K. Watanabe, T. Matsuura, *Tetrahedron Lett.* **1974**, 1291.
34. F.A. Cotton and G. Wilkinson in *Advanced Inorganic Chemistry*, 5th ed., John Wiley & Sons ed, Wiley-Interscience, New York, **1988**, 734.
35. a) V.F. Patel, G. Pattenden, *J. Chem. Soc, Chem. Comm.*, **1987**, 871; b) D.J. Coveney, V.F. Patel, G. Pattenden, *Tetrahedron Lett.*, **1987**, *28*, 5949; c) V.F. Patel, G. Pattenden, *Tetrahedron Lett.*, **1988**, *29*, 707.
36. Y.N. Ito, T. Katsuki, *Tetrahedron Lett.*, **1998**, *39*, 4325.
37. J.M. Ready, E.N. Jacobsen, *J. Am. Chem. Soc.*, **1999**, *121*, 6086.
38. a) M. Tokunaga, J.F. Larrow, F. Kakiuchi, E.N. Jacobsen, *Science*, **1997**, *227*, 936; b) C. Floriani, M. Puppis, F. Calderazzo, *J. Organomet. Chem.*, **1968**, *12*, 209.
39. P.J. McCarthy, R.J. Hovey, K. Ueno, *J. Am. Chem. Soc.*, **1995**, *77*, 5820.
40. X.R. Bu, E.A. Mintz, X.Z. You, R.X. Wang, Y. Qi, Q.J. Meng, Y.J. Lu, *Polyhedron,* **1996,** *15*, 4585.
41. S. Bunce, R.J. Cross, L.J. Farrugia, S. Kunchandy, L.L. Meason, K.W. Muir, M. O' Donnell, R.D. Peacock, D. Stirling, S.J. Teat, *Polyhedron*, **1998,** *17*, 4179.

42. K. Nakajima, M. Kojima, S. Azuma, R. Kasahara, M. Tsuchimoto, Y. Kubozono, H. Maeda, S. Kashino, S. Ohba, Y. Yoshikawa, J. Fujita, *Bull. Chem. Soc. Jpn.*, **1996**, *69*, 3207.
43. J-P Costes, M.I. Fernandez_Garcia, *Transition Met. Chem.*, **1988**, *13*, 131.
44. J-P Costes, G.Cros, M.H. Darbieu, J.P. Laurent, *Inorg. Chim. Acta*, **1982**, *60*, 111.

Chapter 4 Asymmetrical Schiff base ligands

4.1. Introduction

The interest in the design and synthesis of asymmetrical Schiff base ligands stems from the realisation that co-ordinated ligands around central metal ions in natural systems are asymmetrical [**1**]. An important feature of asymmetrical complexes is expected to be the unique structural properties, which may differ both sterically and electronically from those of their symmetrical counterparts. In salen-type ligands, substituents in the aromatic ring of the aldehydes play a key role in determining the general properties of the metal complexes due to their influence on the reactivity of the central metal ion. Further, keeping one site constant and changing the substituents on the other allows fine-tuning of the electronic properties of the complexes.

Although asymmetrical ligands offer many advantages over the symmetrical counterparts in elucidation of the composition and geometry of metal ion binding sites in biological systems, progress in this field has been hampered by their difficult preparation. Strategies proposed for the synthesis of asymmetrical Schiff base ligands involve: (i) a stepwise procedure with or without isolation of the intermediate mono Schiff base [**2, 3**]; (ii) blocking of one of the two active sites in the diamine [**4, 5**]; or (iii) separation of the mono Schiff base from the double Schiff base as a nickel(II) complex [**6**].

Recent studies concerning the reactivity of asymmetrical Schiff base complexes confirmed the potential of such complexes. Jacobsen and co-workers reported the preparation of asymmetrical complex **175**, an intermediate which was further used in synthesis of dimer **55b** [7]. Kinetic studies with monomeric (symmetrical and asymmetrical) and dimeric chromium salen complexes **175, 54** and **55b** demonstrated that the ring opening of *meso* epoxides catalysed by these complexes proceeds *via* a co-operative mechanism between two metal centres in solution and it was also found that the asymmetrical complex **175** was twice as reactive as its symmetrical counterpart **54**.

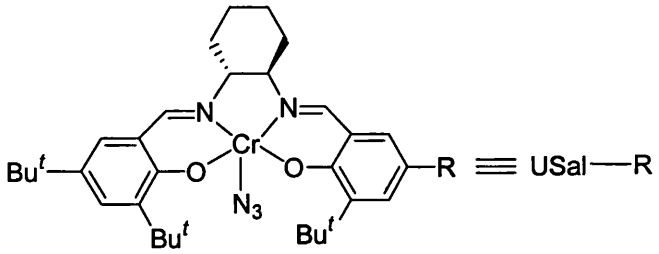

175: R = OAc
54: R = ^{t}Bu

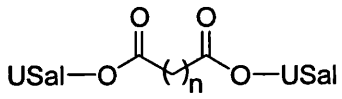

55b: n = 2-10

Figure 4.1. Jacobsen's monomer and dimer - catalysts in ring opening of epoxides

While the work described in this thesis was in progress the asymmetrical chromium complexes **176, 177** were prepared [3] and their catalytic activity in stoichiometric epoxidation of E-β-methylstyrenes was tested.

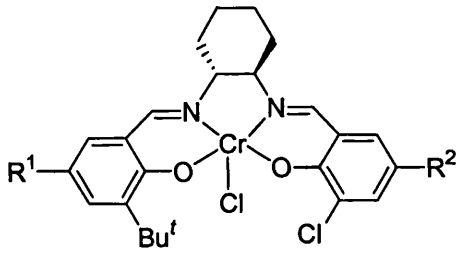

176: R^1 = ^{t}Bu; R^2 = H
177: R^1 = H; R^2 = Cl

Figure 4.2. Gilheany's asymmetrical chromium salen epoxidation catalysts

Enantioselectivities were not as good as those obtained in the case of the corresponding symmetrical Schiff base complexes, but in the presence of Ph_3PO as donor ligand they increased substantially and became close to the latter. The authors consider that these results are determined by the fact that the employed asymmetrical complexes were not bent like their symmetrical counterparts are and thus preserve the C_2-symmetry around the metal centre.

Figure 4.3. Planar *cf.* bent conformation in Cr(salch) complexes

4.2. Nomenclature of asymmetrical salen ligands

Abbreviated names for asymmetrical salen ligands are obtained using the same method as that employed for the family of symmetrical salen ligands. The abbreviated name of the diamine is placed between the two abbreviated names of the aldehydes employed in the synthesis. Abbreviations for the parent aldehydes salicylaldehyde, 3,5-di-*t*-butylsalicylaldehyde, aminobenzaldehyde, 3-methyl and 5-methyl-aminobenzaldehydes, thiosalicylaldehyde are: sal, 3,5-di-^{t}Bu-sal, amb, 3-Me-amb, 5-Me-amb, t-sal while for the diamines 1,2-diaminocyclohexane and 1,3-diaminopropane they are ch and pr.

4.3 Strategies applied for the synthesis of asymmetrical salchsal and ambchsal ligands

This section describes the results obtained in syntheses of new asymmetrical salchsal (**178**) and ambchsal (**179 - 183**) ligands shown in Figure 4.4.

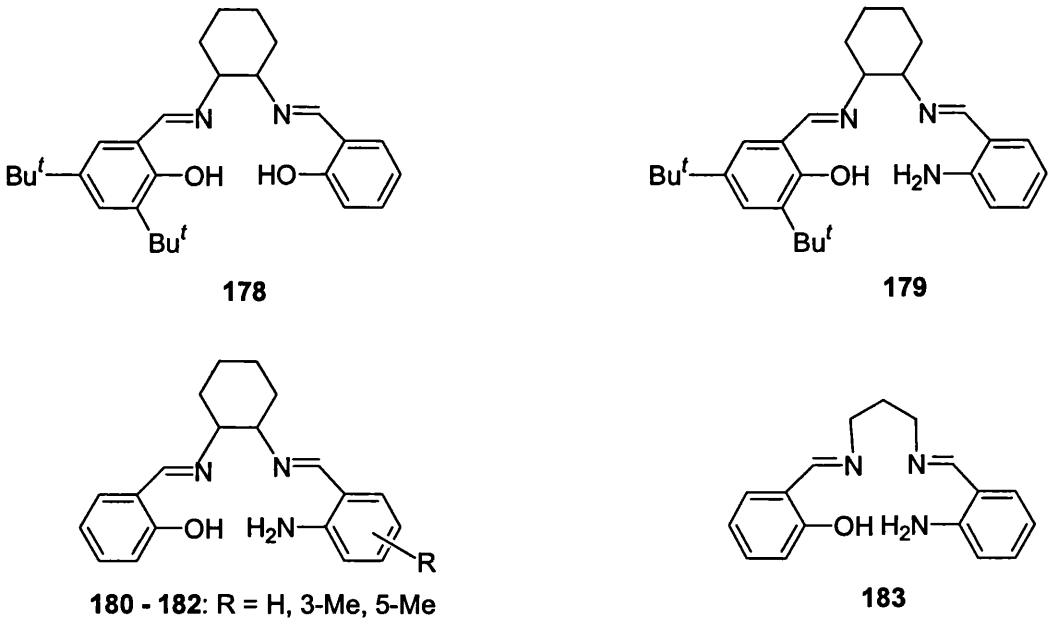

Figure 4.4. Asymmetrical salchsal and ambchsal ligands synthesized

After studying the reactivity of several aromatic aldehydes towards 1,2-diaminocyclohexane, the strategies for preparation of asymmetrical salen ligands

proposed in the literature were tested. New strategies (sections **4.3.1.2. - 4.3.1.4.**) were also developed in the search for better synthetic routes to compounds **178 - 183**. Further more, preparation of nickel asymmetrical Schiff base complexes derived from ligands **178** and **180 - 182** under mild conditions are discussed in section **4.4.**

4.3.1. Stepwise procedure

This procedure implies the synthesis of the mono Schiff base **185a-d** and its subsequent condensation with a second carbonyl compound to give the asymmetrical Schiff base ligand.

4.3.1.1 Study of the reactivity of different aromatic aldehydes toward 1,2-diaminocyclohexane

The reactivity of several aromatic aldehydes toward 1,2-diaminocyclohexane was studied in ethanol at reflux, using a 1 : 3 ratio between the aromatic aldehyde and diamine.

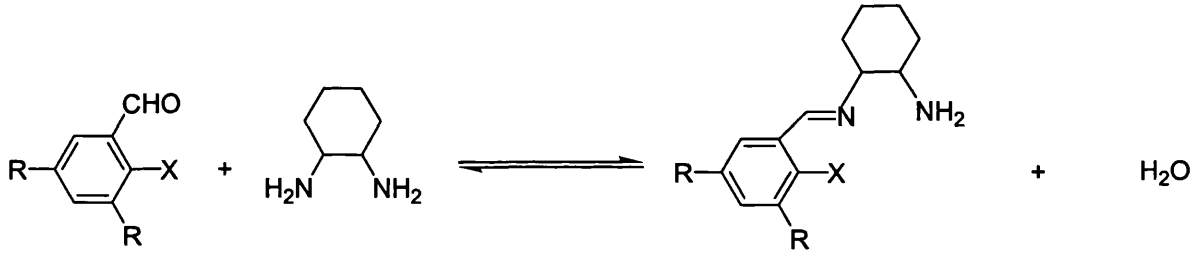

184a-d **185a-d**

a-c: R = H; X = NH_2, HO, MeO

d: R = ^{t}Bu; X = HO

Scheme 4.1. First step condensation

Condensation yields an equilibrium mixture of mono (**185**), double Schiff base (**107** or **186b, c**) and free amine. An excess of the diamine and dropwise addition of the aldehyde over the diamine ensured a higher ratio of mono to double Schiff base. This ratio for different aldehydes was determined by ^{1}H-NMR and was used to estimate their reactivity (Table 4.1). A lower ratio of mono to double Schiff base corresponds to a higher reactivity of the aldehyde.

Table 4.1. Reactivity of benzaldehydes **184a-d** toward 1,2 diaminocyclohexane

Compound	X	R	Ratio of Schiff bases	
			mono	double
a	NH_2	H	32.5	1
b	HO	H	5	1
c	MeO	H	29	1
d	HO	*t*-Bu	8	1

Salicylaldehyde was much more reactive than 2-aminobenzaldehyde (Table 4.1., entries 1, 2) and for this reason we aimed to transform salicylaldehyde into a derivative which would have a lower reactivity and would undergo a more selective condensation. It was expected that substitution of the proton in the phenolic group of salicylaldehyde with a protective R group, that could be later removed under mild conditions would increase the ratio of mono to double Schiff base. Protection of the hydroxyl group as *t*-butyldimethylsilyl ether (TBDMS) is widely used in organic synthesis because it involves an easy preparation, has a good stability under a wide range of reaction conditions and can be removed in mild conditions [**8**].

2-Methoxy-benzaldehyde was used as model compound to test this approach and indeed the reactivity of the aldehyde decreased almost six times (entry 3). A similar effect, although of lower magnitude, was obtained when bulky tert-butyl groups were introduced in *ortho-* and *para-* positions to the hydroxyl groups (entry 4).The mono Schiff bases obtained when X = NH_2, MeO (entries 1 and 3) contained only traces of double Schiff base. Attempts to remove the excess of the diamine by washing with water or ether were accompanied by modification of the ratio mono to double Schiff bases due to the shift of the equilibrium between them.

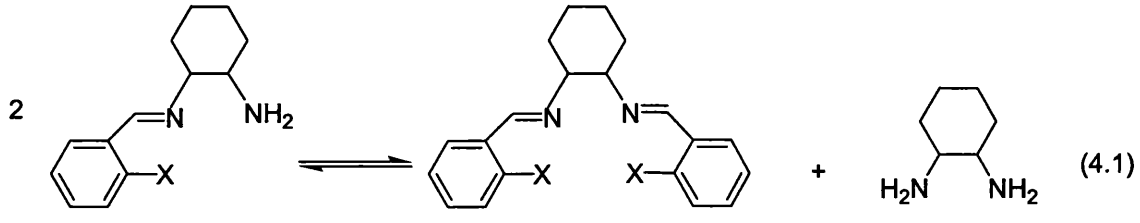

185a: X = NH_2
185b: X = HO
185c: X = MeO

107
186b
186c

ch

Scheme 4.2. Equilibrium generating the double Schiff base from the mono Schiff base

Results from entry 4 in Table 4.1, at first sight, are in contradiction with the data reported by Gilheany (Table 4.2)[3].

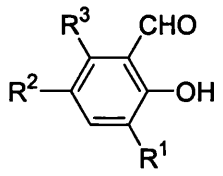

187

Table 4.2. Reactivity of benzaldehydes **187** toward 1,2-diaminocyclohexane

Ligand	R_1	R_2	R_3	Ratio of Schiff base ligands	
				Mono	Double
a	Cl	H	H	3	1
b	Cl	Cl	H	6	1
c	Cl	Cl	Cl	10	1
d	H	NO_2	H	30	1

In a similar way he measured the equilibrium ratios between mono and double Schiff bases obtained from condensation of 1,2-diaminocyclohexane with salicylaldehyde derivatives **187** substituted with electron-withdrawing groups and found that the reactivity of the aromatic aldehydes decreased with introduction of such substituents onto the aromatic ring. These data point out two different factors which influence the equilibrium below (Scheme 4.3), namely the electrophilicity of the benzaldehyde derivative, and the acidity of hydroxy group.

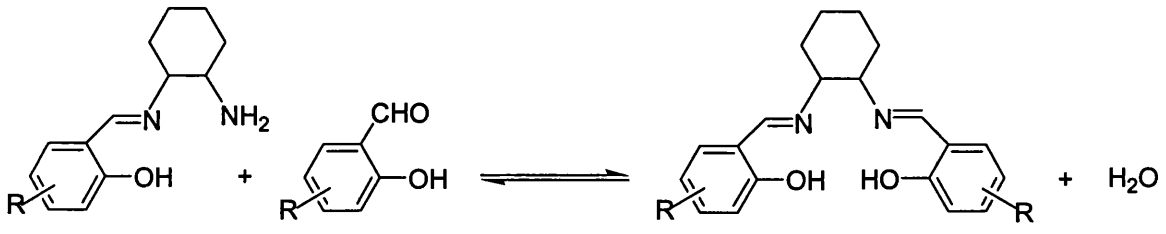

Scheme 4.3. Formation of symmetrical double Schiff base in the first step condensation

In the condensation reaction the aldehyde acts as an electrophile and electron-donating substituents in the aromatic ring will increase the electron density at the carbon atom

from the carbonyl group which will lower the aldehyde electrophilicity. In the salicylaldehyde derivatives substituted with electron-withdrawing groups, the substituents at the aromatic ring increase the acidity of the hydroxy group and for this reason the more probable structure of the mono Schiff base is zwitterionic:

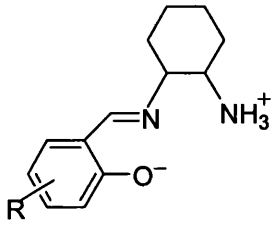

Figure 4.5. Structure of the mono Schiff base when R is an electron-withdrawing substituent

The effect increases with the number of electron-withdrawing groups (Table 4.2, entries 1-3) and also depends on the nature of the substituents (entries 1, 4). Protonation of the mono Schiff base (Figure 4.5) reduces considerably the rate of condensation with a second mole of aldehyde, therefore the ratio of mono to double Schiff base decreases. These two effects combine together to give the observed reactivity of the salicylaldehyde derivatives.

4.3.1.2 Procedure 1

Condensation of 3,5-di-*t*-butyl-2-hydroxybenzaldehyde with 1,2-diaminocyclohexane (Scheme 4.4) was performed as described in the section **4.3.1.1**. In the second condensation the aldehyde was added dropwise over the mixture of mono and double Schiff bases (**185d**, **186d**) in dichloromethane at 25 °C. Then the temperature was increased slowly to 55 °C and it was maintained for 3 hours.

First step

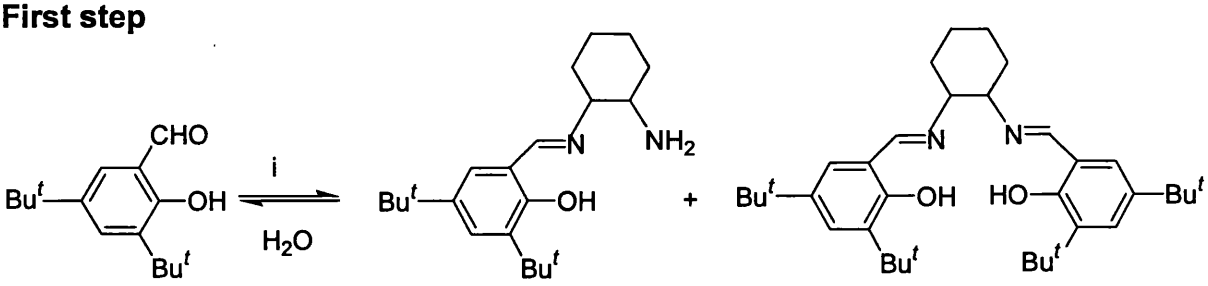

185d **186d**

i: 1,2-diaminocyclohexane

Second step

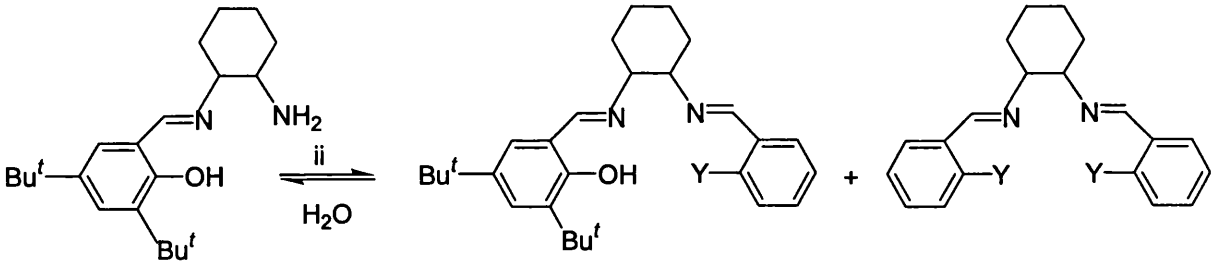

185d

178: Y = OH
179: Y = NH_2

107: Y = NH_2
186b: Y = OH

ii: 2-Y-C_6H_4-CHO

RESULTS

Synthesis of **178**

First step: **185d** : **186d** = 6 : 1
Second step: **186d** : **178** : **186b** = 0.29 : 1 : 0.93

Synthesis of **179**

First step: **185d** : **186d** = 6 : 1
Second step: **186d** : **179** : **107a** = 0.26 : 1 : 1

Scheme 4.4. Condensation steps in Procedure 1

Higher temperatures or rapid heating of the reaction mixture dramatically modified the ratios of asymmetrical to symmetrical Schiff bases. A lower temperature, which involved longer periods to complete the reaction, had similar effects. The results obtained from each step are given in Scheme 4.4. When the reaction was complete the mixture was concentrated and the addition of petroleum spirit led to precipitation of symmetrical Schiff base **186b** and **107** respectively. After filtration, the solvent was evaporated and the asymmetrical ligand **178** precipitated on crystallisation from ethanol.

The asymmetrical ligand **179** could not be isolated in the same way as it was more soluble in ethanol than the symmetrical Schiff base **186d**. 3,5-Di-*t*-butyl-2-hydroxybenzaldehyde was added first because the separation of the asymmetrical ligands from the symmetrical **186b** and **107** proved to be less difficult than from the other symmetrical Schiff base. A higher ratio of mono Schiff base **185d** to **186d** was desired to ensure a lower amount of the latter Schiff base in the reaction mixture obtained after the second step condensation.

4.3.1.3 Procedure 2

In a different procedure, both aldehydes were added dropwise to the diamine dissolved in dichloromethane at room temperature. (ratio aldehyde 1: amine: aldehyde 2 = 1:1:1). The temperature was then increased gradually to 55 °C and held at this value for 3 h. After this period, more of the second aldehyde was added to the reaction mixture in order to transform all the mono Schiff bases into double Schiff bases. The results obtained in this case are given in Scheme 4.5.

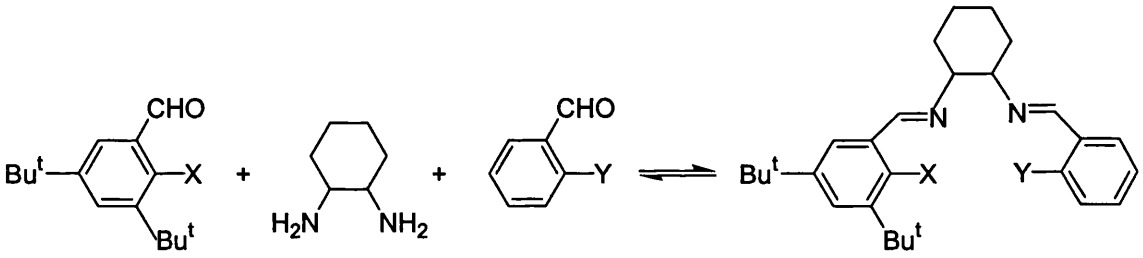

178: X = Y = OH;
179: X = OH, Y = NH_2

RESULTS

Synthesis of **178**
First step:
186d : **178** : **186b** = 0.55 : 1 : 0.83
Second step:
186d : **178** : **186b** = 0.3 : 1 : 0.96

Synthesis of **179**
First step:
186d : **179** : **107** = 1.48 : 1: 0.2
Second step:
186d : **179** : **107** = 0.41 : 1 : 0.69

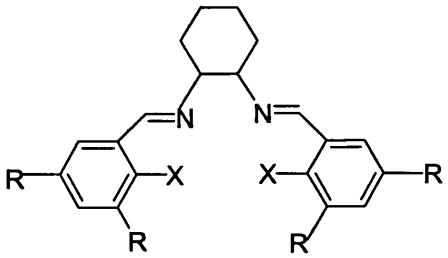

107: X = NH_2, R = H
186b: X = OH, R = H
186d: X = OH, R = ^{t}Bu

Scheme 4.5. Synthesis involving addition of both benzaldehydes in the first step

The work-up procedure was similar to that presented in 4.3.1.2. The asymmetrical ligand **178** was isolated by a two-step recrystallisation, while the asymmetrical ligand **179** could not be isolated pure. The composition of the reaction mixture obtained from these two procedures were similar for synthesis of **178**. In the case of asymmetrical ligand **179** better results (in terms of the ratio of asymmetrical ligand to each symmetrical Schiff base) were obtained using the first procedure.

4.3.1.4. Procedure 3

Another way of generating the mono Schiff base **185d, b** is by making use of the equilibrium below :

First step

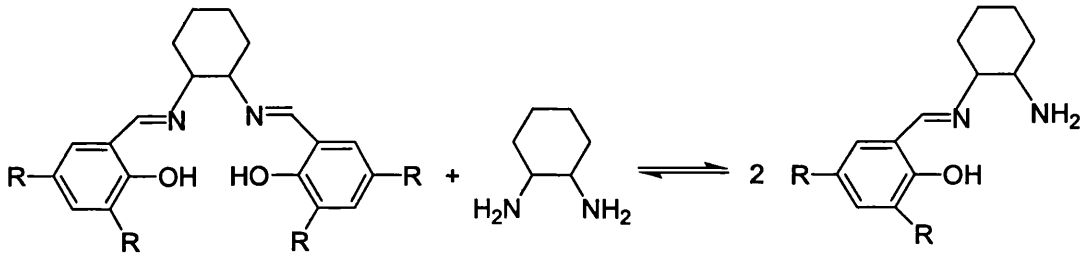

186b: R = H
186d: R = ^{t}Bu

185b: R = H
185d: R = ^{t}Bu

Second step

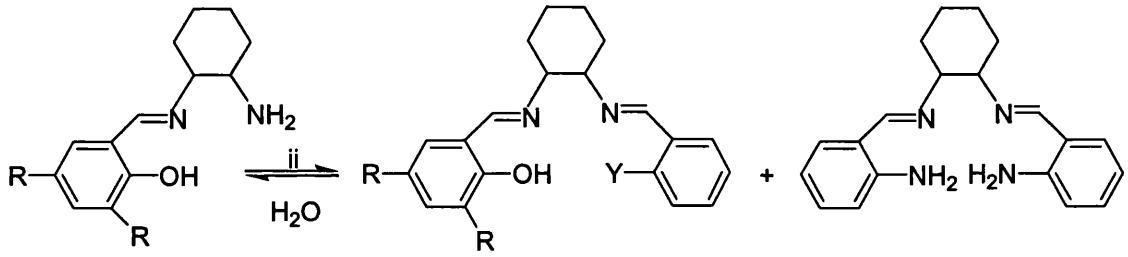

179: Y = NH_2, R = ^{t}Bu
180: Y = NH_2, R = H

107

ii: 2-H_2N-C_6H_4-CHO

RESULTS

Synthesis of **179**
First step: **185d** : **186d** = 3.4 : 1
Second step: **186d** : **179** : **107** = 0.4 : 1 : 1.1

Synthesis of **180**
First step: **185b** : **186b** = 4 : 1
Second step: **186b** : **180** : **107** = 0.1 : 1 : 0.03

Scheme 4.6. Reaction steps in Procedure 3

The mono Schiff base **185d, b** was obtained upon mixing the double Schiff base **186d, b** and the diamine in stoichiometric amounts in CH_2Cl_2 and stirring the obtained mixture for 3 days at room temperature. After this step the solvent was not evaporated and the second condensation (Scheme 4.6) leading to asymmetrical ligand was performed in the same manner as described before. When the solvent is evaporated part of the diamine is removed from the system and this shifts the equilibrium (4.1) back to the symmetrical Schiff base **186d, b**, a process which is not desired. The composition at each stage was established by ^{1}H-NMR.

Although the asymmetrical ligand was not isolated, very good results were obtained in the synthesis of **180**. Thus, the ratio of symmetrical **186b** to asymmetrical **180** was 1 : 10 and symmetrical **107** to asymmetrical **180** was 1 : 30. In the case of ligand **179** the results were not as good as those obtained in procedure 1, which seems to be the best synthetic method for it.

4.3.1.5. Characterisation of the symmetrical and asymmetrical salen ligands by ^{1}H-NMR

C_2-symmetrical ligand **186b** contains two equivalent aromatic rings substituted with hydroxy groups placed *ortho-* to the imine groups. The ^{1}H-NMR spectrum recorded in $CDCl_3$ presents a broad signal at δ 13.30 which was assigned to the phenolic protons, while the protons from the imine group (H^7) appear at δ 8.27 as a singlet. In the region corresponding to aromatic protons, the spectrum exhibits four signals due to the presence of four non-equivalent aromatic protons in the molecule. Protons H^6 and H^3 appear as two doublets at δ 7.15 and 6.89, and H^5 and H^4 as triplets at δ 6.80 and δ 7.24 respectively. The signal for H^6 appears at lower field than the one for H^3 due to the vicinity of the former proton to the imine group. The magnetic anisotropy of this group is also responsible for a higher δ value found in for H^4 as compared to the one for H^5.

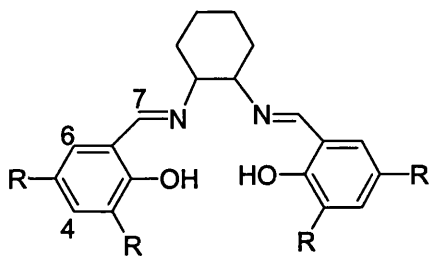

186b: R = H
186d: R = ^{t}Bu

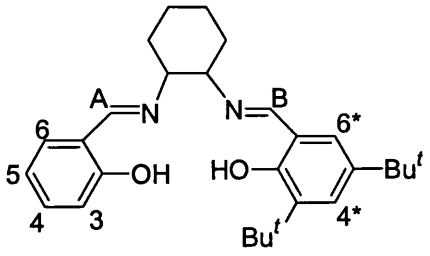

178

Figure 4.6. Symmetrical salch and asymmetrical salchsal ligands and the proton labelling in ^{1}H-NMR

The protons from the cyclohexane moiety appear as four multiplets at δ 3.33 and between δ 1.98 and 0.87.

Symmetrical Schiff base **186d** shows signals for phenolic and imine protons at δ 13.72 and 8.30 (H^7) respectively, similar to those obtained in the case of **186b**. The aromatic H^4 and H^6 protons appear as two doublets at δ 6.98 and 7.30 due to the *meta-* coupling between them (J=2.4 Hz). The chemical shifts were assigned on similar considerations with those for the **186b**, therefore H^6 will appear at a lower field than H^4. The protons from the cyclohexyl moiety appear as multiplets in the aliphatic region, which also shows two singlets (δ 1.41 and 1.25) corresponding to the protons from the *t*-butyl groups present in the molecule in *ortho-* and *para-* positions respectively to the hydroxyl group.

In the asymmetrical ligand **178** the two aromatic rings are non-equivalent. The molecule contains two different imine groups appearing as singlets at δ 8.29 (H^B) and 8.26 (H^A) and two hydroxy groups seen as broad resonances at δ 13.66 and 13.41. Assignment of the two imine protons was done by comparison with similar protons in the corresponding symmetrical Schiff bases **186b** and **186d**. In the aromatic region, the spectrum shows four doublets, two at δ 7.31 and 6.97 have a coupling constant of 2.4 Hz and the other two at δ 7.14 and 6.88 have a coupling constants of 7.8 Hz. Comparing these signals with those obtained in the spectra of symmetrical double Schiff bases, one can establish that the first two correspond to protons from the aromatic ring substituted with *t*-butyl groups (H^{6*}, H^{4*}) and the others to protons from the unalkylated ring (H^6,

H^3). The two triplets at δ 7.24 and 6.80 are due to protons (H^4, H^5) from the same, unalkylated, aromatic ring. The spectrum also contains the multiplet resonance of the cyclohexylidene moiety in the aliphatic region and two singlets at δ 1.41 and 1.24, each of them corresponding to nine protons from the *t*-butyl groups.

4.3.1.6. Attempt to synthesize N-(2-hydroxy-benzylidene)-1,2-diamino-cyclohexane

The procedure for synthesis of mono Schiff base **185b** has been published by Lopez *et.al.* [2], who reported that an almost pure product could be obtained by condensation of 1,2-diaminocyclohexane with salicylaldehyde in chloroform at 0 °C. The very slow addition of the aldehyde (5 h) and a lower temperature contributed to a better selectivity in the first step condensation and led to a higher ratio of mono : double Schiff base. A small excess (1-1.5 equiv) of the diamine is employed which is then removed with the solvent on distillation under vacuum. The second condensation took place in ethanol at 60 °C leading to compounds **188** in 77-97 % yield.

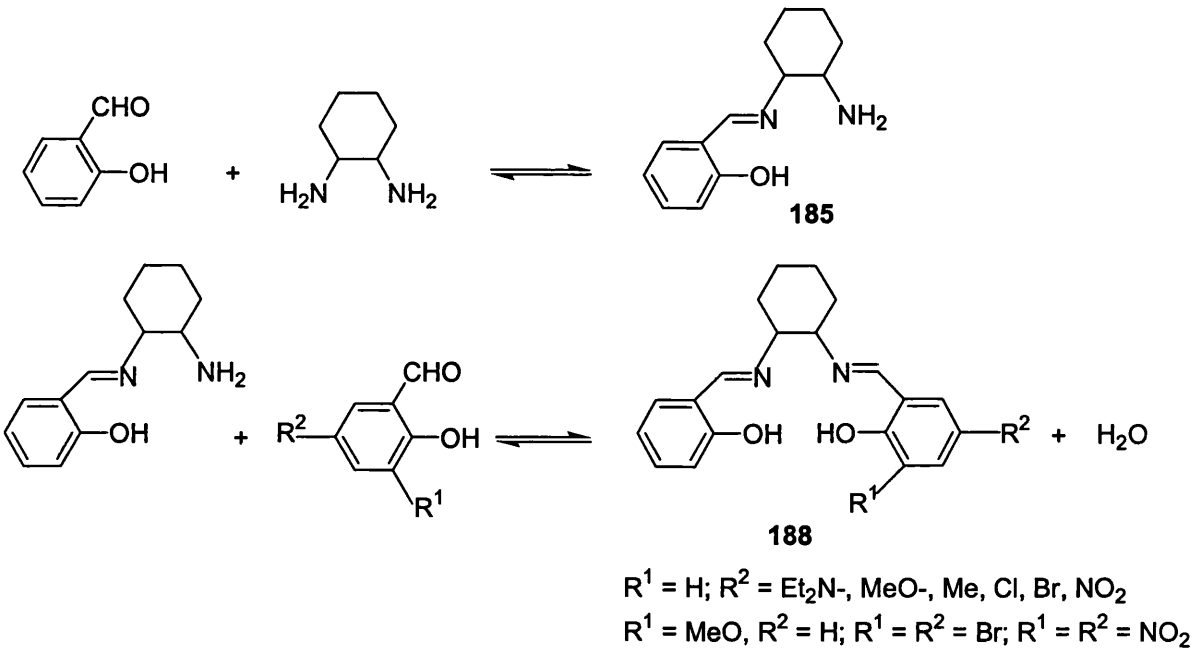

Scheme 4.7. Condensation steps in Lopez' procedure

Employing Lopez' method I obtained a different composition of the reaction mixture after the first condensation. As the authors did not give enough details regarding the

work-up procedure, samples were taken from the reaction mixture at different moments and their composition was determined by ^{1}H-NMR to check the reported results. The heating procedure (from 0 °C to 70 °C) is very important because during it the ratio mono: double Schiff base varies considerably. Different parameters such as period spent by the mixture at room temperature, period used to remove the solvent and the time spent at 60°- 70°C were varied. When the solvent was removed together with the diamine the equilibrium was shifted back to the double Schiff base (Scheme 4.8) and periods longer than 5 minutes even at 60 °- 70 °C resulted into massive decomposition of the product.

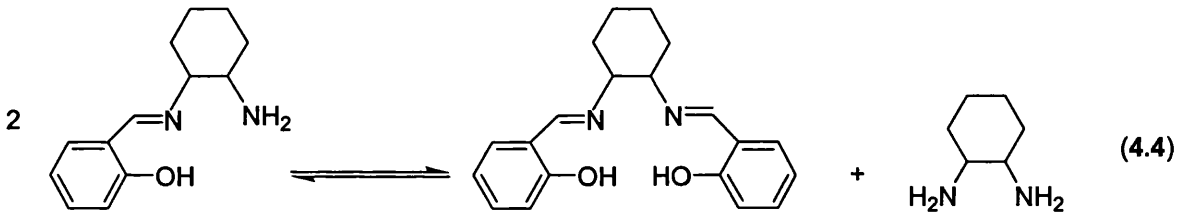

(4.4)

Scheme 4.8. Decomposition of the mono Schiff base

After all these tests I obtained the best result (mono **185b** : double Schiff base **186b** = 7 : 1) when the ratio diamine : salicylaldehyde was 1.5 : 1 (heating period between 0-70 °C aprox. 15 min). Later, independently two other research groups [**3, 4**] reported that Lopez' procedure could not be reproduced and questioned his data. Following the mentioned procedure, Gilheany [**3**] reported a ratio mono **185b** : double Schiff base **186b** equal to 3 : 1. Due to the problems encountered it was decided to do the synthesis of asymmetrical complexes using my own procedures.

4.3.2. Synthesis involving blocking of one of the active sites in the diamine

This strategy was proposed by Katsura who used it in synthesis of asymmetrical salen ligand **189** [**5**]. Acetic acid reacts with 1 equivalent of 1,3-diamino-propane in methanol generating the corresponding mono ammonium salt. The reaction blocked one of the active sites of the diamine, leaving the other one able to give condensation with salicylaldehyde. Then the blocked site is neutralised with triethylamine in the presence

of 2-hydroxy-acetophenone and the second condensation takes place. The reaction mixture was heated for a short period for completion, total reaction time was less than 2 h, and the product was isolated by recrystallisation from methanol.

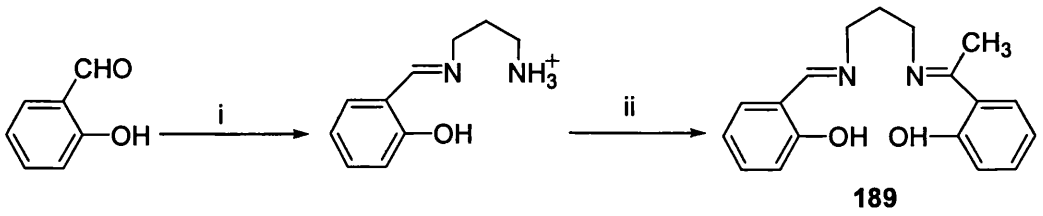

189

i: 1,3-diamino-propane, CH_3COOH, CH_3OH
ii: 2-hydroxy-acetophenone, Et_3N, 50°C

Scheme 4.9. Katsura's strategy for the synthesis of **189**

This approach has been recently used in the synthesis of several asymmetrical salen ligands **190** having an (N_2O_2) donor atom set [**4**]. The authors took advantage of insolubility of ammonium salts in ethereal solution and used anhydrous hydrochloric acid instead of acetic acid as the blocking reagent. In this way they isolated the mono Schiff base ammonium salts which were subsequently treated with the second salicylaldehyde derivative. The first condensation reaction was done in a mixture of methanol-ethanol, while the second condensation reaction took place in absolute ethanol in the presence of molecular sieves at room temperature. The reaction time for each step was rather long; the whole synthesis lasting 60-72 h. At the end of the reaction the solvent was removed under vacuum to give a solid which was extracted with dry diethyl ether and after filtration and solvent evaporation led to the desired products in 60-87 % yield.

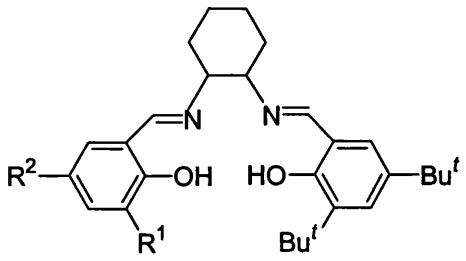

190

a-c: $R^1 = {}^tBu$; R^2 = H, NMe_2, O^iPr
d : $R^1 = R^2$ = Br
e : $R^1 = R^2 = NO_2$

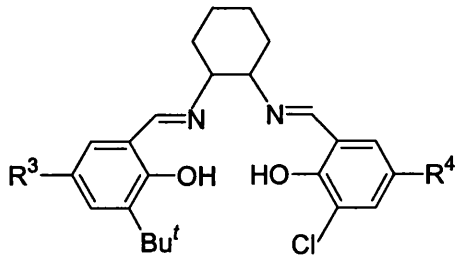

191

a: $R^3 = {}^tBu$; R^4 = H
b: R^3 = H; R^4 = Cl

Figure 4.7. Nguyen's and Gilheany's asymmetrical salchsal ligands

A slightly different procedure was reported by Gilheany [3] for the synthesis of asymmetrical ligands **191**. After the first condensation performed at room temperature in diethyl ether, the mono Schiff base was separated from the double Schiff base as a salt with (+)-O,O'-dibenzoyl-D-tartaric acid. He showed that better results are obtained on salicylaldehyde derivatives substituted with electron withdrawing groups which are less reactive in the condensation with 1,2-diaminocyclohexane. The second step was performed in refluxing ethanol and the product was isolated by flash chromatography in low yields.

We adapted the procedure described by Katsura [5] toward the synthesis of asymmetrical ligand **183** derived from salicylaldehyde, 1,3-diamino-propane and 2-aminobenzaldehyde using acetic acid for generation of the mono Schiff base ammonium salt. The latter was neutralised *in situ* with triethylamine in the presence of 2-aminobenzaldehyde and the reaction mixture was heated for a short period to ensure the completion of the second condensation. The solvent was removed under vacuum and the composition of the reaction mixture was determined by ^{1}H-NMR.

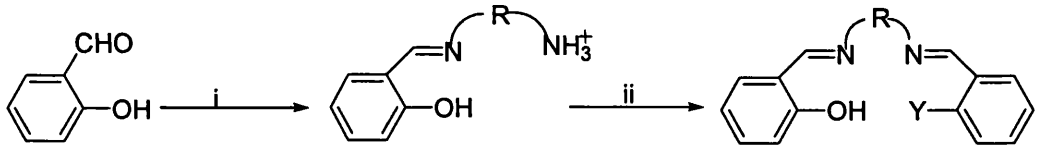

i: 1,3-diamino-propane, CH_3COOH, CH_3OH, 25 °C
ii: 2-amino-benzaldehyde, Et_3N, 50 °C

183: Y = NH_2, R = -$(CH_2)_3$-
192: Y = OH, R = -$(CH_2)_3$-

180: Y = NH_2, R = -C_6H_{10}-
186: Y = OH, R = -C_6H_{10}-

Scheme 4.10. Our synthesis of **183** using Katsura's strategy

The NMR spectrum of the mixture showed two singlets at δ 8.39 and 8.37 in the ratio 1.2 : 1 which correspond to the imine group protons from symmetrical **192** and asymmetrical **183** Schiff bases. The first assignment was done by comparison with the signal obtained for a pure sample of **192**. This result is comparable with that reported by Brewer [9], who obtained the nickel complex of **183** in 19 % yield using a different strategy.

The method proved to be not that effective for the synthesis of asymmetrical ligand **183** derived from 1,3-diamino-propane and it was expected that in the case of the more reactive 1,2-diamino-cyclohexane the ratio symmetrical **186b** : asymmetrical **180**

complex would be higher. For this reason we decided to use other procedures for synthesis of ligands with an N_3O donor atom set.

4.3.3. Attempted synthesis of asymmetrical ligand from the nickel (II) complex of the mono Schiff base

Introduced by Elder [6], this approach involves separation of the mono Schiff base from the reaction mixture obtained after the first condensation as a nickel complex **194** (Scheme 4.11). The latter is formed on addition of nickel(II) acetate to the obtained solution and heating at reflux.

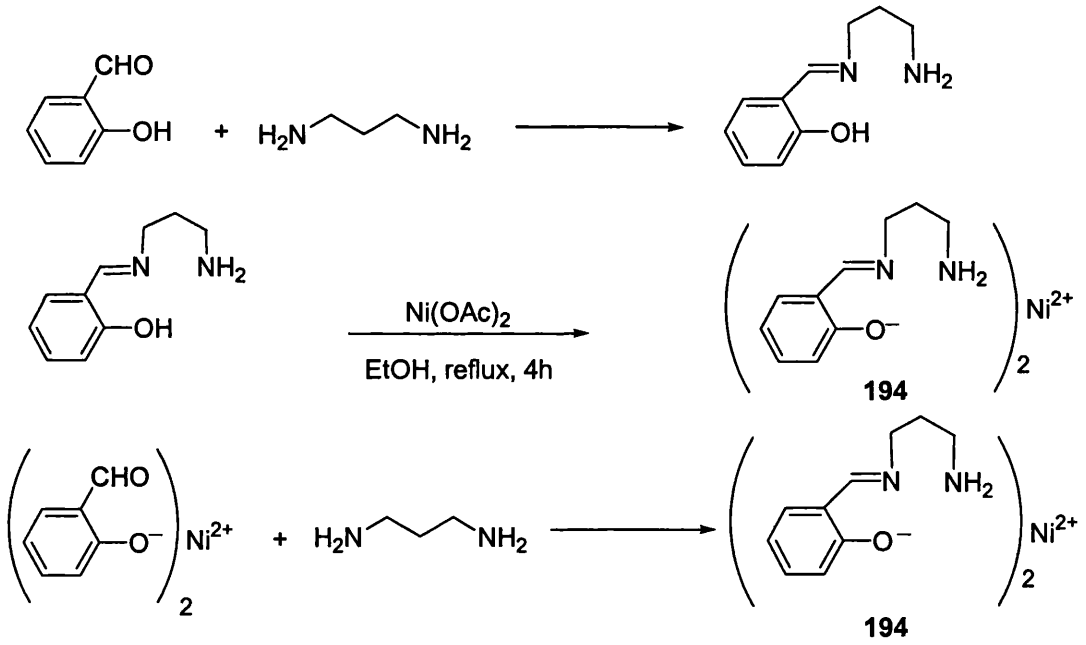

Scheme 4.11. Synthesis of nickel complex of the mono Schiff base

An alternative route to complex **194** is by reaction of the salicylaldehyde nickel complex with an excess of diamine. In the next step, complex **194** is treated with dimethylglyoxime (H_2dmg) in refluxing methanol for several hours to give $Ni(Hdmg)_2$ as a precipitate, leaving the free mono Schiff base **193** in solution. After filtration the latter undergoes condensation with a different aldehyde and generates the asymmetrical tetradentate Schiff base ligand.

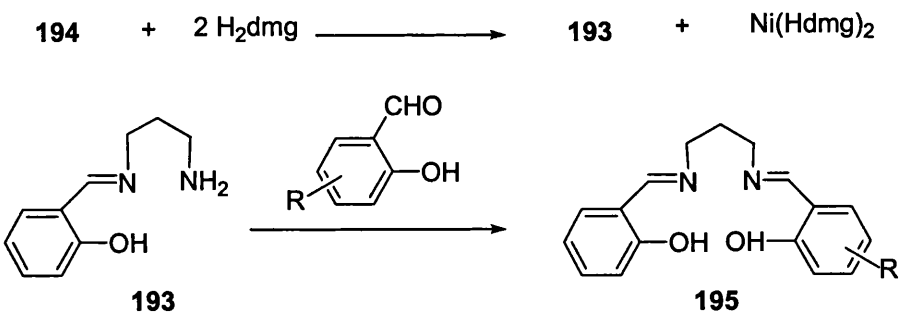

Scheme 4.12. Elder's proposed strategy to nickel salprsal complexes

Elder prepared the asymmetrical nickel complex **195a** by reaction of **194** with the nickel complex of 5-chloro-salicylaldehyde. The procedure was applied successfully for complexation of N_3O ligands **195b-d** with nickel and copper [**9, 10**]. The '*in-situ*' solution of asymmetrical ligands reacted with nickel(II) and copper(II) nitrates to give mixtures of symmetrical and asymmetrical Schiff base complexes.

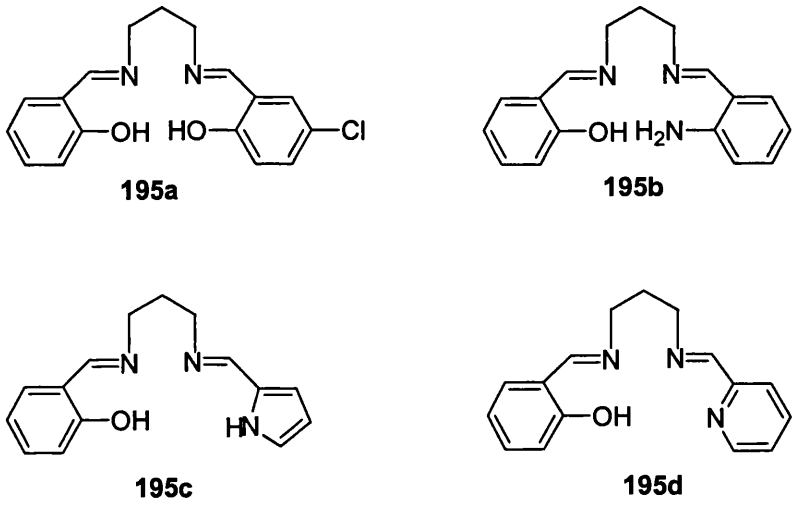

Figure 4.8. Asymmetrical ligands generated by Elder's strategy (not isolated)

In the case of **195b** and **195c**, the metal (M = Ni, Cu) complexes precipitated from solution at room temperature or upon cooling below 0 °C, while those from **195d** were more soluble than the metal symmetrical Schiff base complexes. Filtration of the reaction mixtures followed by neutralisation of the filtrates led to precipitation of the corresponding complexes.

Recently this method has been employed to synthesise nickel salen complexes with an N_2OS donor atom set **196** [**11**] by condensation of nickel complex **194** with

bis(thiosalicylaldehydate) nickel (II) in methanol-dichloromethane at room temperature overnight. The product precipitated from the reaction mixture and was separated by filtration.

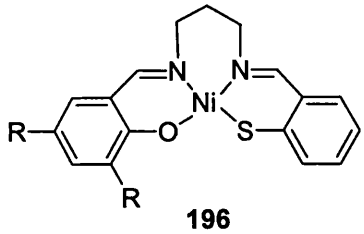

196

R = H, Cl

Figure 4.9. Nickel asymmetrical salprt-sal prepared by Elder's strategy

Attempts to prepare the free asymmetrical ligand using a similar procedure in the absence of nickel or by demetallation of the nickel asymmetrical complexes were not successful, mixtures of symmetrical and asymmetrical ligands were obtained in both cases. These reports show that when there is a big difference in reactivity between the two aromatic aldehydes used in the synthesis of asymmetrical salen-type complexes, the isolation of the free ligand becomes more difficult presumably due to a faster equilibrium between the symmetrical and asymmetrical double Schiff bases in solution. In both cases the synthesis and isolation of the desired metal complexes relied on differences in solubility between the asymmetrical and the corresponding symmetrical complexes.·

We applied Elder's strategy to the syntheses of nickel complexes of **185a** and **185b**. After the condensation of the salicylaldehyde or 2-aminobenzaldehyde with 1,2-diaminocyclohexane, using a ratio 1 : 3 between the reagents, complexation was performed following the conditions employed by Elder in refluxing methanol [**6**].

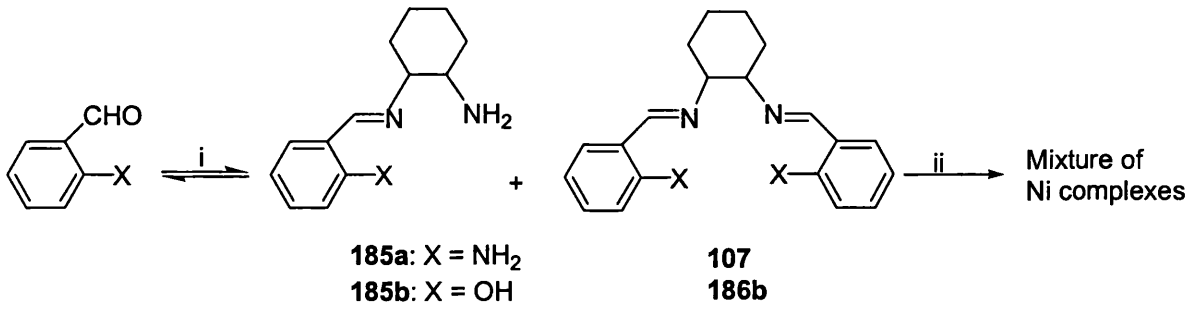

185a: X = NH_2
185b: X = OH

107
186b

i: 1,2-diaminocyclohexane, EtOH reflux, 3 h;
ii: $Ni(OAc)_2 \cdot 4H_2O$, EtOH reflux, 4 h

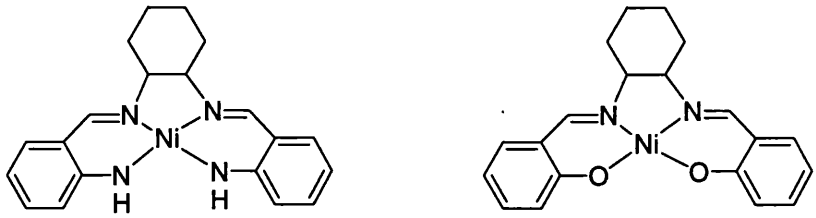

113 **119**

Scheme 4.13. Attempted synthesis of Ni complexes of **185 a,b** and the isolated products **113, 119**

In both reactions the nickel complexes of the double Schiff bases **113** and **119** precipitated from the reaction mixture and were isolated by filtration. This result was unexpected as in the case of aminobenzaldehyde, at the end of the first step condensation, the ^{1}H-NMR spectrum showed that the mixture contained only mono Schiff base **185a** and diamine and no double Schiff base **107**. The IR spectra of the precipitate resulted from the complexation reaction showed that it contained pure nickel complex **113**, while the IR of the remaining solution indicated that it contained **113** and uncomplexed mono Schiff base **185a**.

Complexations of mixtures of mono Schiff base **185b** and double Schiff base **186b** were performed at room temperature and the results compared with those obtained at reflux. The IR spectra of the two precipitates obtained in this manner presented the same bands, however differences in the relative intensity of some of the bands were found, which suggested that the precipitate obtained at room temperature was a mixture of two compounds. The intensities of these IR bands, in the reactions carried out at 25°C, varied in time and they also depended on the presence/ absence of a base during the process.

An explanation for these results is that the octahedral nickel complex of the mono Schiff base **185** is not stable under the reaction conditions and is transformed into the more stable square planar complex of the double Schiff base **113, 119**. The rate of this reaction is faster in our case as 1,2-cyclohexane diamine is more basic than 1,3-propane diamine employed by Elder in his studies [**6**]. The process becomes slower and can be detected when the complexation is performed at room temperature or at a lower temperature.

We consider that even when the nickel complex of **185** can be isolated, this procedure involving the removal of the metal ion by reaction with dimethylglyoxime at reflux for several hours will not give good yields of asymmetrical ligand due to the following equilibrium (Scheme 4.14) which is set up in solution as soon as the free mono Schiff base **185** is generated and which is shifted toward double Schiff base (**107** or **186**) in these conditions.

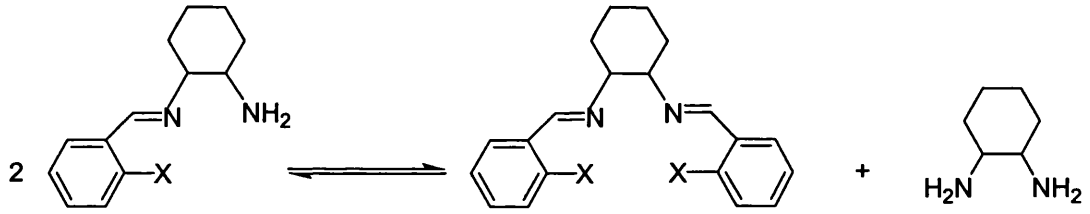

185
a: X = NH_2
b: X = HO

107: X = NH_2
186b: X = HO

ch

Scheme 4.14. Equilibrium leading to decomposition of mono Schiff base

However, these experiments led us to the realisation that all the complexations of the asymmetrical Schiff base ligands should be performed under mild conditions (*i.e.* room temperature) to avoid formation of the more stable symmetrical Schiff bases.

4.4. Synthesis of asymmetrical nickel(II) salchsal and R-ambchsal complexes

4.4.1. Synthesis from the free ligand

Treatment of asymmetrical ligand **178** with stoichiometric amounts of triethylamine and nickel(II) acetate in ethanol at room temperature gave the nickel complex **197** as an orange precipitate (89 % yield).

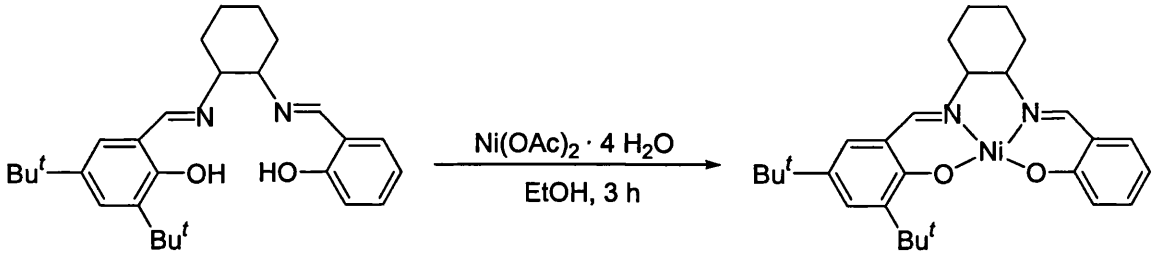

178 **197**

Scheme 4.15. Synthesis of nickel salchsal **197** using optimised conditions

At higher temperatures, mixtures of asymmetrical and symmetrical Schiff base complexes were obtained suggesting that the free asymmetrical ligand was not stable in solution at these temperatures. Crystals for X-ray experiments were grown from CH_2Cl_2 and petroleum spirit.

The IR spectrum of **197** presents an absorption band at 1612 cm^{-1} assigned to C=N bond. The ^{1}H-NMR spectrum resembles with the one of the free ligand, but in the complex the imine and the aromatic protons give resonance at higher field. Another difference is the disappearance of the signals associated with the hydroxyl groups, which is expected on complexation of the free ligand. The assignment of the imine protons was done in a similar way as described for the free ligand. By comparing the values obtained for these protons in the complex and in the free ligand a difference in chemical shift of about 0.9 ppm was found, which is equal to that for related protons in symmetrical Ni(salch). The ^{1}H-NMR spectrum of the solution indicated that it was a mixture of asymmetrical and both symmetrical Schiff base complexes.

4.4.2. Synthesis of nickel (R-ambchsal) complexes

Since the discovery of Le Chatelier's principle, different equilibria in solution have been investigated. Recently, a few research groups [**12**] have been focusing their work on using the dynamic aspect of the chemical equilibrium to generate libraries of compounds in equilibrium and introduced a new concept in organic chemistry called Dynamic Combinatorial Chemistry (DCC). In the presence of a target able to react selectively with one member of the library all the equilibria are shifted, acting in favour of this reaction, according to Le Chatelier's principle.

An example of such a system involved a dynamic library of imines obtained by reversible combination of four amines and three aldehydes. Treating this library with carbonic anhydrase it was found that one of its members (Figure 4.10) was a strong inhibitor of this enzyme. The advantage of such an approach is the simple way of building and testing the library with the aid of the target molecule. J.M. Lehn considers that DCC may represent a powerful methodology for discovery of new substrates, inhibitors, receptors and catalysts for a variety of processes.

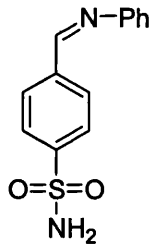

Figure 4.10. Compound with biological activity discovered by DCC

As it was shown in section **4.3**, condensation of 1, 2-diaminocyclohexane with two different bezaldehydes gives a mixture of symmetrical and asymmetrical Schiff bases and the major challenge in synthesis of asymmetrical Schiff base ligands arise from their instability in solution leading to an equilibrium mixture of the above mentioned compounds. For this reason we were interested to gain more information regarding the equilibrium illustrated in Scheme 4.16 at room temperature.

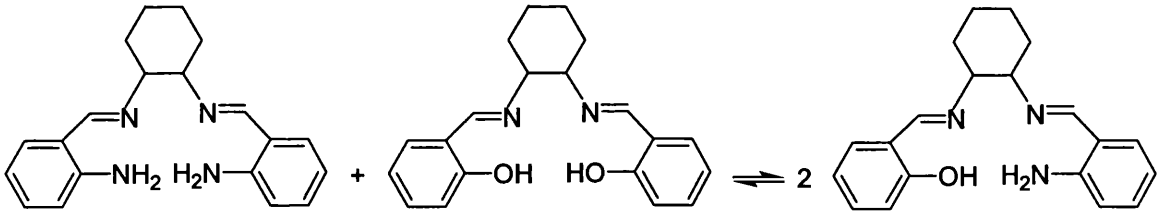

107 186b 180

Scheme 4.16. Equilibrium between symmetrical and asymmetrical double Schiff bases

The study performed by ^{1}H-NMR consisted in monitoring the evolution of a mixture of **107** and **186b** in time until the equilibrium was reached, the composition of the system being determined from integration of the imine proton peaks in the symmetrical and asymmetrical ligand **180**. In of adventitious amounts of water the equilibrium was reached in 60 h and the ratio between the compounds was 1 : 1 : 1, however in the presence of water the equilibrium state was reached faster (after 40h). The peaks corresponding to the asymmetrical ligand **180** appear after 1 h implying that at the end of the second condensation the desired asymmetrical ligand should be isolated from the mixture in 1 h, after this time the asymmetrical Schiff base ligand starts to decompose into the thermodynamically more stable symmetrical double Schiff bases **107** and **186b**. These suggested that the mentioned equilibrium is quite rapid and determined us to explore the possibility of using it as driving force toward synthesis of asymmetrical nickel N_3O complexes **198 - 200**.

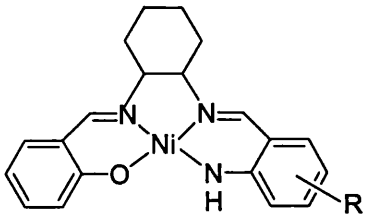

198 - 200

R = H, 3-Me, 5-Me

Figure 4.11. Asymmetrical Ni(R-ambchsal) complexes synthesized

In the present work a different consequence of the Le Chatelier's principle was used which is illustrated in Scheme 4.17. Considering **107** and **186b** in equilibrium with **180**, if one of the starting material species (**186b**) is in excess then the chemical equilibrium will be shifted toward the formation of **180**.

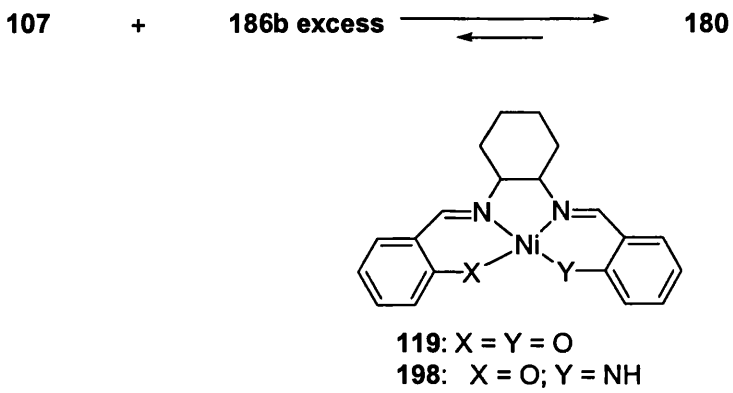

Scheme 4.17. Strategy used for synthesis of Ni(ambchsal) complexes and the two nickel complexes from the final reaction mixture

Indeed, it was found that by addition of one of the symmetrical Schiff bases in excess it was possible to generate a composition at the equilibrium (**186b** : **180** : **107** = 2.7 : 1 : 0.1) in which the Schiff base **107** was present only in a negligible amount (*i.e.* this compound is chemically 'removed'). In this way from a mixture of three species, the system passes into a state where only two species were present in solution. Then reacting the mixture with nickel acetate in the conditions employed in section **4.4.1** a mixture of nickel complexes **198** and **119** was obtained. This mixture was separated by filtration and NMR analysis indicated that the asymmetrical nickel(II) complex **198** was obtained in quatitatively yield. Its isolation from the nickel(II) complex **119** was done by multiple recrystallisations. The related methyl substituted asymmetrical complexes **199** and **200** were synthesised following the same strategy.

4.4.3. ^{1}H-NMR spectra of asymmetrical Ni(R-ambchsal) complexes

The ^{1}H-NMR spectra of nickel(II) complexes **198 - 200** are in agreement with the assigned structures. The resonances corresponding to imine group protons are shifted upfield upon complexation with nickel by 0.6 ppm (H^{B}) and 0.8-0.9 ppm (H^{A}), similar to that found for symmetrical nickel ambch and salch complexes.

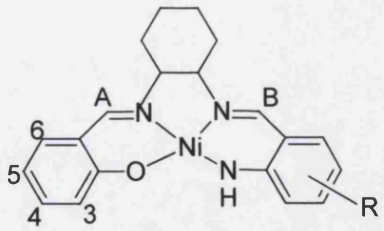

198 - 200

The variation of the imine proton chemical shifts (δ) with the coordination sphere in the free ligand and nickel complexes is presented in Table 4.3. The signals for H^A and H^B appear at values intermediate between those corresponding to the same protons in symmetrical compounds which indicates that asymmetrical ligands allow a better tunning of electronic properties in their complexes. A gradual shift of δ towards higher field was observed upon changing the donor atom set from N_2O_2 to N_3O and N_4 (entries 1, 3, 5, 6, 7).

It can also be seen (Figure 4.12) that in spite of the differences between ambch and salch compounds, appropriate substitution of the aromatic rings determines important variations in chemical shifts of imine protons leading to compounds like **110** which have properties closer to alkyl substituted 3,5-di-^{t}Busalch **186d**, while **111** is expected to have very different properties. The effect of donor atom substitution can also be seen in the difference of chemical shifts $\delta(H^A - H^B)$ in asymmetrical ligands **178** and **182**. In the other two synthesised asymmetrical ambchsal compounds (**181** and **180**) the differences between the two halves of the molecule are much smaller.

Figure 4.12. Variation of imine proton chemical shift in symmetrical and asymmetrical ligands

Table 4.3. Variation of imine protons chemical shift (δ, ppm) in symmetrical and asymmetrical complexes

No	Ligand	Label of the compound*	δH^A, δH^{B**} in ligand	δH^A, δH^{B**} in Ni complex
1	**186d**	Bu-N_2O_2	8.30	-
2	**110**	3-Me-N_4	8.29	7.70
3	**178**	N_2O_2	8.29; 8.26	7.42; 7.35
4	**181**	3-Me-N_3O	8.27; 8.26	7.64; 7.51
5	**186b**	N_2O_2	8.26	7.27
6	**180**	N_3O	8.25; 8.24	7.47; 7.32
7	**107**	N_4	8.25	7.64
8	**182**	5-Me-N_3O	8.24; 8.18	7.56; 7.37
9	**111**	5-Me-N_4	8.19	7.60

*used in Figures 4.12 and 4.14; ** H^A, H^B imine protons

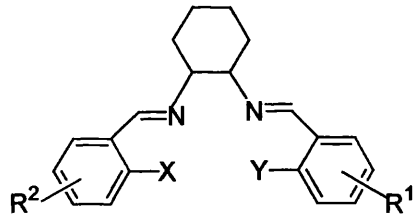

107: X = Y = NH_2; R^1 = R^2 = H
110: X = Y = NH_2; R^1 = R^2 = 3-Me
111: X = Y = NH_2; R^1 = R^2 = 5-Me
180: X = NH_2; R^2 = H; Y = OH; R^1 = H
181: X = NH_2; R^2 = 3-Me; Y = OH; R^1 = H
182: X = NH_2; R^2 = 5-Me; Y = OH; R^1 = H

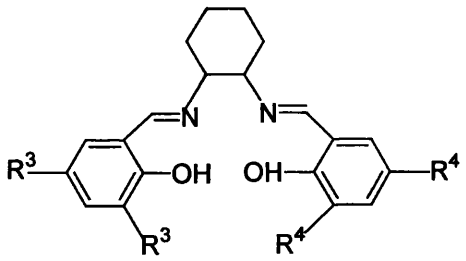

186b: R^3 = R^4 = H
186d: R^3 = R^4 = ^{t}Bu
178: R^3 = ^{t}Bu, R^4 = H

Figure 4.13. Symmetrical and asymmetrical ligands synthesized

The results from Table 4.3 indicate that substitution of the amb ring in nickel symmetrical complexes with an alkyl group determines absolute shifts with 0.04-0.06 ppm of the imine proton (entries 7, 2 and 9), while shifts of 0.08 ppm are found for substitution of the sal ring with 3 and 5-*t*-butyl groups in the nickel complex (entries 3, 5). An interesting variation of the NMR imine protons signals was presented by the different asymmetrical nickel N_3O complexes **198-200** compared with the values of these protons for the corresponding symmetrical complexes (δ_1, δ_2 in Table 4.4). These

data show the interaction between the two moieties in the asymmetrical ligand of these complexes, referred as amb and sal rings.

Table 4.4. Variation of imine protons chemical shift (δ, ppm) in N_3O complexes **198 - 200**

Complex	H^B	H^A	$\delta_1=H^B-H^{*a}$	$\delta_2=H^A-H^{*a}$
198	7.47	7.32	0.17	0.05
199	7.64	7.51	0.06	0.24
200	7.56	7.37	0.04	0.1

$^aH^*$-imine proton chemical shift in symmetrical complexes

While in complexes **199** and **200,** δ_1 was 0.06 and 0.04 (Table 4.4, entries 2, 3), comparable with introduction of an alkyl substituent in the amb ring, sal ring suffered more important modifications as indicated by δ_2 = 0.24 and 0.1 ppm. A different situation was found in the complex **198** (entry 1) in spite of the same co-ordination sphere (N_3O) with previously mentioned compounds. In this complex, the sal ring suffered small variations (δ_2 = 0.05 ppm), while the amb moiety changed much more as indicated by δ_1 = 0.17 ppm. The results suggest that **198** resembles more with Ni(salch) **119**, whereas **199** and **200** are closer to Ni(ambch) **113**(Figure 4.14). The difference between the two moieties amb and sal reflected by the difference (δH^A - δH^B) is smaller for complexes **198** and **199** than the difference found in the **200** complex.

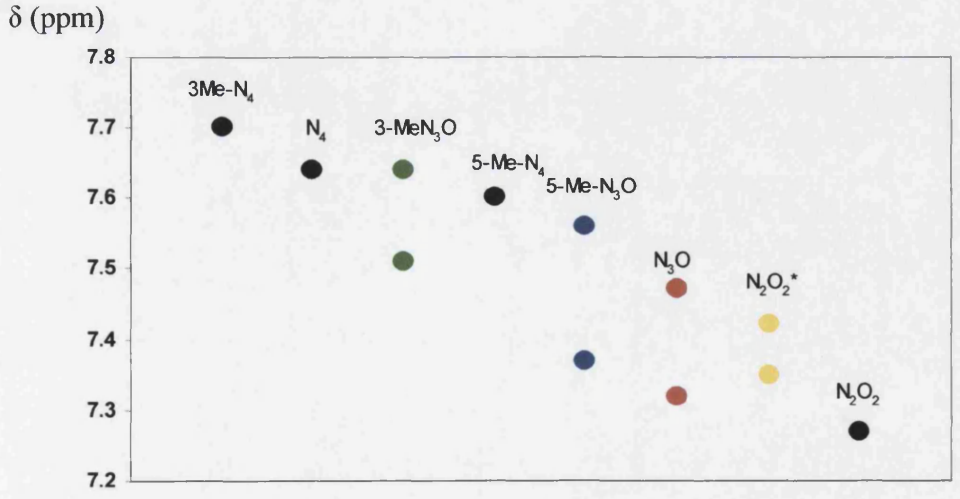

Figure 4.14. Variation of imine proton chemical shift in Nickel symmetrical and asymmetrical complexes

4.4.4 Crystal structures of asymmetrical nickel complexes

The crystal structure of Ni(ambchsal) **198** is presented in Figure 4.15. The complex has a square planar geometry with the nickel atom lying at 0.0091 (molecule A) and 0.0136Å (molecule B) above the plane formed by N_3O donor atoms. In the asymmetrical molecule there is a 50:50 disorder of metal bound NH and O positions. The data presented in Table 4.5 indicate that in complex **198** three bonds Ni-donor atoms are statistically equal, the forth (Ni-inner N donor) is slightly shorter. Similar values were obtain for the bonds between Ni and neutral nitrogen donor, as well as anionic donors in both molecules present in the unit cell. The bond lengths in this complex have intermediate values between those corresponding to symmetrical Ni(ambch) **113** and Ni(salch) **119** complexes, being closer to the latter.

Table 4.5. Selected bond lengths (Å) in Ni ambchsal **198**, Ni salchsal **197** and related symmetrical and asymmetrical complexes

Complex	Donor set	Ni-X	Ni-N	Ref
113	N_4	1.833(15) 1.888(10)	1.874(15) 1.910(10)	-
198 Molecule A	N_3O	1.845(6) 1.849(6)	1.852(6) 1.864(6)	-
198 Molecule B	N_3O	1.841(6) 1.842(5)	1.851(6) 1.860(6)	-
119	N_2O_2	1.835(3) 1.852(3)	1.861(4) 1.852(4)	**13**
197	N_2OO	1.844(2) 1.829(2)	1.844(3) 1.846(3)	-
201	N_3O	1.847(2)	1.905(2)	**9**

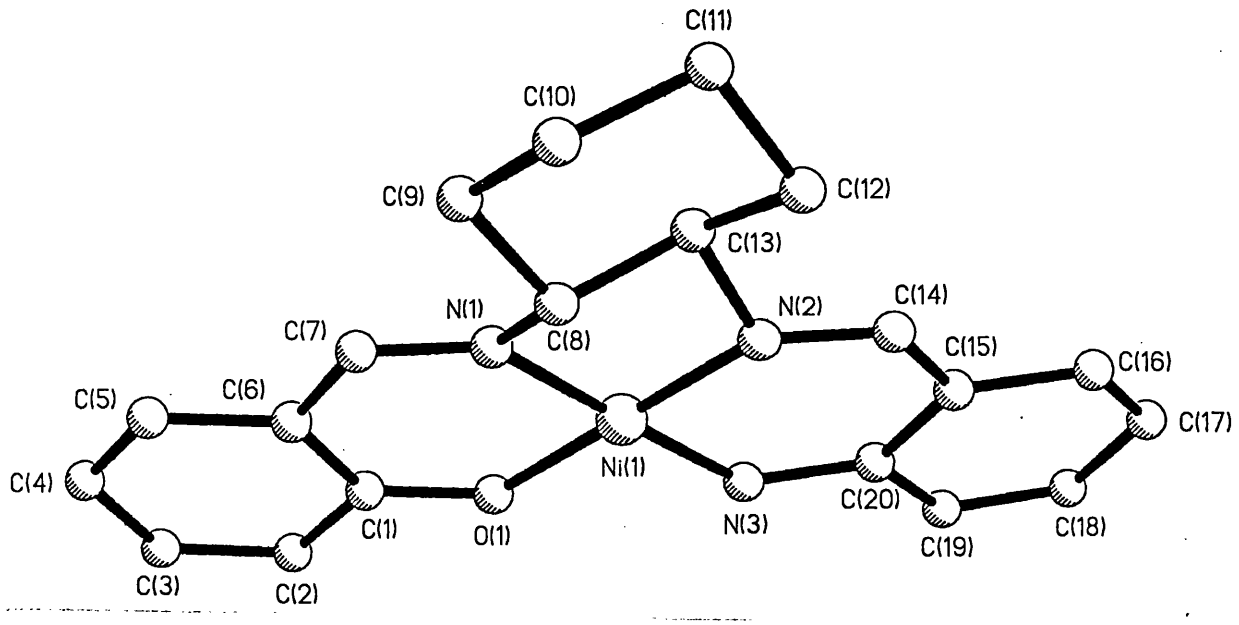

Ni(1)–N(1)	1.852(6)
Ni(1)–N(2)	1.864(6)
Ni(1)–N(3)	1.849(6)
Ni(1)–O(1)	1.845(6)
N(1)–Ni(1)–N(2)	85.4(3)
O(1)–Ni(1)–N(3)	87.1(2)
O(1)–Ni(1)–N(2)	178.6(3)

Figure 4.15. Crystal structure of Ni(ambchsal) **198** with selected bond lengths (Å) and angles(°)

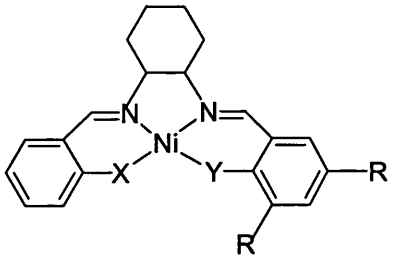

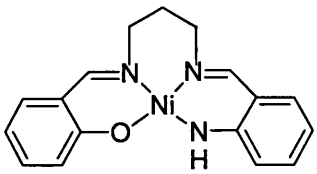

201

113: X = Y = NH, R = H
119: X = Y = O, R = H
197: X = Y = O, R = ^{t}Bu
198: X = O; Y = NH, R = H

Figure 4.16. Symmetrical and asymmetrical N_2O_2 and N_3O complexes

Table 4.6. Selected bond angles (°) for Ni(ambchsal) **198** , Ni (salchsal) **197** and related symmetrical and asymmetrical complexes

Complex	Donor set	X-Ni-X α	N-Ni-N β	Difference α-β
113	N_4	88.27(57)	85.03(55)	3.24
198 (Molecule A)	N_3O	87.1(2)	85.4(3)	1.7
198 (Molecule B)	N_3O	86.3(2)	85.5(3)	0.8
119	N_2O_2	84.5(1)	85.7(2)	-1.2
197	N_2OO^*	84.47(10)	86.91(12)	-2.44
201	N_3O	82.07(13)	95.99(14)	-13.92

Defining α the angle X-Ni-Y and β the angle N-Ni-N, one can notice that the change in the co-ordination sphere around the metal determines a variation of the difference (α-β) from 3 ° in **113** to 1.7 ° (molecule A) and 0.8 ° (molecule B) in **198** and -1.2 ° in **119**. This difference is mainly due to a decrease in α with introduction of O atoms in the donor atoms set, while angle β is not influenced by changes in the co-ordination sphere around the metal. The result found for complex **119** in which α is smaller than β was explained by the fact that Ni(salch) adopts a slightly distorted square planar geometry in which the two O atoms are above and below the plane formed by Ni and the two neutral N atoms, while the other complexes are square planar. Thus, they will place the amide nitrogens at bigger distance one from another, by modifying the value of α. The dihedral angles between the two aromatic rings in complex **198** are 8.8° and 13.4° which implies

that the molecule has an umbrella shape. The conformation of the five membered chelate ring formed by the nickel, azomethine nitrogens and the two carbon atoms from the diimine bridge is a half chair.

While this work was in progress, the crystal structure of **201** has been reported [**9**]. Comparing the data for the two nickel N_3O complexes, having a different diimine bridge, one can observe that the bonds between nickel and the outer donor atoms have similar values in both, while the reported complex has longer bonds Ni-imine N atoms. The latter complex has C_2-symmetry, both halves of the complex are identical in spite of substitution of one oxygen atom from a symmetrical salpr complex for a nitrogen atom in the co-ordination sphere. The presence of a different diimine brige in complex **201** determines a decrease in α and an increase in β angle compared with the same angles in complex **198**, reflecting a higher flexibility allowed by the former ligand. The molecule shows a more important distortion as results from the difference α-β which is –13.9°.

The Ni(salchsal) complex **197** has a slightly distorted square planar geometry (Figure 4.17) which resemble with that found in Ni(salch) **119**. Comparing the bond lengths in these two related complexes it can be seen that substitution of one of the aromatic rings with electron donating groups led to a decrease in the bond distances between nickel and all the donor atoms. In complex **197** three bonds Ni-donor atoms are equal, while the bond Ni-O_2 is statistically different, the oxygen atom attached to the substituted ring being placed in closer proximity to nickel as expected. Although the asymmetrical nickel complex **197** resembles with the symmetrical Ni(salch) **119**, the distortion in the former compound is more important as revealed by the difference α-β = -2.44°, comparing with -1.2° in Ni(salch). This was determined by an increase of β angle, while α has the same value in both.

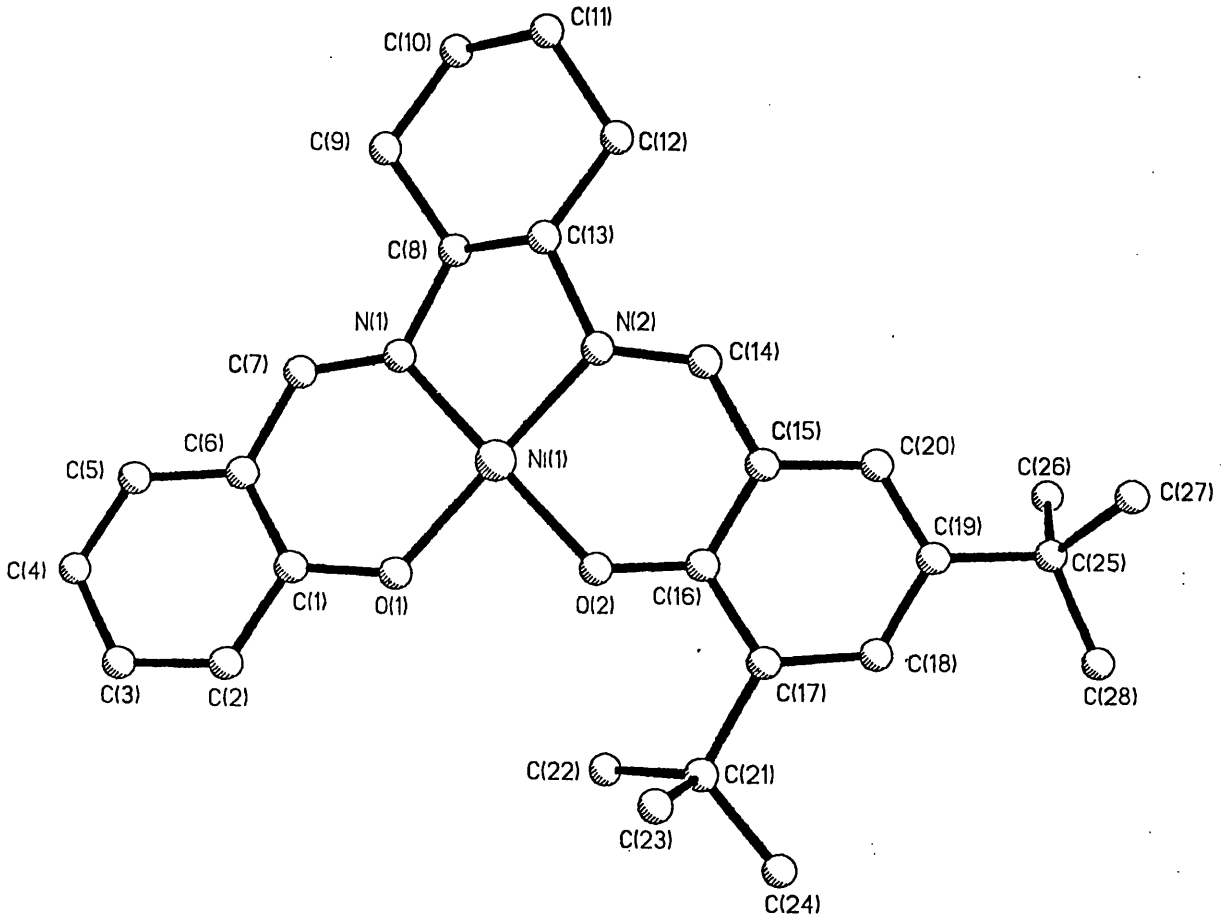

Ni(1)–N(1)	1.844(3)
Ni(1)–N(2)	1.846(3)
Ni(1)–O(1)	1.844(2)
Ni(1)–O(2)	1.829(2)
N(1)–Ni(1)–N(2)	86.91(12)
O(1)–Ni(1)–O(2)	84.47(10)
N(1)–Ni(1)–O(2)	174.65(11)

Figure 4.17. Crystal structure of Ni(salchsal) **197** with selected bond lengths (Å) and angles(°)

4.5 Conclusions

The strategies proposed in the literature were tested in preparation of new asymmetrical salchsal and ambchsal ligands **178 - 183**. All of them led to mixtures of asymmetrical and the corresponding symmetrical ligands from which the desired products could not be isolated.

New strategies were developed in a search for better synthetic routes to these compounds (sections **4.3.1.2-4.3.1.4**). The asymmetrical salchsal ligand (**178**) was prepared using two different stepwise procedures. The first employed an excess of diamine in the condensation with di-*t*-Bu-salicylaldehyde to ensure a good ratio mono : double Schiff base. This step was followed by condensation with salicylaldehyde. In the second procedure both aldehydes are added in stoichiometric amounts over the diamine and then the reaction mixture was gradually heated to reach the optimum temperature. This was very important also in the second step condensation as fast heating or a higher temperature modified the ratio mono : double Schiff base obtained in the first step. Very promising results were obtained for ambchsal **180** using a new strategy, from which the product was obtained in 80 % purity. The remaining 20 % consist of symmetrical double Schiff bases. In this procedure the mono Schiff base was generated from double Schiff base and diamine mixed together in stoichiometric amounts. The second condensation with aminobenzaldehyde was performed in the same way as in the previous procedures.

The results demonstrated that the route to asymmetrical double Schiff base ligands is not general and has to take into account the difference in reactivity between the two aldehydes and also the nature of the diamine involved in the condensation reaction. Syntheses of asymmetrical nickel N_2O_2 and N_3O complexes was achieved under mild conditions in high yields. While synthesis of **197** has involved careful ligand complexation to avoid generation of symmetrical double Schiff base ligands, synthesis of complexes **198 – 200** involved controlling the composition of a mixture of symmetrical and asymmetrical ligands in equilibrium, followed by complexation with the nickel salt.

The information obtained from X-ray crystal structures and ^{1}H-NMR spectra of the symmetrical and asymmetrical nickel complexes proved that the geometry and

electronic properties of asymmetrical complexes are different than those of corresponding symmetrical complexes. It is expected that these will determine a different reactivity of the asymmetrical complexes in catalytic processes.

4.6 References

1. R. Atkins, G. Brewer, E. Kokot, G.M. Mockler, E.Sinn, *Inorg. Chem.*, **1985**, *24*, 127.
2. J. Lopez, S. Liang, X.R. Bu, *Tetrahedron Lett.*, **1998**, *39*, 4199.
3. A.M. Daly, C.T. Dalton, M.F. Renehan, D.G. Gilheany, *Tetrahedron Lett.*, **1999**, *40*, 3617.
4. E.J. Campbell, S.T. Nguyen, *Tetrahedron Lett.*, **2001**, *42*, 1221.
5. C. Fukuhara, E. Asato, T. Shimoji, K. Katsura, *J. Chem. Soc., Dalton Trans.* **1987**, 1305.
6. R.C. Elder, *Aust. J. Chem.*, **1978**, *31*, 35.
7. R.G. Konsler, J. Karl, E.N. Jacobsen, *J. Am. Chem. Soc.*, **1998**, *120*, 10780.
8. B.C. Ranu, U. Jana, A. Majee, *Tetrahedron Lett.*, **1999**, *40*, 1985.
9. G. Brewer, P. Kamaras, L. May, S. Prytkov, M. Rapta, *Inorg. Chim. Acta.*, **1998**, *279*, 111.
10. P.J. Burke, D.R. McMillin, *J. Chem. Soc., Dalton Trans.*, **1980**, 1794.
11. L. Gomez, E. Pereira, B de Castro, *J. Chem. Soc., Dalton Trans.*, **2000**, 1373.
12. J-M. Lehn, *Chem. Eur. J.*, **1999**, *5*, 2455.
13. A. Wojtczak, E. Szlyk, M. Jaskolski, E. Larsen, *Acta Chem. Scand.*, **1997**, *51*, 274.

Chapter 5. Experimental

5.1 Preparation and instrumentation

Unless otherwise stated, all manipulations involving synthesis of aldehydes, Schiff bases and their complexes were carried out in air. The work done under an atmosphere of nitrogen involved using standard vacuum line, Schlenk and glove box techniques. All solvents and reagents were obtained from commercial sources and the reagents were used without further purification. In the synthesis of 5-chloro-2-amino-benzaldehyde it was used starting material of technical purity because it was found that the impurities present do not affect the reduction of 5-chloro-2-nitrobenzaldehyde and isolation of the product. Solvents used in synthesis of 2-amino-methyl-benzaldehyde, methylation of 3-hydroxy-nitrobenzaldehydes and preparation of vanadyl complexes were distilled under an atmosphere of nitrogen over drying agents. Dichloromethane and acetonitrile were distilled from calcium hydride, diethyl ether was distilled from sodium/ potassium alloy, while benzene and toluene were distilled from sodium. The dried solvents were stored in ampoules over activated 4 Å sieves or sodium mirrors, after being degassed thoroughly. Glassware was dried in ovens at 110°C minimum 5 h prior to use.

NMR spectra were recorded on Bruker AMX400 and Bruker AC300 spectrometers. Proton NMR spectra were recorded at 400 MHz and 300 MHz on corresponding instruments. Spectra were recorded in $CDCl_3$ and the solvent was used as internal reference. Chemical shifts are reported in parts per million (ppm, δ) and coupling constants J in Hertz (Hz). Mass spectra were recorded on a VG ZAB-SE mass spectrometer for both electron impact (EI) and fast atom bombardment (FAB) analyses. High-resolution mass spectrometry was performed on a VG ZAB-SE mass spectrometer using fast atom bombardment (FAB) ionisation at the School of Pharmacy, University of London. Ion fragments masses are given with relative abundances stated as a percentage in brackets. Infra-red (IR) spectra were recorded on Nicolet 205 FTIR spectrophotometer in solid state (KBr) and the wavelength for specific absorptions are given. Elemental analyses were carried out by the Microanalytical Section of the Chemistry Department, University College London.

Numbering schemes used for description of ^{1}H-NMR signals

Unless given in the following sections, the numbering schemes used to describe the ^{1}H-NMR signals of the compounds are presented below.

• Hydroxy- and methoxy-nitro-benzaldehydes

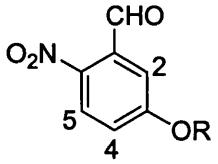

R = H, Me

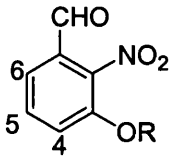

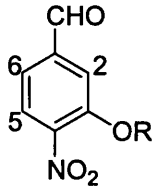

• Aminobenzaldehydes

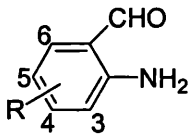

• Mono and double Schiff bases and their Nickel complexes

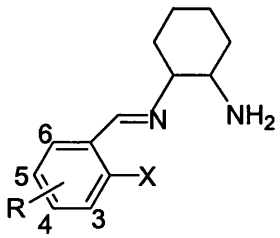

X = OH, NH_2

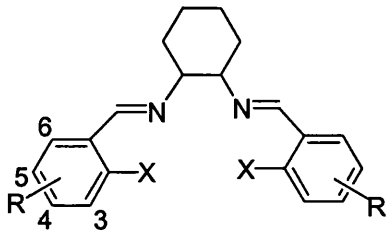

X = OH, NH_2

5.2 Preparation of 2-nitrobenzaldehydes

5.2.1 Nitration of 3-hydroxy-benzaldehyde[1]

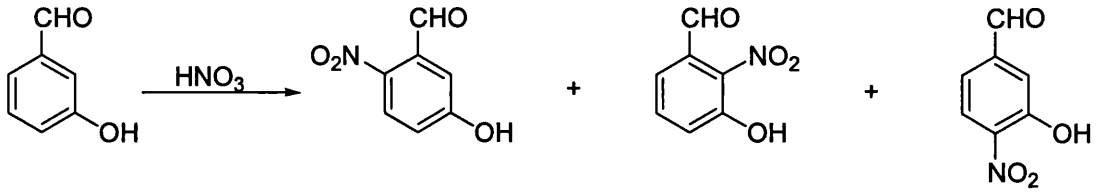

Molar ratio: 1 1.25 1.4

3-Hydroxy-benzaldehyde (10.84 g, 0.089 mole) was added in portions to a well stirred mixture of concentrated nitric acid (10 mL) and water (44 mL) so that the reaction temperature did not exceed 5 °C. After addition, the temperature was increased gradually to 40 °C, later to 50-55 °C and then maintained at this value for 4 h. Stirring was continued until the reaction temperature dropped to 30 °C. Then the reaction mixture was poured into the ice water to give a yellow precipitate (13.17 g) which was washed thoroughly with water and air dried (89 % yield).

The crude product was stirred 30 min in benzene at reflux, cooled to 45 °C and filtered to give a brown precipitate of 5-hydroxy-2-nitro-benzaldehyde (3.64 g). The filtrate was further cooled to room temperature when 3-hydroxy-2-nitro-benzaldehyde (orange) precipitated from solution (4.55 g). After filtration, the latter was evaporated to dryness to give 4-nitro-3-hydroxy-benzaldehyde (4.98 g, yellow powder). The structure of all nitro-hydroxy-benzaldehydes was established by ^{1}H-NMR.

MS (EI) (m/z) 168, no peak for dinitro-hydroxy-benzaldehyde

EA: Calculated for $C_7H_5NO_4$: C: 50.31, H: 3.01; N: 8.38; Found: C: 50.28, H: 2.74, N: 8.34

5-hydroxy-2-nitro-benzaldehyde (83)

^{1}H-NMR ($CDCl_3$): δ, 10.48 (1H, s, CHO); 8.16 (1H, d, J = 8.8, H^3); 7.53 (1H, s, OH); 7.29 (1H, d, J = 2.8, H^6); 7.13 (1H, dd, J = 8.8, J = 2.8, H^4)

3-hydroxy-2-nitro-benzaldehyde (84)

^{1}H-NMR ($CDCl_3$): δ, 10.44 (1H, br, s, OH); 10.33 (1H, s, CHO); 7.68 (1H, t, J = 8, H^5); 7.39 (1H, dd, J = 8, J = 1.2, H^6); 7.33 (1H, dd, J = 8, J = 1.2, H^4)

3-hydroxy-4-nitro-benzaldehyde (85)

^{1}H-NMR ($CDCl_3$): δ, 10.59 (1H, br, s, OH); 10.07 (1H, s, CHO); 8.30 (1H, d, J = 8.6, H^5); 7.67 (1H, d, J = 1.6, H^2); 7.52 (1H, dd, J = 8.6, J = 1.6, H^6)

5.2.2 Nitration of 3-methoxy-benzaldehyde

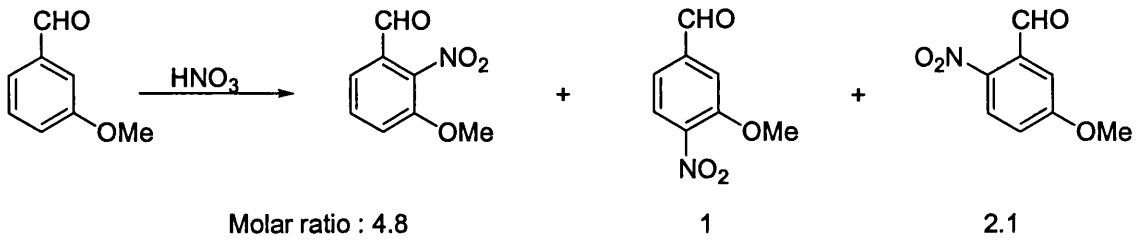

Molar ratio : 4.8 1 2.1

Over 3-methoxy-benzaldehyde (10.6 g, 0.077 mol) cooled in an ice bath and well stirred was added dropwise concentrated nitric acid (25 mL) at a rate so that the temperature did not exceed 10 °C. Then the homogeneous mixture was heated gradually to 45-48 °C and this temperature was preserved for 4 h. After this time heating was stopped and ice was added directly in the reaction flask. Stirring was interrupted 30 min later allowing the two liquid phases to separate. The aqueous layer was removed with a pipette from the orange red oil containing the product and unreacted substrate. To the latter was added a fresh quantity of nitric acid (25 mL) in the same manner as described above for the pure substrate. The procedure was repeated (4 times) until complete conversion of the 3-methoxy-benzaldehyde. The time spent by the reaction mixture at 48 °C was 14 h. On addition of ice to the final mixture the product precipitated and it was separated by filtration. The yellow precipitate was washed several times with water to remove the excess acid and air dried.

The crude product was stirred 30 min in benzene at reflux and filtered while still hot (aprox. 45 °C) to give a white off solid. Then fractional crystallisation led to isolation of pure isomers in the order 3-methoxy-2-nitro (5.51 g), 3-methoxy-4-nitro (1.16 g) and 5-methoxy-2-nitrobenzaldehydes (2.45 g)(65 % yield). Separation was harder than the one of crude mixture obtained from nitration of 3-hydroxy-benzaldehyde.

5-methoxy-2-nitro-benzaldehyde (87)

^{1}H-NMR ($CDCl_3$): δ, 10.50 (1H, s, CHO); 8.17 (1H, d, J = 9, H^3); 7.34 (1H, d, J = 2.8, H^6); 7.16 (1H, dd, J = 9, J = 2.8, H^4); 3.97 (3H, s, CH_3O)

3-methoxy-2-nitro-benzaldehyde (86)

^{1}H-NMR ($CDCl_3$): δ, 9.96 (1H, s, CHO); 7.63 (1H, t, J = 7.5, H^5); 7.52 (1H, d, J = 7.5, H^6); 7.35 (1H, d, J = 7.5, H^4); 3.97 (3H, s, CH_3O)

3-methoxy-4-nitro-benzaldehyde (88)

^{1}H-NMR ($CDCl_3$): δ, 10.07 (1H, s, CHO); 7.94 (1H, d, J = 8.3, H^5); 7.61 (1H, s, H^2); 7.55 (1H, d, J = 8.3, H^6); 4.05 (3H, s, CH_3O)

5.3 Reduction of nitrobenzaldehydes

5.3.1 Reduction of 2-nitrobenzaldehyde[2]

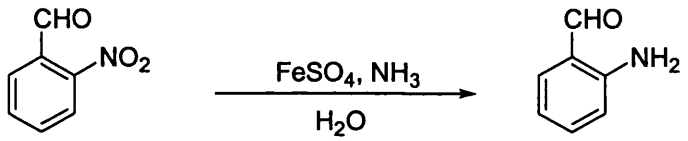

61a

Hydrochloric acid (0.15 mL) and 2-nitro-benzaldehyde (1.5 g, 0.01 mol) were added over a stirred aqueous solution of hydrated iron (II) sulfate (26.25 g, 0.094 mol, 44 mL). The mixture was heated until it became homogeneous and at 90 °C ammonia solution was added to it in four aliquots (6.25 mL and 3 x 2.5 mL). The colour of the solution changed from green to black after the addition of the first aliquot. The product was then removed from the reaction mixture by fast steam distillation to avoid its degradation. The aqueous light yellow distillate (125 mL) was saturated with sodium chloride and cooled with ice to give a light yellow precipitate of 2-amino-benzaldehyde (0.84 g) which was separated by filtration (70% yield).

2-Amino-benzaldehyde has been reported [**2**] to be unstable at room temperature due to a self condensation reaction. It cannot be dried completely as removal of water favours this process, therefore it should be used immediately after synthesis. However, we were able to preserve it for two weeks at 25 °C without degradation in a small amount of mother solution and isolate it just before addition to the next reaction.

^{1}H-NMR ($CDCl_3$): δ 9.88 (1H, s, CHO); 7.49 (1H, d, J = 7.8, H^6); 7.32 (1H, t, J = 7.8, H^4); 6.76 (1H, t, J = 7.8, H^5); 6.66 (1H, d, J = 7.8, H^3); 6.12 (2H, br, NH_2).

5.3.2 Reduction of 5-chloro-2-nitro-benzaldehyde

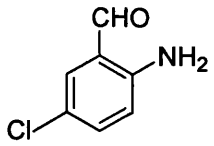

61b

This reaction was performed in a similar way as described in 5.3.1. The starting material, 5-chloro-2-nitrobenzaldehyde, is commercially available as a technical mixture containing also 3-chloro-4-nitro-benzaldehyde (15%), 5-chloro-2-nitrobenzoic acid (5 %) and H_2SO_4 (3 %). The reducing agent was added in excess to reduce all the nitro derivatives present in the starting material to the corresponding aromatic amines. The product was obtained as a yellow powder (0.46 g, yield 55 %).

^{1}H-NMR ($CDCl_3$): δ 9.81 (1H, s, CHO); 7.46 (1H, d, J = 2.5, H^6); 7.26 (1H, dd, J = 2.5, J = 8.8, H^4); 6.63 (1H, d, J = 8.8, H^3); 6.14 (2H, br, NH_2).

5.3.3 Reduction of 2-nitro-3-methoxy-benzaldehyde

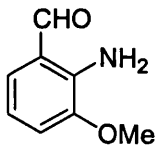

61c

This reaction was performed in a similar way as described in 5.3.1 using 2-nitro-3-methoxy-benzaldehyde. The product, 2-amino-3-methoxy-benzaldehyde, obtained in 50 % yield by extraction of the distillate with dichloromethane (yellow solution) was used directly in the condensation with diaminocyclohexane.

^{1}H-NMR ($CDCl_3$): δ 9.90 (1H, s, CHO); 7.14 (1H, d, J = 8, H^6); 6.89 (1H, d, J = 8, H^4); 6.69 (1H, t, J = 8, H^5); 6.40 (2H, br, NH_2); 3.89 (3H, s, OCH_3)

5.3.4 Reduction of a mixture of 2-nitro, 4-nitro and 6-nitro-3-methoxy-benzaldehydes

Reduction of an equimolecular mixture of 3-methoxy-n-nitro-benzaldehydes (where n = 2, 4, 6) was done using similar conditions to those described in 5.3.1. Then different work-up procedures were tested.

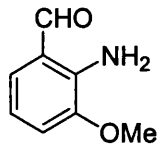

61c

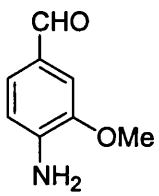

61g

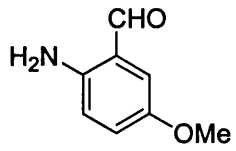

61d

In one experiment, the mixture resulted from reduction was steam-distilled for 1 h giving an intense yellow distillate which was extracted with dichloromethane until colourless.

- Composition of the distillate (by integration of the aldehyde proton signals in the ^{1}H-NMR spectrum): **61c** : **61g** = 4 : 1

In a different experiment, reduction was followed by extraction in dichloromethane.

- Composition of the reaction mixture (by integration of aldehyde protons in the ^{1}H-NMR spectrum): **61c** : **61d** : **61g** = 0.5 : 0.3 : 1.

5.4 Duff reaction

5.4.1 Attempt to synthesize the 2-amino-3,5-dimethyl-benzaldehyde

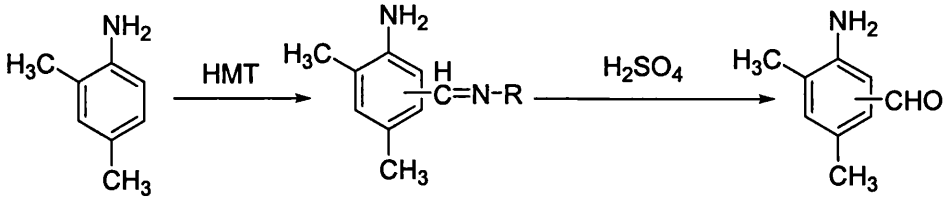

The procedure described in [3] was adapted for 2, 4-dimethyl-aniline. A mixture of hexamethylene tetramine (11.2 g, 0.08 mol) and 2,4-dimethyl-aniline (4.93 g, 98 %, 0.04 mol) in glacial acetic acid (40 mL) was stirred and gradually heated (1 h) to 100 °C. After 4 h at this temperature, the solution was cooled to 50 °C and upon addition of aqueous H_2SO_4 (33 %) a red precipite was formed which dissolved when the

temperature was brought back to 100 °C. One hour later the reaction mixture was cooled to room temperature and extracted with ether (2 x 100 mL). Addition of more ether (100 mL) led to the formation of an orange-red precipitate which was separated by filtration. NMR samples were taken from the reaction mixture before addition of H_2SO_4 and after hydrolysis from the orange-red precipitate.

Reaction mixture before hydrolysis: mixture of aldehydes (singlets at δ = 9.29 and 9.26 ppm in the ratio 1:1) and Schiff bases (imine proton singlets at δ = 8.61, 8.19 (major compound) and 8.08 ppm in the ratio 1.1 : 5.3 : 1).

After hydrolysis:

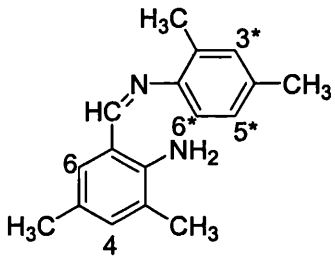

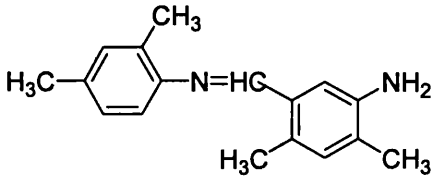

• **Orange-red precipitate**: mixture of 3 Schiff bases (imine proton singlets at δ = 8.57, 8.36 (major compound) and 8.21 ppm in the ratio 1: 17: 3).
Major compound: 8.36 (1H, s, CH=N); 7.35 (1H, d, J = 7.7 Hz, H^{6*}); 7.14 (1H, s, H^{6}); 7.13 (1H, d, J = 7.7, H^{5*}); 6.94 (1H, s, H^{3*}); 6.64 (1H, s, H^{4}); 4.91 (2H, s, NH_2); 2.41 (3H, s, CH_3); 2.35 (3H, s, CH_3); 2.33 (3H, s, CH_3); 2.28 (3H, s, CH_3).

A new amount of aqueous H_2SO_4 was added to the orange-red precipitate which was kept under stirring in acetic acid. The mixture was heated for several hours in an attempt to complete the hydrolysis of the Schiff bases present in the mentioned precipitate, then it was extracted with ether to give a slightly yellow solution and a white-yellow precipitate. Part of the white-yellow precipitate in water was steam distilled for 1 h and the distillate was extracted in DCM and analysed by NMR.

• **Distillate:** 2-amino-3,5-dimethyl-benzaldehyde, 9.84 (1H, s, CH=N); 7.17 (1H, s, H_{arom}); 7.09 (1H, s, H_{arom}); 5.31 (2H, s, NH_2); 2.27 (3H, s, CH_3); 2.16 (3H, s, CH_3).

5.4.2 Attempt to synthesize 2-amino-5-methyl-benzaldehyde

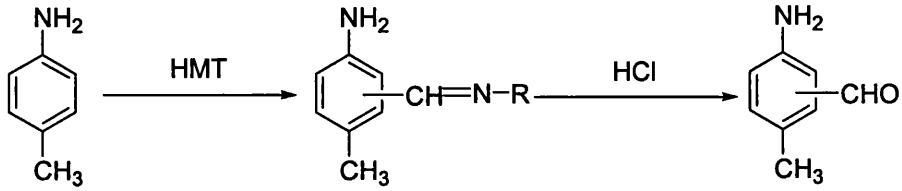

Hexamethylenetetramine (11.2 g, 0.08 mol), *p*-methyl-aniline (4.28 g, 0.04 mol) and glacial acetic acid (40 mL) were combined in a round bottom flask. Under stirring, the temperature of the reaction mixture was increased gradually (1 h) to 100 °C and this value was kept for 4 h. The solution was cooled to 50 °C and aqueous HCl (41 mL, 30 %) was added to it. The temperature was then increased to 95-100 °C and heating continued for one more hour. NMR samples were taken from the reaction mixture before acid addition (HCl) and at the end of the reaction. After cooling to room temperature the mixture was extracted with diethyl ether (2 x 100 mL). Addition of a new amount of ether (100mL) led to precipitation of an orange product which was separated from the aqueous solution with a pipette and analyzed by NMR.

Reaction mixture before hydrolysis : mixture of aldehydes (singlets at δ = 9.36, 9.28, 9.27, 9.24 ppm in the ratio 1: 1: 1: 4) and Schiff bases (singlets at δ = 8.63, 8.57, 8.42, 8.15 (major compound) in the ratio 1.3 : 1: 1 : 5.7);

Reaction mixture after hydrolysis : mixture of aldehydes (singlets at δ = 9.77, 9.74, 9.65 (major), 9.28, 9.27 ppm in the ratio 1 : 4.7 : 16 : 1 : 3) and Schiff bases (singlets at δ = 8.61, 8.58, 8.43 (major) ppm in the ratio 1 : 1 : 6);

- **Orange precipitate:**

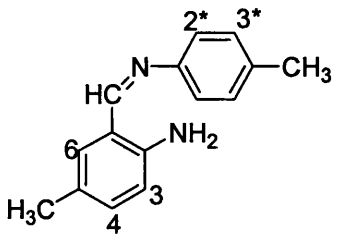

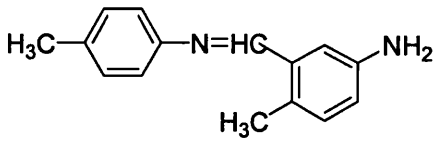

8.27 (1H, s, CH=N); 7.49 (1H, d, J = 8.1, H^3); 7.34 (2H, d, J = 8.4, H^{2*} and H^{6*}); 7.26 (2H, d, J = 8.4, H^{3*} and H^{5*}); 7.15 (1H, d, J = 8.1, H^4); 6.89 (1H, s, H^6); 5.15 (2H, s, NH_2); 2.42 (3H, s, CH_3); 2.35 (3H, s, CH_3).

Attempt to achieve hydrolysis

• in basic conditions

Part of the orange precipitate was dissolved in ethanol and saturated aqueous sodium carbonate solution was added carefully until pH=8-9. The mixture was then heated at 80 °C for 2 h and the composition of the mixture was analysed by NMR.

NMR: signal at δ=8.27 ppm small, but no aldehyde is present in solution.

• in neutral conditions

The ether layer was washed with saturated sodium carbonate and water until pH=7. Then it was concentrated and put on an alumina column which was eluted with petroleum spirit : ethyl acetate = 19 : 1. All the fractions collected from the column were analysed by NMR indicating that they were mixtures of double Schiff bases and aldehydes.

5.5 Oxidation of amino-benzyl alcohols

5.5.1 Activation of MnO_2[4]

A round bottom flask containing a suspension of wet MnO_2 (8.53 g) in benzene (100 mL) was connected to a Dean-Stark apparatus having a reflux condenser at the top. The heterogeneous mixture was brought under vigorous stirring to 80 °C in approximate 1 h, then the temperature of the oil bath was gradually increased to 115 °C. The system was left to run under these conditions overnight to ensure complete separation of the water in the trap. Activated MnO_2 was used in oxidation of 2-amino-R-benzyl alcohol (R=H, 3-Me, 5-Me) either in the next day or in the following 1-2 days. In the latter case it was kept under benzene in a closed round bottom flask.

5.5.2 Oxidation of 2-amino-3-methyl-benzyl alcohol

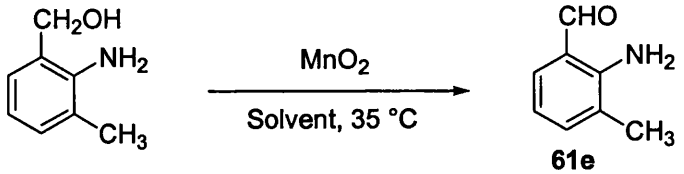

61e

The general procedure for the oxidation of amino-benzyl-alcohols [**5**] was adapted for 2-amino-3-methyl-benzyl alcohol. Activated MnO_2 (7.8 g) in benzene (95 mL) was transferred to a Schlenk tube and the solvent was degassed by passing nitrogen through the solution for 30 min. A solution of 2-amino-3-methyl-benzyl alcohol (0.978 g, 7.1 mmol) in dry, degassed solvent (100 mL of benzene, ether or DCM) was added with a cannula over the MnO_2 under stirring. After addition, the system was heated gently to 35 °C under nitrogen for at least 6 h or left to run overnight. Filtration of the heterogeneous mixture under nitrogen gives a yellow solution of 2-amino-3-methyl-benzaldehyde. The black solid was extracted with dry, degassed diethylether and filtered again for at least three times to separate the entire product (0.82 g, 85 % yield).

^{1}H-NMR ($CDCl_3$): δ, 9.89 (1H, s, CHO); 7.39 (1H, d, J = 7.5, H^6); 7.24 (1H, d, J = 7.5, H^4); 6.71 (1H, t, J = 7.5, H^5); 6.21 (2H, br, NH_2); 2.18 (3H, s, CH_3)

5.5.3 Oxidation of 2-amino-benzyl alcohol

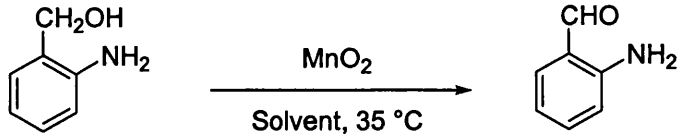

61a

The reaction was performed in a similar way as described in 5.5.2, but using DCM for addition of the benzyl alcohol to the activated MnO_2 and the extraction of the product (0.717 g, 81 % yield) was done using warm (35 °C) dichloromethane.

^{1}H-NMR ($CDCl_3$): δ 9.88 (1H, s, CHO); 7.49 (1H, d, J = 7.8, H^6); 7.32 (1H, t, J = 7.8, H^4); 6.76 (1H, t, J = 7.8, H^5); 6.66 (1H, d, J = 7.8, H^3); 6.12 (2H, br, NH_2).

5.5.4. Oxidation of 2-amino-5-methyl-benzyl alcohol

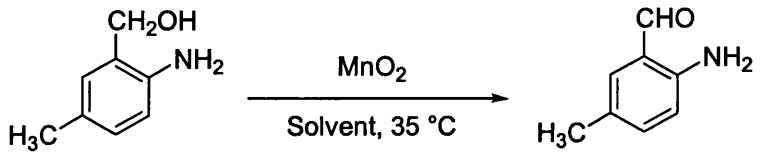

61f

The reaction was performed in a similar way as described in 5.5.2, the product (0.774 g, 83 % yield) being extracted in dichloromethane at room temperature.

^{1}H-NMR ($CDCl_3$): δ, 9.85 (1H, s, CHO); 7.28 (1H, d, J = 2, H^6); 7.15 (1H, dd, J = 8.4, J = 2, H^4); 6.59 (1H, d, J = 8.4, H^3); 5.95 (2H, br, NH_2); 2.27 (3H, s, CH_3)

The products, 2-amino-R-benzaldehydes (R = H, 3-CH_3, 5-CH_3), as solutions in dichloromethane were preserved at room temperature under nitrogen. This solution was added directly to the 1,2-diamino-cyclohexane in the synthesis of amben-type ligands. The amino-benzaldehydes kept in this way were stable for several weeks without any degradation as resulted from ^{1}H-NMR.

5.6 Bromination of 2-nitro-5-methoxy-toluene

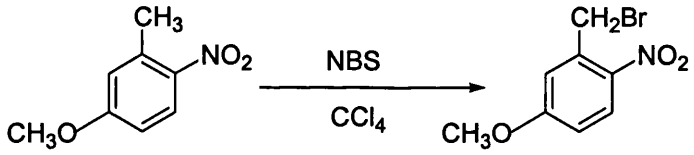

78a

The procedure described in [6] was adapted for 2-nitro-5-methoxy-toluene. To a solution of 2-nitro-5-methoxy-toluene (1 g, 6 mmol) in CCl_4 (75 mL) were added *N*-bromosuccinimide (2.13 g, 12 mmol) and benzoyl peroxide (30 mg, 0.12 mmol). The reaction mixture was refluxed for 5.5 days during which time samples were taken from the mixture and were analysed by ^{1}H-NMR. After 60 h and 93 h new amounts of benzoyl peroxide (30 mg) were added to the mixture. At the end of the reaction the mixture was cooled to 0 °C; filtered and concentrated. Attempts to crystallise the product from the reaction mixture with ether-hexane were not successful.

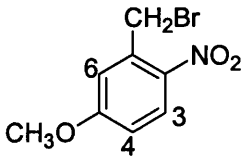

78a

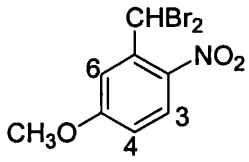

78b

Table 5.1. Composition of the bromination mixture in time

Sample No.	Time/h	Conversion of the starting material / %	ratio **78a** : **78b**
1	23	29.4	9.3 : 1
2	44	36.5	7.4 : 1
3	61.5	55	4.1: 1
4	69.5	60	3.9: 1
5	90.5	62.8	3.9: 1
6	132.5	67.4	2.8: 1

5-methoxy-2-nitro-toluene: 8.1(1H, d, J = 8.8 Hz, H^3); 6.82-6.78 (2H, m, H^4, H^6); 3.88 (3H, s, OCH_3); 2.65 (3H, s, CH_3);

***N*-bromo-succinimide**: 2.97; 1.56

5-methoxy-2-nitro-benzyl bromide (78a)

^{1}H-NMR ($CDCl_3$): δ, 8.16 (1H, d, J = 9.1 Hz, H^3); 7.03 (1H, d, J = 2.8 Hz, H^6); 6.93 (1H, dd, J = 9.1 Hz, J = 2.8 Hz, H^4); 4.87 (2H, s, CH_2); 3.92 (3H, s, CH_3O).

5-methoxy-2-nitro-benzylidene dibromide (78b)

^{1}H-NMR ($CDCl_3$): δ, 8.03 (1H, d, J = 9.1 Hz, H^3); 7.69(1H, s, CH), 7.68 (1H, d, J = 2.8 Hz, H^6); 6.95 (1H, dd, J = 9.1 Hz, J = 2.8 Hz, H^4); 3.98 (3H, s, CH_3O)

5.7 Methylation of 5-hydroxy-2-nitro-benzaldehyde

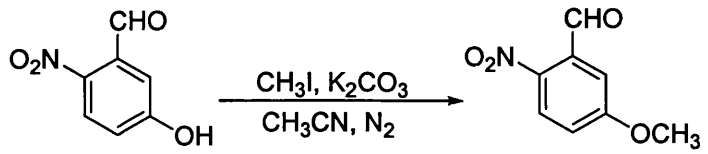

87

The general procedure described in [7] was adapted for methylation of 5-hydroxy-2-nitro-benzaldehyde. This reaction was performed under nitrogen. To a solution of 5-hydroxy-2-nitro-benzaldehyde (1.29 g, 7.7 mmol) in dry, degassed acetonitrile (40 mL) was added K_2CO_3 (1.067 g, 7.7 mmol) under a nitrogen flow. Then methyl iodide (0.75 mL) was added with a syringe. A condenser and a nitrogen bubbler were placed on the top of the Schlenk tube and after air removal, nitrogen was passed through the system in a gently flow. The reaction mixture was left overnight, under stirring at 55 °C.

Next day the mixture was cooled to room temperature and the decanted solution was separated from the small amounts of brown precipitate (unreacted substrate) by transferring it with a cannula into another Schlenk tube. The solvent was removed under low pressure to give 1.37 g orange powder of 5-methoxy-2-nitro-benzaldehyde in high yield (98 %).

5-methoxy-2-nitro-benzaldehyde (87)

^{1}H-NMR ($CDCl_3$): δ, 10.50 (1H, s, CHO); 8.17 (1H, d, J = 9, H^3); 7.34 (1H, d, J = 2.8, H^6); 7.16 (1H, dd, J = 9, J = 2.8, H^4); 3.97 (3H, s, CH_3O)

5.8 Synthesis of symmetrical ambch ligands

5.8.1 Synthesis of the *N,N'*-bis-(2,2'-aminobenzylideneimino)-cyclohexane

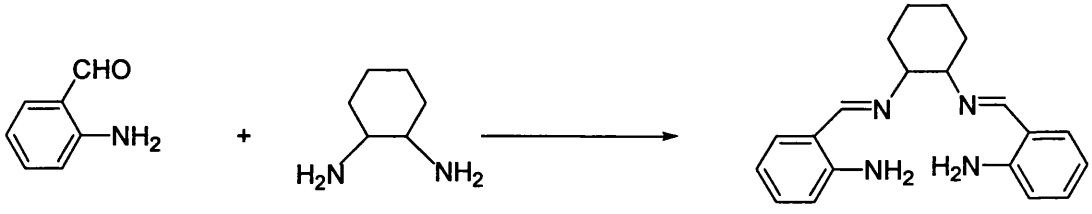

107

2-Amino-benzaldehyde (1.4 g, 0.011 mol) in ethanol (20 mL) was added dropwise with a syringe over a stirred ethanolic solution (20 mL) of 1,2-diaminocyclohexane (0.66 g, 0.005 mol). Then the temperature of the reaction mixture was increased to 90 °C and it was maintained for 3 h. After this time the solvent was evaporated under vacuum and the resulted oil was dissolved in CH_2Cl_2 (50 mL), washed with H_2O (5 mL) and dried. Solution was concentrated and addition of petroleum spirit to it led to precipitation of a white yellow product (1.5 g, 81% yield). Purification can also be performed by recrystallization from ethanol.

^{1}H-NMR ($CDCl_3$): δ, 8.25 (1H, s, CH=N); 7.08 (2H, q, H^4, H^6); 6.60 (2H, t, H^3, H^5); 6.29 (2H, s, NH_2), 3.24 (1H, m); 1.92-1.24 (4H, m).
IR (KBr, cm^{-1}): 3474 m, 3250 w, 2938 w, 2916 m, 2854 m, 2835 w, 1627 vs, 1603 m, 1581 s, 1559 m, 1490 m, 1459 m, 1390 m, 1325 m, 1153 w, 1092 w, 946 w, 752 s.
MS (EI) (*m/z*) 320(66), 200(25), 157(9), 145(16), 131(32), 120(100), 106(38), 93(22), 77(15);

5.8.2 Synthesis of the *N, N'*-bis-(2,2'-amino-5-chloro-benzylideneimino)-cyclohexane

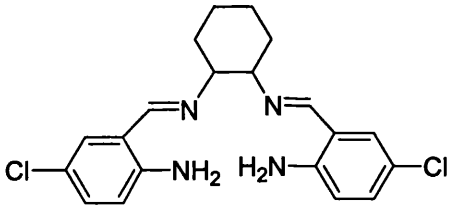

108

Preparation of 5-Cl-ambch **108** was performed using a procedure similar to that described for ambch ligand. The product (0.57 g) was obtained in 76 % yield.

^{1}H-NMR ($CDCl_3$): δ, 8.14 (1H, s, CH=N); 7.02 (2H, m, H^4, H^6); 6.54 (1H, d, J = 8.5 Hz, H^3); 6.30 (2H, br, NH_2); 3.22 - 2.25 (1H, m, aliph); 2-1 (4H, m, aliph)
IR (KBr, cm^{-1}): 3467 s, 3237 m, 2931 m, 2919 m, 2853 s, 1629 vs, 1579 s, 1548 s, 1483 vs, 1445 m, 1376 m, 1312 w, 1206 w, 1155 m, 1138 w, 1083 m, 941 w, 889 w, 815 s, 716 w, 646 m, 560 m.
MS (EI) (*m/z*) 388(51.3), 291(2.7), 248(3.3), 234(21.2), 205(3.8), 179(8.6), 165(20.6), 154(100), 140(24), 127(11.5), 118(3.3), 90(2.4), 77(6.1);

Elemental analysis calculated for: $C_{22}H_{28}N_4Cl_2$: C, 61.70; H, 5.69; N, 14.39. Found: C, 58.11; H, 6.20; N, 14.03.

5.8.3 Synthesis of the *N,N'*-bis-(2,2'-amino-5-methyl-benzylideneimino)-cyclohexane

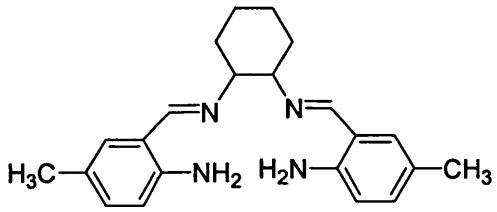

111

Preparation of 5-CH_3-ambch (**111**) was performed using a procedure similar to that described for ambch ligand. The product (0.206 g) was obtained in 78 % yield.

^{1}H-NMR ($CDCl_3$): δ, 8.19 (1H, s, CH=N); 6.89 (1H, d, J = 8 Hz, H^4); 6.88 (1H, s, H^6); 6.52 (1H, d, J = 8 Hz, H^3); 6.3 (2H, br, NH_2); 3.22 (1H, m, aliph); 2.18 (3H, s, CH_3); 1.9-1 (4H, m, aliph).

IR (KBr, cm^{-1}): 3465 s, 3273 w, 2935 s, 2919 s, 2854 s, 1629 vs, 1578 s, 1560 s, 1496 vs, 1446 m, 1375 m, 1314 m, 1245 m, 1159 s, 1088 m, 1035 w, 947 m, 859 w, 819 s, 675 w, 565 m.

MS (EI) (*m/z*) 348(44), 250(8), 236(4), 214(17.5), 185(3), 159(8), 145(26), 134(100), 120(28), 106(13), 91(9), 77(7);

Elemental analysis calculated for: $C_{22}H_{28}N_4$: C, 75.82; H, 8.09; N, 16.07. Found: C, 75.41; H, 7.92; N, 15.84.

5.8.4 Synthesis of the *N,N'*-bis-(2,2'-amino-3-methyl-benzylideneimino)-cyclohexane

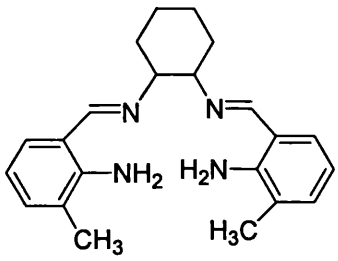

110

Preparation of 3-CH_3-ambch (**110**) was performed using a procedure similar to that described for ambch ligand. The product (0.363 g) was obtained in 85 % yield.

^{1}H-NMR ($CDCl_3$): δ, 8.28 (1H, s, CH=N); 7.01(1H, d, J = 7.8 Hz, H^6); 7.00 (1H, d, J = 7.8 Hz, H^4); 6.57 (1H, t, J = 7.8, H^5); 6.40 (2H, br, NH_2); 3.27 (1H, m, aliph); 2.12 (3H, s, CH_3); 2-1.3 (4H, m, aliph).

IR (KBr, cm^{-1}): 3458 s, 3242 m, 2924 s, 2855 s, 2827 m, 1630 vs, 1566 s, 1466 s, 1443 m, 1381 m, 1335 w, 1300 w, 1232 m, 1140 w, 1080 w, 1007 w, 951 w, 770 w, 742 s.

MS (EI) (*m/z*) 348(92.1), 250(8.2), 228(6), 214(29), 201(4), 185(6), 171(13.4), 159(12.4), 145(39.5), 134(100), 120(39.8), 107(15.2), 91(14.5), 77(8).

Elemental analysis calculated for: $C_{22}H_{28}N_4$: C, 75.82; H, 8.09; N, 16.07. Found: C, 75.22; H, 7.95; N, 15.73.

5.8.5 Synthesis of the *N,N'*-bis-(2,2'-amino-3-methoxy-benzylideneimino)-cyclohexane

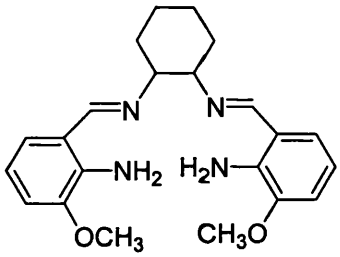

109

Preparation of 3-CH_3O-ambch (**109**) was performed using a procedure similar to that described for ambch ligand. The product (0.413 g) was obtained in 82 % yield.

^{1}H-NMR ($CDCl_3$): δ, 8.27 (1H, s, CH=N); 6.76 (1H, d, J = 7.7 Hz, H^6); 6.7 (1H, d, J = 7.7 Hz, H^4); 6.54 (1H, t, J = 7.7 Hz, H^5); 6.5 (2H, br, NH_2); 3.86 (3H, s, OCH_3); 3.25 (1H, m, H); 2-1.2 (4H, m, aliph).

IR (KBr, cm^{-1}): 3474 s, 3268 m, 2927 s, 2855 m, 2838 w, 1629 vs, 1546 s, 1479 vs, 1462 m, 1442 m, 1383 m, 1272 s, 1229 vs, 1208 m, 1176.5 w, 1139 w, 1062 w, 953 w, 775 w, 735 s

MS (FAB) (*m/z*) 381(54.5), 339(3), 307(19.4), 289(9.5), 248(58.1), 230(11.4), 214(6.4), 187(5.3), 154(54), 137(100), 120(23.5), 107(41), 89(34.6), 77(34.1).

Elemental analysis calculated for: $C_{22}H_{28}N_4O_2$: C, 69.44; H, 7.42; N, 14.72. Found: C, 65.36; H, 7.58; N, 14.13.

Preparation of salch, 3, 5-di-Busalch and salpr was done using a procedure similar to that employed for ambch. The products were characterized by ^{1}H-NMR.

5.9 Synthesis of symmetrical ambch complexes

5.9.1 Synthesis of nickel ambch complexes

5.9.1.1. Synthesis of the Ni(ambch) complex·

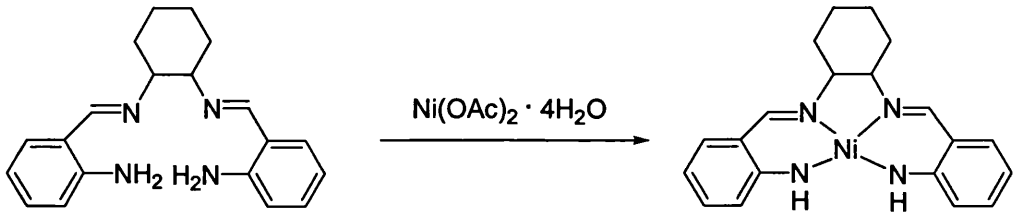

113

To an ethanolic solution containing ambch (0.13 g, 0.4 mmol, 60 mL) the stoichiometric amount of nickel (II) acetate (0.1 g, 0.4 mmol) was added at once as a powder. The solution turned from yellow to dark red in only a few minutes. The reaction mixture was kept under stirring at 25 °C for 3 hours. Filtration of the solution afforded a red precipitate of the nickel (II) ambch complex **113** which was washed with cold ethanol (5 mL) and dried under vacuum (0.09 g, 60% yield). Dark-red crystals for X-ray experiments were grown from CH_2Cl_2 and petroleum spirit.

^{1}H-NMR ($CDCl_3$): δ, 7.64 (1H, s, CH=N); 7.02 (1H, d, J = 7.8 Hz, H^6); 6.94 (1H, t, J = 7.8 Hz, H^4); 6.55 (1H, d, J = 7.8 Hz, H^3); 6.22 (1H, t, J = 7.8 Hz, H^5); 3.21 (1H, m, aliph); 2.46 (1H, m, aliph); 1.95(1H, m, aliph); 1.56 (1H, m, aliph); 1.34 (1H, m, aliph).
^{13}C-NMR ($CDCl_3$): δ, 153.74 (C^7), 133.36 (C^2), 133.25 (C^4), 131.72 (C^6), 119.35 (C^1), 115.54 (C^5), 111.56 (C^3), 70.06 (C^8), 29.13 (C^9), 24.69 (C^{10}).
IR (KBr, cm^{-1}): 3439 br, w, 3342 w, 3042 w, 2937 w, 2859 w, 1610 vs, 1540 s, 1459 s, 1389 m, 1366 m, 1340 w, 1307 w, 1241 m, 1218 w, 1192 w, 1155 w, 1122 w, 1045 w, 1022.2 w, 910 w, 932 w, 747 m, 735 m, 643 w, 571 w, 463 w, 445 w.
Elemental analysis calculated for: $C_{20}H_{22}N_4Ni$: C, 63.70; H, 5.88; N, 14.85. Found: C, 62.88; H, 5.72; N, 14.62.

5.9.1.2 Synthesis of the Ni(5-Cl-ambch) complex

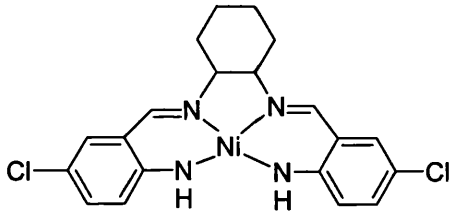

114

Synthesis of this complex was performed using a procedure similar to that employed for Ni ambch. The product (0.133 g), a red powder, was obtained in 91 % yield.

NMR ($CDCl_3$): δ, 7.59 (1H, s, CH=N); 7.00 (1H, d, J = 2.2 Hz, H^6); 6.85 (1H, dd, J = 2.2 Hz, J = 9.0 Hz, H^4); 6.49 (1H, d, J = 9.0 Hz, H^3); 3.2-3.1 (1H, m, aliph); 2.5-2.4 (1H, m, aliph); 2.05-1.95 (1H, m, aliph); 1.6-1.2 (5H, m, aliph); 0.9-0.8 (2H, m, aliph).

IR (KBr, cm^{-1}): 3437 br, m, 3344 m, 2934 m, 2856 w, 1611 vs, 1535 m, 1472 s, 1435 m, 1391 m, 1344 w, 1304 w, 1229 m, 1178 m, 1130 w, 1042 w, 934 w, 870 w, 804 m, 737 m, 671 w, 638 w.

MS (FAB) (*m/z*) 445(95), 410(4.1), 367(2), 302(2), 252(4.4), 230(6), 117(14.6), 37(8.7)

HRMS calculated for $C_{20}H_{20}N_4Cl_2Ni$ (M+1) 445.0487, found 445.0496.

Elemental analysis calculated for $C_{20}H_{20}N_4Cl_2Ni$: C, 53.86; H, 4.52; N, 12.56. Found: C, 53.66; H, 4.40; N, 12.60.

5.9.1.3. Synthesis of the Ni(3-MeO-ambch) complex

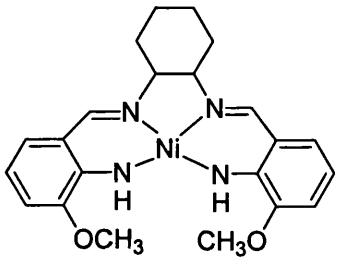

115

Procedure 1

To an ethanolic solution of 3-MeO-ambch (0.116 g, 0.3 mmol, 20 mL) was added $Ni(OAc)_2 \cdot 4H_2O$(0.076 g, 0.3 mmol) and the obtained solution was kept at room temperature under stirring for 3 h. No precipitate was formed and after the mentioned time, solution was concentrated under vacuum, transferred to a sample tube and layered with petroleum spirit. Next day the liquid phase was separated with a pipette from the purple precipitate formed at the bottom of the tube and the solid was washed two times

with petroleum spirit. Both the solution and the purple solid were analysed by ^{1}H-NMR. The NMR of the solution indicated that it contained only unreacted ligand. The purple solid had low solubility in $CDCl_3$ and it presented no signals in the aromatic region of the spectrum.

IR (KBr, cm^{-1}): 3600 s, 3427 vs, 3292 vs, 3270 vs, 3171 s, 3157 s, 2947 s, 2926 vs, 2899 m, 2859 m, 1598 vs, 1576 vs, 1456 m, 1440 m, 1406 s, 1343 w, 1232 w, 1123 m, 1021 vs, 925 w, 859 w, 668 m, 558 w, 497 w.

Complexation was also attempted in the presence of stoichiometric amount of NEt_3 which was added as a solution in ethanol, after the metal salt. The reaction took place under stirring at room temperature for 4 h. However, at the end of this period the NMR of a sample indicated only unreacted ligand.

Procedure 2

The reaction was performed using a similar procedure as described before, with the difference that after addition of all the reagents, the mixture was heated to 60-65 °C and stirred at this temperature for 3 h. After this time, a dark brown precipitate of Ni (3-MeO-ambch) **115** (0.082 g, 62 % yield) was separated by filtration from a dark-brown solution.

^{1}H-NMR (Precipitate, $CDCl_3$): δ, 7.67 (1H, s, CH=N); 6.72 (1H, d, H^6, J = 7.5 Hz); 6.45 (1H, d, H^4, J = 7.5 Hz); 6.17 (1H, t, H^5, J = 7.5 Hz); 4.16 (1H, br, NH); 3.85 (3H, s, OCH_3); 3.18 (1H, m, aliph); 2.5 (1H, m, aliph); 1.96 (1H, m, aliph); 1.3-1.26 (2H, m, aliph).

^{13}C-NMR ($CDCl_3$): δ, 152.96 (C^7), 148.55 (C^3), 145.88 (C^2), 124.71 (C^6), 115.00 (C^4), 109.68 (C^5), 108.20 (C^1), 70.14 (C^8), 55.62 (OCH_3), 29.22 (C^9), 24.77 (C^{10}).

IR (KBr, cm^{-1}): 3446 br, m, 3351 m, 2932 w, 1611 vs, 1543 w, 1481 s, 1442 m, 1386 w, 1344 w, 1227 vs, 1164 w, 1095 w, 1074 w, 1040 w, 975 w, 872 w, 725 m, 673 w.

MS (FAB) (*m/z*) 437(100), 422(9), 371(3), 301(3), 268(3), 248(6), 225(8), 213(4), 183(2.2), 158(4.3), 129(4), 99(7);

Elemental analysis calculated for $C_{22}H_{26}N_4O_2Ni$: C, 60.44; H, 5.99; N, 12.81. Found: C, 59.02; H, 6.02; N, 11.82.

5.9.1.4. Synthesis of the Ni(3-Me-ambch) complex

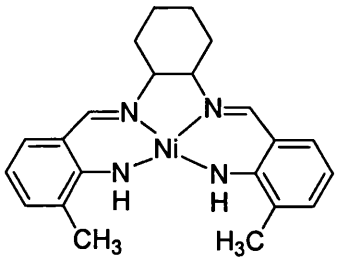

116

Synthesis of this complex was performed using a procedure similar to that employed for the nickel (II) ambch-3MeO. The compound (0.247 g) was obtained in 85 % yield.

^{1}H-NMR ($CDCl_3$): δ, 7.70 (1H, s, CH=N); 6.99 (1H, d, H^6, J = 7.5 Hz); 6.94 (1H, d, H^4, J = 7.5 Hz); 6.20 (1H, t, H^5, J = 7.5 Hz); 5.31 (1H, br, NH); 3.20 (1H, m, aliph); 2.53-2.50 (1H, m, aliph); 2.17 (3H, s, CH_3); 1.97 (1H, m, aliph); 1.39-1.25 (2H, m, aliph).

^{13}C-NMR ($CDCl_3$): δ, 154.1 (C^7), 152.34 (C^2), 131.9 (C^4), 131.8 (C^6), 123.97 (C^3), 115.28 (C^5), 111.21 (C^1), 70.20 (C^8), 29.09 (C^9), 24.73 (C^{10}), 17.56 (CH_3)

IR (KBr, cm^{-1}): 3444 w, 3375 w, 3364 w, 3050 w, 3024 w, 2962 w, 2933 m, 2855 w, 1609 vs, 1548 s, 1459 s, 1440 m, 1412 w, 1377 w, 1342 w, 1311 w, 1226 s, 1089 m, 1044 m, 1032 w, 741 m, 733 s, 623 m, 571 w, 509 w.

Elemental analysis calculated for $C_{22}H_{26}N_4Ni$: C, 65.22; H, 6.46; N, 13.83. Found: C, 64.11; H, 6.42; N, 13.42.

5.9.1.5 Synthesis of the Ni(5-Me-ambch) complex

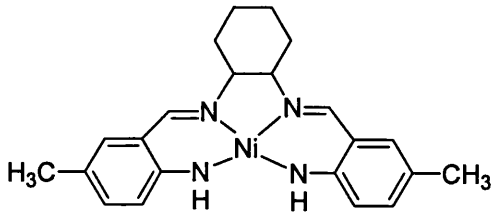

117

Synthesis of this complex was performed using a procedure similar to that employed for the nickel (II) 3-MeO-ambch. The product (0.098 g, dark-red powder) was obtained in 32 % yield.

^{1}H-NMR ($CDCl_3$): δ, 7.60 (1H, s, CH=N); 6.80 (1H, s, H^6); 6.78 (1H, d, H^4, J = 8.4 Hz); 6.50 (1H, d, H^3, J = 8.4 Hz); 3.15 (1H, m, aliph); 2.47 (1H, m, aliph); 2.14 (3H, s, CH_3); 1.95 (1H, m, aliph); 1.36 (2H, m, aliph).

IR (KBr, cm^{-1}): 3439 br, w, 3337 w, 3012 w, 2928 m, 2855 m, 1622 vs, 1601 vs, 1541 vs, 1479 vs, 1452 s, 1393 s, 1348 s, 1306 w, 1246 s, 1200 m, 1165 s, 1130 w, 1045 w, 945 w, 870 w, 808 m, 781 w, 638 m, 563 w, 451 w.

MS (FAB) (*m/z*) 405(100), 352(3.2), 267(2.7), 192(12.5), 145(6), 58(3)

HRMS calculated for $C_{22}H_{26}N_4Ni$ (M^+) 404.1501, found 404.1511.

Elemental analysis calculated for $C_{22}H_{26}N_4Ni$: C, 65.22; H, 6.46; N, 13.83. Found: C, 62.81; H, 6.25; N, 12.91.

5.9.2 Synthesis of Copper amch complexes

5.9.2.1 Synthesis of Cu(ambch) complex

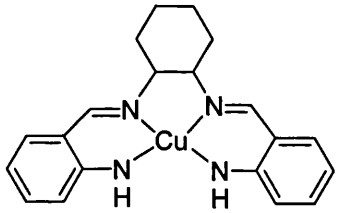

132

A solution of triethylamine (0.06 g, 0.6 mmol) in ethanol (2.5 mL) was added to a stirred ethanolic solution of the free ligand (0.1 g, 0.3 mmol, 40mL). The stoichiometric amount of copper(II) acetate (0.06 g, 0.3 mmol) was then added as a powder to the above solution. The latter changed its colour in few minutes from yellow to brown indicating the formation of the complex. After 3 h at 25 °C the solution was filtered to give a brown precipitate which was washed with cold ethanol and dried under vacuum. The desired product (0.07 g) was obtained in 59 % yield. Brown crystals for X-ray experiments were grown from CH_2Cl_2 and petroleum spirit.

IR (KBr, cm^{-1}): 3440 br, w, 3340 br, w, 2935 w, 2856 w, 1616 vs, 1535 s, 1475 sh, m, 1450 s, 1389 m, 1355 m, 1309 w, 1235 m, 1179 m, 1157 m, 1117 m, 1022 m, 909 w, 746 sh, m, 738 m, 664 w, 566 w, 460 w, 414 w.

MS (FAB) (*m/z*) 382(60.4), 321(2), 263(9.6), 182(7.2), 131(9.1), 81(2.8)

HRMS calculated for $C_{20}H_{22}N_4Cu$ (M^+) 381.1134, found 381.1140.

Elemental analysis calculated for $C_{20}H_{22}N_4Cu$: C, 62.89; H, 5.80; N, 14.67; Found: C, 62.03; H, 5.68; N, 14.38.

5.9.2.2 Synthesis of the Cu(5-Cl-ambch) complex

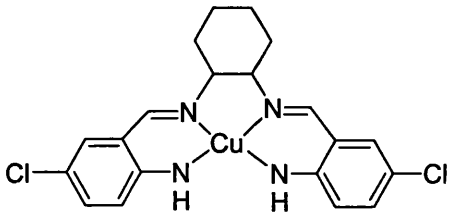

133

Synthesis of this complex was performed using a procedure similar to that employed for the copper (II) ambch. The product (0.113 g, brown powder) was obtained in 80 % yield.

IR (KBr, cm^{-1}): 3442 br, w, 3341 w, 2936 w, 2855 w, 1609 vs, 1528 s, 1463 s, 1426 m, 1390 s, 1367 w, 1349 w, 1327 w, 1308 w, 1228 m, 1167 s, 1122 w, 807 m, 732 m, 662 m.

MS (FAB) (*m/z*) 451(65), 415(4), 389(6.5), 369(3), 297(11), 252(4.5), 216(15.5), 191(4.5), 130(4.6), 81(3.1), 37(3).

HRMS calculated for $C_{20}H_{20}N_4Cl_2Cu$ (M+1), 450.0432, found 450.0439.

Elemental analysis calculated for $C_{20}H_{20}N_4Cl_2Cu$: C, 53.28; H, 4.47; N, 12.42. Found: C, 53.31; H, 4.60; N, 12.49.

5.9.2.3 Synthesis of the Cu(3-MeO-ambch) complex

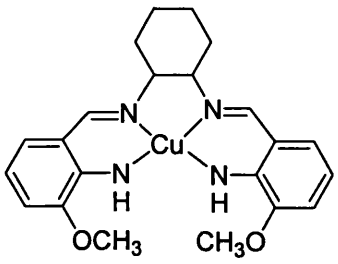

134

Synthesis of this complex was achieved by addition of $Cu(OAc)_2 \cdot H_2O$ (0.204 g, 1.0 mmol) to a solution of ligand (0.34 g, 0.9 mmol) in ethanol (85 mL), previously deprotonated with NEt_3 (0.207 g, 2 mmol). The reaction was carried out under stirring at 60°C for 2.5 h and led to formation of Cu(3-MeO-ambch) complex which precipitated from the system and was separated by filtration (0.194 g, 49 % yield).

IR (KBr, cm^{-1}): 3441 br, w, 3355 m, 3055 w, 2998 w, 2931 m, 2855 w, 2829 w, 1609 vs, 1542 s, 1479 s, 1459 m, 1440 s, 1384 s, 1349 m, 1341 m, 1335 m, 1235 s, 1215 vs, 1163 w, 1091 w, 1073 m, 1028 w, 970 s, 954 m 749 w, 726 s, 690 w, 562 w.

Elemental analysis calculated for $C_{22}H_{26}N_4O_2Cu$: C, 59.78; H, 5.93; N, 12.67. Found: C, 58.97; H, 5.85; N, 12.27.

5.9.2.4 Synthesis of the Cu(3-Me-ambch) complex

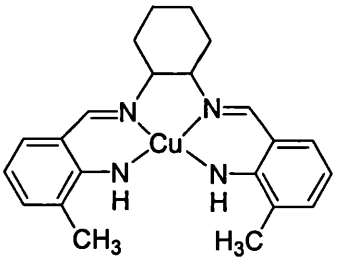

135

Synthesis of this complex was performed using a procedure similar to that employed for the copper (II) 3-MeO-ambch. The product (0.796 g) was obtained in 80 % yield.

IR (KBr, cm^{-1}): 3443 br, w, 3371 w, 3020 w, 2932 w, 2856 w, 1612 vs, 1545 s, 1450 m, 1439 sh, m, 1393 m, 1371 m, 1339 w, 1302 w, 1221 m, 1090 w, 1034 w, 959 w, 858 w, 741 m, 648 w, 549 w, 502 w.

MS (FAB) (*m/z*) 410(100), 348(11.78), 277(6.9), 223(4), 198(7.3), 145(16), 117(5).

HRMS calculated for $C_{22}H_{26}N_4Cu$ (M+1) 410.1524, found 410.1531.

Elemental analysis calculated for $C_{22}H_{26}N_4Cu$: C, 64.44; H, 6.39; N, 13.66. Found: C, 63.77; H, 6.30; N, 13.35.

5.9.2.5 Synthesis of the Cu(5-Me-ambch) complex

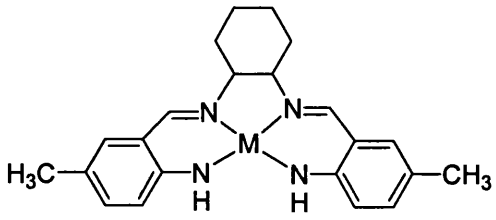

136a: M = CuOAc
136b: M = CuCl

From $Cu(OAc)_2$

Complexation of 5-Me-ambch with Cu^{2+} was performed using a procedure similar to that employed for 3-MeO-ambch. After 3 h heating was stopped and the reaction

mixture was evaporated to dryness to give a brown-black residue. This was washed with ethanol and petroleum spirit, then was analysed by IR and elemental analysis.

IR (KBr, cm^{-1}): 3429 s, 2932 m, 2860 w, 1626 vs, 1570 vs, 1485 m, 1420 s, 1344 m, 1236 w, 1169 w, 1038 w, 826 w, 679 w, 623 w, 561 w.
MS (FAB) (*m/z*) 410(55.3), 395(7.1), 352(100), 248(41.1), 145(51.2)
Peaks higher than M^+: 838, 816, 761, 644, 601, 525, 464;
Elemental analysis calculated for $C_{24}H_{29}N_4O_2Cu \cdot 4H_2O$: C, 53.27; H, 6.89; N, 10.35. Found: C, 56.57; H, 6.66; N, 9.60.

From $CuCl_2$
This reaction was performed in a similar way as described above, but using $CuCl_2$ as a copper source. After 3 h at 60 °C, the mixture was cooled to room temperature and was filtered to give a brown precipitate.

IR (KBr, cm^{-1}): 3445 vs, 2972 m, 2936 vs, 2760 sh, m, 2743 m, 2677 vs, 2629 m, 2610 m, 2492 m, 1629 sh, vs, 1612 br, vs, 1576 vs, 1535 s, 1474 vs, 1447 sh, vs, 1393 s, 1308 s, 1236 w, 1171 s, 1036 m, 827 br, w.
MS (FAB) (*m/z*) 410, 352, 239; peaks higher than M^+: 814, 752, 640, 525, 466.
Elemental analysis calculated for $C_{22}H_{26}N_4ClCu \cdot 3H_2O$: C, 52.9; H, 6.45; N, 11.26. Found: C, 54.07; H, 7.05; N, 10.86.

5.9.3 Synthesis of Manganese amch complexes

5.9.3.1 Synthesis of the Mn(ambch)(Cl)

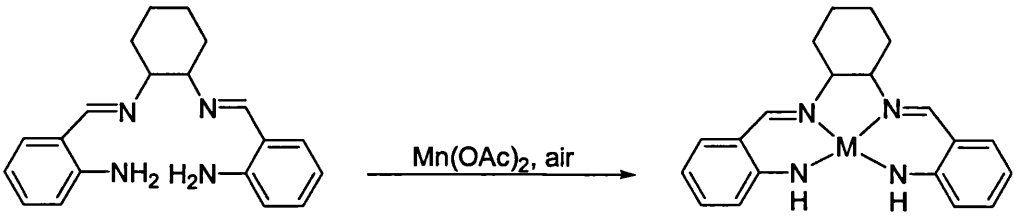

M = MnCl

143

Method A.

The procedure described in [3] was adapted for complexation of ambch. Hydrated manganese (II) acetate (0.87 g, 3.5 mmol) was dissolved in ethanol (11 mL) and the solution was heated to reflux (80-85 °C) until it became homogeneous. To this solution the free ligand (0.38 g, 1.2 mmol) dissolved in toluene (26 mL) was added dropwise. The mixture was kept at reflux for 3 hours, then air was gently bubbled through the solution for 6 hours, during this time the reaction being followed by TLC on alumina using ethyl acetate : hexane = 1 : 4. When the spot corresponding to the free ligand decreased considerably, the heating was stopped and saturated sodium chloride solution (1.5 mL) was added. The mixture was cooled to room temperature and the two layers were separated. The organic layer was washed with water and dried over Na_2SO_4, then removal of the solvent led to a solid which was redissolved in DCM. Addition of hexane and concentration of this solution, followed by cooling in the fridge gave a brown precipitate which was collected by filtration and analysed by IR.

IR (KBr, cm^{-1}): 3439 s, 2936 m, 2860 w, 1612 vs, 1543 s, 1445 s, 1391 w, 1344 m, 1312 s, 1286 s, 1204 m, 1151 m, 1124 , 1018 w, 908 m, 812 m, 760 m, 629 m, 571 w, 426 m

Method B.

To an ethanolic solution containing manganese(II) acetate (1.06 g, 4.3 mmol, 23 mL), heated to reflux, the free ligand (ambch) (0.46 g, 1.4 mmol) dissolved in ethanol (60 mL) was added dropwise over 2 h. Solution changed its colour gradually during this period from white-off to brown and later black (dark brown under light). Then triethylamine (0.28 g, 2.8 mmol) was added to the reaction mixture and this was kept for 2.5 h under stirring at 90 °C, then air was bubbled gently through the solution, which became completely black 5-10 min later. After 3.5 h in these conditions, saturated aqueous solution of NaCl was added and reflux continued for another 40 min.

Filtration of the cold mixture and evaporation of the filtrate gave a dark-brown solid which was extracted with CH_2Cl_2. After filtration of the obtained solution, followed by drying with Na_2SO_4, the solvent was removed under vacuum to give a brown residue. This was washed with Et_2O, then was dissolved in a small quatity of CH_2Cl_2 and layered

with petroleum spirit. A brown precipitate (0.11 g) separated overnight which was analyzed by MS, IR and elemental analysis. The orange ethereal solution became a brown oil on standing in air. It contained a paramagnetic compound as indicated by ^{1}H-NMR.

brown precipitate

IR (KBr, cm^{-1}): 1627 s, 1609 vs, 1564 br, s, 1538 br, s, 1496 m, 1480 m, 1448 s, 1422 br, s, 1387 s, 1355 m, 1236 w, 1185 w, 1157 m, 1118 w, 1048 w, 1023 br, m.

MS: $(M\text{-}Cl)^+$, Calculated: 372.9. Found: 373.

Elemental analysis calculated for $C_{20}H_{22}N_4MnCl$: C, 58.76; H, 5.42; N, 13.70; Found: C, 46.60; H, 6.20; N, 10.18.

Method C. Synthesis of the Mn(ambch)(Cl)

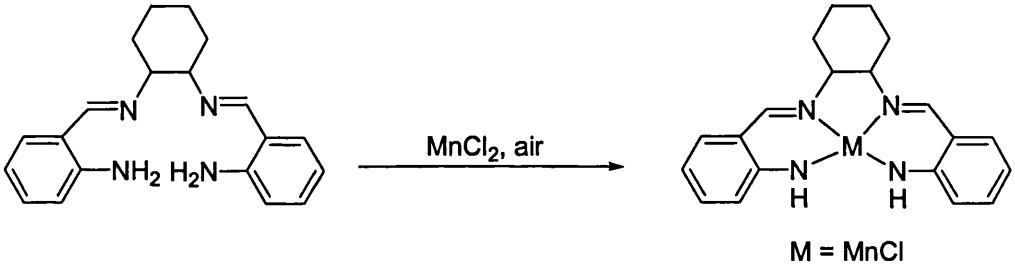

143

The procedure described in [**8**] was adapted for complexation of ambch. To a solution of ambch ligand (0.15 g, 0.47 mmol) in ethanol (20 mL) was added NEt_3 (0.094g, 0.93 mmol, in 10 mL ethanol) followed by $MnCl_2 \cdot H_2O$ (0.092 g, 0.46 mmol). Solution changed its colour from yellow to orange and later brown orange within 15 minutes. The reaction mixture was kept 20 h under stirring at 55-60 °C in air, during this time the mixture being monitored by ^{1}H-NMR. The product is insoluble in $CDCl_3$, however the consumption of the ligand in time was followed (using the imine proton signal), allowing the determination of the reaction time. At the end of the reaction, the mixture was filtered to give a dark brown precipitate of Mn(ambch)(Cl) (0.102 g, 53.4 % yield) and a brown solution.

Brown precipitate **143**

IR (KBr, cm^{-1}): 3437 s, 3261 m, 2937 w, 2858 w, 1607 vs, 1537 m, 1447 s, 1389 m, 1352 s, 1238 w, 1188 w, 1155 w, 1124 w, 1020 w, 910 w, 758 m, 567 w, 523 w, 463 w, 422 w.

MS (FAB) (*m/z*) 373(24), 321(100), 248(15.2), 218(41), 200(8), 184(11.4), 131(17.3), 106(12.7), 81(7)

Elemental analysis calculated for $C_{20}H_{22}N_4ClMn{\cdot}3H_2O$: C, 51.89; H, 6.09; N, 12.10; Cl, 7.67.Found: C, 51.49; H, 5.92; N, 11.95; Cl, 7.62.

5.9.3.2 Synthesis of Mn(3-Me-ambch)(Cl)

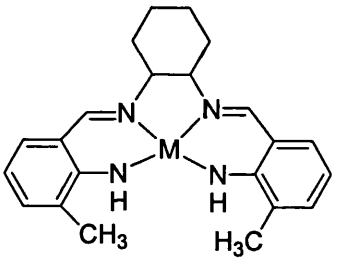

M = MnCl

144

This reaction was performed using a procedure similar to that employed for synthesis of Mn(ambch)(Cl). The mixture was kept under stirring at 55 °C for 19 h in air, during this period the consumption of ligand was monitored by ^{1}H-NMR. After this period the reaction mixture was filtered to give brown precipitate. The filtrate was concentrated under vacuum and addition of diethyl ether to this solution led to precipitation of more product (0.085 g, 47 % yield). This was washed several times with ether and dried.

brown precipitate **144**

IR (KBr, cm^{-1}): 3435 m, 3366 m, 2937 w, 2855 w, 1607 vs, 1547 s, 1448 w, 1429 w, 1387 m, 1362 m, 1325 m, 1219 m, 1090 w, 1036 w, 959 w, 860 w, 795 w, 748 w, 671 w, 567 w, 503 w, 469 w.

MS (FAB) (*m/z*) 436(1), 401(36), 348(22), 268(2), 232(3), 198(6), 171(3), 134(16), 118(4.1), 94(100), 81(5)

HRMS calculated for $C_{22}H_{26}N_4ClMn$ (M^+), 436.1217, found 436.1226.

Elemental analysis calculated for $C_{22}H_{26}N_4ClMn{\cdot}3H_2O$: C, 53.82; H, 6.57 ; N: 11.41; Found: C: 48.61; H: 6.29; N: 10.53.

5.9.4 Synthesis of Cobalt (II) ambch complexes

5.9.4.1. Synthesis of the Co(ambch) complex

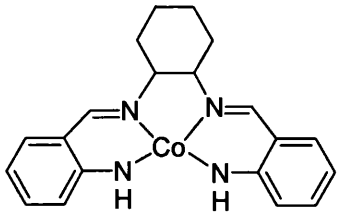

154

The procedure described in [9] was adapted for complexation of ambch. Synthesis of this complex was performed under nitrogen. To a hot ethanolic solution of the ligand (0.2 g, 0.62 mmol, 10 mL) kept under stirring at 55-60 °C, was added dropwise with a cannula a degassed aqueous solution of $Co(OAc)_2 \cdot 4H_2O$ (0.202 g, 0.81 mmol, 9 mL). After addition of the metal salt heating was stopped and solution was allowed to cool to 40 °C. Filtration under nitrogen led to the separation of a bright-red precipitate (0.144 g, 61 % yield) from a red-orange solution. The precipitate was heated to 40 °C in vacuum for 30 min - 1h to remove the traces of solvents. The dried product is air stable. When the precipitate is not completely dry or in solution, in presence of oxygen, the Co(II) ambch is readily oxidized to Co(III) and the solution turns brown-red.

IR (KBr, cm^{-1}): 3443 br, s, 3042 w, 2936 w, 2858 w, 1603 vs, 1582 m, 1539 s, 1443 s, 1381 m, 1346 m, 1306 w, 1238 w, 1190 m, 1155 m, 1126 w, 1022 w, 912 w, 746 s, 694 w, 571 w, 457 w.

Elemental analysis calculated for: $C_{20}H_{22}N_4Co$: C, 62.17; H, 6.00; N, 14.5. Found: C, 61.96; H, 5.88; N, 13.52.

5.9.4.2 Synthesis of the Co(3-Me-ambch) complex

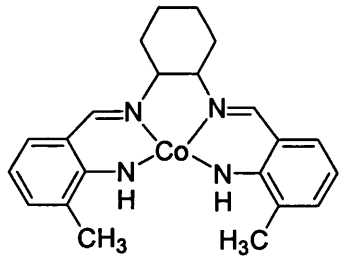

155

Synthesis of this complex was performed using a procedure similar to that employed for the Co(ambch). Before addition of the metal salt, the ligand was deprotonated with NEt_3. The product (0.135 g, red-orange powder) was obtained in 73 % yield.

IR (KBr, cm^{-1}): 3437 s, 3018 w, 2930 s, 2855 w, 2361 w, 2332 w, 1626 w, 1601 vs, 1547 vs, 1450 s, 1433 s, 1371 s, 1337 m, 1312 w, 1231 s, 1088 w, 1043 w, 743 s, 677 m, 573 w, 513 w.

Elemental analysis calculated for $C_{22}H_{26}N_4Co$: C, 65.18; H, 6.46; N, 13.82. Found: C, 63.99; H, 6.43; N, 13.41.

5.9.4.3 Synthesis of the Co(5-Me-ambch) complex

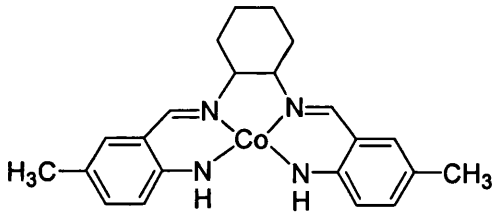

156

Synthesis of this complex was performed using a procedure similar to that employed for the Co(ambch). Before addition of the metal salt, the ligand was deprotonated with NEt_3. The product (0.088 g, red powder) was obtained in 80 % yield.

IR (KBr, cm^{-1}): 3435 br, vs, 3012 w, 2930 m, 2857 w, 1623 vs, 1581 vs, 1565 vs, 1547 vs, 1492 s, 1447 vs, 1419 vs, 1385 s, 1341 m, 1243 w, 1169 s, 1129 m, 1101 m, 1041 m, 1013 sh, 954 w, 875 w, 819 m, 808 m, 695 w, 566 w.

Elemental analysis calculated for $C_{22}H_{26}N_4Co$: C, 65.18; H, 6.46; N, 13.82. Found: C, 64.42; H, 6.29; N, 12.58.

5.9.5 Oxidation of Co(II) ambch

NMR experiment 1

The reaction between Co(II)ambch **154** and *t*-butyl-phenol (molar ratio 1 : 3.6) in $CDCl_3$ was followed by ^{1}H-NMR. Experiments were run after 30 min, 45 min, 1 h and 2.5 h. Broad signals appeared in the sample after 30 min, but after 1 h the compound seemed to be diamagnetic. After 2.5 h the product (red-brown) precipitated at the bottom of the tube and the solution presented NMR signals only for unreacted 4- tert-butyl-phenol.

The aromatic protons overlap forming multiplets between 8.8 and 6.2 ppm, while two singlets at 5.91 and 5.39 ppm could be distinguished. These two singlets might indicate the presence of quinones in the system, but the complexity aromatic region prevented full interpretation. However, they are present in low amount (less than 10 %) as resulted from integration of the corresponding tert-butyl-proton signals.

NMR experiment 2

NMR experiments were run after 30 min, 45 min and 3 h on a red-brown solution obtained by mixing Co(ambch) **154** and *t*-butyl-phenol (molar ratio 1 : 1) in $CDCl_3$. Broad signals appear in the sample even after 1h and the sample proved hard to shim. Compared with the previous ^{1}H-NMR experiments, a new peak at 3.54 ppm appeared in the spectra which indicated a side reaction that occurred in $CDCl_3$. This reaction seemed rather fast in the conditions employed. Signals in the aromatic region are broad and they overlap, making the NMR spectra not very informative. However, in the region corresponding to the tert-butyl protons only one singlet (at δ 1.1) could be distinguished apart from that of the *t*-butyl-phenol (δ 1.35) which suggested that the reaction led mainly to one product. After 3 h the solvent was evaporated and the IR of the sample was obtained. The sample was a mixture of Co(ambch), *t*-butyl-phenol and Co(ambch)(O-C_6H_4-4-Bu^t) complex.

IR (KBr, cm^{-1}): 3443 br, s, 3042 w, 2936 w, 2858 w, 1603 vs, 1582 m, 1539 s, 1443 s, 1381 m, 1346 m, 1306 w, 1238 w, 1190 m, 1155 m, 1126 w, 1022 w, 912 w, 746 s, 694 w, 571 w, 457 w.

5.9.5.1 Oxidation of Co(ambch) in benzene

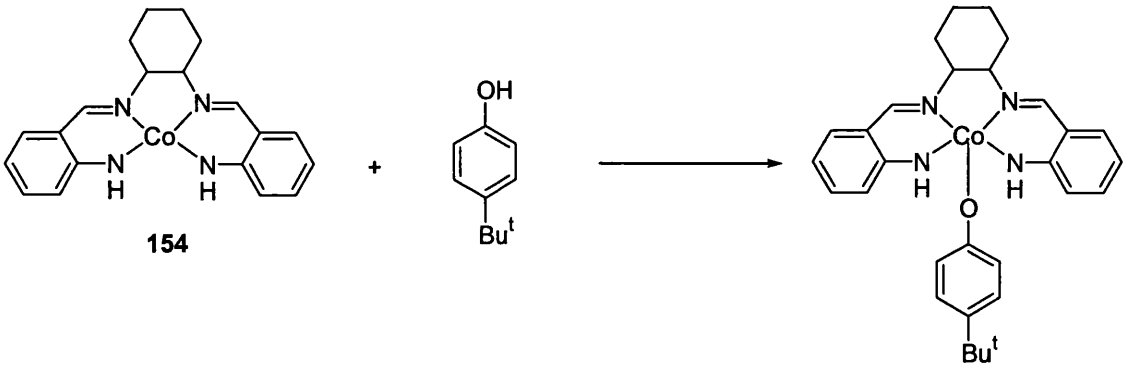

154 158

To a solution of tert-butyl-phenol (0.095 g, 0.6 mmol) in benzene (22 mL) was added Co(ambch) (0.08 g, 0.2 mmol) under stirring. The solid dissolves quickly and the solution changes its colour from bright red to dark-brown red in about 5 min. The mixture was stirred at room temperature for 1 h, then it was filtered to give a dark filtrate. This was concentrated and addition of diethyl ether to it induced precipitation of a dark-black precipitate of Co(ambch)(O-C_6H_4-4-Bu^t)(**158**, 83 % yield).

The precipitate was washed several times with diethyl ether and analyzed by IR and EA, while the brown ethereal washings were analyzed by IR and NMR. The brown solution contained mainly unreacted *t*-butyl-phenol according to ^{1}H-NMR and IR, additionally the IR spectrum presented bands which might be assigned to a substituted benzoquinone.

IR (brown sample, KBr, cm^{-1}): 3435 br, vs, 2963 s, 2905 w, 2868 w, 1650 m(*), 1614 s, 1599 m(*), 1514 vs, 1447 w, 1385 m, 1362 w, 1244 s, 1182 m, 1113 w, 829 s, 816 w, 550 m, 478 w (main component – tert-butyl-phenol; * band assigned to a quinone).

IR (dark-black precipitate, KBr, cm^{-1}): 3441 br, vs, 2947 m, 2858 w, 1609 vs, 1535 w, 1514 w, 1493 s, 1445 s, 1385 s, 1362 w, 1344 w, 1277 m, 1261 m, 1240 w, 1175 w, 1153 m, 1124 m, 1020 w, 912 w, 833 w, 746 s, 567 w, 552 w.
Elemental analysis calculated for: $C_{30}H_{35}N_4OCo(C_{10}H_{14}O)$: C, 70.98; H, 7.29; N, 8.28. Found: C, 67.96; H, 7.48; N, 7.84.

5.9.5.2 Reaction of Co(ambch) with 2,4-di-*t*-butyl-phenol

This reaction was performed in a similar manner as described for 4-*t*-butyl-phenol. The solution changed more slowly the colour from red to brown. After 1 h it was filtered to give a red precipitate containing mainly unreacted Co(ambch) and a brown solution. Bands characteristic of quinones indicated their presence in small amounts in the precipitate, while in solution these bands were more intense.

IR (precipitate, KBr, cm^{-1}): 3038 w, 2936 m, 2861 w, 1654 w(*), 1603 vs, 1580 s, 1560 w, 1541 vs, 1509 w, 1476 w, 1450 s, 1440 vs, 1400 m, 1381 m, 1348 s (*), 1340 m, 1306 m, 1238 m, 1217 w, 1190 m, 1155 m, 1124 w, 1022 w, 910 w, 825 w (*), 748 s, 737 s, 694 m (main component – Co(II)(ambch), * band assigned to a quinone)

IR (solution, KBr, cm^{-1}): 2954 vs, 2906 s, 2866 s, 1654 m(*), 1604 s, 1590 (sh) s(*), 1577 s, 1571 m, 1561 s, 1540 m, 1534 m, 1528 m, 1524 m, 1520 m, 1509 s, 1475 s, 1458 s, 1447 s, 1439 s, 1408 s, 1389 s, 1361 s, 1306 m, 1278 s, 1255 s, 1232 s, 1201 s, 1176 m, 1155 m, 1122 w, 1088 w, 1023 w, 824 w(*), 749 m, 738 m (contains 2,4-di-*t*-butyl-phenol; * band assigned to a quinone)

5.9.5.3 Oxidation of Co(ambch) in chloroform

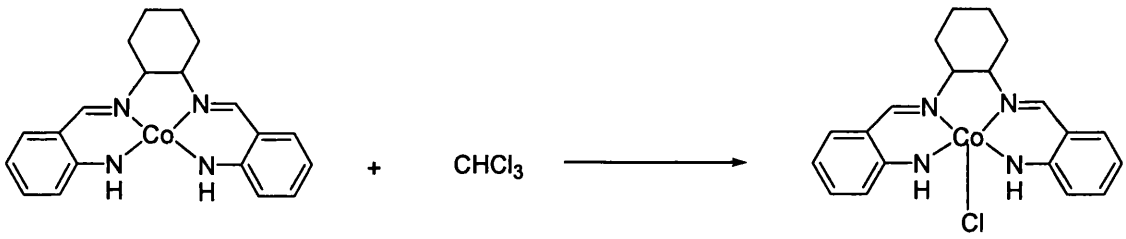

162

Upon stirring Co(ambch) at room temperature in $CHCl_3$, the system changed colour from red to brown and a fine homogeneous suspension was formed within 5 min. This was stirred overnight and the following day, evaporation of the solvent under vacuum led to a black-grey residue that was washed several times with petroleum spirit and analyzed by IR. The attempt to run an NMR experiment was not successful, due to the paramagnetism of the compound.

IR (KBr, cm^{-1}): 1602.7 vs, 1570 m, 1543 m, 1440.7 s, 1384.8 vs, 1355.9 m, 1325 w, 1193.9 m, 1153.4 s, 1124.4 s, 1024 m, 916.1 w, 758 s, 619 w

Elemental analysis calculated for: $C_{20}H_{22}N_4ClCo \cdot CH_2Cl_2$: C, 50.66; H, 4.82; N, 11.25. Found: C, 52.99; H, 5.11; N, 11.20.

5.9.5.4 Oxidation of Co(ambch) in 2-butanol

Co(ambch) (0.022 g, 0.06 mmol) was stirred at room temperature in 2-butanol (7.5 mL). After 30 min DCM and H_2O were added to the system, but even so the solution maintained its initial red colour. Therefore, the mixture was left under stirring at 50 °C overnight. The following day, unreacted Co(ambch) complex was separated by filtration from the dark black solution which was concentrated and layered with petroleum spirit. More red precipitate deposited overnight and after its separation, the filtrate was evaporated to give a brown powder which was washed with petroleum spirit and dried under vacuum.

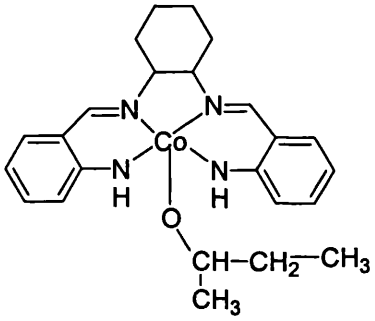

159

brown powder

IR (KBr, cm^{-1}): 2980 w (*), 2933 m, 2860 w, 1720 m (*), 1660 s, 1634 s, 1607 vs, 1576 s, 1559 s, 1539 s, 1526 s, 1509 m, 1448 m, 1384 s, 1321 m, 1260 m, 1208 w, 1120 w, 1031 w, 763 w (main component Co(ambch)(OBu); * band which might indicate the presence of 2-butanone)

5.9.5.5 Oxidation of Co(ambch) in ethanol

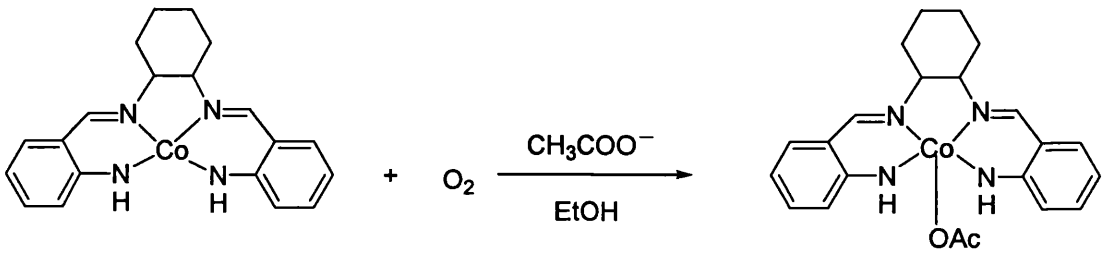

163

A solution of Co(II) ambch (0.5 mmol in 10 mL ethanol), generated as described in section **5.9.4.1** was opened to air and stirred at room temperature for 2 h. After this period, the solvent was evaporated and the obtained dark residue (0.163 g, 80 % yield) was washed several times with petroleum spirit. The product was analysed by elemental analysis and IR.

IR (KBr, cm^{-1}): 3423 s, 2936 w, 2860 w, 1649 s, 1597 vs, 1570 vs, 1447 m, 1400 m, 1335 m, 1256 w, 1231 w, 1157 w, 1123 w, 1024 w, 764 w, 671 w, 617 w, 573 w, 461 w.

Elemental analysis calculated for: $C_{22}H_{25}N_4O_2Co\cdot(CH_3COOH)(H_2O)$: C, 56.03; H, 6.07; N 10.89 . Found: C, 53.74; H, 5.84; N, 10.57.

5.10 Synthesis of VO (ambch) complexes

5.10.1 Complexation of ambch with $VO(acac)_2$

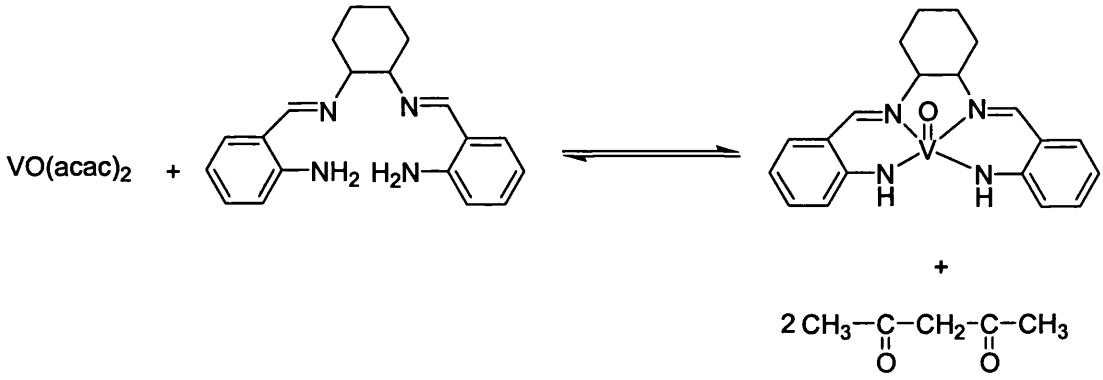

This reaction was performed under nitrogen. Ethanol was degassed by bubbling nitrogen through it for minimum 30 min before the beginning of the reaction. Under stirring, to a warm (50 °C) ethanolic solution of ligand (0.216 g, 0.67 mmol, 15 mL) was added dropwise a solution of $VO(acac)_2$ (0.179 g, 0.67 mmol) in ethanol (30 mL). At the end of the addition, temperature was raised to 90 °C and kept constant for 3 h. After this period, the reaction mixture was filtered hot to give a green-grey precipitate and a green-yellow solution. The latter was concentrated to half of the initial volume and cooled. Light-blue crystals were formed overnight which were decanted from the yellow-brown solution with a cannula. Evaporation of this solution gave a brown-orange oil. The oil was washed with dry petroleum spirit to give a yellow solution and a brown-orange

solid. The blue crystals were analysed by IR and the yellow solution by ^{1}H-NMR in $CDCl_3$.

green-grey precipitate

IR (KBr, cm^{-1}): 3439 vs, 2937 vs, 2864 s, 1628 s (br), 1497 m, 1450 m, 1128 m, 1119 m, 1096 m, 1030 m, 968 vs (br), 810 vs (br), 762 vs, 667 vs (br).

blue crystals

IR (KBr, cm^{-1}): 3419 m, 2976 m, 2892 w, 1570 vs, 1526 vs, 1428 m, 1382 s, 1370 s, 1352 s, 1289 m, 1096 w, 1042 s, 1003 s, 935 w, 896 w, 794 w, 684 w, 597 s, 467 w.

$VO(acac)_2$

IR (KBr, cm^{-1}): 3431 w, 1559 vs, 1529 vs, 1419 m, 1374 s, 1358 s, 1287 m, 1023 w, 998 s, 937 w, 799 w, 790 w, 686 w, 610 w, 485 m.

yellow solution:

1 : 1 mixture of symmetrical ligand ambch and asymmetrical ligand ambchac

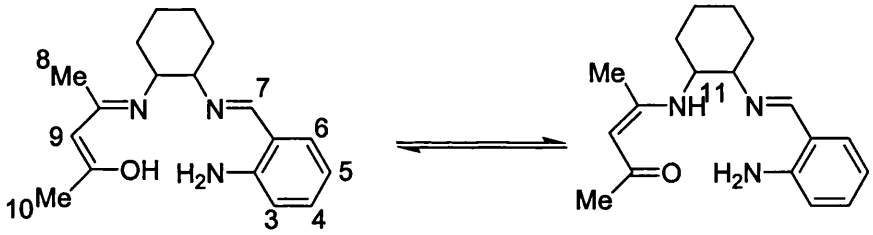

171 **171**

ambchac **171**:

^{1}H-NMR ($CDCl_3$): δ, 10.9 (1H, br, s, NH), 8.50 (1H, s, H^7), 8.05 (1H, d, H^6); 7.88 (1H, d, H^3); 7.80 (1H, t, H^4); 7.55 (1H, t, H^5); 6.30 (2H, br, s, NH_2); 4.73 (1H, s, H^9); 2.93 (3H, s, H^{10}); 2.74 (3H, s, H^8).

5.10.2 Complexation of ambch with $VO(acac)_2$ in presence of a base

Synthesis was performed under nitrogen. Ethanol was degassed by bubbling N_2 through it for minimun 30 min before the beginning of the reaction. Under stirring, to a hot solution (75 °C) of ambch ligand (0.207 g, 0.64 mmol) and NEt_3 (0.13 g, 1.28 mmol) in

ethanol (20 mL), was added dropwise a solution of $VO(acac)_2$ (0.171 g, 0.64 mmol) in ethanol (40 mL). Then the temperature was raised to 90 °C and kept constant for 3.5 h. After this time, the solution was filtered cold to give a white precipitate and a green filtrate. Evaporation of this to dryness produced an orange-brown oil which was dissolved in dry DCM. Addition of diethylether to this solution gave a green-brown precipitate and a light solution. Upon addition of more ether and after shaking the Schlenk tube, the precipitate became yellow-orange and the solution turned brown. After filtration the solution was evaporated to dryness to give a brown solid.

The brown solid was extracted twice with hot toluene to give a green solution which was decanted with the cannula from 0.153 g orange solid (65 % yield).

yellow-orange precipitate

IR (KBr, cm^{-1}): 1624 s, 1593 s, 1128 s, 1094 s, 1045 s, 982 vs, 802 m, 704 m, 671 m, 619 m.

orange solid VO(ambchac) (173)

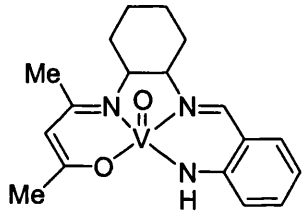

173

IR (KBr, cm^{-1}): 3414 m, 3247 w, 2929 m, 2856 w, 1611 vs, 1594 s, 1543 s, 1524 m, 1510 w, 1449 s, 1389 m, 1356 m, 1236 w, 1188 w, 1157 w, 1122 w, 1025 w, 962 m, 937 m, 909 w, 807 m, 750 m, 624 w, 569 w, 463 w.

Elemental analysis calculated for: $C_{18}H_{23}N_3O_2V$: C, 59.33; H, 6.36; N, 11.53. Found: C, 57.48; H, 6.62; N, 11.21.

green solution

IR (KBr, cm^{-1}): 1628 vs, 1611, 1558 vs, 1526 vs, 1491 s, 1420 s, 1375 vs, 1286 s, 1022 s, 997 s, 939 m, 797 m, 750 s (main component $VO(acac)_2$, contains also VO ambchac)

5.10.3 Complexation of ambch with $VOSO_4$

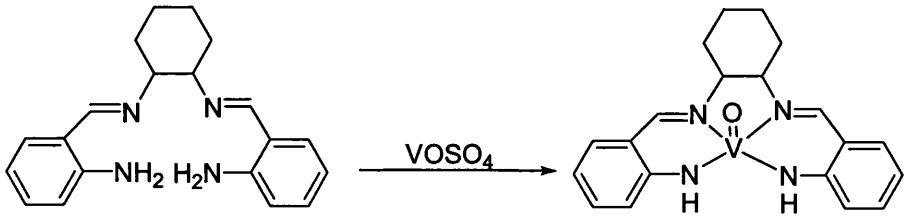

170

Method A

This reaction was performed under nitrogen. A mixture of ligand (0.215 g, 0.67 mmol) and NEt_3 (0.136 g, 1.34 mmol) in ethanol (20 mL) was heated to 60 °C under stirring to obtain a homogeneous system. Then $VOSO_4 \cdot 5H_2O$ (0.17 g, 0.67 mmol) disolved in 15 mL water was added dropwise with a cannula over the deprotonated ligand. In few minutes the solution turned from yellow to orange and the system became heterogeneous. After 70 min at 60 °C the reaction mixture was cooled to room temperature and filtered to give an orange-brown precipitate of VO(ambch) (0.122 g, 47 % yield) and a dark orange solution.

Orange precipitate:

IR (KBr, cm^{-1}): 3439 m, 3269 w, 2936 w, 2858 w, 1614 vs, 1545 s, 1447 s, 1393 m, 1354 m, 1313 w, 1236 w, 1188 m, 1153 m, 1124 m, 1024 m, 962 m, 932 w, 912 w, 808 w, 752 w, 623 w, 569 w, 517 w.

Elemental analysis calculated for: $C_{20}H_{22}N_4VO$: C, 62.33; H, 5.75; N 14.54, . Found: C, 61.15; H, 5.52; N, 14.39.

Method B

This reaction was performed under nitrogen. A solution of ligand (0.215 g, 0.67 mmol) in ethanol (15 mL) deprotonated with NEt_3 (0.136 g, 1.34 mmol in 5 mL ethanol) was added to a Schlenk tube containing solid $VOSO_4$ at 25 °C. After addition, solution turned from yellow to green while the metal salt only partially soluble at this temperature. The mixture was heated to 70 °C and after aprox. 20 min solution turned from green to orange. Heating and stirring were stopped after 90 min and upon cooling an orange-brown precipitate was formed which was separated by filtration. The solid was washed with degassed EtOH, then dried under vacuum to give the product (0.187 g, 73 % yield).

5.11 Synthesis of asymmetrical Schiff base ligands

5.11.1 Reactivity of different benzaldehydes towards 1,2-diaminocyclohexane

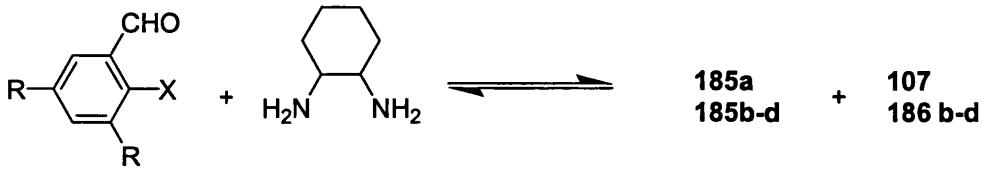

a-c: R = H; X = NH_2, HO, MeO;
d : R = ^{t}Bu; X = HO

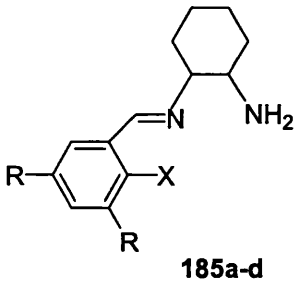

185a-d

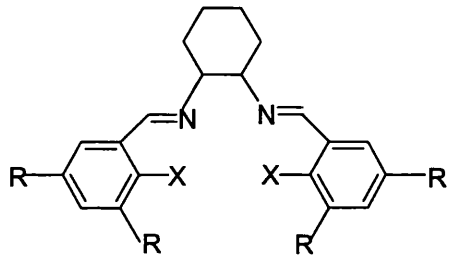

107
186 b-d

The monotartrate salt of 1,2-diaminocyclohexane (1.53 g, 5.8 mmol) was mixed with K_2CO_3 (1.61 g, 11.6 mmol) in 8 mL water and after complete dissolution, 10.4 mL of EtOH were added to the obtained solution. Then, the cloudy mixture was heated to 75-80 °C and X-R-benzaldehyde (1.9 mmol) in ethanol (4.3 mL) was added dropwise to it. The temperature was increased to 90-95 °C and it was maintained for 3 h. The composition of the reaction mixture was determined by ^{1}H-NMR (Table 5.2).

Table 5.2. Reactivity of benzaldehydes towards 1,2-diaminocyclohexane

No	X	R	Ratio of Schiff bases	
			mono	double
1	NH_2	H	32.5	1
2	OH	H	5	1
3	OMe	H	29	1
4	OH	*t*-Bu	8	1

Isolation of (R, R)-*N*-(2-aminobenzylidene)-1,2-diaminocyclohexane (185a)

After this time the solvent was evaporated under vacuum at 50-60 °C and water (5 mL) was added over the yellow oily residue. The aqueous layer was extracted with CH_2Cl_2 (3 × 20 mL) and after separation of the organic layer, it was dried over anhydrous Na_2SO_4 and the solvent was removed to give a white precipitate of *N*-(2-aminobenzylidene)-1,2-cyclohexanediamine (0.28 g, 68 % yield).

^{1}H-NMR ($CDCl_3$): δ, 8.41 (1H, s, CH=N); 7.21 (1H, dd, J = 1.5 Hz, J = 8 Hz, H^6); 7.15 (1H, dt, J = 1.5 Hz, J = 8.5 Hz, H^4); 6.69 (2H, m, H^3, H^5); 6.38 (2H, s, NH_2); 2.9-2.8 (1H, m, aliph); 2.8-2.65 (1H, m, aliph); 2-1.1 (10H, m, NH_2 + aliph).

Isolation of (R, R)-*N*-(2-methoxybenzylidene)-1,2-diaminocyclohexane (185c)

The work-up procedure was similar to that described for the mono Schiff base derived from 2-amino-benzaldehyde.

^{1}H-NMR ($CDCl_3$): δ, 8.78 (1H, s, CH=N); 7.94 (1H, dd, J = 1.8 Hz, J = 8.0 Hz, H^6); 7.38 (1H, dt, J = 1.8 Hz, J = 8.0 Hz, H^4); 6.97 (1H, t, J = 8.0 Hz, H^5); 6.91 (1H, d, J = 8.0 Hz, H^3); 3.86 (3H, s, CH_3O); 2.95-2.8 (2H, m, aliph); 2-1.1 (10H, m, aliph + NH_2)

5.11.2 Stepwise procedures

5.11.2.1 Procedure 1.

First step condensation was performed in the way described in section 5.11.1.

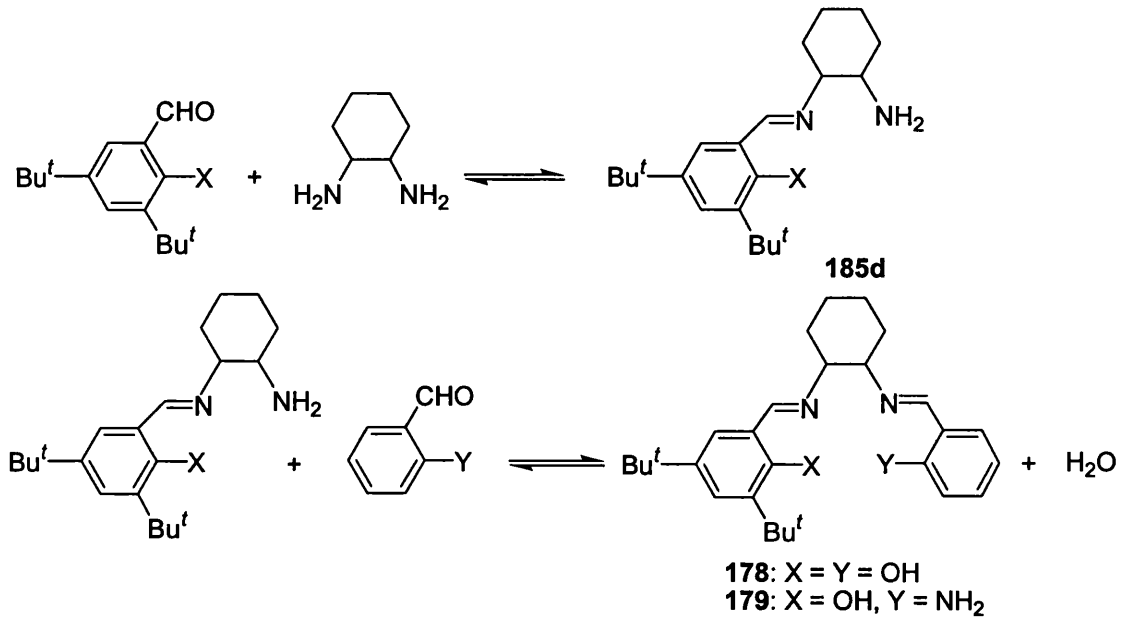

Second step condensation

Over a stirred mixture of mono and double Schiff base (0.68 g, 60 % mono Schiff base, 16 % double and 24 % diamine), obtained from condensation of 3,5-di-*t*-butyl-salicylaldehyde with (R,R)-1,2-diaminocyclohexane, dissolved in CH_2Cl_2 (15 mL) was added dropwise salicylaldehyde (0.498 g, 4 mmol) in CH_2Cl_2 (10 mL). At the end of addition the temperature was gradually increased to reflux (50-55 °C) and was kept at that value for 3 h. After that time, the solution was dried, filtered and the solvent was evaporated to give a yellow powder (1.08 g). Its composition was determined by ^{1}H-NMR. The powder was dissolved in CH_2Cl_2 and addition of petroleum spirit led to precipitation of salch. After filtration and evaporation to dryness the solid was dissolved in EtOH and on slow evaporation under vacuum the asymmetrical ligand (R,R)-3,5-di-^{t}Bu-salchsal **178** was separated as a light yellow precipitate. The amount of 3,5-di-^{t}Bu-salchsal generated in this reaction was 0.52g (58 % yield).

Synthesis of ligand **179** was achieved following a similar procedure in 49 % yield. In this case the product could not be isolated from the reaction mixture as it was more soluble in ethanol than the 3,5-di-^{t}Bu-salch.

Table 5.3 Results obtained using procedure 1

No	X	Y	1st step condensation	2nd step condensation	U
			185d: SB_1 **185d** : ch*	SB_1 : U : SB_2*	
1	HO	HO	6 : 1 0.85 : 1	0.29 : 1 : 0.93	**178**
2	HO	NH_2	6 : 1 0.66 : 1	0.26 : 1 : 1	**179**

*Ch = unreacted 1,2-diaminocyclohexane
U = asymmetrical ligand
SB_1 = symmetrical double Schiff base from X-substituted benzaldehyde
SB_2 = symmetrical double Schiff base from Y-substituted benzaldehyde

3,5-di-^{t}Bu-salchsal

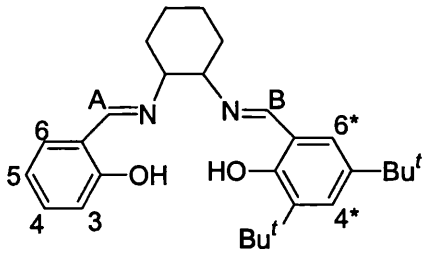

178

^{1}H-NMR ($CDCl_3$): δ, 13.66 (1H, br, HO); 13.41 (1H, br, HO); 8.29 (1H, s, CH^B=N); 8.26 (1H, s, CH^A=N); 7.31 (1H, d, J = 2.4 Hz, H^{6*}); 7.24 (1H, t, J = 7.8 Hz, H^4); 7.14 (1H, d, J = 7.8 Hz, H^6); 6.97 (1H, d, J = 2.4 Hz, H^{4*}); 6.88 (1H, d, J = 7.8 Hz, H^3); 6.80 (1H, t, J = 7.8 Hz, H^5); 3.32 (2H, m); 1.46-2.18 (8H, 3m)

IR (KBr, cm^{-1}): 3436 br, m, 2954 s, 2922 s, 2861 m, 1631 vs, 1583 s, 1502 w, 1469 s, 1443 s, 1422 w, 1385 w, 1362 w, 1253 w, 1174 w, 1095 w, 851 w.

MS: Calculated: 434.62. Found: 434.

5.11.2.2 Procedure 2.

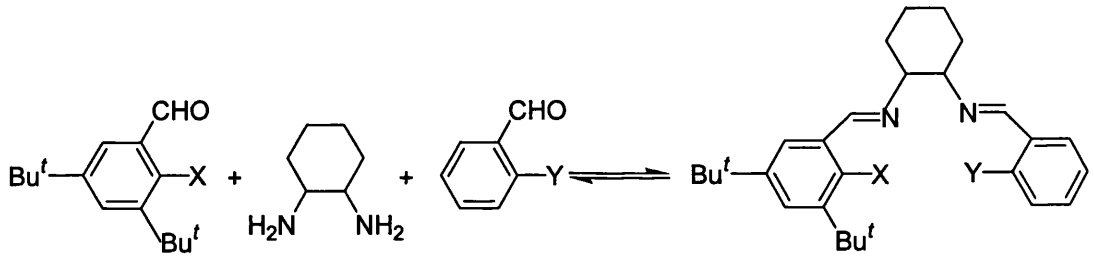

4.5 : X = Y = OH
4.6 : X = OH, Y = NH_2

1,2-diaminocyclohexane (0.22 g, 2 mmol) was dissolved in CH_2Cl_2 (10 mL) and to the stirred solution were added dropwise 3,5-di-*t*-butyl-salicylaldehyde (0.5 g, 2 mmol) and salicylaldehyde (0.23 g, 2 mmol) as solutions in CH_2Cl_2 (11 mL together). After the addition of the second aldehyde the mixture was gradually heated to 55 °C and this value was preserved for 3 h. The composition of the solution was determined by ^{1}H-NMR. To the above solution was added a new amount of salicylaldehyde (0.11 g, 0.9 mmol) at room temperature to transform all the mono Schiff bases in double Schiff bases and the heating procedure was repeated. The asymmetrical ligand (0.18 g, 0.4 mmol) was isolated from the reaction mixture by a two step recrystallization procedure from CH_2Cl_2/ petroleum spirit and EtOH. The amount of asymmetrical ligand **178** in the final reaction mixture was 0.39 g (43 % yield).

Synthesis of ligand **179** was achieved following a similar procedure in 42 % yield. The product could not be isolated from the reaction mixture as it was more soluble in ethanol than the 3,5-di-^{t}Bu-salch.

Table 5.4 Results obtained using Procedure 2

No	X	Y	1st step condensation	2nd step condensation	U
			$SB_1 : U : SB_2$*	$SB_1 : U : SB_2$	
1	HO	HO	0.55 : 1 : 0.83	0.3 : 1 :0.96	**178**
2	HO	NH_2	1.48 : 1 : 0.19	0.41 : 1 : 0.69	**179**

*U = asymmetrical ligand
SB_1 = symmetrical double Schiff base from X-substituted benzaldehyde
SB_2 = symmetrical double Schiff base from Y-substituted benzaldehyde

5.11.2.3 Procedure 3.

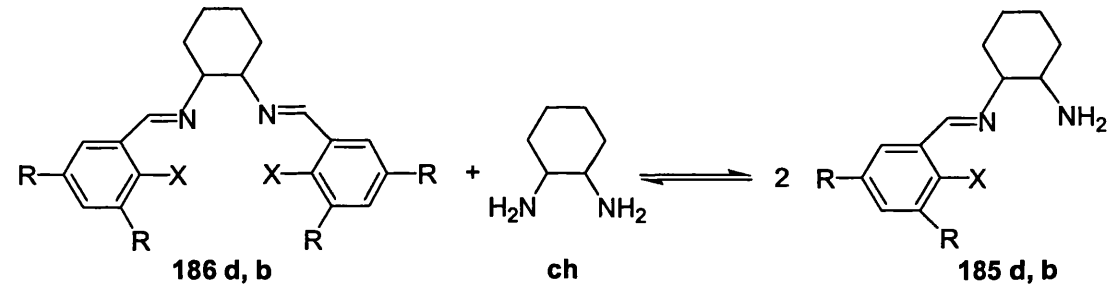

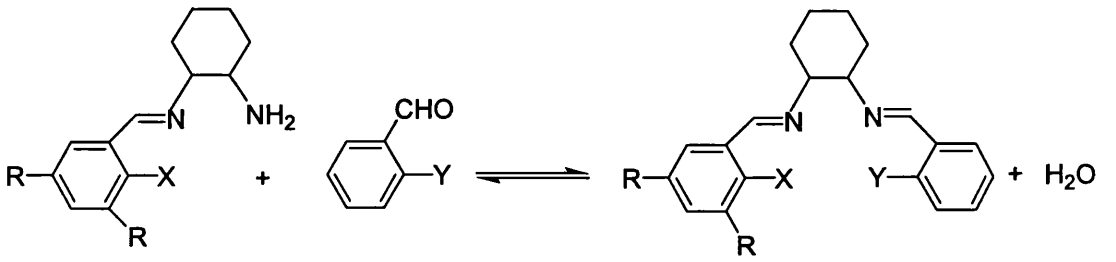

179: X = OH; Y = NH_2, R = ^{t}Bu
180: X = OH; Y = NH_2, R = H

(R,R)-*N,N'*-bis(salicylidene)-1,2-diaminocyclohexane (0.74 g, 2.3 mmol) and 1,2-diaminocyclohexane (0.26 g, 2.3 mmol) were dissolved in CH_2Cl_2 (75 mL) and the mixture was kept under stirring at room temperature for 3 days. Composition of the solution after this period was determined by ^{1}H-NMR.

Further on, to the homogeneous system was added dropwise a solution of 2-aminobenzaldehyde (0.55 g, 4.6 mmol) in ethanol, then the temperature was increased gradually to reflux (50-55 °C) and maintained for 3 h. The reaction mixture was dried over Na_2SO_4, filtered and the solvent was removed under vacuum at room temperature. The composition of the mixture was determined by ^{1}H-NMR. Recrystallization from ethanol did not lead to any improvement in the ligand purity. The amount of ambchsal in the final mixture was 1.2 g (82 % yield).

Synthesis of ligand **179** was achieved following a similar procedure in 53 % yield. The product could not be isolated from the reaction mixture.

Table 5.5. Results from Procedure 3

X	X	R	1st step	2nd step condensation	U
			185 : SB_1 **185** : ch*	SB_1 : U : SB_2*	
HO	NH_2	H	4 : 1 2 : 1	0.1 : 1 : 0.03	**180**
HO	NH_2	*t*-Bu	3.4 : 1 2 : 1	0.4 : 1 : 1.08	**179**

*Ch = unreacted 1,2-diaminocyclohexane
U = asymmetrical ligand
SB_1 = symmetrical double Schiff base from X-substituted benzaldehyde
SB_2 = symmetrical double Schiff base from Y-substituted benzaldehyde

5.11.3 Synthesis of *N*-(2-hydroxybenzylidene)-1,2-diaminocyclohexane [10]

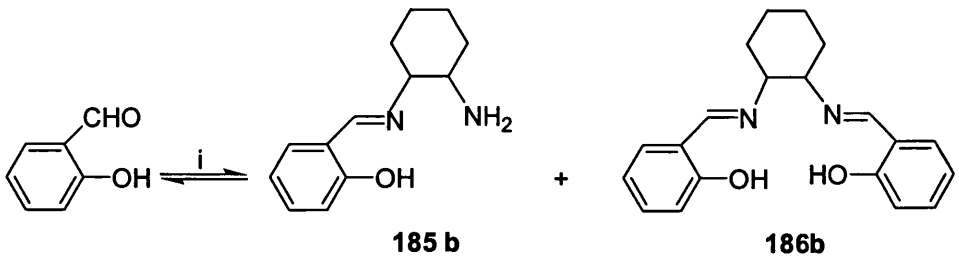

185 b **186b**

i: 1,2-diamino-cyclohexane : diamine = 1 : 1.5; $CHCl_3$, 0°C

The procedure described in [**10**] was attempted. Salicylaldehyde (0.332 g, 2.7 mmol) in chloroform (20 mL) was added dropwise (2.5 h) to a vigorously stirred solution of 1,2-diaminocyclohexane (0.468 g, 4 mmol) in $CHCl_3$ (60 mL) containing anhydrous Na_2SO_4 at 0 °C. Different parameters were tested in the work-up procedure in order to obtain a high ratio mono : double Schiff base salch. This ratio was determined by integration of the NMR signals given by the imine protons of the mentioned Schiff bases. The results are summarised in Table 5.6.

Table. 5.6. Optimization of the work-up procedure

No	Ratio diamine : salicylaldehyde	Time used to remove $CHCl_3$ (min)	Temperature (°C)	Time used to remove the diamine (min)	Ratio **185 b**: **186 b**
1	1 : 1	10	50-55	5	3.2 : 1
2	1 : 1	30	60	20	2 : 1
3	1.5 : 1	5	60-63	35	0.9 : 1
4	1.5 : 1	5-7	65-70	5	7 : 1
5	1.5 : 1	5-7	70	25	0.6 : 1

In the following, the procedure that gave the best results is described. The drying agent was removed by filtration and the filtrate was collected in an ice cooled flask. This solution was transfered directly in an oil bath maintained at 40 °C and the solvent was evaporated in 5-7 min at 50-55 °C. Then the compound was heated at 65-70 °C for 5 min to remove the excess of diamine from the system. The ^{1}H-NMR indicated a ratio mono Schiff base : salch = 7 : 1.

5.11.4 Synthesis involving blocking of one active sites in the diamine

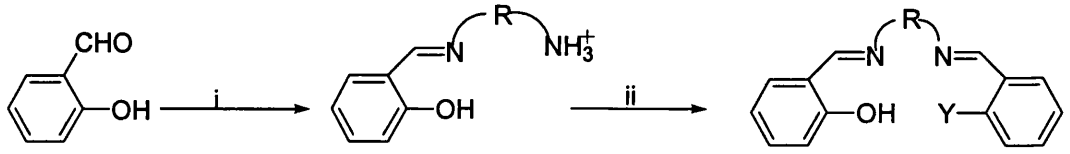

i: 1,3-propanediamine, CH_3COOH, CH_3OH, 25 °C
ii: 2-amino-benzaldehyde, Et_3N, 50 °C

183: Y = NH_2, R = -$(CH_2)_3$-
192: Y = OH, R = -$(CH_2)_3$-

The procedure described in [**11**] was adapted for synthesis of ambprsal (**183**). To a solution of propane-1,3-diamine (0.37 g, 5 mmol) in methanol (2 mL) was added dropwise acetic acid (0.3 g, 5 mmol) diluted with methanol (1:1 vol). The mixture was stirred vigorously for 20 minutes. Salicylaldehyde (0.606 g, 5 mmol) was then added and the mixture was stirred for 40 minutes at room temperature. After addition of aminobenzaldehyde (0.6 g, 5 mmol) the mixture was stirred 10 minutes then the reaction mixture was neutralized with triethylamine (0.5 g, 5 mmol) and was allowed to warm to 30 °C, followed by stirring for 10 minutes at this temperature. The composition of the reaction mixture was determined by integration of the signals presented by imine group protons in symmetrical and asymmetrical ligands salpr : ambprsal = 1.22 : 1.

Salpr (**192**)

^{1}H-NMR ($CDCl_3$): δ, 13.45 (1H, s, HO); 8.39 (1H, s, CH=N); 7.32 (1H, t, J = 7.8 Hz, H^4); 7.26 (1H, d, J = 7.8 Hz, H^6); 6.98 (1H, d, J = 7.8 Hz, H^3); 6.89 (1H, t, J = 7.8 Hz, H^5); 3.73 (2H, t, CH_2); 2.13 (1H, q, CH_2).

^{1}H-NMR ($CDCl_3$): $\delta_{CH=N}$ in ambprsal 8.39 and 8.36 ppm

5.11.5 Synthesis of asymmetrical ligands from nickel complex of the mono Schiff base

5.11.5.1. Attempt to synthesize the nickel complex of *N*-(2-amino-benzylidene)-1,2-diaminocyclohexane

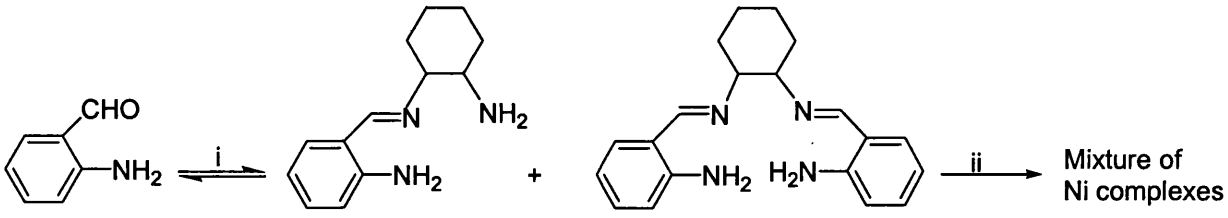

185a **107**

i: 1,2-diaminocyclohexane, EtOH reflux, 3 h;
ii: $Ni(OAc)_2$, EtOH, reflux 4 h

The procedure described in [**12**] was adapted for the mono Schiff base derived from 2-amino-benzaldehyde and 1,2-diaminocyclohexane. $Ni(OAc)_2 \cdot 4H_2O$ (0.45 g, 1.8 mmol) was added as a fine powder to a stirred ethanolic solution containing (R,R)-*N*-(2-amino-benzylidene)-1,2-diaminocyclohexane (0.68 g, 3.1 mmol, 7 mL). The reaction mixture

was heated to 60-65 °C for 2 h. Solution became red-orange after 2-3 min and changed to red-blood during heating. After this time, H_2O (0.5 mL) was added to this solution and the heating continued for two more hours. The dark-red solution was filtered to give a red precipitate which was washed with ethanol. Based on ^{1}H-NMR was established that the product was the Ni(ambch) **113** (0.24 g, 40 % yield).

Evaporation of the filtrate led to a darker red solid whose IR spectrum was recorded and indicated a mixture of Ni(ambch) and the uncomplexed ligand.

^{1}H-NMR ($CDCl_3$) precipitate (Niambch, **113**): 7.64 (1H, s, CH=N); 7.02 (1H, d, J = 7.8 Hz, H^6); 6.94 (1H, t, J = 7.8 Hz, H^4); 6.55 (1H, d, J = 7.8 Hz, H^3); 6.22 (1H, t, J = 7.8 Hz, H^5); 3.21 (2H, m, aliph); 2.46 (2H, m, aliph); 1.95(2H, m, aliph); 1.56 (2H, m, aliph); 1.34 (2H, m, aliph).

IR (KBr, cm^{-1}) precipitate (Ni ambch): 3439 br, w, 3342 w, 3042 w, 2937 w, 2859 w, 1610 vs, 1540 s, 1459 s, 1389 m, 1366 m, 1340 w, 1307 w, 1241 m, 1218 w, 1192 w, 1155 w, 1122 w, 1045 w, 1022 w, 910 w, 932 w, 747 m, 735 m, 643 w, 571 w, 463 w, 445 w.

Elemental analysis calculated: C, 63.70; H, 5.88; N, 14.85. Found: C, 62.88; H, 5.72; N, 14.62.

IR (KBr, cm^{-1}) filtrate: 3448 vs, 2937 w, 2856 w, 1633 sh, s, 1610 vs, 1540 s, 1468 s, 1458 s, 1401 m, 1387 s, 1366 m, 1307 m, 1241 m, 1155 m, 1122 m, 1043 w, 1022 m, 747 m, 735 m, 642 m, 619 m, 602 m.

5.11.5.2. Attempt to synthesize the nickel complex of *N*-(2-hydroxy-benzylidene)-1,2-diaminocyclohexane

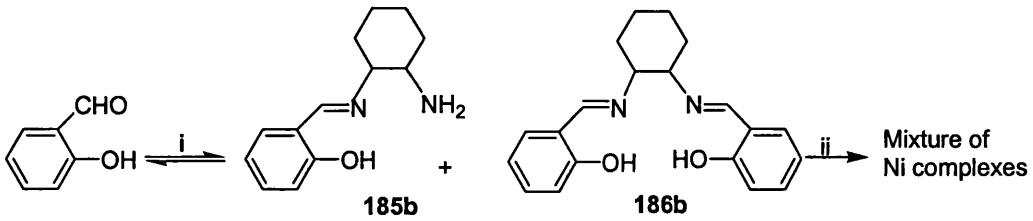

i: 1,2-diaminocyclohexane, EtOH reflux, 3 h;
ii: $Ni(OAc)_2$, EtOH, reflux 4 h or 25 °C

The monotartrate salt of 1,2-diaminocyclohexane (1.54 g, 6 mmol) and K_2CO_3 (1.63 g, 12 mmol) were mixed together in an aqueous solution (8 mL). The mixture was stirred

until dissolution was achieved and then ethanol (10.5 mL) was added. The resulted mixture was heated to reflux (80 °C) and a solution of salicylaldehyde (0.24 g, 2 mmol) in ethanol (4.4 mL) was added dropwise. The reaction took place at 90 °C during 3 h. Then the mixture was cooled to 70-75 °C and $Ni(OAc)_2 \cdot 4H_20$ (0.24 g, 1 mmol) was added as a fine powder. The mixture changed its colour from yellow to brown-orange in few minutes, then it became red. The heating continued for 2 h. Filtration of the solution led to a red-orange precipitate of Ni(salch) **119** (0.29 g, yield 78 %). The compound was characterized by ^{1}H-NMR, IR, elemental analysis.

• Precipitate obtained from complexation at 70-75 °C

^{1}H-NMR ($CDCl_3$): δ, 7.27 (1H, s, CH=N); 7.18 (1H, t, J = 7.7 Hz, H^4); 6.98 (1H, d, J = 7.7 Hz, H^6); 6.94 (1H, d, J = 7.7 Hz, H^3); 6.49 (1H, t, J = 7.7 Hz, H^5); 3.30 (m); 2.35 (m); 1.90 (m); 1.61 (m), 1.33 (m) (5H).

IR (KBr, cm^{-1}) : 3421 br, m, 3048 w, 3027 w, 2931 w, 2855 w, 1619 vs, 1600 s, 1537 s, 1469 s, 1455 s, 1349 m, 1325 s, 1224 w, 1202 w, 1147 m, 1124 w, 1108 w, 1046 w, 1027 w, 908 m, 848 w, 811 w, 752 s, 739 m, 569 w, 469 w, 447 w.

Elemental analysis calculated for $C_{20}H_{20}N_2O_2Ni$: C, 63.37; H, 5.31; N, 7.39. Found: C, 62.89; H, 5.15; N, 7.34.

Complexation of the mixture containing mono and double Schiff bases, obtained by condensation of salicylaldehyde with 1, 2-diaminocyclohexane, with nickel acetate was also studied at room temperature. Samples were taken from the reaction mixture at different moments which after evaporation of the solvent were analysed by IR.

The IR spectra of these samples resembled with that of Ni (salch) isolated as described before, however some differences in the relative intensities of some bands were observed. These bands appear at 1351, 1331, 1044, 1022, 842 and 812 cm^{-1} and their intensities will be noted as I_1 to I_6.

Complexation at 25°C

after 2 h: $I_1 > I_2$; $I_3 < I_4$; $I_5 > I_6$.

after 24 h (precipitate): $I_1 > I_2$; $I_3 > I_4$; $I_5 > I_6$

Complexation at 70 °C (precipitate): $I_1 < I_2$; $I_3 \approx I_4$; $I_5 \approx I_6$

Complexation at 25 °C in presence of a base

after 1 h: $I_1 > I_2$; $I_3 \approx I_4$; $I_5 > I_6$

after 3 h: (precipitate) $I_1 > I_2$; $I_3 > I_4$; $I_5 > I_6$

• Precipitate obtained from complexation at 25 °C (orange-yellow)

IR (KBr, cm^{-1}) : 1622 vs, 1602 s, 1541 s, 1469 s, 1456 s, 1351 s, 1331 m, 1227.5 w, 1201 w, 1145.4 s, 1125.2 m, 1044.2 m, 1022 m, 946.5 w, 908.3 m, 842 m, 812 w, 746.9 s, 737.2 s, 569 w, 447 w

5.12 Synthesis of asymmetrical nickel salchsal and ambchsal complexes

5.12. 1 Synthesis of Ni (3,5-di-^{t}Bu-salchsal)

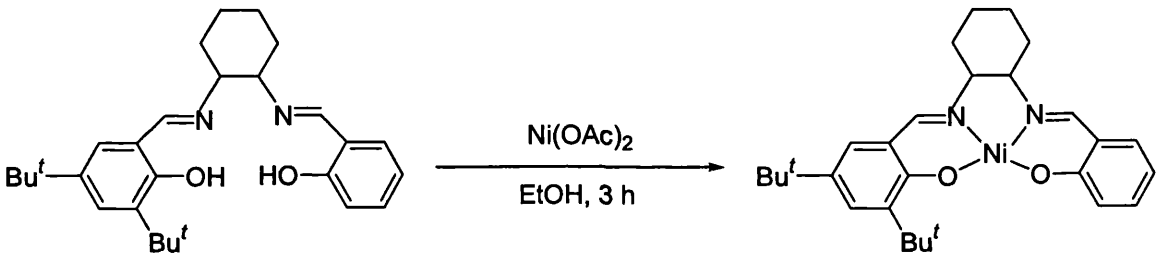

197

To a solution of (R, R)-3,5-di-^{t}Bu-salchsal (0.1 g, 0.23 mmol) in ethanol (70 mL) was added triethylamine (0.05 g, 0.49 mmol) in ethanol (5 mL). After stirring for 5 min, $Ni(OAc)_2 \cdot 4H_2O$ (0.06 g, 0.24 mmol) was added as a fine powder. The mixture changed its colour within few minutes from yellow to orange. The reaction proceeded in 3 h, under stirring at room temperature. After that period, the mixture was filtered to give an orange precipitate which was washed with ethanol and dried. The product (0.1 g, yield 89 %), Ni(3,5-di-^{t}Bu-salchsal), was characterized by ^{1}H-NMR, IR, MS. The ^{1}H-NMR spectrum of a sample taken from the filtrate indicated a mixture of nickel symmetrical and asymmetrical complexes.

Precipitate Ni (3,5-di-^{t}Bu-salchsal) (197)

^{1}H-NMR ($CDCl_3$): δ, 7.42 (1H, s, CH^B=N); 7.35 (1H, s, CH^A=N); 7.29 (1H, d, J = 2.6 Hz, H^{6*}); 7.18 (1H, t, J = 7.6 Hz, H^4); 7.07 (1H, d, J = 7.6 Hz, H^6); 6.89 (1H, d, J = 7.6 Hz, H^3); 6.88 (1H, d, J = 2.6 Hz, H^{4*}); 6.49 (1H, t, J = 7.6 Hz, H^5); 3.12 (1H, m); 3.05

(1H, m); 2.42 (2H, m); 1.91 (2H, m); 1.56 (2H, m); 1.42 (9H, s, ^{t}Bu); 1.32 (2H, m); 1.27 (9H, s, ^{t}Bu).

IR (KBr, cm^{-1}): 3447 br, s, 2948 s, 2906 m, 2864 m, 1613 vs, 1548 w, 1531 s, 1455 s, 1439 s, 1359 m, 1330 s, 1258 w, 1202 w, 1173 w, 1149 w, 1129 w, 1044 w, 1023 w, 930 w, 912 w, 861 w, 844 w, 786 w, 767 m, 617 w, 586 w, 555 w.

MS: Calculated 491.3; Found 491.

Filtrate: ^{1}H-NMR ($CDCl_3$): imine group protons: δ, 7.42 (s); 7.39 (s); 7.35 (s).

5.12.2 Study of the equilibrium involving symmetrical and asymmetrical Schiff bases

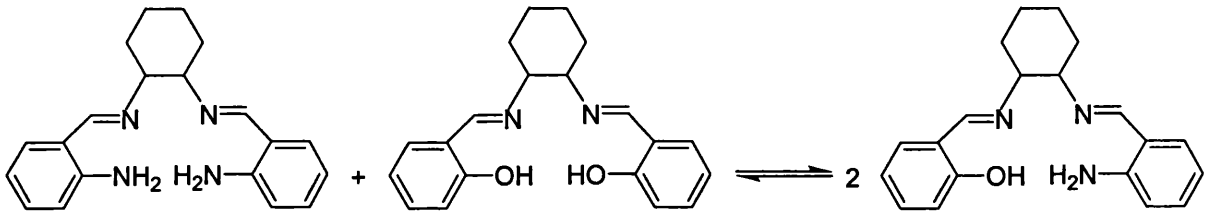

107 **186b** **180**

Salch (10 mg) and ambch (10 mg) were dissolved and mixed in $CDCl_3$, then the obtained homogeneous solution was transferred to an ^{1}H-NMR tube. The spectra were recorded at different moments and the composition of the solution was determined from the ratios between the imine group protons in the mentioned compounds. After 63 h the composition at the equilibrium was: salch : ambch : ambchsal = 1 : 1.2 : 1.2.

In the presence of water the experiment was carried out in a similar way, except that the initial ratio salch : ambch was 5 : 1.

composition after 1 h: salch : ambch : ambchsal = 29 : 5.2 : 1

composition after 40 h (equilibrium):

salch : ambch : ambchsal = 26 : 1 : 9.5

5.12.3 Synthesis of Ni(ambchsal)

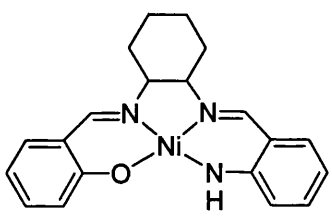

198

A mixture of salch **186b** (0.4 g, 1.24 mmol) and ambch **107** (0.081 g, 0.25 mmol) dissolved in ethanol (80 mL) reacted under stirring for 3 days at room temperature to generate the asymmetrical Schiff base ambchsal **(180)** which is in dynamic equilibrium with the symmetrical ligands. After the mentioned period, nickel acetate was added as a powder to the solution and the reaction mixture was stirred for 3 h at room temperature. The nickel complexes precipitated from solution and were separated by filtration. Separation of the two complexes was done by multiple recrystallizations from DCM-Et_2O. Red plates of Ni (ambchsal) **198** suitable for X-ray studies were grown in this way. Slow evaporation of the filtrate led to formation of orange needles of Ni (salch). The identity of the crystals was established by ^{1}H-NMR.

Composition of the mixture before complexation:

salch : ambchsal = 2.94 : 1 ; ambch : ambchsal = 1 : 9

Composition of the mixture after complexation:

Ni (salch) : Ni (ambchsal) = 2.1 : 1

Ni (ambchsal) 198

7.47 (1H, s, CH^B=N); 7.32 (1H, s, CH^A=N); 7.18 (1H, t, H^4); 7.00 (1H, d, H^{6*}); 6.96 (1H, t, H^{4*}); 6.95 (1H, d, H^6); 6.80 (1H, d, H^3); 6.64 (1H, d, H^{3*}); 6.50 (1H, t, H^5); 6.22 (1H, t, H^{5*}); 3.99 (1H, br, NH); 3.51-3.3 (2H, m, aliph); 2.32 (2H, m, aliph); 1.87 (2H, m, aliph); 1.61 (1H, m, aliph); 1.31-1.2 (3H, m, aliph).

5.12.4 Synthesis of Ni(3-Me-ambchsal)

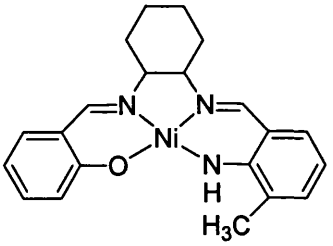

199

Preparation of this complex was performed using a procedure similar to that employed for nickel ambchsal. Composition of the reaction mixture before and after complexation with nickel acetate was determined by integration of the signals in the NMR spectra corresponding to the imine and methyl group protons.

Composition of the mixture before complexation:

salch : 3-Me-ambchsal = 3.3 : 1 ; 3-Me-ambch : 3-Me-ambchsal = 1 : 23

Composition of the mixture after complexation:

Ni (salch) : Ni (3-Me-ambchsal) = 2.2 : 1

Ni (3Me-ambchsal) 199

7.64 (1H, s, CH^{B}=N); 7.51 (1H, s, CH^{A}=N); 7.20 (1H, t, H^{4}); 7.12 (1H, d, H^{6}); 7.07 (1H, d, H^{6*}); 7.03 (1H, d, H^{3}); 7.00 (1H, t, H^{5}); 6.86 (1H, d, H^{4*}); 6.53 (1H, t, H^{5*}); 6.30 (1H, br, NH); 3.75-3.72 (1H, m, aliph); 3.26-3.16 (1H, m, aliph); 2.23 (3H, CH_3); 2.6-1.2 (8H, m, aliph).

5.12.5 Synthesis of Ni(5-Me-ambchsal)

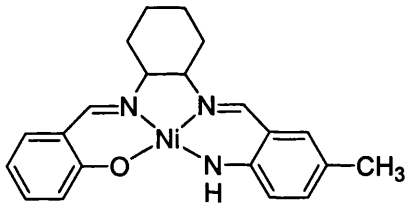

200

Preparation of this complex was performed using a procedure similar to that employed for nickel ambchsal. Composition of the reaction mixture before and after complexation with nickel acetate was determined by integration of the signals in the NMR spectra corresponding to the imine and methyl group protons.

Composition of the mixture before complexation:

salch : 5-Me-ambchsal = 3 : 1 ; 5-Me-ambch : 5-Me-ambchsal = 1 : 18

Composition of the mixture after complexation:

Ni(salch) : Ni(5-Me-ambchsal) = 3.4 : 1

Ni(5-Me-ambch) 200

7.56 (1H, s, CH^{B}=N); 7.37 (1H, s, CH^{A}=N); 7.20 (1H, t, H^{4}); 7.08 (1H, d, H^{6}); 6.82 (1H, d, H^{3}); 6.81 (1H, d, H^{4*}); 6.78 (1H, s, H^{6*}); 6.65 (1H, d, H^{3*}); 6.53 (1H, t, H^{5}); 4.05 (1H, br, NH); 2.15 (3H, CH_3)

5.13 References

1. W.S. Saari, S.W. King, V.J. Lotti, A. Scriabine, *J. Med. Chem.*, **1974**, *17*,1086.
2. L.I. Smith, J.W. Opie, *Org. Syn.*, **1948**, *28*, 11.
3. J.F. Larrow, E.N. Jacobsen, *J. Org. Chem.*, **1994**, *59*, 1939.
4. I. M. Goldman, *J. Org. Chem.*, **1969**, *34*, 1979.
5. R.F. Nystrom, W.G. Brown, *J. Am. Chem. Soc.*, **1947**, *69*, 2548.
6. M.C. Wani, M.E. Wall, *J. Org. Chem.*, **1969**, *34*, 1364.
7. T. W. Green, P.G.M. Wuts, *Protective Groups in Organic Synthesis*, 3rd ed., Wiley, New York, **1999**, p 23.
8. D. Das, C.P. Cheng, *J. Chem. Soc., Dalton Trans.*, **2000**, 1081.
9. B.M. Higson, E.D. McKenzie, *J.Chem.Soc., Dalton Trans.*, **1972**, 269.
10. J. Lopez, S. Liang, X.R. Bu, *Tetrahedron Lett.*, **1998**, *39*, 4199.
11. C. Fukuhara, E. Asato, T. Shimoji, K. Katsura, *J. Chem. Soc., Dalton Trans.* **1987**, 1305.
12. R.C. Elder, *Aust. J. Chem.*, **1978**, *31*, 35.

Appendix 1 – Crystal Data

Cu(ambch) 3.21

Empirical formula	$C_{20}H_{22}N_4Cu$	
Formula weight	381.96	
Temperature	100(2) K	
Wavelength	0.71073 Å	
Crystal system	Triclinic	
Space group	P-1	
Unit cell dimensions	a = 9.8965(11) Å	α = 100.406(6)°
	b = 10.0512(13) Å	β = 101.388°
	c = 18.920(2) Å	γ = 106.160(5)°
Volume	1715.7(3) $Å^3$	
Z	2	
Density (calculated)	1.479Mg/m^3	
Absorption coeficient	1.283 mm^{-1}	
F(000)	796	
Crystal size	0.2 x 0.2 x 0.1 mm^3	
Theta range for data collection	1.13 to 25.00°	
Index ranges	-11<=h<=11, -11<=k<=11, -22<=l<=22	
Reflections collected	9376	
Independent reflections	5954 [R(int) = 0.0928]	
Completeness to theta = 25.00°	98.5 %	
Absorption correction	Scalepack	
Max. and min. trasmission	0.8824 and 0.7835	
Refinement method	Full-matrix least-squares on F^2	
Data / restraints / parameters	5954 / 0 / 456	
Goodness-of-fit on F^2	1.022	
Final R indices [I>2sigma(I)]	R1 = 0.0768, wR2 = 0.1510	
R indices (all data)	R1 = 0.1439, wR2 = 0.1776	
Extinction coefficient	0.0010(6)	
Largest diff. peak and hole	0.621 and –0.565 e.$Å^{-3}$	

Ni(ambchsal) 4.26

Empirical formula	$C_{20}H_{21}N_3ONi$	
Formula weight	379.09	
Temperature	100(2) K	
Wavelength	0.71070 Å	
Crystal system	Triclinic	
Space group	P-1	
Unit cell dimensions	a = 9.7892(7) Å	α = 101.307(3)°
	b = 10.0122(4) Å	β = 101.439(3)°
	c = 18.7217(8) Å	γ = 104.386(3)°
Volume	1682.92(16) $Å^3$	
Z	2	
Density (calculated)	1.479Mg/m^3	
Absorption coeficient	1.169 mm^{-1}	
F(000)	792	
Crystal size	0.4 x 0.2 x 0.2 mm^3	
Theta range for data collection	1.15 to 26.00°	
Index ranges	-11<=h<=12, -12<=k<=12, -22<=l<=23	
Reflections collected	26461	
Independent reflections	6550 [R(int) = 0.0456]	
Completeness to theta = 25.00°	99.3 %	
Absorption correction	Scalepack	
Refinement method	Full-matrix least-squares on F^2	
Data / restraints / parameters	6550 / 0 / 523	
Goodness-of-fit on F^2	1.313	
Final R indices [I>2sigma(I)]	R1 = 0.0869, wR2 = 0.2066	
R indices (all data)	R1 = 0.0980, wR2 = 0.2108	
Extinction coefficient	0.0010(6)	
Largest diff. peak and hole	0.713 and –0.794 e.$Å^{-3}$	

Ni(salchsal*) 4.25

Empirical formula	$C_{28}H_{36}N_2O_2Ni$
Formula weight	491.30
Temperature	100(2) K
Wavelength	0.71070 Å
Crystal system	Monoclinic
Space group	P21/c
Unit cell dimensions	a = 13.6744(9) Å α = 90°
	b = 15.8398(9) Å β = 96.640(4)°
	c = 11.6016(11) Å γ = 90°
Volume	2496.0(3) $Å^3$
Z	4
Density (calculated)	1.307Mg/m^3
Absorption coeficient	0.804 mm^{-1}
F(000)	1048
Crystal size	0.4 x 0.1 x 0.1 mm^3
Theta range for data collection	2.19 to 27.50°
Index ranges	-17<=h<=17, -17<=k<=20, -15<=l<=12
Reflections collected	16034
Independent reflections	5715 [R(int) = 0.1367]
Completeness to theta = 25.00°	99.7 %
Absorption correction	Scalepack
Max. and min. trasmission	0.9239 and 0.7391
Refinement method	Full-matrix least-squares on F^2
Data / restraints / parameters	5715 / 0 / 305
Goodness-of-fit on F^2	0.949
Final R indices [I>2sigma(I)]	R1 = 0.0561, wR2 = 0.1052
R indices (all data)	R1 = 0.1341, wR2 = 0.1299
Extinction coefficient	0.0009(8)
Largest diff. peak and hole	0.628 and –0.770 e.$Å^{-3}$

Appendix 2-Bond lengths [Å] and angles [°] of structures solved by Single crystal X-ray analysis

Cu(ambch) 3.21

Cu(1)-N(1)	1.907(6)	C(8)-C(13)	1.594(16)
Cu(1)-N(4)	1.923(6)	C(9)-C(10)	1.49(2)
Cu(1)-N(3)	1.946(6)	C(10)-C(11)	1.569(19)
Cu(1)-N(2)	1.956(6)	C(11)-C(12)	1.67(2)
N(1)-C(1)	1.355(8)	C(12)-C(13)	1.667(19)
C(1)-C(2)	1.419(9)	C(14)-C(15)	1.422(10)
C(1)-C(6)	1.437(10)	C(15)-C(16)	1.411(9)
Cu(2)-N(8)	1.894(6)	C(15)-C(20)	1.439(9)
Cu(2)-N(5)	1.903(6)	C(16)-C(17)	1.383(10)
Cu(2)-N(7)	1.946(6)	C(17)-C(18)	1.389(10)
Cu(2)-N(6)	1.958(5)	C(18)-C(19)	1.353(9)
N(2)-C(7)	1.289(8)	C(19)-C(20)	1.435(9)
N(2)-C(8A)	1.512(19)	C(21)-C(26)	1.435(9)
N(2)-C(8)	1.528(12)	C(21)-C(22)	1.436(10)
C(2)-C(3)	1.357(9)	C(22)-C(23)	1.363(10)
N(3)-C(14)	1.299(9)	C(23)-C(24)	1.406(10)
N(3)-C(13A)	1.47(2)	C(24)-C(25)	1.366(10)
N(3)-C(13)	1.536(14)	C(25)-C(26)	1.398(9)
C(3)-C(4)	1.377(11)	C(26)-C(27)	1.429(10)
N(4)-C(20)	1.332(8)	C(28)-C(29)	1.50(2)
C(4)-C(5)	1.378(10)	C(28)-C(33)	1.53(2)
N(5)-C(21)	1.353(9)	C(29)-C(30)	1.56(3)
C(5)-C(6)	1.407(9)	C(30)-C(31)	1.47(2)
N(6)-C(27)	1.294(9)	C(31)-C(32)	1.59(2)
N(6)-C(28)	1.507(16)	C(32)-C(33)	1.56(3)
N(6)-C(28A)	1.538(15)	C(34)-C(35)	1.430(9)
C(6)-C(7)	1.414(10)	C(35)-C(36)	1.401(10)
N(7)-C(34)	1.288(9)	C(35)-C(40)	1.446(10)
N(7)-C(33A)	1.515(14)	C(36)-C(37)	1.368(9)
N(7)-C(33)	1.566(15)	C(37)-C(38)	1.411(10)
N(8)-C(40)	1.349(9)	C(38)-C(39)	1.340(10)

C(8)-C(9)	1.45(2)	C(39)-C(40)	1.421(9)
C(8A)-C(13A)	1.43(3)	C(28A)-C(33A)	1.509(19)
C(8A)-C(9A)	1.58(3)	C(28A)-C(29A)	1.53(2)
C(9A)-C(10A)	1.54(3)	C(29A)-C(30A)	1.53(2)
C(10A)-C(11A)	1.41(2)	C(30A)-C(31A)	1.47(2)
C(11A)-C(12A)	1.56(3)	C(31A)-C(32A)	1.49(2)
C(12A)-C(13A)	1.61(3)	C(32A)-C(33A)	1.46(2)

N(1)-Cu(1)-N(4)	94.8(3)
N(1)-Cu(1)-N(3)	173.6(3)
N(4)-Cu(1)-N(3)	91.1(3)
N(1)-Cu(1)-N(2)	91.0(3)
N(4)-Cu(1)-N(2)	174.2(3)
N(3)-Cu(1)-N(2)	83.2(2)
C(1)-N(1)-Cu(1)	130.6(5)
N(1)-C(1)-C(2)	122.1(7)
N(1)-C(1)-C(6)	121.1(6)
C(2)-C(1)-C(6)	116.8(6)
N(8)-Cu(2)-N(5)	95.2(3)
N(8)-Cu(2)-N(7)	90.6(3)
N(5)-Cu(2)-N(7)	174.1(3)
N(8)-Cu(2)-N(6)	174.2(3)
N(5)-Cu(2)-N(6)	90.7(3)
N(7)-Cu(2)-N(6)	83.6(2)
C(7)-N(2)-C(8A)	120.0(9)
C(7)-N(2)-C(8)	119.6(7)
C(8A)-N(2)-C(8)	31.8(8)
C(7)-N(2)-Cu(1)	126.9(5)
C(8A)-N(2)-Cu(1)	109.2(8)
C(8)-N(2)-Cu(1)	112.5(5)
C(3)-C(2)-C(1)	122.3(7)
C(14)-N(3)-C(13A)	120.6(9)
C(14)-N(3)-C(13)	119.4(7)
C(13A)-N(3)-C(13)	29.7(8)

C(2)-C(3)-C(4)	120.7(7)	C(17)-C(16)-C(15)	122.8(7)
C(20)-N(4)-Cu(1)	130.2(5)	C(16)-C(17)-C(18)	117.8(6)
C(3)-C(4)-C(5)	120.1(7)	C(19)-C(18)-C(17)	121.7(7)
C(21)-N(5)-Cu(2)	131.2(5)	C(18)-C(19)-C(20)	122.9(7)
C(4)-C(5)-C(6)	121.1(7)	N(4)-C(20)-C(19)	122.2(6)
C(27)-N(6)-C(28)	119.8(7)	N(4)-C(20)-C(15)	122.3(6)
C(27)-N(6)-C(28A)	119.1(7)	C(19)-C(20)-C(15)	115.5(6)
C(28)-N(6)-C(28A)	30.3(7)	N(5)-C(21)-C(26)	121.4(7)
C(27)-N(6)-Cu(2)	127.3(5)	N(5)-C(21)-C(22)	122.4(6)
C(28)-N(6)-Cu(2)	112.0(6)	C(26)-C(21)-C(22)	116.2(6)
C(28A)-N(6)-Cu(2)	110.1(6)	C(23)-C(22)-C(21)	122.3(7)
C(5)-C(6)-C(7)	118.2(7)	C(22)-C(23)-C(24)	120.3(7)
C(5)-C(6)-C(1)	119.0(6)	C(25)-C(24)-C(23)	119.1(7)
C(7)-C(6)-C(1)	122.8(6)	C(24)-C(25)-C(26)	122.5(7)
C(34)-N(7)-C(33A)	121.1(7)	C(25)-C(26)-C(27)	118.2(6)
C(34)-N(7)-C(33)	117.9(8)	C(25)-C(26)-C(21)	119.5(7)
C(33A)-N(7)-C(33)	32.3(7)	C(27)-C(26)-C(21)	122.3(6)
C(34)-N(7)-Cu(2)	127.5(5)	N(6)-C(27)-C(26)	126.7(6)
C(33A)-N(7)-Cu(2)	110.8(6)	C(29)-C(28)-N(6)	115.1(13)
C(33)-N(7)-Cu(2)	109.9(6)	C(29)-C(28)-C(33)	115.2(15)
N(2)-C(7)-C(6)	127.1(7)	N(6)-C(28)-C(33)	101.4(11)
C(40)-N(8)-Cu(2)	131.4(5)	C(28)-C(29)-C(30)	108.3(15)
C(9)-C(8)-N(2)	118.8(11)	C(31)-C(30)-C(29)	115.1(15)
C(9)-C(8)-C(13)	110.2(12)	C(30)-C(31)-C(32)	117.7(15)
N(2)-C(8)-C(13)	97.9(8)	C(33)-C(32)-C(31)	103.5(14)
C(8)-C(9)-C(10)	113.5(15)	C(28)-C(33)-C(32)	114.3(14)
C(9)-C(10)-C(11)	111.4(13)	C(28)-C(33)-N(7)	103.2(11)
C(10)-C(11)-C(12)	102.8(11)	C(32)-C(33)-N(7)	110.4(11)
C(11)-C(12)-C(13)	98.9(11)	N(7)-C(34)-C(35)	126.4(7)
N(3)-C(13)-C(8)	102.9(8)	C(36)-C(35)-C(34)	118.1(7)
N(3)-C(13)-C(12)	107.1(9)	C(36)-C(35)-C(40)	119.8(6)
C(8)-C(13)-C(12)	103.0(10)	C(34)-C(35)-C(40)	122.2(7)
N(3)-C(14)-C(15)	126.6(7)	C(37)-C(36)-C(35)	122.2(7)
C(16)-C(15)-C(14)	118.4(6)	C(36)-C(37)-C(38)	118.2(7)
C(16)-C(15)-C(20)	119.2(6)	C(39)-C(38)-C(37)	121.2(7)
C(14)-C(15)-C(20)	122.3(6)	C(38)-C(39)-C(40)	123.1(7)

C(28A)-C(33A)-C(32)	111.1(12)
C(28A)-C(33A)-N(4)	102.3(11)
C(32)-C(33A)-N(4)	109.7(10)

Ni(ambchsal)

Ni(1)-O(1)	1.845(6)	C(9)-C(10)	1.568(17)
Ni(1)-O(2)	1.849(6)	C(12)-C(11)	1.559(16)
Ni(1)-N(1)	1.852(6)	C(12)-C(13A)	1.583(15)
Ni(1)-N(2)	1.864(6)	C(12)-C(13)	1.585(16)
Ni(2)-O(3)	1.841(6)	C(12)-C(11A)	1.603(17)
Ni(2)-O(4)	1.842(5)	C(14)-C(15)	1.435(10)
Ni(2)-N(4)	1.851(6)	C(15)-C(20)	1.427(10)
Ni(2)-N(3)	1.860(6)	C(15)-C(16)	1.428(10)
O(1)-C(1)	1.325(9)	C(16)-C(17)	1.370(11)
O(2)-C(20)	1.329(9)	C(17)-C(18)	1.406(12)
O(3)-C(21)	1.337(9)	C(18)-C(19)	1.372(11)
O(4)-C(40)	1.337(9)	C(19)-C(20)	1.426(10)
N(1)-C(7)	1.314(9)	C(21)-C(26)	1.413(10)
N(1)-C(8)	1.500(15)	C(21)-C(22)	1.427(10)
N(1)-C(8A)	1.510(15)	C(22)-C(23)	1.374(11)
N(2)-C(14)	1.290(10)	C(23)-C(24)	1.404(12)
N(2)-C(13)	1.516(15)	C(24)-C(25)	1.369(11)
N(2)-C(13A)	1.521(15)	C(25)-C(26)	1.418(10)
N(3)-C(27)	1.292(10)	C(26)-C(27)	1.421(10)
N(3)-C(28A)	1.522(14)	C(29)-C(28A)	1.525(16)
N(3)-C(28)	1.554(15)	C(29)-C(30A)	1.528(17)
N(4)-C(34)	1.301(10)	C(29)-C(28)	1.589(16)
N(4)-C(33)	1.464(16)	C(29)-C(30)	1.630(16)
N(4)-C(33A)	1.583(16)	C(32)-C(31)	1.487(16)
C(1)-C(6)	1.424(10)	C(32)-C(33A)	1.557(16)
C(1)-C(2)	1.426(9)	C(32)-C(33)	1.566(15)
C(2)-C(3)	1.371(10)	C(32)-C(31A)	1.634(18)
C(3)-C(4)	1.397(11)	C(34)-C(35)	1.422(11)
C(4)-C(5)	1.377(11)	C(35)-C(36)	1.420(10)
C(5)-C(6)	1.404(10)	C(35)-C(40)	1.425(10)
C(6)-C(7)	1.414(10)	C(36)-C(37)	1.350(12)
C(9)-C(8)	1.531(16)	C(37)-C(38)	1.389(12)
C(9)-C(8A)	1.550(15)	C(38)-C(39)	1.378(11)
C(9)-C(10A)	1.557(19)	C(39)-C(40)	1.431(10)
		C(8)-C(13)	1.50(2)
		C(10)-C(11)	1.52(2)

C(27)-N(3)-C(28)	123.3(8)
C(28A)-N(3)-C(28)	33.6(8)
C(27)-N(3)-Ni(2)	127.1(5)
C(28A)-N(3)-Ni(2)	113.2(6)
C(28)-N(3)-Ni(2)	108.0(6)
C(34)-N(4)-C(33)	117.3(8)
C(34)-N(4)-C(33A)	122.9(8)
C(33)-N(4)-C(33A)	30.5(7)
C(34)-N(4)-Ni(2)	127.2(6)
C(33)-N(4)-Ni(2)	112.4(6)
C(33A)-N(4)-Ni(2)	108.8(6)
O(1)-C(1)-C(6)	122.2(6)
O(1)-C(1)-C(2)	121.1(6)
C(6)-C(1)-C(2)	116.7(6)
C(3)-C(2)-C(1)	121.6(7)
C(2)-C(3)-C(4)	121.1(7)
C(5)-C(4)-C(3)	118.9(7)
C(4)-C(5)-C(6)	121.5(7)
C(5)-C(6)-C(7)	118.0(7)
C(5)-C(6)-C(1)	120.2(6)
C(7)-C(6)-C(1)	121.8(6)
N(1)-C(7)-C(6)	125.3(7)
C(8)-C(9)-C(8A)	28.0(6)
C(8)-C(9)-C(10A)	113.7(10)
C(8A)-C(9)-C(10A)	106.4(9)
C(8)-C(9)-C(10)	108.3(10)
C(8A)-C(9)-C(10)	113.9(10)
C(10A)-C(9)-C(10)	25.0(6)
C(11)-C(12)-C(13A)	115.5(9)
C(11)-C(12)-C(13)	105.3(9)
C(13A)-C(12)-C(13)	32.8(7)
C(11)-C(12)-C(11A)	35.8(7)
C(13A)-C(12)-C(11A)	103.0(9)
C(13)-C(12)-C(11A)	113.9(9)
N(2)-C(14)-C(15)	125.0(7)
C(20)-C(15)-C(16)	120.3(7)

C(28)-C(33)	1.53(2)
C(30)-C(31)	1.52(2)
C(8A)-C(13A)	1.53(2)
C(10A)-C(11A)	1.54(2)
C(28A)-C(33A)	1.48(2)
C(30A)-C(31A)	1.51(2)

O(1)-Ni(1)-O(2)	87.1(2)
O(1)-Ni(1)-N(1)	93.5(2)
O(2)-Ni(1)-N(1)	178.3(3)
O(1)-Ni(1)-N(2)	178.6(3)
O(2)-Ni(1)-N(2)	94.1(3)
N(1)-Ni(1)-N(2)	85.4(3)
O(3)-Ni(2)-O(4)	86.3(2)
O(3)-Ni(2)-N(4)	179.4(3)
O(4)-Ni(2)-N(4)	94.1(3)
O(3)-Ni(2)-N(3)	94.0(3)
O(4)-Ni(2)-N(3)	178.9(3)
N(4)-Ni(2)-N(3)	85.5(3)
C(1)-O(1)-Ni(1)	129.8(5)
C(20)-O(2)-Ni(1)	128.6(5)
C(21)-O(3)-Ni(2)	128.0(5)
C(40)-O(4)-Ni(2)	128.3(5)
C(7)-N(1)-C(8)	119.6(8)
C(7)-N(1)-C(8A)	118.7(7)
C(8)-N(1)-C(8A)	28.7(7)
C(7)-N(1)-Ni(1)	127.4(5)
C(8)-N(1)-Ni(1)	111.7(7)
C(8A)-N(1)-Ni(1)	111.7(6)
C(14)-N(2)-C(13)	118.4(8)
C(14)-N(2)-C(13A)	120.8(8)
C(13)-N(2)-C(13A)	34.3(7)
C(14)-N(2)-Ni(1)	127.6(5)
C(13)-N(2)-Ni(1)	110.5(7)
C(13A)-N(2)-Ni(1)	109.9(6)
C(27)-N(3)-C(28A)	116.6(8)

C(20)-C(15)-C(14)	121.8(6)
C(16)-C(15)-C(14)	117.9(6)
C(17)-C(16)-C(15)	120.6(7)
C(16)-C(17)-C(18)	119.6(7)
C(19)-C(18)-C(17)	121.2(7)
C(18)-C(19)-C(20)	121.5(7)
O(2)-C(20)-C(19)	120.3(6)
O(2)-C(20)-C(15)	122.8(6)
C(19)-C(20)-C(15)	116.9(6)
O(3)-C(21)-C(26)	123.1(6)
O(3)-C(21)-C(22)	120.1(7)
C(26)-C(21)-C(22)	116.8(6)
C(23)-C(22)-C(21)	121.4(7)
C(22)-C(23)-C(24)	120.9(7)
C(25)-C(24)-C(23)	119.5(7)
C(24)-C(25)-C(26)	120.6(7)
C(21)-C(26)-C(25)	120.8(7)
C(21)-C(26)-C(27)	121.6(6)
C(25)-C(26)-C(27)	117.6(7)
N(3)-C(27)-C(26)	125.5(7)
C(28A)-C(29)-C(30A)	108.0(9)
C(28A)-C(29)-C(28)	33.1(7)
C(30A)-C(29)-C(28)	116.6(9)
C(28A)-C(29)-C(30)	112.0(9)
C(30A)-C(29)-C(30)	32.7(7)
C(28)-C(29)-C(30)	101.4(9)
C(31)-C(32)-C(33A)	112.8(9)
C(31)-C(32)-C(33)	109.3(9)
C(33A)-C(32)-C(33)	30.0(7)
C(31)-C(32)-C(31A)	27.9(7)
C(33A)-C(32)-C(31A)	102.3(9)
C(33)-C(32)-C(31A)	113.8(9)
N(4)-C(34)-C(35)	125.8(7)
C(36)-C(35)-C(34)	118.9(7)
C(36)-C(35)-C(40)	120.1(7)
C(34)-C(35)-C(40)	121.0(6)
C(37)-C(36)-C(35)	121.4(8)
C(36)-C(37)-C(38)	119.4(7)
C(39)-C(38)-C(37)	121.7(7)
C(38)-C(39)-C(40)	120.7(8)
O(4)-C(40)-C(35)	123.0(6)
O(4)-C(40)-C(39)	120.5(7)
C(35)-C(40)-C(39)	116.5(6)
C(13)-C(8)-N(1)	101.9(12)
C(13)-C(8)-C(9)	110.5(13)
N(1)-C(8)-C(9)	115.4(11)
C(11)-C(10)-C(9)	110.2(13)
C(10)-C(11)-C(12)	109.4(11)
C(8)-C(13)-N(2)	102.8(11)
C(8)-C(13)-C(12)	108.3(11)
N(2)-C(13)-C(12)	111.8(10)
C(33)-C(28)-N(3)	99.2(10)
C(33)-C(28)-C(29)	109.1(11)
N(3)-C(28)-C(29)	109.0(9)
C(31)-C(30)-C(29)	108.4(11)
C(32)-C(31)-C(30)	107.7(13)
N(4)-C(33)-C(28)	101.5(12)
N(4)-C(33)-C(32)	115.8(11)
C(28)-C(33)-C(32)	105.2(12)
N(1)-C(8A)-C(13A)	101.3(10)
N(1)-C(8A)-C(9)	113.7(10)
C(13A)-C(8A)-C(9)	109.2(11)
C(11A)-C(10A)-C(9)	108.1(13)
C(10A)-C(11A)-C(12)	104.9(10)
N(2)-C(13A)-C(8A)	100.2(10)
N(2)-C(13A)-C(12)	111.6(10)
C(8A)-C(13A)-C(12)	106.1(11)
C(33A)-C(28A)-N(3)	100.9(11)
C(33A)-C(28A)-C(29)	106.1(14)
N(3)-C(28A)-C(29)	114.2(10)
C(31A)-C(30A)-C(29)	106.7(12)
C(30A)-C(31A)-C(32)	111.2(12)

N(8)-C(40)-C(39)	123.8(7)
N(8)-C(40)-C(35)	120.8(6)
C(39)-C(40)-C(35)	115.5(6)
C(13A)-C(8A)-N(2)	106.6(15)
C(13A)-C(8A)-C(9A)	116.1(17)
N(2)-C(8A)-C(9A)	114.1(14)
C(10A)-C(9A)-C(8A)	109.2(15)
C(11A)-C(10A)-C(9A)	116.1(17)
C(10A)-C(11A)-C(12A)	108.8(17)
C(11A)-C(12A)-C(13A)	105.2(15)
C(8A)-C(13A)-N(3)	105.7(15)
C(8A)-C(13A)-C(12A)	105.4(17)
N(3)-C(13A)-C(12A)	113.3(14)
C(33A)-C(28A)-C(29A)	110.3(13)
C(33A)-C(28A)-N(6)	103.5(10)
C(29A)-C(28A)-N(6)	115.7(12)
C(30A)-C(29A)-C(28A)	111.7(14)
C(31A)-C(30A)-C(29A)	110.8(13)
C(30A)-C(31A)-C(32A)	111.0(14)
C(33A)-C(32A)-C(31A)	116.1(14)
C(32A)-C(33A)-C(28A)	110.6(13)
C(32A)-C(33A)-N(7)	118.2(12)
C(28A)-C(33A)-N(7)	102.3(11)

Ni(salchsal*

Ni(1)-O(2)	1.829(2)	C(21)-C(22)	1.545(5)
Ni(1)-N(1)	1.844(3)	C(25)-C(28)	1.525(5)
Ni(1)-O(1)	1.844(2)	C(25)-C(26)	1.532(4)
Ni(1)-N(2)	1.846(3)	C(25)-C(27)	1.542(5)
O(1)-C(1)	1.310(4)		
N(1)-C(7)	1.305(4)	O(2)-Ni(1)-N(1)	174.65(11)
N(1)-C(8)	1.494(4)	O(2)-Ni(1)-O(1)	84.47(10)
C(1)-C(6)	1.406(4)	N(1)-Ni(1)-O(1)	95.44(11)
C(1)-C(2)	1.418(4)	O(2)-Ni(1)-N(2)	93.57(11)
O(2)-C(16)	1.317(4)	N(1)-Ni(1)-N(2)	86.91(12)
N(2)-C(14)	1.297(4)	O(1)-Ni(1)-N(2)	175.36(11)
N(2)-C(13)	1.480(4)	C(1)-O(1)-Ni(1)	127.0(2)
C(2)-C(3)	1.384(5)	C(7)-N(1)-C(8)	120.3(3)
C(3)-C(4)	1.399(5)	C(7)-N(1)-Ni(1)	126.9(2)
C(4)-C(5)	1.366(5)	C(8)-N(1)-Ni(1)	111.9(2)
C(5)-C(6)	1.417(5)	O(1)-C(1)-C(6)	124.3(3)
C(6)-C(7)	1.439(4)	O(1)-C(1)-C(2)	117.7(3)
C(8)-C(13)	1.507(5)	C(6)-C(1)-C(2)	117.9(3)
C(8)-C(9)	1.523(4)	C(16)-O(2)-Ni(1)	126.4(2)
C(9)-C(10)	1.531(5)	C(14)-N(2)-C(13)	123.2(3)
C(10)-C(11)	1.508(5)	C(14)-N(2)-Ni(1)	125.7(2)
C(11)-C(12)	1.524(5)	C(13)-N(2)-Ni(1)	111.0(2)
C(12)-C(13)	1.528(4)	C(3)-C(2)-C(1)	121.0(3)
C(14)-C(15)	1.431(5)	C(2)-C(3)-C(4)	120.8(3)
C(15)-C(20)	1.410(4)	C(5)-C(4)-C(3)	118.8(3)
C(15)-C(16)	1.427(4)	C(4)-C(5)-C(6)	121.9(3)
C(16)-C(17)	1.421(4)	C(1)-C(6)-C(5)	119.4(3)
C(17)-C(18)	1.388(4)	C(1)-C(6)-C(7)	122.2(3)
C(17)-C(21)	1.542(4)	C(5)-C(6)-C(7)	118.4(3)
C(18)-C(19)	1.404(4)	N(1)-C(7)-C(6)	123.8(3)
C(19)-C(20)	1.368(4)	N(1)-C(8)-C(13)	105.1(3)
C(19)-C(25)	1.546(4)	N(1)-C(8)-C(9)	117.2(3)
C(21)-C(24)	1.533(5)	C(13)-C(8)-C(9)	112.0(3)
C(21)-C(23)	1.543(5)	C(8)-C(9)-C(10)	109.0(3)
		C(11)-C(10)-C(9)	112.6(3)
		C(10)-C(11)-C(12)	112.1(3)

C(11)-C(12)-C(13)	109.7(3)
N(2)-C(13)-C(8)	104.4(3)
N(2)-C(13)-C(12)	116.6(3)
C(8)-C(13)-C(12)	111.5(3)
N(2)-C(14)-C(15)	125.3(3)
C(20)-C(15)-C(16)	120.0(3)
C(20)-C(15)-C(14)	119.3(3)
C(16)-C(15)-C(14)	120.7(3)
O(2)-C(16)-C(17)	119.5(3)
O(2)-C(16)-C(15)	121.9(3)
C(17)-C(16)-C(15)	118.6(3)
C(18)-C(17)-C(16)	118.2(3)
C(18)-C(17)-C(21)	122.0(3)
C(16)-C(17)-C(21)	119.9(3)
C(17)-C(18)-C(19)	124.0(3)
C(20)-C(19)-C(18)	117.4(3)
C(20)-C(19)-C(25)	120.6(3)
C(18)-C(19)-C(25)	122.0(3)
C(19)-C(20)-C(15)	121.8(3)
C(24)-C(21)-C(17)	112.1(3)
C(24)-C(21)-C(23)	107.9(3)
C(17)-C(21)-C(23)	110.2(3)
C(24)-C(21)-C(22)	107.1(3)
C(17)-C(21)-C(22)	110.2(3)
C(23)-C(21)-C(22)	109.2(3)
C(28)-C(25)-C(26)	108.5(3)
C(28)-C(25)-C(27)	107.4(3)
C(26)-C(25)-C(27)	109.2(3)
C(28)-C(25)-C(19)	113.1(3)
C(26)-C(25)-C(19)	109.3(3)
C(27)-C(25)-C(19)	109.3(3)